

BIRLA CENTRAL LIBRARY

PILANI [RAJASTHAN]

Class No. 627

Book No. C468C

Accession No. 39367

Centrifugal Pumps and Blowers

BY

AUSTIN H. CHURCH

*Professor of Mechanical Engineering
New York University*

NEW YORK

JOHN WILEY & SONS, INC.

CHAPMAN & HALL, LTD.

LONDON

COPYRIGHT, 1944
BY
AUSTIN H. CHURCH

All Rights Reserved

*This book or any part thereof must not
be reproduced in any form without
the written permission of the publisher.*

FOURTH PRINTING, FEBRUARY, 1950

PRINTED IN THE UNITED STATES OF AMERICA

PREFACE

The application and use of centrifugal pumps and blowers today are universal. Modern public utilities, chemical plants, municipal gas, water, and sewage works, and other fields too numerous to mention would be seriously handicapped if these machines did not exist.

It is surprising therefore that there is no modern textbook in English which may be referred to by young graduate engineers who must deal with such equipment. With that need in mind this book was written.

The book does not attempt to develop new theories nor go into advanced problems; but it does cover the basic principles of design, construction, and application along the conventional lines of present-day practice. References are given to many recent technical papers which may be consulted for more complete or advanced information. With the material given in this book as a basis, the interested reader should be able to assimilate them.

Examples are given to clarify the text, and problems with answers are included by which the reader may test his grasp of the subject matter.

I should like to acknowledge the great help received from Mr. Hans Gartmann of the De Laval Steam Turbine Company in the preparation of the manuscript, and wish to express my deep appreciation for the valuable assistance rendered. I should also like to thank Messrs. F. K. Mäussnest and A. Peterson for valuable suggestions made after reading parts of the manuscript. I have drawn upon technical literature and trade catalogs in preparing the book, and wish to express my appreciation to the authors and companies concerned for allowing me to use their material.

A. H. C.

*University Heights
New York City
April, 1944*

CONTENTS

1. Introduction	1
1-1 Introduction. 1-2 Centrifugal machines. 1-3 Reciprocating machines. 1-4 Operation and nomenclature of centrifugal machines.	
2. Principles of Fluid Flow	6
2-1 Introduction. 2-2 Specific weight, density, and specific gravity. 2-3 Flow. 2-4 Viscosity. 2-5 Reynolds number. 2-6 Continuity equation. 2-7 Head. 2-8 Bernoulli's theorem. 2-9 Loss of head. 2-10 External head required of pump or blower. 2-11 Streamlines and stream-tubes. 2-12 Applications of flow principles.	
3. Basic Theory of Pumps and Blowers	22
3-1 Velocity diagrams. 3-2 Ideal head equation. 3-3 Ideal torque and horsepower equations. 3-4 Incompleteness of the ideal equations. 3-5 Circulatory flow. 3-6 Friction. 3-7 Turbulence. 3-8 Disk friction. 3-9 Leakage. 3-10 Mechanical losses. 3-11 Prerotation of the fluid. 3-12 Coefficients and efficiencies. 3-13 Performance curves. 3-14 Virtual head-capacity curve. 3-15 Effect of speed changes on performance curves. 3-16 Diffusers. 3-17 Influence of the design on the performance. 3-18 The actual head-capacity curve. 3-19 Brake horsepower and efficiency curves. 3-20 Pulsation or surging.	
4. Specific Speed and Efficiency of Pumps	49
4-1 Specific speed. 4-2 Development of the specific speed equation. 4-3 Specific speed in terms of wheel dimensions. 4-4 Specific speed applied to pump classification. 4-5 Pump efficiencies. 4-6 Model tests.	
5. Performance Curves and Cavitation of Pumps	68
5-1 Effect of speed on performance curves. 5-2 Effect of impeller changes on performance curves. 5-3 Performance curves for various types of pumps. 5-4 Effect of viscosity on performance curves. 5-5 Cavitation. 5-6 Suction head or <i>NPSH</i> . 5-7 Available suction head. 5-8 Required suction head. 5-9 Factors affecting cavitation. 5-10 Cavitation parameters.	
6. Design of Radial-Type Pump Stage	90
6-1 Introduction. 6-2 Speed. 6-3 Pipe connections and velocities. 6-4 Leakage losses. 6-5 Impeller inlet dimensions and vane angle. 6-6 Flow in impellers. 6-7 Impeller outlet dimensions and vane angle. 6-8 Design of vanes. 6-9 Example of impeller design. 6-10 Design of volute. 6-11 Example of volute design. 6-12 Design of diffuser. 6-13 Example of diffuser design. 6-14 Disk friction. 6-15 Multistaging.	

- 7. Other Pump Impeller Types** **130**
 7-1 Introduction. 7-2 Francis-type impeller. 7-3 Mixed-flow impeller.
 7-4 Propeller pump.
- 8. Pump Details and Materials** **145**
 8-1 Introduction. 8-2 Shaft and sleeves. 8-3 Bearings. 8-4 Packing boxes. 8-5 Impellers. 8-6 Wearing rings. 8-7 Casing. 8-8 Selection of materials. 8-9 Diffuser. 8-10 Axial thrust. 8-11 Radial thrust. 8-12 Couplings. 8-13 Priming.
- 9. Pump Applications and Selection** **161**
 9-1 Pumping arrangements. 9-2 Prime movers. 9-3 Economic considerations. 9-4 Fire pumps. 9-5 Dredge pumps. 9-6 Slurry pumps. 9-7 Deep well pumps. 9-8 Waterworks, irrigation, and drainage pumps. 9-9 Circulating pumps. 9-10 Boiler feed pumps. 9-11 Condensate pumps. 9-12 Clogless pumps.
- 10. Pump Installation, Operation, and Test** **176**
 10-1 Installation. 10-2 Operation. 10-3 Pump test. 10-4 Test instruments and apparatus. 10-5 Sample pump test.
- 11. Thermodynamic Principles** **189**
 11-1 Introduction. 11-2 Characteristic equation. 11-3 Specific heat. 11-4 Enthalpy. 11-5 Entropy. 11-6 "Standard" air and "free" air. 11-7 Compression of gases. 11-8 Notes on the compression of gases. 11-9 Properties of gas mixtures. 11-10 Effect of altitude on atmospheric conditions.
- 12. Classification and Performance Curves of Blowers** **208**
 12-1 Classification. 12-2 Specific speed. 12-3 Head of blowers and compressors. 12-4 Performance curves. 12-5 Change of speed — other factors constant. 12-6 Constant speed — inlet conditions changed. 12-7 Summary.
- 13. Design of Radial-Type Blower Stage** **217**
 13-1 Introduction. 13-2 Speed. 13-3 Effect of compressibility on design. 13-4 Pipe connections and velocities. 13-5 Impeller inlet dimensions and vane angle. 13-6 Flow conditions in the impeller. 13-7 Impeller outlet dimensions and vane angle. 13-8 Leakage losses. 13-9 Design of vanes. 13-10 Example of impeller design. 13-11 Design of the volute. 13-12 Example of volute design. 13-13 Design of the diffuser. 13-14 Example of diffuser design. 13-15 Disk friction. 13-16 Multi-staging.

14. Construction Details of Blowers	244
14-1 Introduction. 14-2 Shaft and sleeves. 14-3 Leakage. 14-4 Bearings. 14-5 Casing. 14-6 Impeller and vanes. 14-7 Diffuser and diaphragm. 14-8 Axial thrust. 14-9 Couplings. 14-10 Cooling.	
15. Blower Applications	254
15-1 Introduction. 15-2 High pressure air. 15-3 Sewage aeration blowers. 15-4 Scavenging two-cycle Diesels. 15-5 Cupola blowers. 15-6 Blast furnace blowers. 15-7 Bessemer converter blowers. 15-8 Blast furnace gas blowers. 15-9 Water gas blowers. 15-10 Municipal gas plant blowers. 15-11 Coke plant exhausters and boosters. 15-12 Airplane superchargers. 15-13 Other applications.	
16. Regulation of Blowers	260
16-1 Introduction. 16-2 Constant pressure regulation. 16-3 Constant inlet volume or weight flow. 16-4 Pulsation. 16-5 Movable diffuser vanes and prerotation. 16-6 The power wheel.	
17. Blower Installation, Operation, and Test	269
17-1 Installation. 17-2 Operation. 17-3 Blower test. 17-4 Test instruments and apparatus. 17-5 Sample blower test.	
18. Disk Stresses	278
18-1 Introduction. 18-2 Sum and difference curves. 18-3 Disk of any profile. 18-4 Dead weight of vanes. 18-5 Notes on the use of the chart. 18-6 Example.	
19. Critical Speeds	289
19-1 Introduction. 19-2 Action at the critical speed. 19-3 Critical speed of a two-bearing stepped shaft. 19-4 Higher critical speeds of two-bearing shafts. 19-5 Factors influencing the critical speed. 19-6 Critical speeds of three-bearing shafts. 19-7 Torsional critical speeds.	
Index	305

PARTIAL SYMBOL LIST

<i>A</i>	Area	sq. ft. or sq. in.
<i>A</i>	Mechanical equivalent of heat	1/778
a.hp.	Air horsepower	
<i>b</i>	Width of passage	in. or ft.
b.hp.	Brake horsepower	
<i>C, c</i>	Coefficient or constant	
<i>c</i>	Specific heat	B.t.u. per degree
<i>D, d</i>	Diameter	in. or ft.
<i>D</i>	Difference of radial and tangential stresses	lb. per sq. in.
<i>E</i>	Tensile modulus of elasticity	lb. per sq. in.
<i>E_s</i>	Shearing modulus of elasticity	lb. per sq. in.
<i>F</i>	Frequency of vibration	cy. per min.
<i>f</i>	Pipe friction coefficient	
f.hp.	Fluid horsepower	
<i>g</i>	Acceleration due to gravity	32.2 ft. per sec. ²
<i>H</i>	Head	ft.
<i>H</i>	Enthalpy	B.t.u. per lb.
<i>H_{sv}</i>	Suction head above vapor pressure	ft.
<i>h</i>	Height of passage	in. or ft.
hp.	Horsepower	
<i>I</i>	Internal Energy	B.t.u. per lb.
<i>I</i>	Rectangular moment of inertia	in. ⁴
<i>I_p</i>	Polar moment of inertia	in. ⁴
<i>J</i>	Mass moment of inertia	lb.-in.-sec. ²
<i>K</i>	Overall head coefficient at shut-off	
<i>K'</i>	Overall head coefficient at maximum efficiency point	
<i>K</i>	Product of η_{∞} and η_{HY}	
<i>k</i>	Ratio of specific heats	c_p/c_v
<i>L</i>	Length	in. or ft.
<i>M</i>	Molecular weight	
<i>M</i>	Bending moment	in.-lb.
<i>m</i>	Mass	slugs
<i>n</i>	Revolutions per minute	r.p.m.
<i>n_s</i>	Specific speed	r.p.m.
<i>N_R</i>	Reynolds number	
<i>P</i>	Absolute pressure	lb. per sq. ft.
<i>p</i>	Absolute pressure	lb. per sq. in.

Q	Volume flow rate	c.f.s. or g.p.m.
R	Radial stress	lb. per sq. in.
R	Gas Constant	ft.-lb. per deg.
\bar{R}	Radius of gyration	in.
R, r	Radius	ft. or in.
R_m	Hydraulic radius	ft. or in.
S	Entropy	B.t.u. per °F.
S	Suction specific speed	r.p.m.
S	Sum of tangential and radial stresses	lb. per sq. in.
s	Diametral clearance	in.
s	Pitch of labyrinth strips	in.
s_s	Shearing stress	lb. per sq. in.
s_t	Tensile stress	lb. per sq. in.
sg	Specific gravity	
T	Absolute temperature	°F.
T	Torque	in.-lb.
T	Tangential stress	lb. per sq. in.
t	Time	sec.
t	Thickness	in.
u	Tangential velocity	ft. per sec.
V	Absolute velocity of fluid	ft. per sec.
V	Volume	cu. ft.
\bar{V}	Specific volume	cu. ft. per lb.
v	Relative velocity of fluid to impeller	ft. per sec.
W	Weight	lb.
w	Weight flow	lb. per sec.
Wk	Work	ft.-lb.
w.hp.	Water horsepower	
Y	Ratio of adiabatic temperature rise to the actual	
y	Shaft deflection	in.
z	Elevation	ft.
z	Number of impeller vanes	
z'	Number of diffuser vanes	

GREEK LETTERS

α (alpha)	Angle between V and u	deg.
α	Diffuser vane angle	deg.
α	Throttling contraction factor	
β (beta)	Angle between v and u extended	deg.
β	Impeller vane angle	deg.
β	Coefficient	
γ (gamma)	Specific weight	lb. per cu. ft.
γ	Carry-over correction factor	
Δ (delta)	Small change (a prefix)	

Δ	Tip thickness of strip	in.
δ (delta)	Radial clearance	in.
ϵ (epsilon)	Vane thickness factor	
ϵ_p	Pressure ratio	
η (eta)	Efficiency	
η_∞	Circulatory flow coefficient	
θ (theta)	An angle	deg. or rad.
μ (mu)	Absolute viscosity	slugs per ft.-sec.; poise
ν (nu)	Kinematic viscosity	ft. ² per sec.; stoke
ν	Poisson's ratio	
ρ (rho)	Mass density	slugs per cu. ft.
Σ (sigma)	A summation	
σ (sigma)	Cavitation parameter	H_{sv}/H
Φ (phi)	Overall head coefficient at point of maximum efficiency	
Φ'	Overall head coefficient at point of shut-off	
ϕ (phi)	An angle	deg. or rad.
ϕ	Pressure ratio factor	
ω (omega)	Angular velocity	rad. per sec.

SUBSCRIPTS

0	"Eye" of impeller passage
1	Impeller vane inlet edge
2	Impeller vane outlet edge, or impeller rim
3	"Throat" or inlet of diffuser
4	"Mouth" or outlet of diffuser
act.	Actual
ad.	Adiabatic
<i>DF</i>	Disk Friction
<i>f</i>	Friction
<i>H</i>	Hub
<i>HY</i>	Hydraulic
iso.	Isothermal
<i>L</i>	Leakage
<i>M</i>	Mechanical
<i>m</i>	Mean or average
<i>p</i>	Pressure
<i>r</i>	Radial or perpendicular to impeller motion
<i>S</i>	Shaft
su.	Suction
<i>T</i>	Turbulence
<i>u</i>	Tangential or in direction of impeller motion
<i>V</i>	Volumetric, or velocity

vir.	Virtual or ideal
<i>vp</i>	Vapor pressure
<i>z</i>	Height or elevation
∞	Perfect fluid guidance, or infinite number of vanes

CONVERSION FACTORS

Pounds per square inch $\times 2.31 =$ feet of water (60° F.).

Feet of water (60° F.) $\times 0.433 =$ pounds per square inch.

Inches of water (60° F.) $\times 0.0361 =$ pounds per square inch.

Pounds per square inch $\times 27.70 =$ inches of water (60° F.).

Pounds per square inch $\times 2.041 =$ inches of mercury (60° F.).

Inches of mercury (60° F.) $\times 0.490 =$ pounds per square inch.

Horsepower $\times 0.746 =$ kilowatts.

Kilowatts $\times 1.341 =$ horsepower.

Cubic feet $\times 7.48 =$ U. S. gallons.

U. S. gallons $\times 0.1337 =$ cubic feet.

U. S. gallons of water (60° F.) $\times 8.34 =$ pounds

U. S. gallons $\times 0.8327 =$ English gallons.

English gallons $\times 1.201 =$ U. S. gallons.

pure rotation it is easily balanced and contains no inherent inertia forces.

As a result of their higher speeds centrifugal machines are able to handle large volumes at low heads. The fluid is delivered in a steady stream so no receiver is required to even out flow pulsations. They have no internal valves to cause operating difficulties, and it is possible to secure automatic regulation based upon the capacity, the suction pressure, or the discharge pressure. The units are designed to operate with the discharge valve closed ("shut-off"), so there is no likelihood of an expensive or dangerous failure if this valve is inadvertently shut for short periods of time.

If the bearings are located outside the casing, the fluid does not come into contact with the lubricating oil and thus is not contaminated by it. A centrifugal blower tends to act as a cleaner in that impurities in the gas, such as tar, are thrown outward by the centrifugal force and adhere to the walls. The tar then flows to the bottom of the casing, from which it may be removed through suitable drains.

1.3 Reciprocating Machines. Reciprocating units generally have higher efficiencies than the centrifugal but advances in the design of the latter have overcome this advantage when operating under the conditions for which they are most suitable.

Reciprocating pumps have the advantage of being able to start without priming. When operating at constant speed reciprocating machines will deliver a fixed capacity at any discharge pressure. The centrifugal machines may be designed to deliver any capacity from zero to a maximum at practically a constant discharge pressure while operating at constant speed.

Reciprocating machines are ideally suited for applications requiring high heads and small capacities.

Reciprocating compressors introduce oil vapor into the gases from the cylinder lubrication and, if coolers are used, this vapor condenses on the tubes and interferes with the heat transfer. This oil vapor is also objectionable in applications when the air or gas is used in the food or special process industries.

1.4 Operation and Nomenclature of Centrifugal Machines. Figure 1.1 shows an axial section through a three-stage centrifugal compressor with the various parts of the machine labeled.

Assume that the compressor is not rotating but is filled with gas. When rotation starts the gas near the shaft at the first-stage impeller is picked up by the curved vanes and "thrown" outward into the diffuser. This leaves a lower gas pressure at the impeller inlet, so that more gas is forced in by the external pressure in the suction pipe.

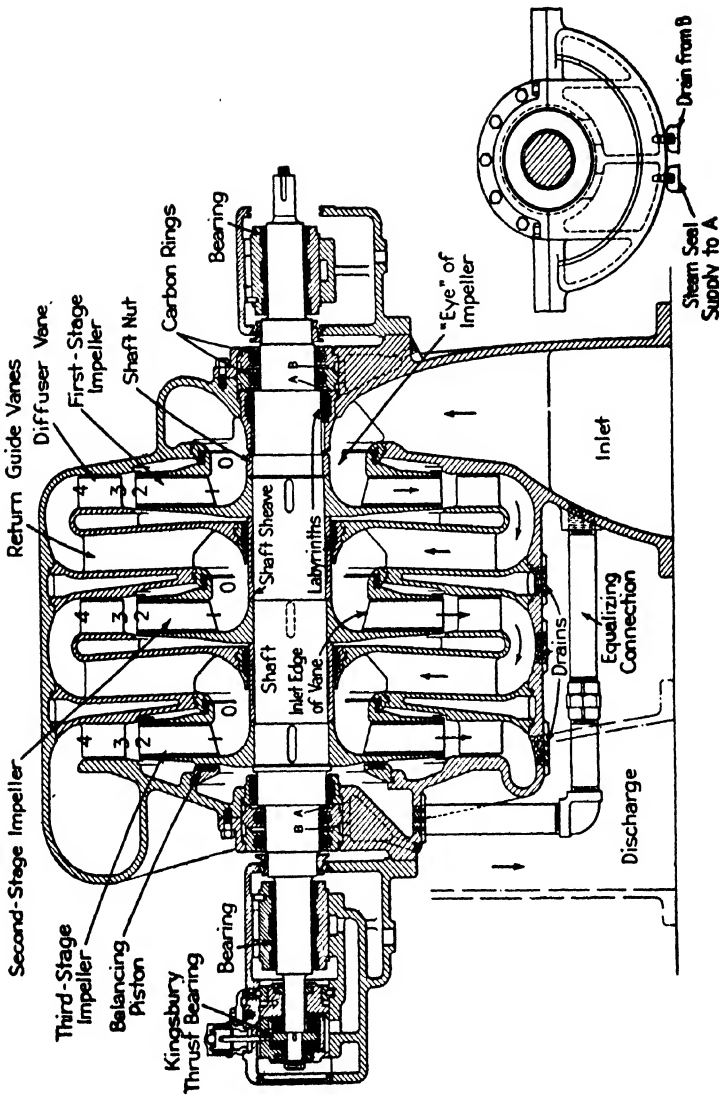
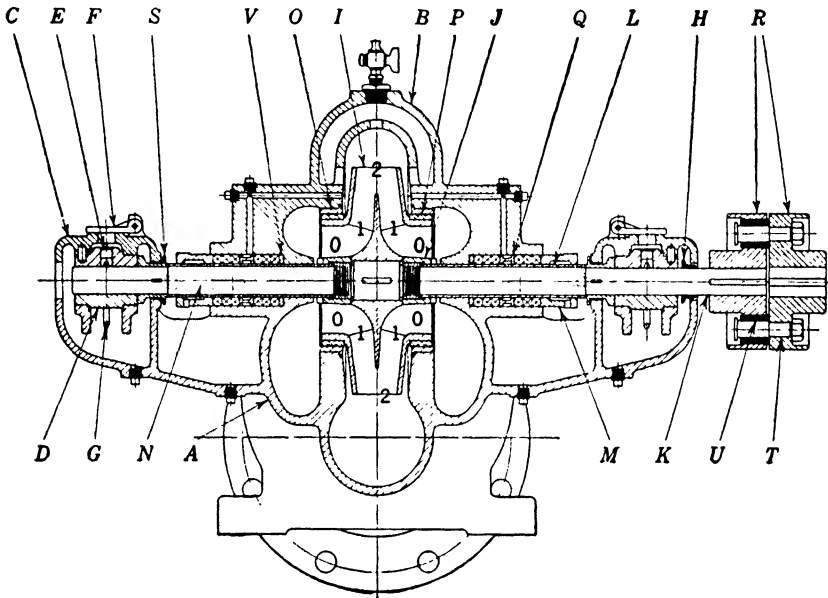


FIG. 1-1. Axial section of three-stage gas compressor provided with steam-sealed packing boxes. Steam is introduced at *A* between the labyrinth and carbon rings to prevent the latter from being fouled by tar. The steam is drained from between the rings at *B* so that it will not blow out around the shaft.

Courtesy De Laval Turbine Steam Co.

The diffuser consists of a number of diverging passages, formed by guide vanes surrounding the impeller, which cause the gas velocity to be decreased and the kinetic energy to be converted into pressure. After leaving the first-stage diffuser the gas passes through the return



Courtesy Dayton-Dowd Co.

- | | |
|-----------------------|---------------------------------|
| A Lower casing | L Shaft sleeve |
| B Upper casing | M Gland halves |
| C Bearing bracket cap | N Gland bolts |
| D Bearing, lower half | O Casing wearing ring |
| E Bearing, upper half | P Impeller wearing ring |
| F Oil-hole cover | Q Lantern ring |
| G Oil ring | R Coupling halves |
| H Oil guard | S Thrust collar and water sling |
| I Impeller | T Coupling pins and nuts |
| J Impeller nut | U Coupling bushings |
| K Shaft | V Packing box bottom |

FIG. 1-2. Single-stage, double-suction centrifugal pump.

guide vanes into the second-stage impeller where the process is repeated. As the gas goes through each stage, its pressure is further increased until it finally leaves at the discharge pressure of the compressor.

The action in a pump is similar to that in a compressor, hence the above description of operation also applies to a multistage pump.

In many machines after the fluid leaves the impeller it does not go to a diffuser but is collected in a spiral-shaped chamber having no guide vanes; this is known as a volute. This volute collects the fluid

Obviously, there must be a transition point from one type of flow to the other; this is known as the *critical* velocity. It is very difficult to observe accurately the exact velocity at which the transition occurs, since it is not entirely consistent for repeated tests and is different when increasing the velocity from laminar to turbulent flow than when decreasing it from turbulent to laminar.

2-4 Viscosity. When laminar flow of a fluid through a passage occurs, the layer of fluid in actual contact with the guiding surface adheres to it, and hence has a zero velocity. The velocity across the section varies (usually parabolically) to a maximum at the center. The resistance to flow is caused by the shearing of adjacent layers of the fluid. This resistance is due to the viscosity of the fluid and is proportional to the rate at which the layers are sheared.

Viscosity is a measure of the resistance to flow of a fluid; or it may be defined as the ratio of the shearing stress or force between adjacent layers of fluid to the rate of change of velocity perpendicular to the direction of motion.

$$\mu = \frac{\tau}{\frac{\partial V}{\partial y}} \tag{2-1}$$

where τ = shearing force or stress
 V = velocity of fluid
 y = distance perpendicular to flow
 μ = absolute viscosity.

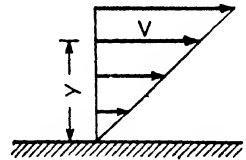


FIG. 2-1. Laminar flow of fluid.

If the absolute viscosity is measured in metric system, the unit is a poise and is measured in grams mass per centimeter-second. In the English system, the units are slugs per foot-second. The following relation is useful for conversions.

$$\mu \text{ in slugs per foot second} = 0.002089 (\mu \text{ in poises}) \tag{2-2}$$

Frequently the viscosity is given in centipoises. A centipoise is $\frac{1}{100}$ of a poise.

It is sometimes more convenient to use *kinematic viscosity* (ν); this is the absolute viscosity divided by the mass density or $\nu = \frac{\mu g}{\gamma} = \frac{\mu}{\rho}$.

In the metric system, the units are called stokes, which are centimeters squared per second; in the English system the units are feet squared per second. For conversion purposes:

$$\nu \text{ in feet squared per second} = 0.001076 (\nu \text{ in stokes}) \tag{2-3}$$

Liquids are frequently specified in terms of Saybolt seconds. A Saybolt second is the time t' in seconds required for 60 cc. of liquid to pass through an opening of standard size. To convert this into kinematic viscosity the following relationships may be used.

$$\nu = 0.0022t' - \frac{1.8}{t'} \text{ cm.}^2 \text{ per sec. or stokes} \quad 2.4$$

$$\nu = \left(0.236t' - \frac{194}{t'} \right) 10^{-5} \text{ ft.}^2 \text{ per sec.} \quad 2.5$$

The above equations apply to the Universal Saybolt viscosimeter. For heavy oils a Saybolt-Furol viscosimeter is used; this is the same as the Universal except that the diameter of the opening is larger. The ratio of the times required for a given liquid to flow through the two viscosimeters is approximately 10 to 1, so that the readings on the Furol machine should be multiplied by 10 before substituting in Eqs. 2.4 and 2.5.

The viscosity is practically independent of the pressure but it varies with the temperature. Helmholtz found the viscosity of water to be

$$\mu \text{ in poises} = \frac{0.01779}{1 + 0.03368t + 0.000221t^2} \quad 2.6$$

and Grindley and Gibson found the viscosity of air to be

$$\mu \text{ in poises} = 0.0001702 (1 + 0.00329t + 0.000007t^2) \quad 2.7$$

where t for both cases is the temperature in degrees centigrade.

Values of viscosity and specific weight for the two common fluids, water and air, at 59° F. and atmospheric pressure are as follows.

Fluid	Absolute Viscosity μ		Kinematic Viscosity ν		Specific Weight γ	
	poises	slugs per ft.-sec.	stokes	sq. ft. per sec.	g. per cc.	lb. per cu. ft.
Air	$0.1783 (10)^{-3}$	$0.3723 (10)^{-6}$	0.1455	$0.1566 (10)^{-3}$	0.001224	0.0765
Water	0.01144	$23.890 (10)^{-6}$	0.01145	$12.32 (10)^{-6}$	1.000	62.34

2.5 Reynolds Number. It is desirable to be able to compare the flow of fluids under different conditions of velocity, viscosity, density, and passage size for similarly shaped channels. It has been found that the resistance to flow of the fluid, or of an object moved through a body of fluid, is a function of a dimensionless ratio known as Reynolds

number, N_R .

$$N_R = \frac{\gamma Vd}{\mu g} = \frac{\rho Vd}{\mu} = \frac{Vd}{\nu} \quad 2.8$$

where γ = specific weight of fluid

V = velocity of fluid or body

μ = absolute viscosity of fluid

ν = kinematic viscosity of fluid

d = some characteristic dimension of the passage or of an object in the path (as a diameter).

Since the ratio is dimensionless, the actual units are immaterial as long as they are consistent. Thus the number could be calculated by using metric units and used in connection with English units, if desirable.

As noted previously in Section 2-3, there are three types of flow, turbulent, critical, and laminar. Large Reynolds numbers indicate turbulent flow, whereas low values indicate laminar flow. The critical flow generally occurs at a Reynolds number of about 2300.

2-6 Continuity Equation. After steady conditions have been established, the weight of fluid per unit of time passing any point is constant. The weight of fluid per second equals $\gamma A V$ where V is the average velocity across the section, A the area, and γ the weight per unit volume or specific weight. For any two sections, a and b , $\gamma_a A_a V_a = \gamma_b A_b V_b$, or for any section

$$\gamma A V = \text{constant} = \text{weight flow in pounds per second} \quad 2.9$$

This is known as the continuity equation and it is very useful in fluid flow work.

For liquids such as water, γ is practically constant, and the equation reduces to

$$Q = A V \quad 2.10$$

where Q is the quantity flowing per unit of time (as cubic feet per second). Hence, as the cross-sectional area of a pipe is decreased gradually the velocity will increase, and vice versa.

2-7 Head. The energy of a fluid, which is its ability to do work, is specified in feet of head of the fluid flowing. The head is the height to which a column of the fluid must rise to contain the same amount of energy as is contained in one unit weight of the fluid under the conditions considered. It may appear in three different forms, which are interchangeable.

The *potential* or *actual head* is based upon the elevation of the fluid

above some arbitrarily chosen datum plane. Thus, a column of water z ft. high contains a certain amount of energy because of its position, and is said to have a head of z ft. of water.

The *kinetic* or *velocity head* is a measure of the kinetic energy contained in a unit weight of the fluid due to its velocity, and is given by the familiar expression for kinetic energy, $V^2/2g$. It may be measured by a pitot tube placed in the stream as shown in Fig. 2·2. The second leg of the manometer is connected to the passage at right angles to the flow to equalize the pressure existing in the passage at this point.

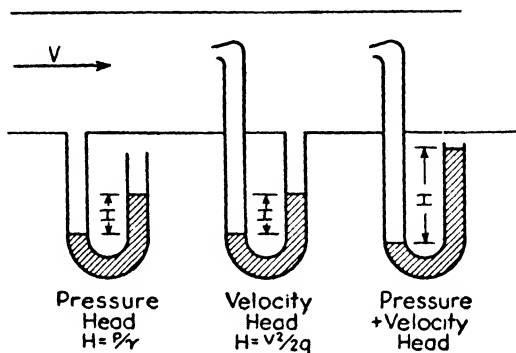


FIG. 2·2. Methods of measuring the various forms of head.

The *pressure head* is the energy contained in the fluid as a result of its pressure, and is equal to P/γ . If an open manometer tube is connected at right angles to the flow, the fluid will rise in the tube to a height equal to P/γ .

2·8 Bernoulli's Theorem. The total energy of the fluid is equal to the sum of the three heads just mentioned or

$$\frac{P}{\gamma} + \frac{V^2}{2g} + z = H \quad 2·11$$

and, since energy cannot be created or destroyed, H is constant (neglecting losses). This equation is known as Bernoulli's theorem. The various forms of head may vary in magnitude at different sections but, neglecting losses, their sum is always the same.

In actual passages, the head does not remain constant because of the friction and turbulence losses. Hence, the equation may be written:

$$H = \frac{P_a}{\gamma_a} + \frac{V_a^2}{2g} + z_a = \frac{P_b}{\gamma_b} + \frac{V_b^2}{2g} + z_b + \text{losses between } a \text{ and } b \quad 2·12$$

If the cross-sectional area of a horizontal pipe is increased gradually,

the velocity will be decreased. The total head H must remain the same, and since the potential head remains constant; as the pipe is horizontal, the pressure head is increased at the expense of the kinetic energy. Therefore, the velocity is decreased and the pressure increased.

2-9 Loss of Head. The loss of head in a passage may be due either to friction or to the turbulence occurring when the fluid passes an obstruction, sudden change of section, etc. These losses will now be considered briefly.

Friction Loss in Passage. Many formulas have been proposed and used to determine the loss of head due to friction of a fluid flowing through a passage. One of the most generally accepted of these is the Darcy equation:

$$\Delta H = f \frac{L}{d} \frac{V^2}{2g} \quad 2-13$$

where V is the average fluid velocity in feet per second

L is path length

d is the pipe diameter

f is an empirical coefficient dependent upon the Reynolds number

ΔH is the lost head in feet of fluid flowing.

The ratio L/d is dimensionless, so any consistent units may be used for L and d .

The value of f for a particular Reynolds number may be taken from Fig. 2-3. This diagram and the Darcy equation may be used for any fluid (liquid or gas) as the value of f depends only upon Reynolds number, N_R , which in turn may be found for any fluid, passage size, or velocity.

If the passage is not circular, or if it has an annular shape (i.e., if the flow takes place between two pipes one of which is inside the other), the hydraulic radius R_m may be used in place of d in calculating the Reynolds number and in the Darcy equation.

$$\text{Hydraulic radius} = R_m = \frac{\text{cross-sectional area}}{\text{wetted perimeter of cross section}} \quad 2-14$$

Since for a circular pipe

$$R_m = \frac{\pi}{4} d^2 \times \frac{1}{\pi d} = \frac{d}{4} \quad \text{or} \quad d = 4R_m$$

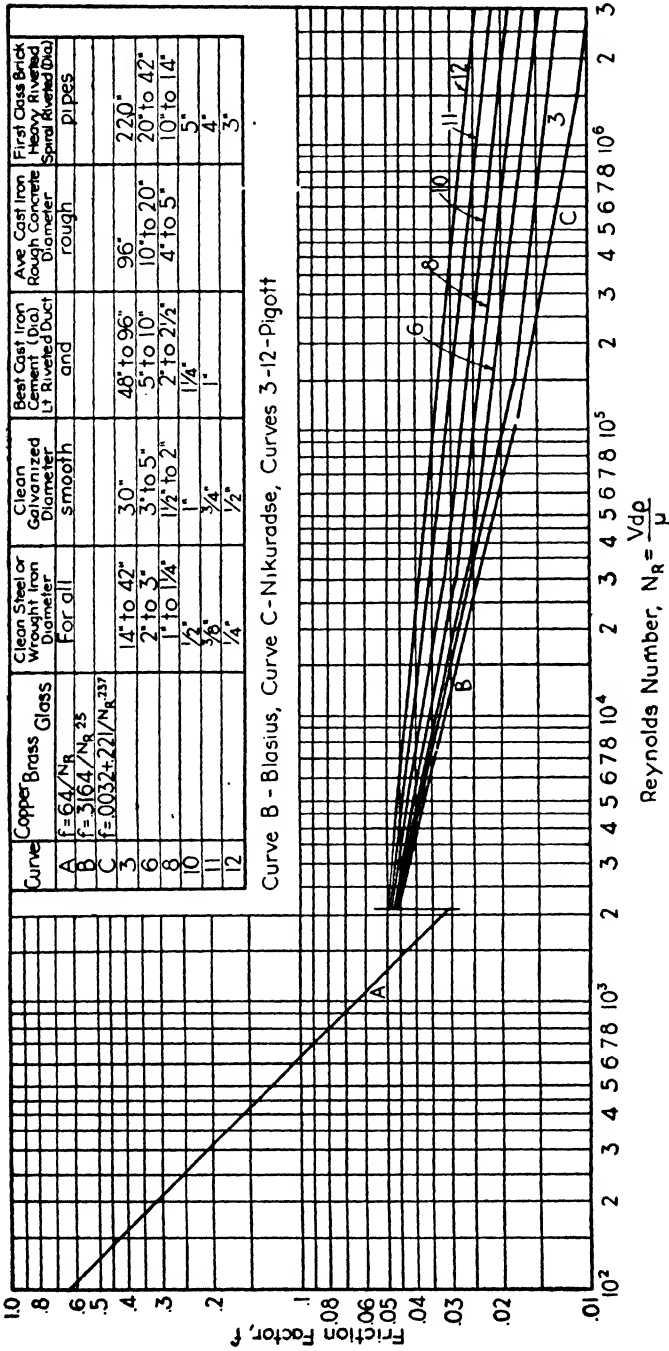


FIG. 2-3. Relation of friction factor, Reynolds number, and roughness for commercial pipes. (Reprinted by permission from *Fluid Mechanics*, by J. K. Vennard, John Wiley & Sons, Inc.)

the Reynolds number becomes

$$N_R = \frac{\gamma V 4R_m}{\mu g} \quad 2-15$$

and the Darcy equation is

$$\Delta H = f \frac{L}{4R_m} \frac{V^2}{2g} \quad 2-16$$

The results obtained by using the hydraulic radius are only approximate as the velocity distribution across the passage is different from that of a circular pipe. However, a good estimate of the losses may be obtained by its use.

If the passage area changes along its length or if it is made up of a series of passages, each may be dealt with separately and the pressure drops for each section added to find the total drop.

If several passages are arranged in parallel, the pressure drop across each must be the same. To find this resultant pressure drop of the system, the partial volume handled by each passage must be proportioned to make the pressure drop the same for all the passages.

Change of Section, Fittings, etc. Any sudden change in section is accompanied by disturbances and eddies, and results in a loss of head. If V_a represents the average velocity of the fluid before an enlarged section and V_b the velocity after the change, the lost head is given by

$$\Delta H = C_1 \frac{(V_a - V_b)^2}{2g}$$

At a sudden contraction in pipe size, the fluid is forced toward the axis and does not contact the walls just beyond the contraction. If the velocity before a reduced section is called V_a and the velocity of the fluid after contact has been reestablished in the reduced section V_b , the lost head is

$$\Delta H = C_2 \frac{(V_b - V_a)^2}{2g}$$

The lost head in various types of fittings may be given by

$$\Delta H = C_3 \frac{V^2}{2g}$$

where C_3 is a coefficient dependent on the type of fitting. Extensive lists of values of these coefficients for many types of fittings may be found in textbooks on hydraulics.

The important fact to observe is that in all cases the losses are

proportional to the velocity squared, so that, at any point of this nature, the velocity should be kept as low as possible in order to minimize the losses.

2-10 External Head Required of Pump or Blower. Before a pump or blower may be designed it is necessary to find the external head against which it is to operate. This may be determined by adding the friction and turbulence losses occurring in the pipe line to the total increase in elevation or pressure head acquired by the fluid, or referring to Fig. 2-4,

$$H = \Delta H_{f_{AS}} + \Delta H_{f_{DB}} + \Delta H_{T_{AS}} + \Delta H_{T_{DB}} + z_{TOT} \quad 2-17$$

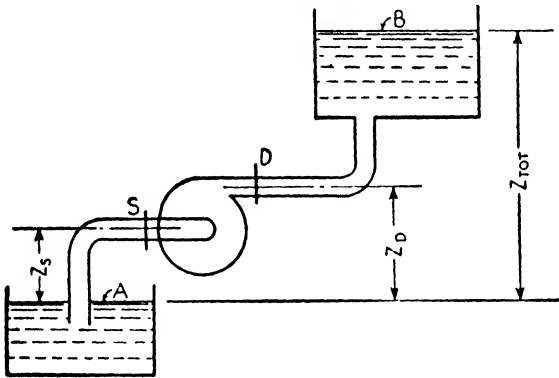


FIG. 2-4. Head on a pump.

The losses due to turbulence, $\Delta H_{T_{AS}}$ and $\Delta H_{T_{DB}}$, include the losses at the pipe entrance and exit, fittings and bends. Since these losses are difficult to evaluate they are frequently included with the friction losses, $\Delta H_{f_{AS}}$ and $\Delta H_{f_{DB}}$. However, since the latter may be approximated by the Darcy equation, the losses are listed separately above.

Additional losses will occur in the pump or blower itself, i.e., from S to D , but they will be cared for in its design and do not affect the external head required. Hence, the head developed by the pump or blower must be the difference between the total head at the center of the discharge flange and that at the center of the suction flange. Referring again to Fig. 2-4,

$$H = z_D - z_S + \frac{P_D}{\gamma_D} - \frac{P_S}{\gamma_S} + \frac{V_D^2}{2g} - \frac{V_S^2}{2g} \quad 2-18$$

To illustrate the method of calculating the total head of a centrifugal pump and the use of the Darcy equation, consider the following data (refer to Fig. 2-4): water temperature = 60°F. , $z_{TOT} = 65 \text{ ft.}$, flow of

water = 1500 g.p.m., diameter of suction line = 8 in., diameter of discharge line = 6 in., length of suction line = 10 ft., length of discharge line = 70 ft., turbulence loss in suction line = 0.3 ft., turbulence loss in discharge line = 0.6 ft., and pipe roughness corresponds to "best cast iron." Determine the total head which must be delivered by the pump.

$$\text{Area of the suction line, } A_S = \frac{\pi}{4} d_S^2 = \frac{\pi}{4} 8^2 = 50.27 \text{ sq. in.}$$

$$\text{Area of the discharge line, } A_D = \frac{\pi}{4} d_D^2 = \frac{\pi}{4} 6^2 = 28.27 \text{ sq. in.}$$

$$\begin{aligned} \text{Velocity in the suction line, } V_S &= \frac{\text{g.p.m.} \times 0.1337^* \times 144}{60 \times A_S} \\ &= \frac{1500 \times 0.1337 \times 144}{60 \times 50.27} = 9.56 \text{ ft. per sec.} \end{aligned}$$

$$\begin{aligned} \text{Velocity in the discharge line, } V_D &= \frac{\text{g.p.m.} \times 0.1337 \times 144}{60 \times A_D} \\ &= \frac{1500 \times 0.1337 \times 144}{60 \times 28.27} = 17.0 \text{ ft. per sec.} \end{aligned}$$

Absolute viscosity of water at 60° F., $\mu = 23.89 (10)^{-6}$ slugs per ft.-sec. (Section 2.4)

Specific weight of water at 60° F., $\gamma = 62.34$ lb. per cu. ft. (Section 2.4)

Reynolds number for the suction line,

$$N_{RS} = \frac{\gamma V_S d_S}{\mu g} = \frac{62.34 \times 9.56 \times \frac{8}{12}}{23.89 (10)^{-6} \times 32.2} = 5.16 (10)^6$$

Reynolds number for the discharge line,

$$N_{RD} = \frac{\gamma V_D d_D}{\mu g} = \frac{62.34 \times 17.0 \times \frac{6}{12}}{23.89 (10)^{-6} \times 32.2} = 6.88 (10)^6$$

From curve 6 of Fig. 2-3, the friction factor corresponding to a Reynolds number of $5.16 (10)^6$ is 0.018, which applies to the suction line.

Lost friction head in suction line,

$$\Delta H_{fAS} = f \frac{L_S V_S^2}{d_S 2g} = 0.018 \frac{10}{\frac{8}{12}} \frac{9.56^2}{2 \times 32.2} = 0.383 \text{ ft., say } 0.4 \text{ ft.}$$

* U.S. gallon = 0.1337 cu. ft.

The friction factor corresponding to a Reynolds number of 6.88 (10)⁵ taken from curve 6 of Fig. 2-3 is 0.0175, which applies to the discharge line.

Lost friction head in discharge line,

$$\Delta H_{f_{DB}} = f \frac{L_D}{d_D} \frac{V_D^2}{2g} = 0.0175 \frac{70}{\frac{9}{12}} \frac{17.0^2}{2 \times 32.2} = 11.0 \text{ ft.}$$

The external head against which the pump must operate is given by Eq. 2-17:

$$H = \Delta H_{f_{AS}} + \Delta H_{f_{DB}} + \Delta H_{T_{AS}} + \Delta H_{T_{DB}} + z_{TOT}$$

$$H = 0.4 + 11.0 + 0.3 + 0.6 + 65.0 = 77.3 \text{ ft.}$$

2-11 Streamlines and Streamtubes. As an aid in analyzing the flow conditions for any particular machine two concepts, streamlines and streamtubes, are often employed.

A *streamline* is an imaginary line drawn through a fluid so that a tangent to it at any point gives the direction of the average velocity at that point.

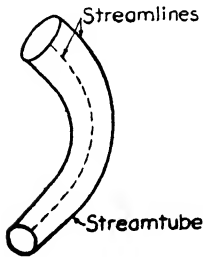


FIG. 2-5. Streamlines and streamtubes.

A *streamtube* is an imaginary closed canal or pipe bounded by streamlines. The cross section of the tube may be any closed curve, and is usually not constant in shape or area along the tube. The tube is so formed that the weight flow, or pounds of fluid per second, is the same at all sections of the tube; i.e., the continuity equation is satisfied. Since the weight flow is constant, if losses are neglected, the total energy at any point in the tube is also constant.

If the flow is laminar, the streamlines trace the actual path of a particle. When the flow is turbulent, they give only an approximation; i.e., they represent the time-average motion on which are superposed the turbulent motions. The latter are neglected in setting up the idealized flow pattern but are actually present at all usual velocities which are well above the critical. For either type of flow, the concepts are quite useful for design purposes.

2-12 Applications of Flow Principles. In order to illustrate the use of streamlines and streamtubes, a few cases of frictionless flow of liquids will be considered. It is important to bear in mind that the following discussion applies to incompressible liquids only; that is, it is based upon the assumption that the volume flow remains constant.

For gases, the specific weight depends upon the pressure and temperature existing at any section and the volume flow, therefore, varies with the pressure and temperature.

(a) *Straight-Line Flow.* Consider first straight-line flow in a rectangular channel. The streamlines will be parallel to the edges of the

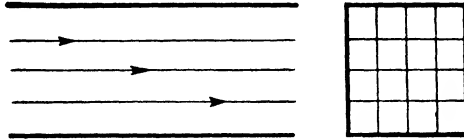


FIG. 2-6. Straight-line flow showing streamlines.

channel, since the total area and velocity remain constant. The streamtubes may be considered to have a rectangular section, and, if each is to carry the same weight flow, the bounding streamlines will be equally spaced, as shown in Fig. 2-6. As the flow is assumed to be frictionless, the velocity at all points of the section will be the same.

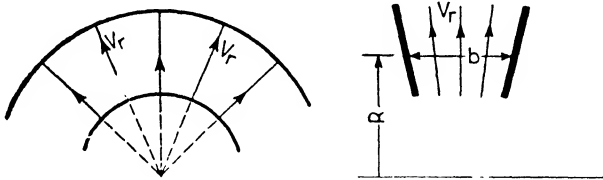


FIG. 2-7. Radial flow showing streamlines.

(b) *Radial Flow.* If the liquid flows radially between two uniformly diverging plates, the streamlines will appear as shown in Fig. 2-7. The streamtubes may be considered to have a rectangular cross section of area $2\pi Rb$, where R is any radius and b is the distance between the plates at this radius.

In order for the continuity equation to be satisfied,

$$Q = A V_r = 2\pi Rb V_r$$

where V_r is the radial velocity.

Since for any tube $Q/2\pi$ is constant,

$$bR V_r = C_1 \tag{2-19}$$

If the plates are parallel, b is also constant and Eq. 2-19 becomes

$$R V_r = C_2 \tag{2-20}$$

(c) *Rotary Flow.* If a fluid has pure rotation (no radial velocity component) and flows between two parallel or uniformly diverging

plates, the streamlines will be concentric circles (Fig. 2-8). The streamtubes may have a rectangular or trapezoidal cross section. In order to find the spacing between the bounding streamlines of the

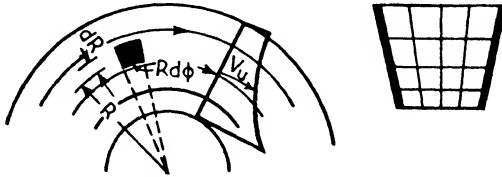


FIG. 2-8. Rotary flow showing streamlines.

streamtubes, a relationship between the tangential velocity V_u and the radius R must be determined. The centrifugal force acting on the liquid will produce a higher pressure at the periphery; this, according to Bernoulli's theorem, means a lower velocity. Consider a differential volume dV of liquid as shown in Fig. 2-8:

$$dV = bR d\phi dR$$

where b is the width perpendicular to the paper.

The centrifugal force dF on the element is

$$dF = dm \frac{V_u^2}{R} = \frac{\gamma b R d\phi dR}{g} \frac{V_u^2}{R}$$

The pressure increase in distance dR is

$$dP = \frac{dF}{dA} = \frac{\gamma b d\phi dR V_u^2}{g b R d\phi} = \frac{\gamma V_u^2 dR}{g R}$$

Note that in this step the term b drops out of the equation; therefore, the results obtained below apply to either parallel or diverging plates.

The total differential of Bernoulli's equation, assuming that the total head H and the elevation z are constant, is given by the expression

$$\frac{dP}{\gamma} + \frac{V_u dV_u}{g} = 0$$

Inserting in this the above equation for dP ,

$$\frac{\gamma V_u^2 dR}{g R \gamma} + \frac{V_u dV_u}{g} = 0$$

Multiplying both sides of the equation by g/V_u^2 ,

$$\frac{dR}{R} + \frac{dV_u}{V_u} = 0$$

Integrating between the limits a and b ,

$$\int_{R_a}^{R_b} \frac{dR}{R} = - \int_{V_{u_a}}^{V_{u_b}} \frac{dV_u}{V_u}$$

$$\log_e \frac{R_b}{R_a} = \log_e \frac{V_{u_a}}{V_{u_b}}$$

or

$$R_a V_{u_a} = R_b V_{u_b} = \text{constant} = C_3 \tag{2-21}$$

From this it may be seen that the velocity distribution will be a hyperbola across the flow, and the bounding streamlines will be farther apart at the rim where the velocity is lower and closer together nearer the center as shown in Fig. 2-8.

(d) *Spiral Flow.* If the radial flow (b) is superposed upon the rotary flow (c), as it is between the outlet of the impeller and the inlet of the diffuser, a spiral flow will result.

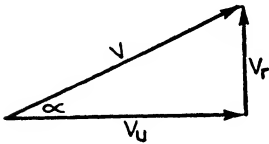


FIG. 2-9. Velocity triangle for spiral flow.

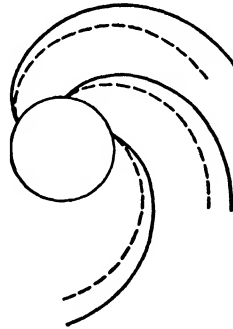


FIG. 2-10. Path of particle having spiral flow.

For *parallel* plates, it was shown that $V_r R = C_2$ (Eq. 2-20) and $V_u R = C_3$ (Eq. 2-21). Hence, the resultant velocity V (Fig. 2-9) will be inversely proportional to the radius R . The tangent of the direction of V is V_r/V_u , which will be constant for all radii. The spiral will make a constant angle α with a tangent, which is the property of a logarithmic spiral. From this, it may be noted that the flow of liquid leaving an impeller is that of a logarithmic spiral, as

shown by the solid lines of Fig. 2-10, if the sides of the passage are parallel.

If the sides of the passage diverge, Eq. 2-21 still holds true, but now $bRV_r = C_1$ (Eq. 2-19) defines the radial component. Hence, the tangential component V_u will still be inversely proportional to the radius, but the radial component V_r will decrease more rapidly. The spiral will no longer be logarithmic since the angle is no longer constant, the spiral now lying "inside" that of the logarithmic, as shown in Fig. 2-10 by the dash line. To determine the exact shape for a given case, a relationship between b and R must first be found. If the passage converges, the spiral will lie "outside" that of the logarithmic.

PROBLEMS

2-1 Using Helmholtz's equation, determine the viscosity of water in poises for a temperature of 60° F. and convert this into English units. If the density of water at this temperature is 1.00 gr. per cc. determine the kinematic viscosity in both sets of units.

Ans. See Section 2-4.

2-2 Using Grindley and Gibson's equation, determine the viscosity of air in poises for a temperature of 60° F. and convert this into English units. If the specific weight of air at this temperature is 0.0765 lb. per cu. ft. determine the kinematic viscosity in both sets of units.

Ans. See Section 2-4.

2-3 No. 6 fuel oil has a viscosity of 300 Saybolt-Furool seconds and a specific gravity of approximately 1. Determine the kinematic and absolute viscosity of the oil in English units.

Ans. $\nu = 708 (10)^{-5}$ ft.² per sec.; $\mu = 0.0137$ slug per ft.-sec.

2-4 Air having a specific weight of 0.063 lb. per cu. ft. and an absolute viscosity of $3.74 (10)^{-7}$ slug per ft.-sec. flows through a 12-in.-diameter pipe at the rate of 4000 lb. per hr. Determine the type of flow existing in the pipe.

Ans. $N_R = 117,000$. \therefore turbulent flow.

2-5 Find the pressure drop in pounds per square inch occurring in 225 ft. of 12-in. "best cast iron" pipe handling 4500 g.p.m. of 60° F. water. The absolute viscosity of the water is $2.389 (10)^{-5}$ slug per ft.-sec. (One gallon = 0.134 cu. ft.)

Ans. 4.22 lb. per sq. in.

2-6 At one point in a horizontal pipe line the pressure of water flowing at a velocity of 15 ft. per sec. is 17 lb. per sq. in. abs.; at another point close by, where the pipe has a smaller section, the pressure is 16 lb. per sq. in. abs. Neglecting losses find the velocity of flow at the latter point.

Ans. 19.4 ft. per sec.

2-7 A pump delivering 8 c.f.s. of water has a 12-in.-diameter suction flange and a 10-in.-diameter discharge flange. The suction pipe is 12 ft. long and the discharge pipe 75 ft. long. The water is delivered to a reservoir 53 ft. above the intake water level. Neglecting turbulence losses in the pipe, find the lead which the pump must deliver. Water temperature 60° F. Assume pipe is "best cast iron."

Ans. 58.45 ft.

2-8 A pump delivering 5000 g.p.m. of 60° F. water has a 16-in.-diameter suction pipe and a 14-in. discharge pipe. The suction vacuum gage, which is 3 in. below the pump centerline, reads 5 in. of mercury (below atmospheric pressure). The discharge gage, which is 18 in. above the pump centerline, reads 10.6 lb. per sq. in. ga. What is the head of the pump? The specific gravity of mercury is 13.6.

Ans. 32.58 ft.

2-9* It is desired to pump 1000 gal. per hr. of gasoline (specific gravity = 0.85) at a temperature of 50° F. (viscosity = 0.8 centipoises) from the bottom of a storage tank at ground level to the top of a fractionating column 90 ft. high. The total length of pipe (actual + equivalent length due to fittings) is 125 ft. The pipe line is 2-in. standard steel. Calculate the motor size (expressed in horsepower) needed, if the efficiency of the pump and drive is assumed to be 55 per cent. *Ans.* 0.59.

2-10* One thousand gallons of benzol are to be pumped per hour through a 1¼-in. standard steel pipe (1.38 in. inside diameter) to the top of a reaction tower. The equivalent length of the line, including pump, is 1000 ft. and the pipe outlet is 50 ft. above the level of the benzol in the supply tank. The temperature is 70° F., the specific gravity of the benzol is 0.88, and the viscosity 0.65 centipoise at this temperature. The pump is a direct-connected electrical centrifugal, with an overall efficiency of 40 per cent. Calculate the electrical input to the motor.

Ans. 0.67 kw.

2-11* Water is pumped from a reservoir to a tank with a lift of 20.0 ft. The suction pipe, which connects the reservoir to the pump, is 12 in. in diameter and 25 ft. long. The discharge pipe, which connects the pump to the tank is 10 in. in diameter and 450 ft. long. Both pipes may be classified as clean, smooth, cast iron pipes. The suction pipe projects into the reservoir and the discharge pipe projects into the tank. The efficiency of the pump is 60 per cent. Considering all losses, calculate the horsepower required to operate the pump to discharge 3 c.f.s. into the tank.

Ans. 14.1.

2-12* It is required to pump 500,000 gallons per day (continuous operation) of an oil having a specific gravity of 0.92 and viscosity of 250 Saybolt Universal seconds through a 6-in.-diameter wrought iron pipe. What pump pressure (in pounds per square inch) must be provided per 1000 ft. of pipe?

Ans. 8.32 lb. per sq. in.

* Taken from New York State examinations for Professional Engineers.

CHAPTER 3

BASIC THEORY OF PUMPS AND BLOWERS

3.1 Velocity Diagrams. The path and velocity of a fluid particle flowing through an impeller would appear to be quite different to an observer standing on the ground, than it would to one stationed inside the rotating impeller, if that were possible. The velocity of the particle relative to the ground is called absolute; the velocity relative to the impeller is called relative. It is important to understand thoroughly these two types of velocities and the relationships between them.

In order to illustrate these relationships, a simple example will be considered. The crane shown in Fig. 3-1 moves along its track at a velocity u of 4 ft. per sec., hence, after 1 sec. it will be 4 ft. from its

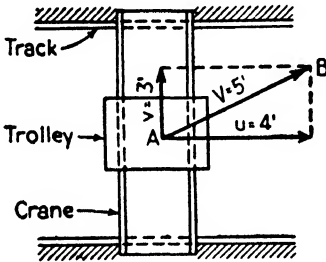


FIG. 3-1. Crane movement illustrating absolute and relative velocities.

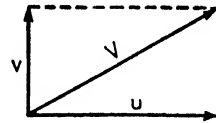


FIG. 3-2. Absolute and relative velocities.

starting point relative to the ground. At the same time, the trolley moves with a velocity v of 3 ft. per sec. on its track across the crane, so that relative to the crane it will have traveled 3 ft. after 1 sec. Relative to the ground, the trolley will have traveled from A to B in this second, a distance of 5 ft. A person following the trolley from the ground would travel in the direction AB with a velocity V of 5 ft. per sec. Hence, the absolute velocity V of the trolley is the vector sum of the absolute velocity u of the crane plus the relative velocity v of the trolley to the crane as shown in Fig. 3-2.

For a fluid flowing through a rotating impeller, u is the velocity of a point on the impeller relative to the ground, V is the absolute velocity of a fluid particle flowing through the impeller relative to the ground, and v is the velocity of a fluid particle relative to the impeller.

The relationship shown for the crane and trolley applies to this case at any point in the impeller. Assuming that the flow takes place in a plane, i.e., that it is two-dimensional, and that the fluid follows the impeller vanes exactly, the inlet and outlet triangles of velocities for an impeller having backward curved vanes are shown in Fig. 3-3.

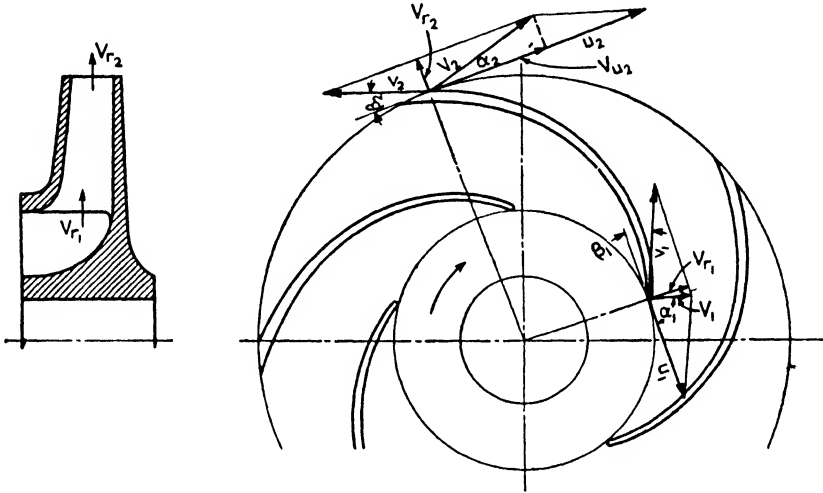


FIG. 3-3. Inlet and outlet velocity diagrams of an impeller having backward-curved vanes.

The angle between V and u is called α ; the angle between v and u extended (or negative u) is β and it is the angle made by a tangent to the impeller vane and a line in the direction of motion of the vane. These angles are shown on the figure as well as V_r , which is the radial component of the absolute velocity V .

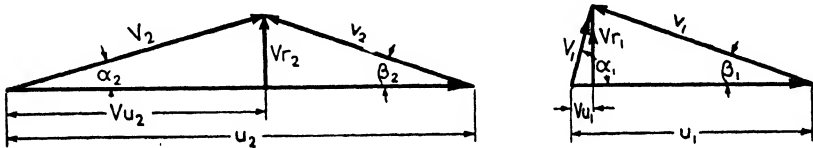


FIG. 3-4. Virtual inlet and outlet velocity diagrams of the impeller of Fig. 3-3.

The velocity symbols used in this book follow the American system. However, many authors use the German system of notation wherein the absolute velocity is designated as C rather than V , and the relative velocity as W rather than v .

Figure 3-4 shows the simplified inlet and outlet diagrams of these

velocities for the impeller shown in Fig. 3-3. Note that V_u is the tangential component of V and equals $V \cos \alpha$.

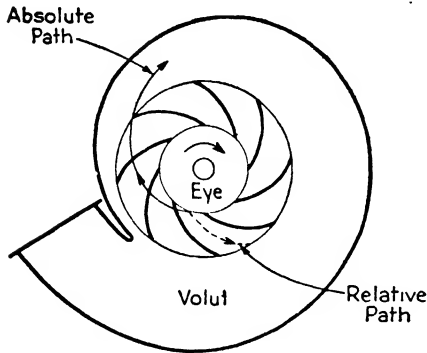


FIG. 3-5. Relative and absolute paths of motion of fluid particle passing through impeller.

In order to illustrate better the difference between the absolute and relative velocities, Fig. 3-5 shows an impeller on which the two paths of the same particle passing through the rotating impeller are shown. The dashed line represents the path of the particle relative to the impeller, and it is seen to follow the vanes as if the impeller were not rotating. The solid line represents the path of the particle relative to the ground and is quite different because of the impeller rotation as just explained.

3-2 Ideal Head Equation. The equation which forms the basis of pump and blower design is based upon three assumptions, none of which is exactly true for actual units. These assumptions are: (1) the fluid leaves the impeller passages tangentially to the vane surfaces, or there is complete guidance of the fluid at the outlet; (2) the impeller passages are completely filled with actively flowing fluid at all times; and (3) the velocities of the fluid at similar points on all the flow lines are the same. The head which is based on these assumptions will be called the "virtual head" and designated by $H_{vir.\infty}$, where the subscript ∞ signifies an infinite number of vanes or perfect guidance of the fluid. The deviation of actual conditions from these assumptions will be considered in later sections.

If a closed container filled with liquid as shown in Fig. 3-6 is rotated at constant speed about its axis, the motion is transmitted to the fluid by its viscosity until the angular velocity ω of the fluid in radians per second is the same as that of the container.

To determine the pressure distribution within the fluid, consider a very small fluid element having a width b , thickness dR , and circumferential length $R d\phi$ rotating with an angular velocity ω . The centrifugal force acting on the particle is

$$dF = dm R\omega^2$$

where the differential mass

$$dm = \frac{\gamma}{g} bR d\phi dR$$

or

$$dF = \frac{\gamma}{g} bR^2\omega^2 d\phi dR$$

This centrifugal force will impart a pressure increase between R and $R + dR$ of

$$dP = \frac{dF}{dA} = \frac{\gamma bR^2\omega^2 d\phi dR}{g bR d\phi} = \frac{\gamma}{g} R\omega^2 dR$$

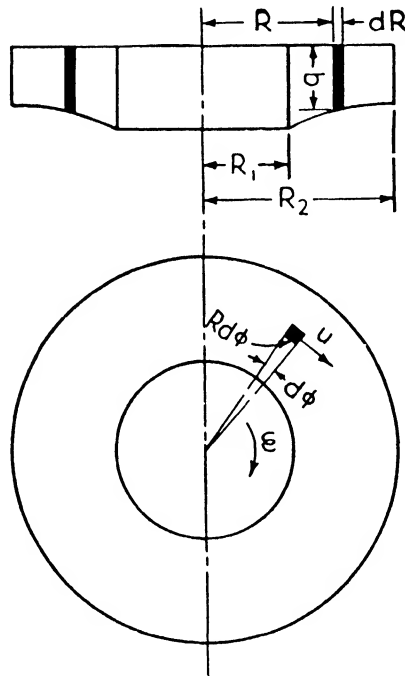


FIG. 3-6. Rotating container filled with liquid.

Integrating between the radii R_1 and R_2 the total pressure rise is

$$P_2 - P_1 = \frac{\gamma}{g} \omega^2 \left(\frac{R_2^2 - R_1^2}{2} \right)$$

or, since $R^2\omega^2 = u^2$

$$P_2 - P_1 = \frac{\gamma}{g} \frac{u_2^2 - u_1^2}{2}$$

As the head in feet of fluid equals P/γ ,

$$H_2 - H_1 = \frac{u_2^2 - u_1^2}{2g} \quad 3.1$$

If turbulence and friction are neglected, the work put into the impeller will equal the total energy of the fluid at the outlet minus the total energy at the inlet. This work may be expressed as head in feet of fluid and is the total virtual head $H_{\text{vir.}\infty}$.

The head is made up of pressure energy $H_{p\infty}$ (as measured by a pressure gage) and of velocity energy or velocity head, so that

$$H_{\text{vir.}\infty} = H_{p\infty} + \frac{V_2^2 - V_1^2}{2g} \quad 3.2$$

The static pressure increase given to the fluid by the impeller consists of the head created by the centrifugal force of the rotating fluid which, according to Eq. 3.1, equals $\frac{u_2^2 - u_1^2}{2g}$, plus the head due to the difference in the relative velocities through the impeller. Hence, the pressure head at the outlet will be increased by the velocity head, $\frac{v_1^2 - v_2^2}{2g}$, and the total static head at the impeller outlet will amount to

$$H_{p\infty} = \frac{u_2^2 - u_1^2 + v_1^2 - v_2^2}{2g}$$

To this pressure energy must be added the increase in absolute velocity energy, $\frac{V_2^2 - V_1^2}{2g}$; hence the total energy increase expressed in head of fluid is

$$H_{\text{vir.}\infty} = \frac{u_2^2 - u_1^2 + v_1^2 - v_2^2 + V_2^2 - V_1^2}{2g} \quad 3.3$$

Referring to the velocity diagrams of Fig. 3.4, v_1 and v_2 can be expressed as functions of u , V and α . From the cosine rule of triangles,

$$\begin{aligned} v_1^2 &= u_1^2 + V_1^2 - 2u_1V_1 \cos \alpha_1 \\ v_2^2 &= u_2^2 + V_2^2 - 2u_2V_2 \cos \alpha_2 \end{aligned}$$

By inserting these values in Eq. 3.3, the theoretical head is

$$H_{\text{vir.}\infty} = \frac{1}{g} (u_2V_2 \cos \alpha_2 - u_1V_1 \cos \alpha_1) \quad 3.4$$

Since $V_{u_1} = V_1 \cos \alpha_1$ and $V_{u_2} = V_2 \cos \alpha_2$, the equation becomes

$$H_{\text{vir.}\infty} = \frac{1}{g} (u_2 V_{u_2} - u_1 V_{u_1}) \quad 3.5$$

Equations 3-3, 3-4, and 3-5 form the basis for the calculation of centrifugal pumps and blowers. It may be noted that they do not contain the specific weight of the medium handled. An impeller operating at a given speed will develop the same head for any medium handled, as the head is expressed in feet of that particular medium.

The virtual horsepower given to the fluid by the impeller is equal to $wH_{\text{vir.}\infty}/550$ which, from Eq. 3-5, equals

$$\text{hp}_{\text{vir.}\infty} = \frac{w}{550g} (u_2 V_{u_2} - u_1 V_{u_1}) \quad 3.6$$

where w is the fluid flow in pounds per second.

3.3 Ideal Torque and Horsepower Equations. A clearer understanding of these equations may be obtained by using the principles of momentum. Momentum is the product of mass and velocity, or mV . The rate of change of momentum with respect to time is a force. Since w is a rate of flow (pounds per second), wV/g is a rate of change of momentum with respect to time, or a force. The tangential component of this force is $(w/g)V_u$. At the inlet $(w/g)V_{u_1}$ represents the force exerted by the fluid on the impeller. At the outlet $(w/g)V_{u_2}$ is a force exerted by the impeller on the fluid. The product of force and radius equals torque. Hence, the net torque exerted by the impeller on the fluid will be

$$T = \frac{w}{g} (R_2 V_{u_2} - R_1 V_{u_1})$$

$$\text{The horsepower input} = \frac{\omega T}{550} = \frac{\omega w}{550g} (R_2 V_{u_2} - R_1 V_{u_1})$$

or, since $\omega = \frac{u}{R}$,

$$\text{hp}_{\text{vir.}\infty} = \frac{w}{550g} (u_2 V_{u_2} - u_1 V_{u_1}) \quad 3.6$$

3.4 Incompleteness of the Ideal Equations. The basic equations just developed are founded upon certain ideal assumptions, namely, frictionless, non-turbulent flow in a plane and complete guidance of the fluid. The actual head developed will be less, and the power consumed may be greater under actual conditions.

These differences will be considered in subsequent sections, but it should be borne in mind that it is not possible to evaluate the exact extent of each of them accurately. Overall coefficients based on test results of previously built pumps and blowers are usually used to evaluate these discrepancies in actual design. These coefficients and efficiencies will be discussed later after the factors upon which they depend have been considered.

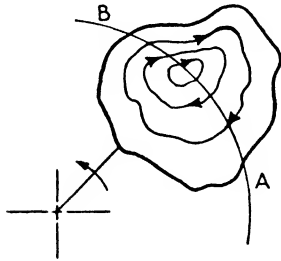


FIG. 3-7. Circulatory flow in a container.

3-5 Circulatory Flow. If a closed container is filled with fluid and rotated about an axis outside itself (Fig. 3-7) the fluid, because of its inertia, will tend to rotate in the opposite direction relative to the container. Thus, if water is placed in a tumbler or pan and the vessel is moved in circles so that one point on it is always nearest the axis

of rotation, it may be observed that the water tends to rotate or circulate in a direction opposite to the direction of rotation of the container, i.e., the fluid tends to remain stationary relative to the ground.

It is apparent that the fluid in contact with the side *A* of the container is at a higher pressure than that at *B*, as the container is exerting a pressure on the fluid on that side while it is being accelerated. As the total head of the fluid along the ring *AB* is approximately constant, the velocity at *B* will be higher than at *A* according to Bernoulli's theorem. This means that the streamlines bounding the streamtubes will be closer together on the *B* side than on the *A* side.

The amount of circulatory flow will depend upon the shape of the container; it will be less if it is long and narrow than if it has a circular section.

In a rotating impeller two flows take place simultaneously, namely, the flow of fluid through the passage plus the circulatory flow. The latter is relatively small and merely modifies the former, the resultant flow being indicated in Fig. 3-8. The resultant effect for a given flow is to cause the fluid to leave the wheel at an angle less than the vane angle (i.e., decrease β_2) and to increase the absolute angle α_2 at which the fluid leaves the wheel.

Since the outlet area A_2 and the flow Q in cubic feet per minute remain the same, the average radial component V_{r_2} remains unchanged. The effect of the circulatory flow on the outlet diagram is shown in solid lines in Fig. 3-9(a); the virtual diagram is dotted.

The effect on the inlet diagram would be to make β_1 larger, as shown in Fig. 3-9(b), the virtual diagram being dotted again. The effect

on the inlet diagram is much less since the vanes are quite close together here.

The exact amount of circulatory flow depends upon the shape of the passage. For a given impeller more vanes make the passage narrower,

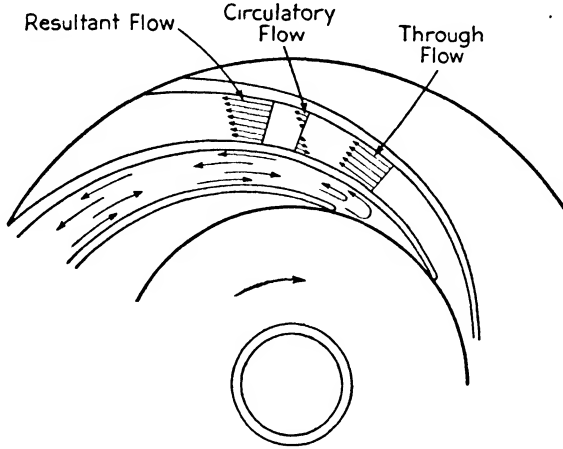


FIG. 3-8. Circulatory, through, and resultant flows in vane passage.

giving greater guidance to the fluid and reducing the circulatory flow effect. The amount of circulatory flow is best determined from test results and experiments. Attempts have been made to set up formulas to calculate it, but they are rather unreliable, particularly for impellers having a small number of vanes.

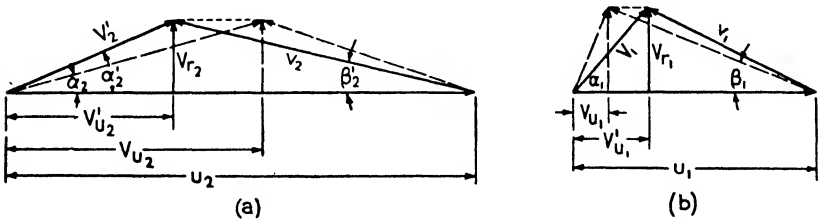


FIG. 3-9. Inlet and outlet velocity diagrams with circulatory flow correction.

3-6 Friction. The method of determining the loss of head due to friction outlined in Section 2-9 could be applied to a given pump or blower by considering it to be a series of short passages and finding the loss in each for a given flow. This procedure is too laborious to be practical and is seldom used.

The loss increases approximately as the square of the velocity. Since the areas remain constant, the velocity is proportional to the

flow and the loss increases approximately with the square of the flow.

The loss also increases with the "wetted areas" of the passages, hence they should be kept small. It increases too with the roughness of the surfaces of the impeller, diffuser or volute, and casing passages. They should, therefore, be made as smooth as practical.

3-7 Turbulence. The type of flow existing in a pump or blower is always turbulent, as shown in the definitions outlined in Section 2-3, i.e., the Reynolds number is always well above the critical value given there. At certain sections in the machine, such as at the inlet and outlet edge of the vanes in both the impeller and diffuser, in the return guide vanes, etc., the flow is seriously disturbed with a resultant loss of head. In this text, these losses are known as turbulence or shock losses. As noted in Section 2-9 the amount of the loss is proportional to the velocity squared, but the coefficient applicable to any particular case is quite difficult to determine.

A pump or blower is designed for a given flow and speed at which it is expected to operate most of the time. The angles of the impeller and diffuser vanes are designed for these conditions. When operating at other flows or speeds (unless the ratio of flow to revolutions per minute is the same as at the design condition), these angles will not be correct and the turbulence losses will increase. Obviously, sudden changes of section or sharp turns should be avoided or minimized as much as possible.

3-8 Disk Friction. The power required to rotate a disk in a fluid is known as the disk friction. The usual impeller has enclosed sides which rotate in the fluid and the power required for this rotation must be supplied by the driver. This power is transformed into heat and may appreciably increase the temperature of the fluid.

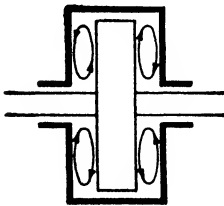


FIG. 3-10. Pumping action due to disk friction.

The disk friction loss is due to two actions which occur simultaneously, namely, (1) the actual friction of the fluid on the disk, which is relatively minor, and (2), a pumping action. The fluid which is in contact with the disk or near it is thrown outward by the centrifugal action

and circulates back toward the shaft to be pumped again as shown in Fig. 3-10.

The energy consumed by the disk friction depends upon the mass of fluid coming into contact with the disk per unit of time and the kinetic energy which the fluid receives. The mass of fluid is proportional to the disk area (D_2^2), the specific weight of the fluid, and the

peripheral speed of the disk u_2 . The kinetic energy varies with the speed squared or u_2^2 . Hence, the horsepower will be proportional to the product of these three factors and a coefficient or

$$\text{Disk friction horsepower} = c_1 D_2^2 u_2^3 \gamma \quad 3-7$$

Since the speed u_2 varies directly with the diameter and the revolutions per minute, Eq. 3-7 may be written

$$\text{Disk friction horsepower} = c_2 D_2^5 n^3 \gamma \quad 3-8$$

Equations 3-7 and 3-8 give the general form of the disk friction equation. Various formulas have been found experimentally for liquids and gases. They are given in Sections 6-14 and 13-15.

It may be noted from Eq. 3-8 that, for a given peripheral speed u_2 , less loss occurs with a small-diameter impeller operating at a high r.p.m. than for a large one operating at a low r.p.m.

The pumping action appears to be reduced with a smaller axial clearance between the disk and casing. The loss is increased with rougher surfaces of the impeller, since it aids the pumping action and also increases the direct friction loss. Hence, the impeller should be as smooth as possible. However, it is doubtful if much is gained by giving it a high polish.

3-9 Leakage. After the fluid has been compressed, it should be prevented from leaking back to its initial condition. This is usually accomplished by using close-clearance labyrinth sealing or wearing rings. There are many types of these rings. Their relative efficiencies and methods of calculating the leakage flow are discussed later for liquids and gases separately.

The leakage has no effect on the head of the pump or blower but it lowers the capacity and increases the brake horsepower required.

3-10 Mechanical Losses. The term mechanical losses includes the frictional losses in the bearings and packing boxes.

It is difficult to predict these losses exactly, but they are usually taken to be 2 to 4 per cent of the brake horsepower, the larger figure being used for the smaller units. They are very nearly constant for a given speed of rotation.

3-11 Prerotation of the Fluid. The usual assumption made in designing is that the fluid enters the impeller vanes radially, so that $\alpha_1 = 90^\circ$. As the fluid approaches the vane inlet, it comes into contact with the rotating shaft and impeller; this tends to cause it to rotate with the wheel. This makes β_1 larger as shown by the solid lines in Fig. 3-11. Prerotation reduces the virtual head, as may be seen from Eq. 3-5, since V_{u_1} is increased. Although this effect is small

in a conventional radial-type impeller, it must be considered when designing by increasing the vane angle β_1 an appropriate amount.

Occasionally, guide vanes are placed at the inlet to insure radial flow, but in most cases this is considered unnecessary. Also, the attendant friction and turbulence losses due to these vanes may overbalance the advantages obtained.

It should be noted that if α_1 equals 90° , i.e., if V_1 is radial, V_{u_1} equals zero, and Eqs. 3-5 and 3-6 become

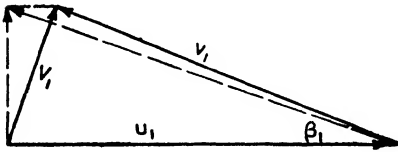


FIG. 3-11. Effect of prerotation on the inlet diagram.

$$H_{\text{vir.}\infty} = \frac{1}{g} u_2 V_u \quad 3-9$$

$$\text{hp}_{\text{vir.}\infty} = \frac{w}{550g} u_2 V_{u_2} \quad 3-10$$

3-12 Coefficients and Efficiencies. The head developed by a pump or blower is less than that given by Eq. 3-5 owing to the losses and circulatory flow discussed in the preceding sections. In designing, these losses are difficult to predict and are usually estimated by coefficients and efficiencies based upon tests and experience. These factors will now be considered.

(a) *Circulatory Flow.* Equation 3-5, which is $H_{\text{vir.}\infty} = (1/g)(u_2 V_{u_2} - u_1 V_{u_1})$, is the virtual head developed when the impeller is considered to have an infinite number of vanes so that no circulatory flow exists. The effect of the circulatory flow is to reduce V_2 as discussed in Section 3-5 and shown in Fig. 3-9. This reduces the virtual head which the impeller is able to develop. As noted in Section 3-5, the circulatory flow also reduces β_2 and increases α_2 . If V'_{u_2} is the tangential component of V_2 based upon a finite number of vanes, and V_{u_2} the tangential component neglecting circulatory flow, then the circulatory flow coefficient is

$$\eta_\infty = \frac{V'_{u_2}}{V_{u_2}} \quad 3-11$$

As stated previously in Section 3-5, attempts have been made to find the relation between η_∞ , the number of vanes, and the outlet vane angle. Because they do not seem to be very reliable, recourse must be made to tests and experience for values of the circulatory flow coefficient. A method for calculating this coefficient from tests is given in part (g) of this section.

The diffuser inlet angle α_2 is based upon the actual absolute outlet angle at which the fluid leaves the impeller after applying the coefficient η_∞ .

If the inlet flow is radial, the head equation for an infinite number of vanes is $H_{\text{vir.}\infty} = \frac{u_2 V u_2}{g}$, hence the virtual head with a finite number of vanes must be

$$H_{\text{vir.}} = \frac{u_2 \eta_{\infty} V u_2}{g} = \eta_{\infty} H_{\text{vir.}\infty} \quad 3.12$$

It should be observed particularly that the reduction in head from $H_{\text{vir.}\infty}$ to $H_{\text{vir.}}$ does not represent a loss but simply accounts for the circulatory flow phenomenon which is not included in the ideal assumptions.

(b) *Hydraulic Efficiency.* The actual head H developed by the unit is less than the virtual head $H_{\text{vir.}}$ given by Eq. 3.12 owing mainly to the friction and turbulence losses discussed in Sections 3.6 and 3.7. The ratio of the actual head developed to the virtual head for a finite number of vanes is the hydraulic efficiency,

$$\eta_{HY} = \frac{\text{actual measured head}}{\text{head imparted to fluid by impeller}} = \frac{H}{H_{\text{vir.}}} \quad 3.13$$

or

$$H = \eta_{HY} H_{\text{vir.}} = \eta_{\infty} \eta_{HY} H_{\text{vir.}\infty} = \frac{u_2 V u_2 \eta_{\infty} \eta_{HY}}{g} \quad 3.14$$

(c) *Factor K.* The product $\eta_{\infty} \eta_{HY}$ may be designated as K so that

$$H = K \frac{u_2 V u_2}{g} = K H_{\text{vir.}\infty} \quad 3.15$$

When the dimensions and speed of the impeller are known, the value of K may be calculated from tests by the use of Eq. 3.15 and the virtual outlet diagram.

(d) *Overall Head Coefficient, Φ .* In deriving Eq. 3.1 it was shown that the pressure head developed by a body of fluid rotating in a closed cylinder is given by

$$H = \frac{u_2^2}{2g} \quad \text{or} \quad u_2 = \sqrt{2gH}$$

Owing to the shape of the vanes and the casing this value is not quite obtained when there is no flow of fluid through the machine. For actual shut-off conditions a factor Φ' may be introduced into the equation:

$$u_2 = \Phi' \sqrt{2gH} \quad 3.16$$

and it will be found by tests that Φ' will be close to unity.

The same equation may be used where H is the head corresponding to the point of best efficiency (design point) and Φ is the corresponding coefficient. If the Φ value is established the equation may be used to determine the required outside impeller diameter since

$$u_2 = \frac{\pi D_2 n}{12 \times 60} = \Phi \sqrt{2g\sqrt{H}}$$

or

$$D_2 = \frac{720}{\pi} \sqrt{2g} \frac{\Phi \sqrt{H}}{n} = \frac{1840\Phi \sqrt{H}}{n} \quad 3.17$$

It should be noted that this coefficient, since it is based upon the total head as measured on test, includes all the losses which occur in the machine. Therefore, the outlet diameter D_2 as found by Eq. 3.17 will be large enough to take care of these losses and still deliver the required head.

(e) *Volumetric Efficiency.* The volumetric efficiency η_v is a measure of the amount of leakage.

$$\eta_v = \frac{\text{delivered weight}}{\text{delivered weight} + \text{internal leakage}} = \frac{w}{w + w_L} \quad 3.18$$

where w_L is the weight of fluid leakage in pounds per second.

(f) *Fluid Horsepower and Overall Efficiency.* The fluid horsepower of a unit is the product of the delivered weight flow in pounds per second w times the actual head H in feet developed by the unit (total head at discharge flange minus the total head at suction flange) divided by 550 or

$$\text{Fluid horsepower} = \frac{w \times H}{550} \quad 3.19$$

Thus, it is the actual useful horsepower output delivered by the unit.

The ratio of the fluid horsepower output to the brake horsepower input of the driver is the overall efficiency of the unit, η .

$$\text{Overall efficiency, } \eta = \frac{\text{fluid horsepower output}}{\text{brake horsepower input}} \quad 3.20$$

The brake horsepower represents the actual horsepower delivered to the pump or blower by the prime mover. This delivered horsepower is used up in the machine in fluid horsepower, leakage, disk friction, hydraulic losses (friction and turbulence), and mechanical losses.

(g) *Relationships Between Various Efficiencies and Coefficients.* As

just noted,

$$\text{b.hp.} = \text{f.hp.} + \text{hp.}_L + \text{hp.}_{DF} + \text{hp.}_{HY} + \text{hp.}_M \quad 3-21$$

where b.hp. = brake horsepower

f.hp. = fluid horsepower

hp._L = horsepower required to overcome leakage

hp._{DF} = horsepower required to overcome disk friction

hp._{HY} = horsepower required to overcome hydraulic losses

hp._M = horsepower required to overcome mechanical losses.

The total energy imparted to the fluid by the impeller is the product of the total weight of fluid handled (delivered plus leakage weights) times the virtual head $H_{\text{vir.}}$, and the horsepower is $\text{hp.} = \frac{(w + w_L)H_{\text{vir.}}}{550}$.

As $\eta_{HY} = \frac{H}{H_{\text{vir.}}}$, this may be written $\text{hp.} = \frac{(w + w_L)H}{550\eta_{HY}}$; it equals the sum of f.hp. + hp._L + hp._{HY}. Then

$$\text{b.hp.} = \frac{(w + w_L)H}{550\eta_{HY}} + \text{hp.}_{DF} + \text{hp.}_M \quad 3-22$$

or

$$\eta_{HY} = \frac{\frac{(w + w_L)H}{550}}{\text{b.hp.} - \text{hp.}_{DF} - \text{hp.}_M} \quad 3-23$$

Equation 3-23 may be used to determine η_{HY} from test results if the disk friction horsepower, mechanical loss horsepower, and the leakage can be estimated fairly accurately. Then from the relation $K = \eta_\infty \eta_{HY}$ the circulatory flow coefficient η_∞ can also be calculated.

(h) *Mechanical Efficiency.* This is the ratio of the power delivered by the impeller to the fluid to the brake horsepower supplied to the pump or blower shaft, i.e.,

$$\eta_M = \frac{\frac{(w + w_L)H_{\text{vir.}}}{550}}{\text{b.hp.}} \quad 3-24$$

This may also be written:

$$\eta_M = \frac{\text{b.hp.} - \text{hp.}_{DF} - \text{hp.}_M}{\text{b.hp.}} \quad 3-25$$

From the foregoing equations it may be seen that

$$\eta = \eta_M \times \eta_{HY} \times \eta_V \quad 3-26$$

as

$$\eta = \frac{\text{f.hp.}}{\text{b.hp.}} = \frac{(w + w_L)H_{\text{vir.}}}{550} \times \frac{H}{H_{\text{vir.}}} \times \frac{w}{w + w_L} = \frac{wH}{550 \text{ b.hp.}}$$

3-13 Performance Curves. The customary method of testing a pump or blower is to run it at constant speed and vary the flow by throttling the discharge. The characteristic curve which shows the performance of the unit, under these conditions, is a curve of head, pressure rise, or discharge pressure plotted against the flow in cubic feet per minute of gas at specified conditions or gallons per minute of liquid. In addition to this curve, it is customary to plot curves of overall efficiency and brake horsepower against the flow. These three curves, shown in Figs. 10-6 and 17-3, describe the performance of the unit and may be used for comparison. The change in these curves due to variations in operating conditions are discussed in Chapters 5 and 12.

3-14 Virtual Head-Capacity Curve. If it is assumed that the inlet flow is radial so that V_{u_1} is zero, the virtual head for an infinite number of vanes is given by Eq. 3-9:

$$H_{\text{vir.}\infty} = \frac{1}{g} u_2 V_u$$

and it is possible to draw some interesting conclusions from it regarding the head-capacity curve.

For a constant speed of rotation, the wheel tip speed u_2 is constant. From Fig. 3-9(a) it may be seen that $V_{u_2} = u_2 - \frac{V_{r_2}}{\tan \beta_2}$ where V_{r_2} is the radial component of V_2 and β_2 is the outlet vane angle. Hence, Eq. 3-9 may be written

$$H_{\text{vir.}\infty} = \frac{1}{g} u_2 \left(u_2 - \frac{V_{r_2}}{\tan \beta_2} \right)$$

or

$$H_{\text{vir.}\infty} = \frac{1}{g} u_2^2 \left(1 - \frac{V_{r_2}}{u_2 \tan \beta_2} \right) \quad 3-27$$

If the flow or capacity of a given unit operating at constant speed is varied, V_{r_2} is the only factor in Eq. 3-27 that will change. Since the outlet area of the impeller is constant, V_{r_2} will be directly proportional to the flow, and the virtual head-capacity curve will be a straight line.

Figure 3-12 shows the virtual outlet diagram of an impeller having an outlet vane angle less than 90° (backward-curved vanes) at half and full capacities. It may be observed that $V_{r_2}/\tan \beta_2$ is directly

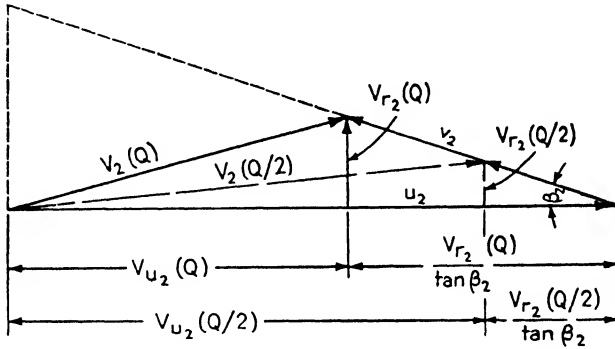


FIG. 3-12. Effect of partial flows on virtual outlet diagram for backward-curved vanes.

proportional to V_{r_2} ; hence from Eq. 3-27 it is apparent that the virtual head $H_{vir.\infty}$ must decrease as V_{r_2} or the flow increases.

Figure 3-13 shows the virtual outlet diagram for radial ($\beta_2 = 90^\circ$) vanes. Since $\tan 90^\circ$ is infinity, the head must be constant for all capacities.

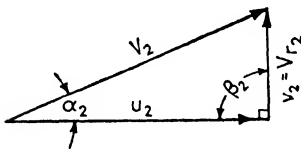


FIG. 3-13. Virtual outlet diagram for radial vanes.

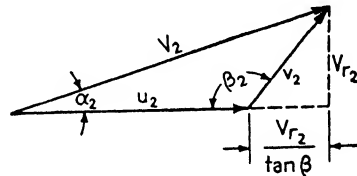


FIG. 3-14. Virtual outlet diagram for forward-curved vanes.

For vane outlet angles greater than 90° , $\tan \beta_2$ is negative; this makes the term $1 - \frac{V_{r_2}}{\tan \beta_2}$ greater than 1 as shown in Fig. 3-14.

Therefore, the head increases with increased capacity.

If the valve in the discharge is closed (shut-off condition) no fluid is delivered and $V_{r_2}/\tan \beta_2$ is zero for any vane outlet angle. The virtual head for an infinite number of vanes is then u_2^2/g .

Figure 3-15(a) shows the virtual head-capacity curves for the above vane angles. The actual curve of a pump or blower, although it differs considerably from the virtual owing to the circulatory flow and friction

and turbulence losses, still retains the inherent characteristics developed above. Figure 3-15(b) shows the outlet diagrams for various vane angles of impellers having the same radial component V_r , to illustrate the relative magnitudes of V_2 .

As has been shown, the principal factors influencing the shape of the characteristic curve are the angles of the impeller vanes at the outlet and the magnitude of the radial velocity. If the vanes are curved

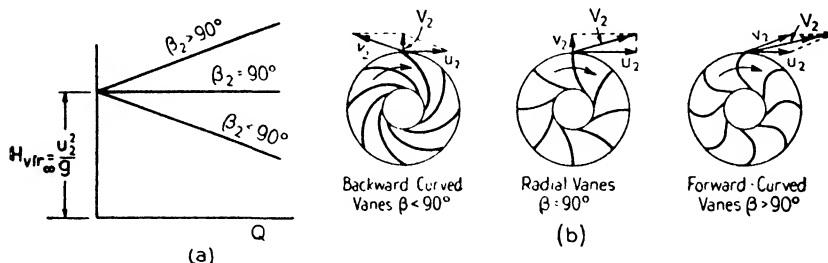


FIG. 3-15. Virtual head-capacity curves and outlet velocity diagrams for various vane angles.

backwards, the head will fall off as the delivery increases. The rate of decrease may be controlled somewhat by the proper selection of the vane outlet angle and outlet area of the impeller.

3-15 Effect of Speed Changes on Performance Curves. When the rotational speed of an impeller is changed from n_a to n_b the peripheral speed u of any point on it will be changed in the same proportion since $u = R\omega$. The vane inlet angle β_1 and the absolute angle of the fluid entering the impeller α_1 remain unchanged. Hence, the inlet triangle and all the velocities of Fig. 3-9(b) will be enlarged or reduced in proportion to $\frac{n_b}{n_a}$, and $Q_b = Q_a \frac{n_b}{n_a}$. In other words, for an impeller of given diameter the fluid capacity is approximately directly proportional to the speed of rotation.

By similar reasoning, it may be seen that the outlet triangle of Fig. 3-9(a) will vary in the same way, neglecting losses. For radial inlet flow $H_{vir.\infty} = \frac{u_2 V_{u_2}}{g}$. Since u_2 and V_{u_2} are both proportional to $\frac{n_b}{n_a}$, $H_{vir.\infty_b} = H_{vir.\infty_a} \left(\frac{n_b}{n_a}\right)^2$. Thus, the head developed is approximately proportional to the square of the speed.

The brake horsepower is approximately proportional to the weight flow and the head developed. Since the former is proportional to the speed and the latter to the speed squared, it follows that the brake

horsepower must be approximately proportional to the cube of the speed. The chief factor determining the brake horsepower in addition to the head and weight flow is the disk friction. From Eq. 3-8 it may be seen that this is also proportional to the speed cubed.

The effect of a speed change on the velocity triangles is to enlarge or reduce their size without changing the angles or the ratio of the fluid velocities. The only factors affected are the friction and turbulence losses due to the change in fluid velocity.

They represent a small part of the total losses, so that for practical purposes it may be assumed that the efficiency will remain approximately constant during a change in speed. Tests show that this is true over a fairly wide speed range.

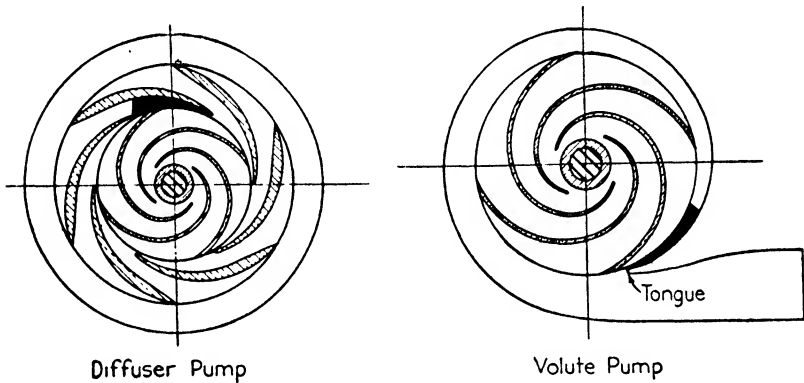


FIG. 3-16. Sections through diffuser and volute pumps.

3-16 Diffusers. As pointed out in Section 3-2, the head imparted to the fluid in the impeller is partly pressure head due to the centrifugal force and partly velocity head. The velocity head must be transformed into pressure head with as little turbulence and loss as possible in a passage or passages surrounding the periphery of the impeller, known as the diffuser.

There are three types of diffusers, all of which surround the periphery of the wheel and are bounded by the sidewalls of the casing. They are: (a) the annular diffuser, which is a ring-shaped space; (b) the volute diffuser, which is a spiral-shaped passage having increasing cross-sectional area as it approaches the discharge; and (c) the diffusing vane diffuser, consisting of a number of relatively short expanding passages. The latter two types are illustrated diagrammatically in Fig. 3-16.

Pumps with diffuser vanes were formerly called turbine pumps

owing to the resemblance of these vanes to the inlet guide vanes of inward flow hydraulic turbines, but the term commonly used today is diffuser pumps.

Annular and volute diffusers require a relatively large outside diameter to insure a reasonable amount of energy conversion. This increases the size and cost of the casing. The volute type is preferred to the annular for pumps, but the latter is widely used for blowers. The walls of the annular diffusers may diverge or may be parallel, and the outside diameter is generally 150 to 180 per cent of the impeller diameter, D_2 .

For either type the fluid flow is very nearly of the form discussed in Section 2-12(*d*), that is, $R \times V$ is constant. Hence, if the outside diameter is made larger a greater conversion of velocity to pressure head will result.

For impellers of relatively small diameter, the ratio of casing diameter to wheel diameter can be made large without unduly increasing the size or cost of the unit.

The vane diffuser is essentially the same as a volute, as shown by the black portions of the two types in Fig. 3-16, except that a number of volutes are used instead of one. For a given impeller and given conditions of flow, the inlet angle α_3 is the same for both, and the inlet velocities of both should be about the same.

A diffuser is used in stages developing high heads and is often used in multistage machines for that reason. If the outside diameter of the impeller is relatively large, it is not economical to make the casing large enough to secure sufficient conversion of the velocity head by means of a volute.

To reduce the cost of making and storing patterns, manufacturers generally adopt a "standard line" or set of casings which cover the usual field of operating conditions. It is necessary to design new volutes and hence casings for each capacity, if maximum efficiency is of importance; but with diffusers the same casing may be used for many different capacities, the variations being secured by a change in the diffusing vanes. Also, a customer may desire to operate a unit for some years at one capacity with the intention of later increasing it to a larger value. This could be done with a diffuser in many instances with no change in the casing and no loss in efficiency. With the volute either the casing would have to be altered, a new one made, or a drop in efficiency accepted.

It is easier to machine a diffuser than a volute, so smoother passages can be obtained more economically. This reduces the frictional losses in the pump.

It has been found that pumps having a volute show an uneven pressure distribution around the periphery of the impeller* particularly when operating at partial flows. This results in an unbalanced load on the shaft which may be partly nullified in a multistage pump by staggering the volutes radially. For single-stage pumps double volutes (each collecting fluid from 180° of impeller circumference) are sometimes used to reduce this radial thrust. The condition does not exist when a diffuser is used.

3-17 Influence of the Design on the Performance. As shown in developing Eq. 3-5 for the virtual head, the total energy of the fluid at the impeller outlet appears as both static and velocity head. The static head at this point is represented by the expression $\frac{u_2^2 - u_1^2 + v_1^2 - v_2^2}{2g}$; the velocity head or kinetic energy is represented

by the expression $\frac{V_2^2 - V_1^2}{2g}$, or $\frac{V_2^2}{2g}$, since the magnitude of $\frac{V_1^2}{2g}$ is usu-

ally negligible. The ratio of these two factors varies according to the outlet angle of the impeller vanes β_2 , the ratio between the velocity of the fluid relative to the impeller v_2 , and the peripheral velocity of the impeller u_2 . As can readily be seen from the outlet diagrams of Fig. 3-15(b) the kinetic energy or velocity head represented by $V_2^2/2g$ is in general large for forward curved and radial vanes and is reduced with a decrease in the outlet angle β_2 . Figure 3-17 shows in a general manner the variation in velocity and pressure at points along the flow path in an impeller and vane diffuser. The values given are relative only and should not be taken literally.

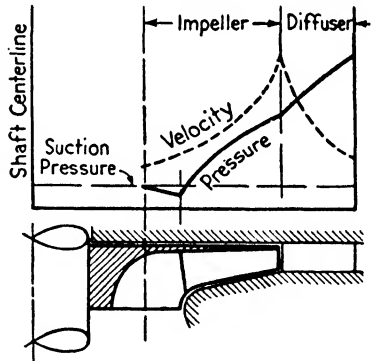


FIG. 3-17. Variation of velocity and pressure through a typical stage having a diffuser.

It has been found that the efficiency when transforming pressure head to velocity head is much greater than the reverse process. In other words the efficiency of energy conversion by increasing the velocity of a fluid is greater than that of slowing it down to develop pressure, owing to the accompanying eddies and turbulence. The pur-

* R. L. Daugherty, "Centrifugal Pumps for the Colorado River Aqueduct," *Mechanical Engineering*, April, 1938, p. 296; R. C. Binder and R. T. Knapp, "Experimental Determinations of the Flow Characteristics in the Volute of Centrifugal Pumps," *A.S.M.E. Trans.*, HYD-58-4, 1936.

pose of the diffuser is to reduce the velocity V_2 to a lower velocity V_4 ; hence, the lower V_2 is the greater the efficiency of the conversion.

The efficiency of transformation of energy within the impeller depends upon correctly designed surfaces, gradual change of areas, and smooth finish. It is an advantage to have a large part of the

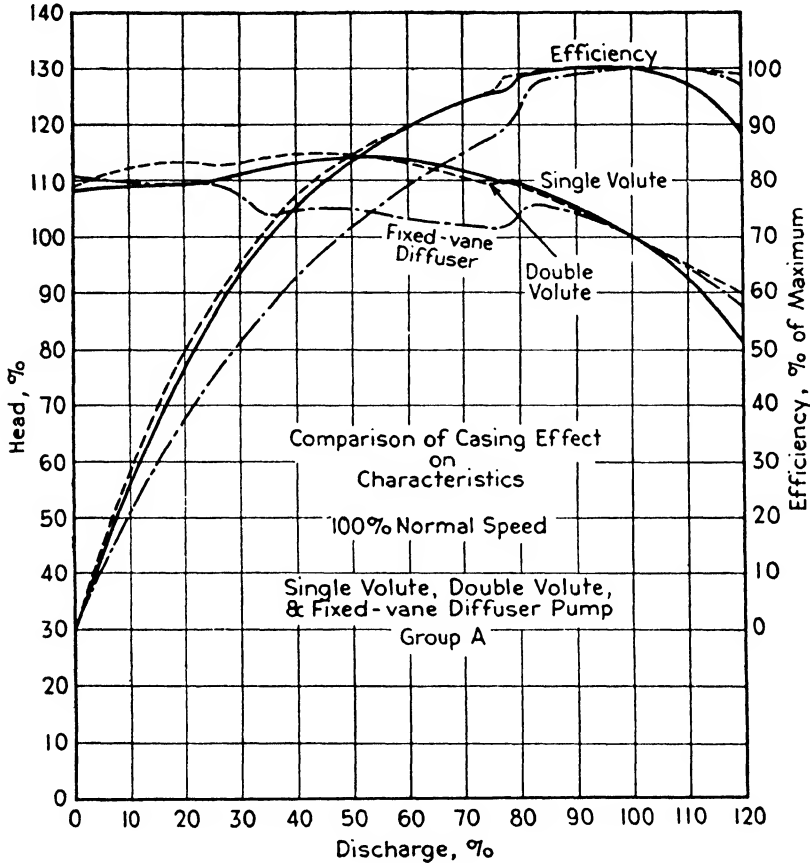


FIG. 3-18. Comparison of casing effect on pump characteristics; Group A pumps. (Taken from "Centrifugal Pump Performance as Affected by Design Features," R. T. Knapp, *A. S. M. E. Trans.*, April, 1941, pp. 251-260.)

total head developed in the impeller, where velocities are relatively low and where the conversion of energy into pressure can be done most efficiently. Moreover, as already mentioned, the presence of a large portion of the energy in the form of velocity in the fluid as it leaves the impeller is accompanied by an unfavorable form of head-capacity characteristic curve.

Tests were made at the California Institute of Technology Laboratory on model pumps for the Grand Coulee Dam and are reported by R. T. Knapp.* A single volute, a double volute, and a diffuser were tested with the same impeller. In the high capacity region it was found that the head curve did not drop off as rapidly for the diffuser

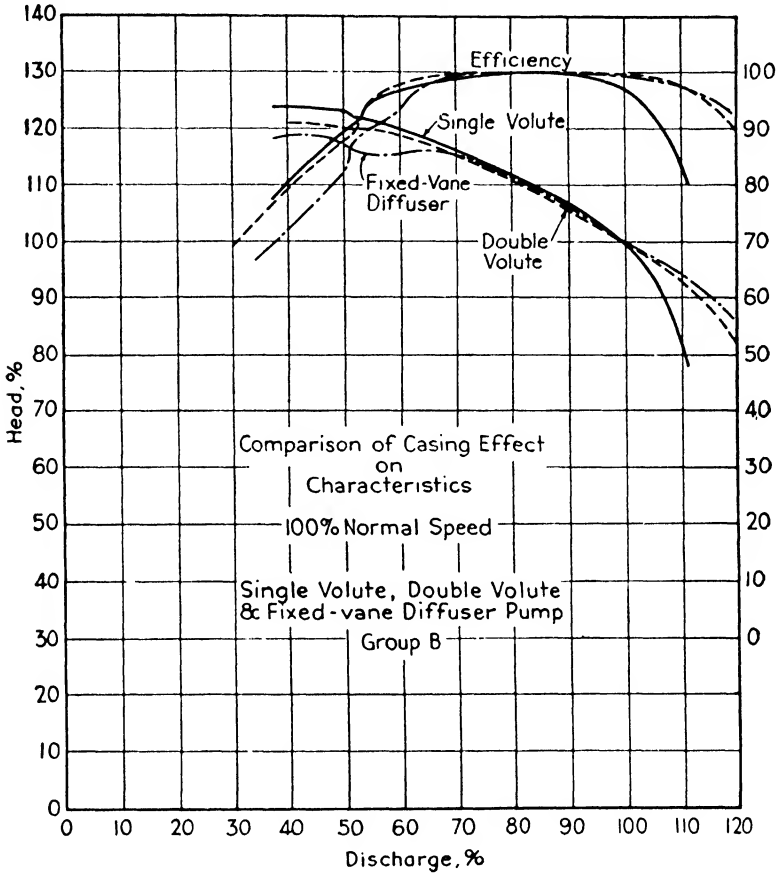


FIG. 3-19. Comparison of casing effect on pump characteristics; Group B pumps. (Taken from "Centrifugal Pump Performance as Affected by Design Features," R. T. Knapp, *A. S. M. E. Trans.*, April, 1941, pp. 251-260.)

or double volute as for the single volute. However, the efficiency and head curves were lower at partial flows because of the increased number of vanes surrounding the impeller at which turbulence losses will occur, as noted in the next section. These are illustrated for two

* "Centrifugal Pump Performance as Affected by Design Features," *A.S.M.E. Trans.*, April, 1941, pp. 251-260.

groups of pumps in Figs. 3-18 and 3-19 which were taken from the paper referred to above.

3-18 The Actual Head-Capacity Curve.* The virtual head-capacity curve, as noted in Section 3-14, is a straight line; for outlet angles less than 90° it has the shape shown in Fig. 3-20 for $H_{vir.\infty}$.

Owing to the circulatory flow effect, the fluid in an actual impeller with a finite number of vanes leaves the impeller at an angle β_2 which

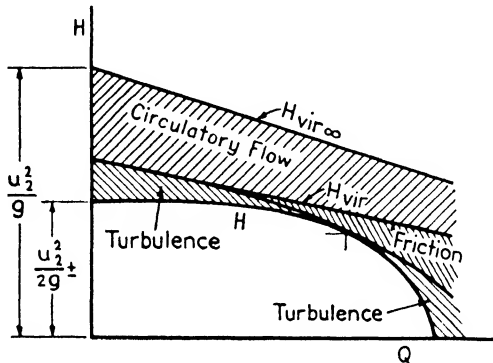


FIG. 3-20. Development of the actual head capacity curve from the virtual.

is smaller than the actual vane angle. This reduces the theoretical head developed in a practically constant ratio and the new virtual head H_{vir} is shown in Fig. 3-20. It should be remembered that this effect is not a loss but a discrepancy not accounted for by the basic assumptions.

The friction losses in the suction passages, interior of the impeller, and the discharge volute will be a minimum at no discharge and will increase approximately as the square of the velocity or capacity, reducing the corrected virtual head H_{vir} , as shown in the figure.

The next losses to be considered are those due to turbulence. Reference to the inlet diagram of Fig. 3-4 shows that for a given impeller operating at a fixed speed (with u_1 constant and the vane inlet angle β_1 fixed) there is only one inlet velocity V_1 that will fulfill the diagram; that is the one corresponding to the rated or design capacity. For reduced or increased capacity, the fluid enters the impeller vanes at

* More complete discussions of the compositions of the actual performance curves may be found in M. D. Aisenstein, "A New Method of Separating the Hydraulic Losses in a Centrifugal Pump," *A.S.M.E. Trans.*, HYD-50-2, 1927, and J. Lichtenstein, "A Method of Analyzing the Performance of Centrifugal Pumps," *A.S.M.E. Trans.*, HYD-50-3, 1927.

an angle different from the inlet vane angle β_1 with resultant turbulence losses. Figure 3-12 shows the change in magnitude and direction of V_2 for various capacities. This is the virtual diagram (uncorrected for the circulatory flow) but the actual diagram will follow the same changes. The vane outlet angle β_2 and peripheral speed u_2 remain the same but the radial component V_{r_2} is directly proportional to the flow. From this figure it may be seen that the inlet angle and area of a diffuser will be correct for only one flow (the design) and the turbulence will increase as the flow gets farther away from this design value. The above is also true for a volute but to a smaller extent, since the incorrect angle will produce turbulence only at the tongue of the volute. This is the reason why it is more difficult to build a diffuser pump with a steadily decreasing head curve from shut-off to full capacity than a pump with a volute. Subtracting this turbulence loss produces the final head-capacity curve H of Fig. 3-20.

It will be found that for most pumps and blowers the head at no delivery or shut-off has a value of about $u_2^2/2g$. The actual value varies from about 0.9 to 1.2 times $u_2^2/2g$. It was shown in Section 3-2 that if there is no flow the static pressure developed in an impeller would be $\frac{u_2^2 - u_1^2}{2g}$, or if all the fluid down to the impeller hub were rotating, the value would be $u_2^2/2g$ since u_1^2 then equals zero. It is an interesting fact that even though the conditions under which a pump or blower impeller operates at no delivery vary considerably from the ideal case with no flow, the head developed is actually very nearly $u_2^2/2g$ and this equation is a convenient means of calculating the approximate impeller diameter required for specified conditions of operation.

3-19 Brake Horsepower and Efficiency Curves. The efficiency and brake horsepower requirement of a pump or blower are affected by the internal leakage losses through the sealing or wearing rings, the disk friction of the exterior of the impeller, the mechanical losses in the bearings and packing boxes, and the fluid friction and turbulence losses in the unit as expressed by Eq. 3-21.

The final brake horsepower curve may be built up in a manner similar to that of the head-capacity curve (Fig. 3-20). In Fig. 3-21 the friction power consumed and the turbulence losses, as discussed in Section 3-17, are added to the useful work or fluid horsepower. The leakage, disk friction, and bearing losses for a machine operating at a constant speed are all practically independent of the capacity and remain approximately constant for all flows as shown in Fig. 3-21, thus giving the final brake horsepower curve shown.

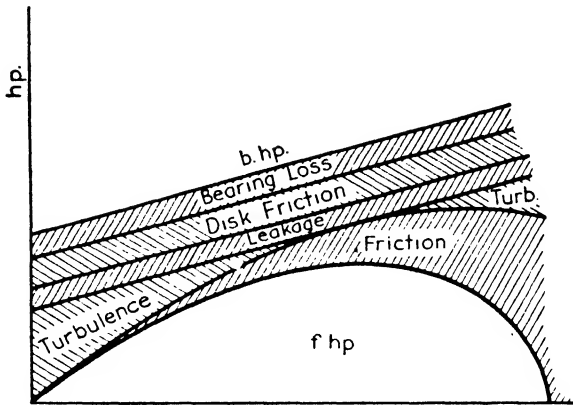


FIG. 3-21. Development of actual brake horsepower-capacity curve from the virtual.

3-20 Pulsation or Surging. Under certain operating conditions, which will be described later, a pump or blower will experience unstable operation and alternately deliver large and small quantities of fluid. This phenomenon is known as pulsation or surging and should be avoided in both design and operation as much as possible since it puts a heavy strain on the unit and also on the whole system.

Figure 3-22 shows a typical characteristic curve for a pump or blower operating at constant speed. Point *D* indicates the normal operating or design point of the curve. Assume that the machine

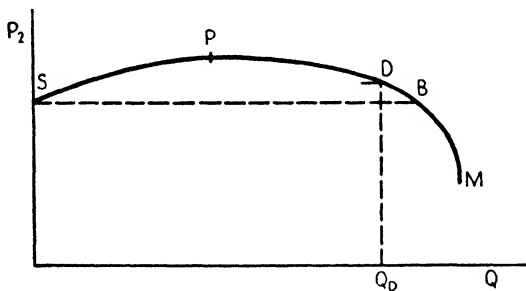


FIG. 3-22. Head-capacity curve to illustrate pulsation.

is delivering fluid to a tank or pipe system from which it is removed for use. If the demand on the system is increased the delivered flow from the unit is also increased and the pressure in the system is reduced, i.e., the operating point moves to the right toward *M* and the delivery pressure is decreased.

If the demand gradually decreases, the system and delivery pressure increase up to point *P* on the curve. For further decrease of demand, the system pressure will be higher than the delivery pressure (since the latter starts to drop off) and the fluid tends to flow back into the unit. Hence delivery from the unit stops and the operating point jumps from *P* to *S*. If fluid is still being removed from the system the pressure gradually will drop below that at *S*. When this occurs the unit starts to deliver fluid but will not build up pressure rapidly enough to follow along the curve from *S* to *P* but instantaneously begins to deliver a flow corresponding to the pressure against it, which is that at point *B*. The increased flow from the machine causes the pressure to rise rapidly along the curve from *B* to point *P* and delivery again ceases until the system pressure drops below *S*. This cycle repeats itself until the conditions causing it are removed, i.e., until the fluid flow from the system is greater than the flow from the machine corresponding to point *P*.

Point *P* is known as the pulsation point and is the highest point on the characteristic curve. Stable conditions prevail on the curve to the right of this point, hence the point should be as far to the left as possible. As will be noted from Section 3-14, backward-curved vanes are the best from this standpoint. It is interesting to note that the pulsation point for a blower having diffuser vanes is usually between 60 and 65 per cent of the rated capacity, whereas for a similar unit having a volute or annular diffuser the pulsation point is between 40 and 50 per cent of the rated capacity.

The frequency and intensity of the pulsation depend upon the slope of the characteristic curve, the rate at which the fluid is being removed, the degree of elasticity of the system, the fluid handled, and the head or number of stages in the unit. If the fluid is a liquid such as water, which is nearly incompressible, the frequency of the pulsations is higher than with a gas. With low head units the pressure variations are proportionately less, but they may be greatly intensified if resonant conditions exist in the system.

PROBLEMS

3-1 An impeller rotating at 3500 r.p.m. has an outside diameter of 8.5 in. The vane outlet angle β_2 is 22° and the radial velocity at the outlet V_{r_2} is 12 ft. per sec. Assuming radial inlet flow to the impeller, draw the virtual outlet diagram to scale, calculating the various velocities and angles. What is the virtual head, $H_{vir.}$?
Ans. 404 ft.

3-2 An impeller rotating at 1150 r.p.m. has the following dimensions: $b_1 = 1\frac{1}{4}$ in., $b_2 = \frac{3}{4}$ in., $D_1 = 7$ in., $D_2 = 15$ in., $\beta_1 = 18^\circ$, $\beta_2 = 20^\circ$ (b_1 and b_2 are the passage widths at inlet and outlet respectively; cross-sectional area $A = \pi Db$ if

vane thickness is neglected). Assuming radial inlet flow and neglecting vane thickness, draw the virtual velocity diagrams and calculate the rated capacity in gallons per minute and the virtual head, neglecting the circulatory flow.

Ans. 980 g.p.m.; 119 ft.

3-3 If the impeller of Problem 3-2 is operated at shut-off (i.e., with $V_{r_2} = 0$) what is the virtual head?

Ans. 176 ft.

3-4 Calculate and draw the outlet velocity triangle for the impeller of Problem 3-2 for $\frac{1}{2}$, $\frac{3}{4}$ and $1\frac{1}{4}$ of the rated capacity and calculate the corresponding virtual heads. Tabulate the values of V_2 and α_2 , including those from Problems 3-2 and 3-3. (Note that this demonstrates the changes causing turbulence losses occurring with the capacity changes.)

3-5 The impeller of Problem 3-2 develops an actual head of 82 ft. and delivers 850 g.p.m. at the point of maximum efficiency, requiring 22 b.hp. The contraction at the discharge due to the vane thickness is 0.92 (i.e., the actual radial outlet velocity is $V_{r_2}/0.92$). Based upon the delivered flow, calculate (a) the overall pump efficiency, (b) the overall pressure coefficient Φ ; (c) the virtual outlet velocities V_2 and v_2 ; (d) virtual outlet angle α_2 ; and (e) coefficient K .

Ans. (a) 80 per cent; (b) 1.037; (c) $V_2 = 53, v_2 = 24.5$; (d) $9^\circ 5'$; (e) 0.67.

3-6 Assume the following losses at the point of maximum efficiency of the impeller of Problem 3-5: mechanical losses in the bearings and packing, 2 per cent of the brake horsepower; disk friction, 1.6 hp.; and leakage loss 35 g.p.m. Determine (a) volumetric efficiency η_V ; (b) hydraulic efficiency η_{HY} ; (c) circulatory flow factor η_∞ ; (d) actual outlet velocity V_2 ; (e) actual absolute outlet angle α_2 ; (f) mechanical efficiency η_M (by two methods); (g) check the equation $\eta = \eta_M \times \eta_{HY} \times \eta_V$.

Ans. (a) 96 per cent; (b) 91.6 per cent; (c) 0.731; (d) 39.2; (e) $12^\circ 25'$; (f) 91 per cent.

CHAPTER 4

SPECIFIC SPEED AND EFFICIENCY OF PUMPS

4.1 Specific Speed. Specific speed is a term used to classify impellers on the basis of their performance and proportions regardless of their actual size or the speed at which they operate. Since it is a function of the impeller proportions it is constant for a series of homologous (having the same angles and proportions) impellers or for one particular impeller operating at any speed.

It is defined as the speed in revolutions per minute at which an impeller would operate if reduced proportionately in size so as to deliver a rated capacity of 1 g.p.m. against a total head of 1 ft. It is designated by the symbol n_s .

4.2 Development of the Specific Speed Equation. The relationships between capacity, head, and speed which were outlined in Section 3.15 will now be applied to develop the equation for the specific speed of an impeller operating at a speed of n r.p.m. and delivering Q g.p.m. against a total head of H ft.

As a first step, let the speed n be reduced to a value n' until the head developed becomes 1 ft. Then $n' = n\sqrt{1/H}$, and the corresponding capacity will be $Q' = Q\sqrt{1/H}$ or $Q\frac{n'}{n}$.

In order to reduce the flow to 1 g.p.m. in accordance with the definition, the dimensions of the impeller must be reduced and at the same time its speed must be increased to maintain the head of 1 ft. (i.e., keep u_1 and u_2 the same). The fluid velocities should also be kept constant in order to maintain the similarity of the velocity diagrams. The impeller inlet area must be reduced in the ratio of $1/Q'$ and all the dimensions in the ratio of $1/\sqrt{Q'}$, since the area is proportional to the linear dimensions squared. To maintain the same peripheral speeds u_1 and u_2 , the rotative speed must be increased by $\sqrt{Q'}/1$.

The final speed for a 1-ft. head and a 1-g.p.m. capacity is

$$n_s = n' \sqrt{Q'} = \frac{n}{\sqrt{H}} \sqrt{\frac{Q}{\sqrt{H}}} = \frac{n\sqrt{Q}}{H^{3/4}} \quad 4.1$$

This is the equation for the specific speed.* It should be noted that

* In solving this equation it may be noted that $H^{3/4} = H/\sqrt{\sqrt{H}}$.

the specific speed is increased with larger capacities and higher operating speeds or with lower heads.

The characteristic curve of a pump varies from zero flow at shut-off to zero head at maximum capacity. Hence the specific speed for one curve varies from zero to infinity. In order to make the term definite it is necessary to select some particular condition. The logical point is that of maximum efficiency, and it is generally understood that this point is meant when the specific speed is stated.

The development of the equation may be made clearer by means of a numerical example. Assume an impeller having a capacity Q of 4000 g.p.m. at a speed n of 2000 r.p.m. against a head H of 100 ft. Its inlet eye diameter is 12 in.

The first step is to reduce the speed n to obtain a head of 1 ft. The new speed $n' = n\sqrt{1/H} = 2000\sqrt{1/100} = 200$ r.p.m., and the corresponding capacity will be $Q' = Q(n'/n) = 4000(200/2000) = 400$ g.p.m.

The next step is to reduce the dimensions of the impeller so that the flow is reduced to 1 g.p.m. and at the same time increase the speed of the impeller to maintain the 1-ft. head. The new inlet area will be $1/Q'$ of the former value, and the new dimensions will be $1/\sqrt{Q'}$ or $1/20$. Hence D' becomes $12/20$ in. or 0.6 in. To keep u_1 and u_2 the same as before the speed must be increased $\sqrt{Q'}/1$ or 20 times. Hence, the final speed will be 20×200 or 4000 r.p.m.; this is the specific speed of the impeller. As a check the original values may be substituted in Eq. 4-1:

$$n_s = \frac{n\sqrt{Q}}{H^{3/4}} = \frac{2000\sqrt{4000}}{100^{3/4}} = \frac{2000 \times 63.2}{31.6} = 4000 \text{ r.p.m.}$$

It is not necessary to grasp the physical significance of the definition of specific speed to use it intelligently. It should be considered as a type characteristic of the impeller which specifies its general proportions and characteristics rather than as an r.p.m. for special conditions.

The chart of Fig. 4-1 may be used to find the specific speed with sufficient accuracy for practical purposes and it avoids the necessity of calculating the head to the $3/4$ power. The point located by plotting the total head and capacity in gallons per minute at the design point is moved parallel to the sloping lines to the corresponding speed in revolutions per minute. The specific speed is read at the top of the chart directly above this final point. The procedure is illustrated by the heavy dashed lines for a pump delivering 1200 g.p.m. against a head of 120 ft. when operating at 3500 r.p.m. The specific speed n_s is then 3350.

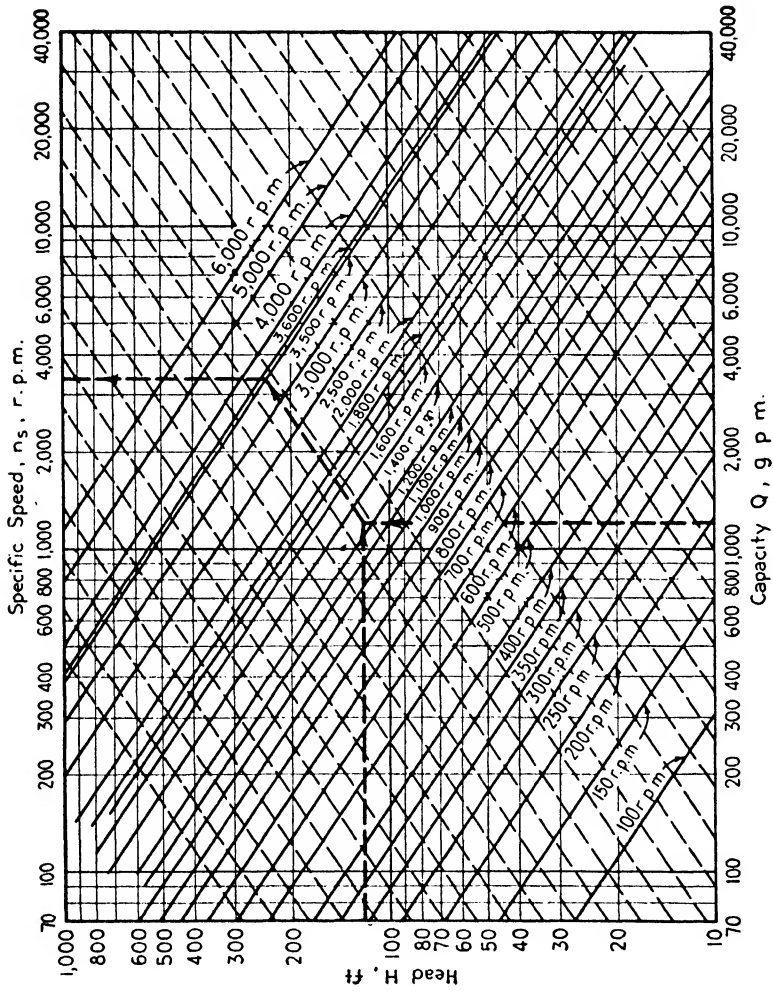


FIG. 4-1. Chart for determination of specific speed.

4-3 Specific Speed in Terms of Wheel Dimensions. From the previous discussion it was seen that the specific speed depends upon the proportions of the impeller rather than the operating speed. An impeller may operate at a high speed and still be classified as a low specific speed wheel and vice versa.

In order to find the relationship between the impeller proportions and the specific speed, it is of interest to develop the following involved approximate formula. Neglecting the vane thickness,

$$Q = A_1 V_1 = \pi D_1 b_1 V_1 = \pi D_1 b_1 (u_1 \tan \beta_1) \quad A$$

From Eqs. 3-15 and 3-27,

$$H = \frac{K}{g} u_2^2 \left[1 - \frac{V_{r_2}}{u_2 \tan \beta_2} \right] \quad B$$

Now,

$$V_{r_2} = \frac{Q}{\pi D_2 b_2} = \frac{\pi D_1 b_1 u_1 \tan \beta_1}{\pi D_2 b_2} = \frac{D_1 b_1}{D_2 b_2} u_1 \tan \beta_1$$

and

$$u_1 = \frac{\pi D_1 n}{12 \times 60} \quad u_2 = \frac{\pi D_2 n}{12 \times 60}$$

Inserting these in A and B,

$$Q = \pi D_1 b_1 u_1 \tan \beta_1 = \pi D_1 b_1 \frac{\pi D_1 n}{720} \tan \beta_1 = \frac{\pi^2}{720} b_1 D_1^2 n \tan \beta_1$$

$$H = \frac{K}{g} u_2^2 \left[1 - \frac{V_{r_2}}{u_2 \tan \beta_2} \right] = \frac{K}{g} \frac{\pi^2 D_2^2 n^2}{720^2} \left[1 - \frac{D_1 b_1 \pi D_1 n \tan \beta_1}{D_2 b_2 720 \tan \beta_2 \pi D_2 n} \right]$$

$$= \frac{K}{g} \frac{\pi^2 D_2^2 n^2}{720^2} \left[1 - \left(\frac{D_1}{D_2} \right)^2 \frac{b_1 \tan \beta_1}{b_2 \tan \beta_2} \right]$$

Substituting these values of Q and H into $n_s = \frac{n\sqrt{Q}}{H^{3/4}}$,

$$n_s = \frac{n \sqrt{\frac{\pi^2}{720} b_1 n D_1^2 \tan \beta_1}}{\left(\frac{K}{g} \right)^{3/4} \left(\frac{\pi^2 D_2^2 n^2}{720^2} \right)^{3/4} \left[1 - \left(\frac{D_1}{D_2} \right)^2 \frac{b_1 \tan \beta_1}{b_2 \tan \beta_2} \right]^{3/4}}$$

$$\begin{aligned}
 n_s &= \left(\frac{g}{K}\right)^{3/4} \frac{n\pi D_1 \sqrt{\frac{b_1 n}{720} \tan \beta_1}}{\left(\frac{\pi D_2 n}{720}\right)^{3/4} \left[1 - \left(\frac{D_1}{D_2}\right)^2 \frac{b_1 \tan \beta_1}{b_2 \tan \beta_2}\right]^{3/4}} \\
 &= \left(\frac{g}{K}\right)^{3/4} \frac{n^{3/2} \pi D_1 720^{3/2} \sqrt{b_1 \tan \beta_1}}{720^{3/2} \pi^{3/2} D_2^{3/2} n^{3/2} \left[1 - \left(\frac{D_1}{D_2}\right)^2 \frac{b_1 \tan \beta_1}{b_2 \tan \beta_2}\right]^{3/4}} \\
 &= \left(\frac{g}{K}\right)^{3/4} \frac{720}{\sqrt{\pi}} \frac{\frac{D_1}{D_2} \sqrt{\frac{b_1}{D_2} \tan \beta_1}}{\left[1 - \left(\frac{D_1}{D_2}\right)^2 \frac{b_1 \tan \beta_1}{b_2 \tan \beta_2}\right]^{3/4}}
 \end{aligned} \tag{4-2}$$

Equation 4-2 illustrates the effect of impeller dimensions and vane angles upon the specific speed and may be summarized as follows:

(a) It will be higher with larger ratios of D_1/D_2 , b_1/D_2 or b_1/b_2 , of which the factor having the greatest influence is D_1/D_2 . This is illustrated in the lower part of Fig. 4-12 which shows various impeller forms with their approximate specific speeds indicated on the chart above. A propeller-type pump will have the highest specific speed since D_1/D_2 is unity or less.

(b) It is higher for a larger inlet angle β_1 and, since $\tan \beta_1 = V_1/u_1$ for axial fluid entrance, for larger values of V_1 . From this consideration it may be noted that a high specific speed reduces the ability of an impeller to operate under a high suction lift because high inlet velocities reduce the available static pressure at the inlet, as will be shown in the next chapter.

(c) If the hydraulic efficiency η_{HY} is constant, the specific speed is increased with smaller K or smaller η_∞ and consequently fewer vanes and shorter vane length, since $K = \eta_{HY}\eta_\infty$.

Another limiting factor should be mentioned at this point. With increasing head it is not possible to increase the inlet velocity indefinitely since cavitation will begin, as explained in the next chapter. Therefore the specific speed must be reduced for wheels operating with higher suction heads.

For specific speed to retain its significance when applied to double-suction impellers (Figs. 1-2 and 4-3) it is necessary to consider such impellers as being equivalent to two single-suction impellers placed back to back or operating in parallel. This means that in applying Eq. 4-1 to double suction impellers the capacity used should be one-half of that handled by the pump.

4-4 Specific Speed Applied to Pump Classification. One use of specific speed is to classify the various types of pump impellers. It has been shown in the previous section that there is a definite correlation between the impeller proportions and the specific speeds. Each type of impeller has a range of specific speeds for which it is best suited, though these ranges are only approximate. There are no sharp dividing lines of demarcation between the various types.

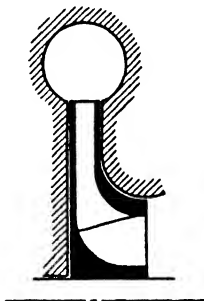


FIG. 4-2. Radial-type impeller.

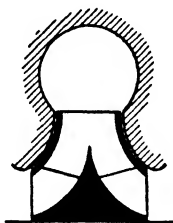


FIG. 4-3. Double-suction impeller.

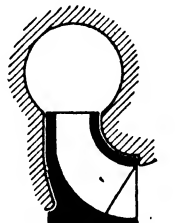


FIG. 4-4. Francis-type impeller.

(a) *Radial-Type Impeller.* The head is developed largely by the action of centrifugal force. The stage shown in Fig. 4-2 is used for medium and high heads (above about 150 ft.). It is the conventional type of impeller, and is used in practically all multistage machines. The range of specific speed is generally between 500 and 3000. The ratio of discharge diameter to inlet eye diameter is in the neighborhood of 2.

When larger volumes must be handled, a double-suction impeller, as shown in Fig. 4-3, may be used. The head and specific speed range are about the same as for a single-suction impeller. This impeller has the advantage of being hydraulically balanced, i.e., the end thrusts are opposed and balance each other.

(b) *Francis-Type Impeller.* For lower heads an axial-inlet radial-discharge impeller, as illustrated in Fig. 4-4, is frequently used. The ratio of the discharge diameter to the inlet eye diameter is usually much smaller than in the previous case. For a given capacity and head this type operates at a higher speed than the conventional impeller. The specific speeds are slightly higher (1500 to 4500). The inlet vane angle must decrease with the radius (or peripheral impeller velocity) in order to insure smooth entry of the fluid, so that it resembles a Francis turbine wheel in shape. This type of impeller may also be made double-suction.

(c) *Mixed-Flow-Type Impeller.* The head developed in this type is due partly to the centrifugal force and partly to the push of the vanes. The discharge is partly radial and partly axial; this is the reason for the name mixed-flow. The mean discharge diameter is usually about equal to the eye inlet diameter, although it may be less than that. The impeller is made screw-shaped (doubly curved) for the same reason as the Francis-type wheel of Fig. 4-4. The specific speed range is usually between 4500 and 8000.

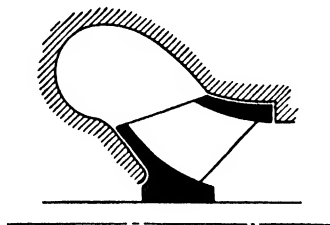


FIG. 4-5. Mixed-flow-type impeller.

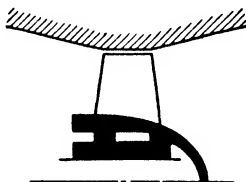


FIG. 4-6. Propeller-type impeller.

(d) *Propeller-Type Impeller.* Practically all the head developed by this type is due to the push of the vanes, the flow being almost entirely axial as shown in Fig. 4-6. It has the highest specific speed (above 8000) and is used for low heads (3 to 40 ft.), low r.p.m. (200 to 1800), and large capacities. Owing to the small amount of guidance given the liquid, it is not suitable for high suction lifts.

(e) *Multistaging.* The impellers described above are for a single stage. When the head to be developed becomes too great for one stage, several impellers are mounted on one shaft in series as shown in Fig. 4-7. These impellers are usually of the radial type shown in Fig. 4-2 since they develop greater heads than the other types.

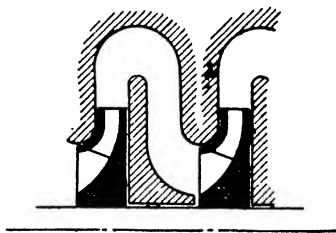


FIG. 4-7. Multistaging.

The specific speed of a multistage pump is taken to be the specific speed of any stage. The speed and flow through all the stages is the same, and the total head is usually equally divided between the stages. Hence all the stages will have the same specific speed, which is considered to be that of the unit.

Figure 4-8 illustrates the types of impellers commonly used for various heads and capacities and supplements the information given above. The limits shown on this chart for each type of pump are

based upon Pomona design, but other manufacturers offer the same types for approximately the same head-capacity conditions.

The water horsepower may be found for a given flow in gallons per minute and the head in feet from the sloping lines of the chart. An estimate of the required brake horsepower can then be obtained by dividing the water horsepower by the estimated pump efficiency.

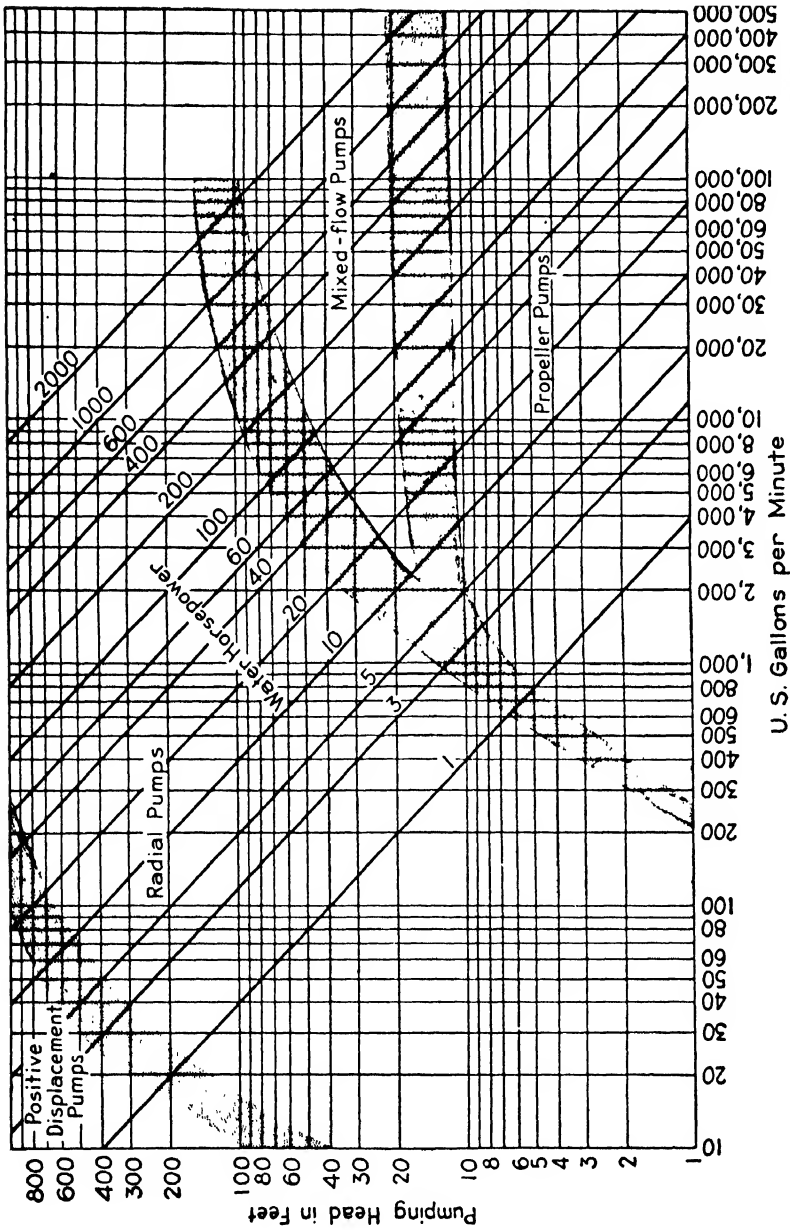
4-5 Pump Efficiencies. The efficiency of a centrifugal pump depends upon a number of factors, the more important of which are: (a) hydraulic losses (friction and turbulence); (b) disk friction; (c) mechanical losses in the bearings and packing; and (d) leakage losses.

From the standpoint of performance the efficiency depends upon capacity, head, and speed, all of which are included in the specific speed. Therefore it would be expected that there should be some relation between the specific speed and efficiency.

Of these items the most important is the capacity. The friction and turbulence losses are a smaller percentage of the total power when large capacities are being handled. Also the disk friction and mechanical losses are relatively smaller when the flows are large. In Fig. 4-9 efficiency is plotted against capacity for about 300 pumps manufactured by about a dozen pump companies. These points were taken from witness tests, or other reliable data in technical literature, and in general they represent average recent commercial practice rather than maximum values or tests on special pumps. As would be expected with the many designs and conditions represented, there is a range of efficiencies for a given capacity rather than single values. The points do show a definite trend toward increased efficiency with higher capacities, and also a marked falling off at low capacities.

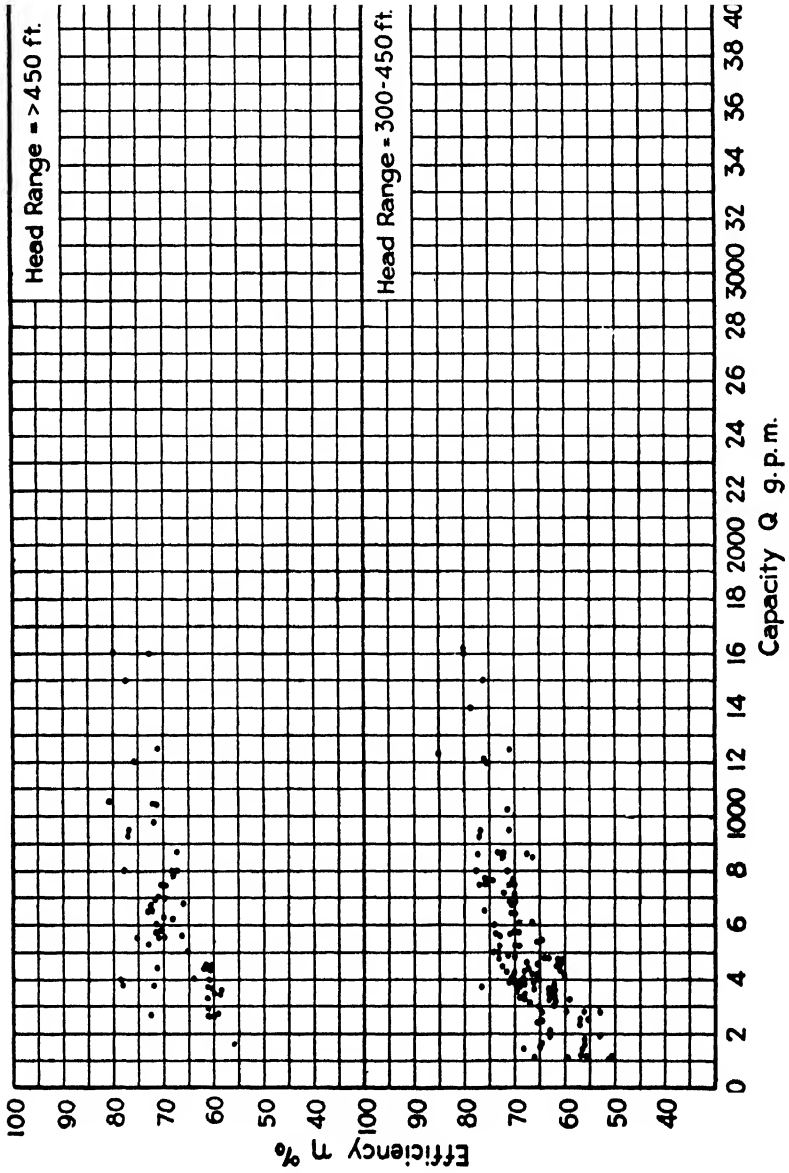
It would be expected that increased head for a given capacity would result in lower efficiency since increased head involves either a larger-diameter impeller or a higher r.p.m. In either case increased disk friction and mechanical losses result. Points of efficiency plotted against head for the same pumps of Fig. 4-9 are shown in Fig. 4-10 for various capacities. Again a range of points occurs, and it may be observed that the efficiency decreases rapidly with smaller capacities.

Various curves of efficiency plotted against specific speed have been published, which in general show that the maximum efficiency occurs at a specific speed in the neighborhood of 2000 to 2500 r.p.m. *Points of specific speed and efficiency for the pumps mentioned above are plotted for various capacities in Fig. 4-11. These points agree



Courtesy Joshua Hendy Iron Works, Pomona Pump Co. D.

FIG. 4-8. Pump-type allocation chart.



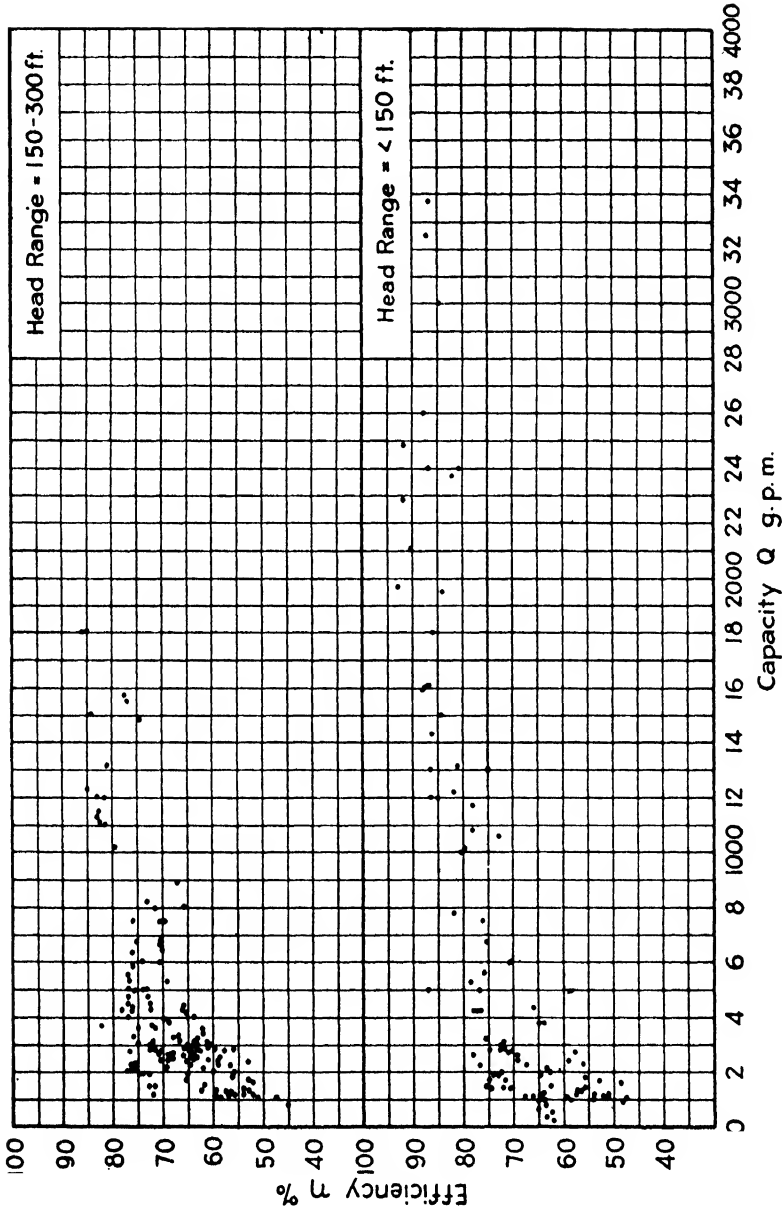


FIG. 4-9. Efficiency-capacity points for various head ranges.

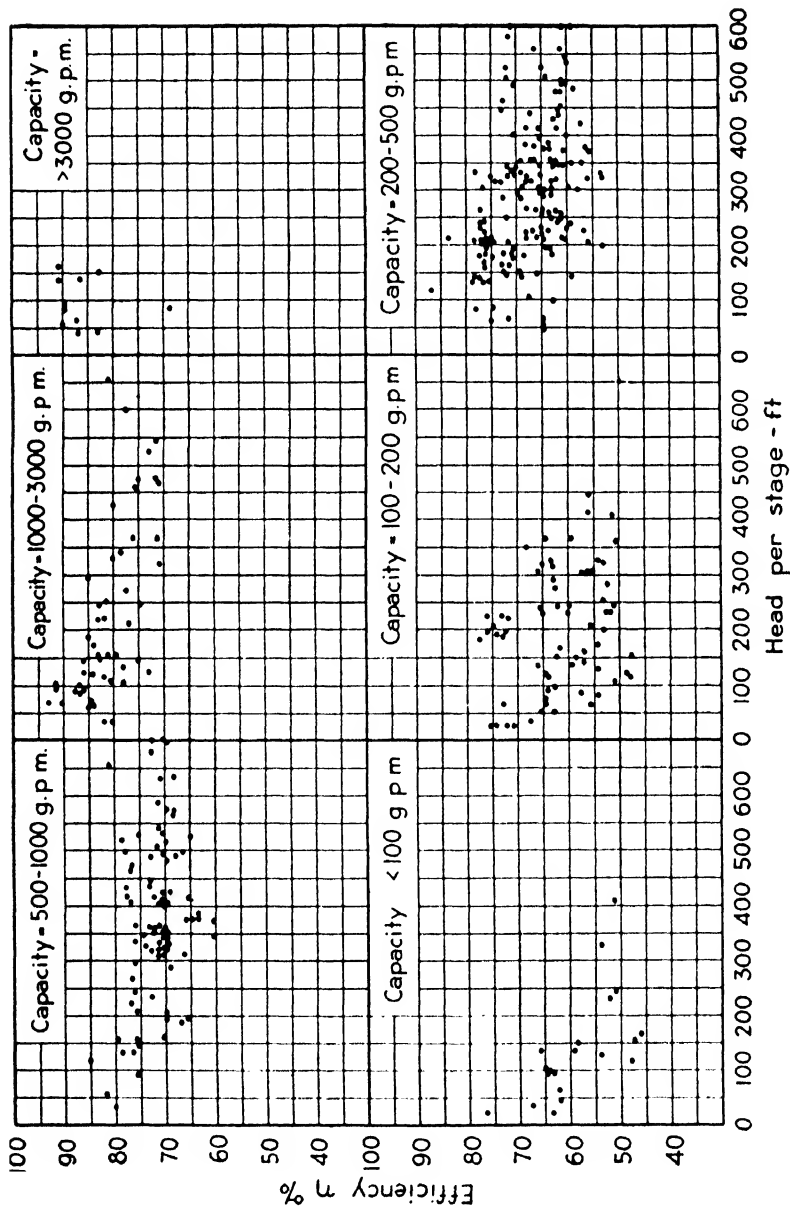


Fig. 4-10. Efficiency-head points for various capacity ranges.

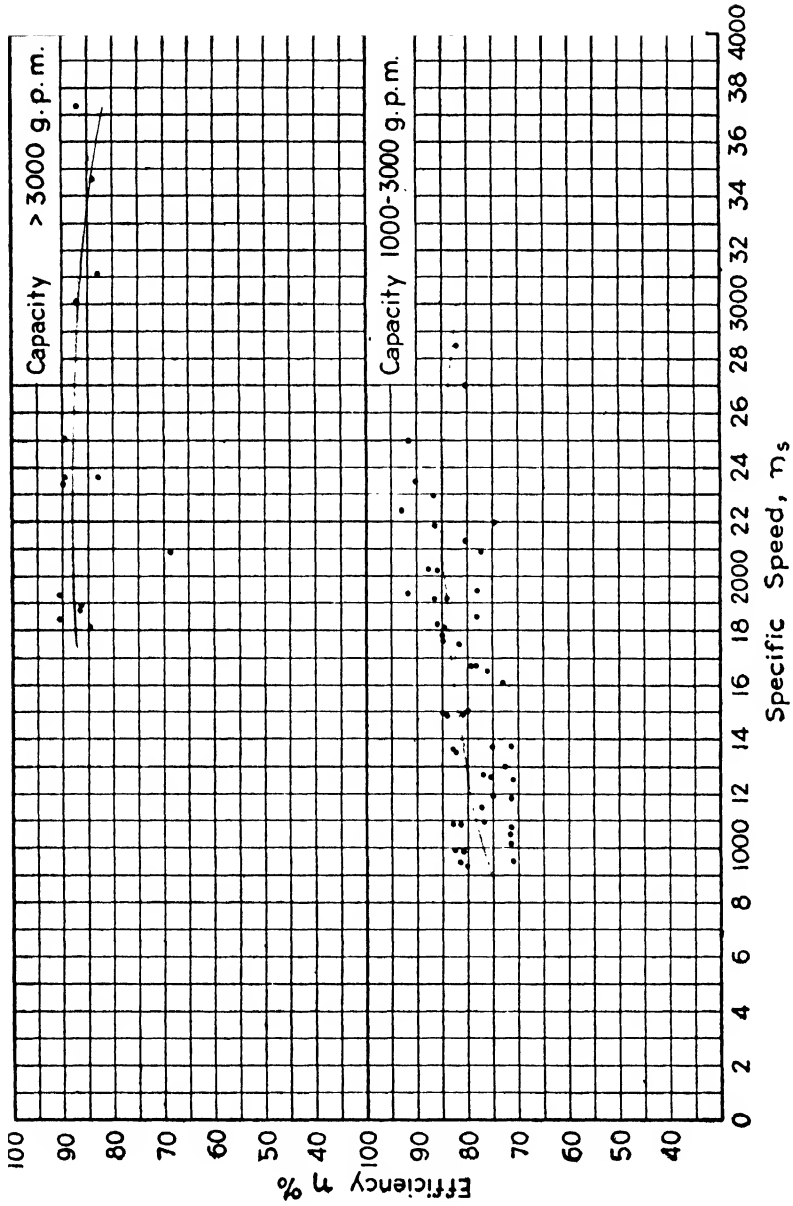
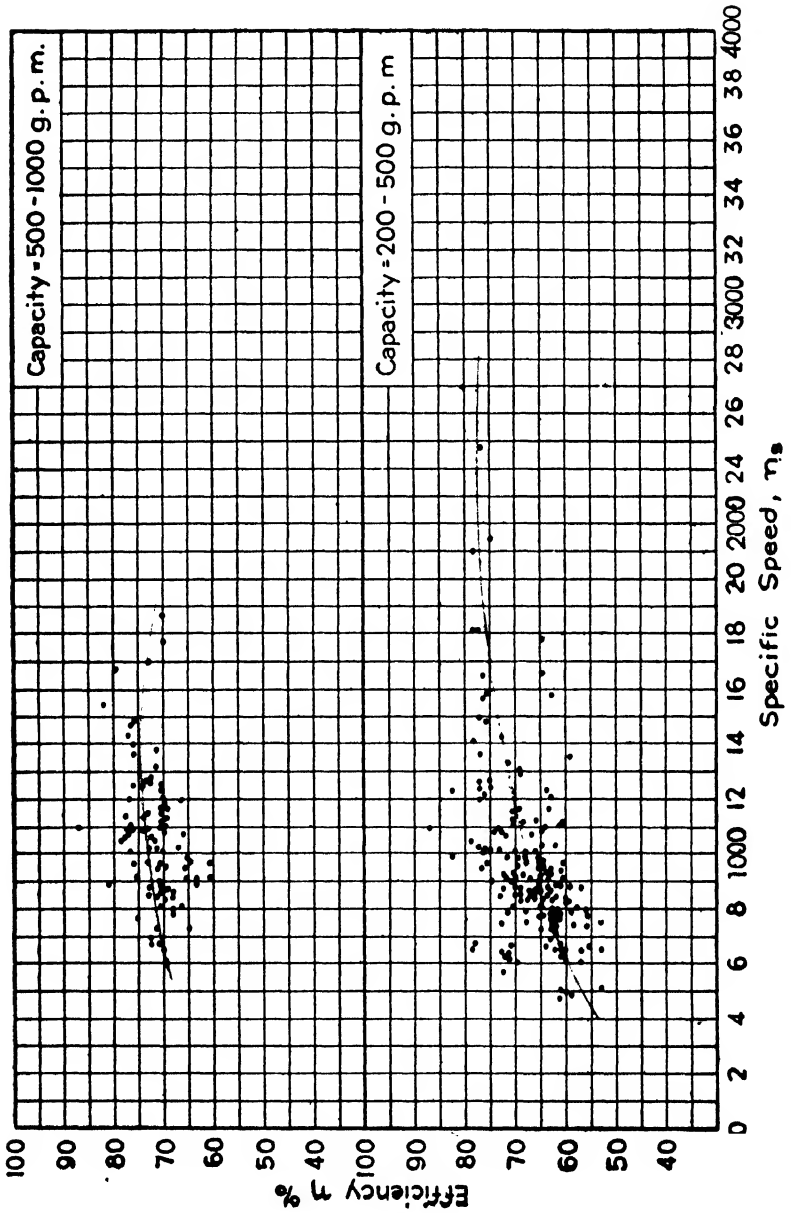


FIG. 4-11. Efficiency-specific speed points for various capacity ranges.



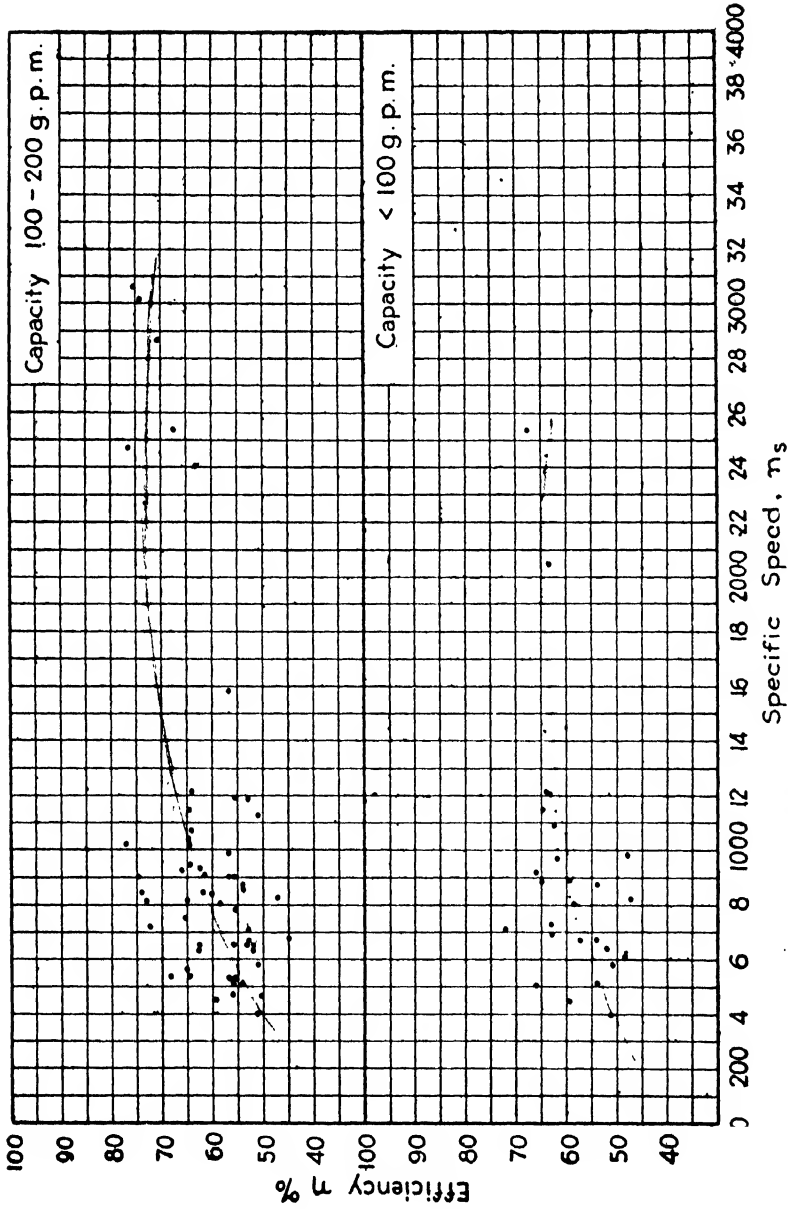


FIG. 4.11. Efficiency-specific speed points for various capacity ranges. (Continued.)

very well with the curve issued by the Worthington Pump & Machinery Corporation which is reproduced as Fig. 4-12.

The efficiency of pumps falls off very rapidly for specific speeds less than about 1000, because low specific speed impellers have long narrow vane passages which result in large fluid friction losses and greater disk friction losses. In addition, the amount of leakage is propor-

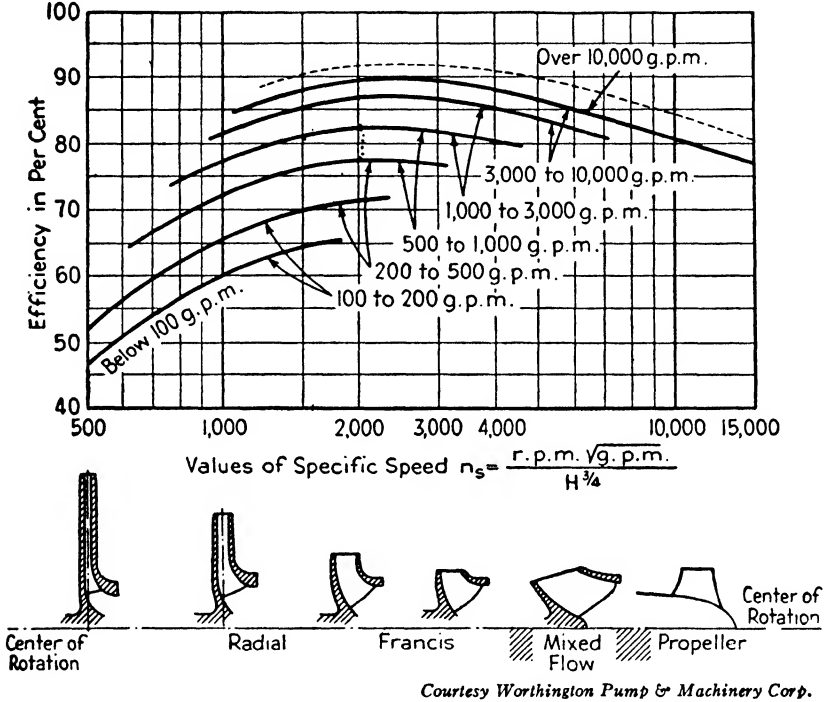


FIG. 4-12. Approximate relative impeller shapes and efficiencies as related to specific speed.

tionally greater as the leakage area is a greater percentage of the passage area for small flows and the pressure differential is greater.

For a given head and capacity it is desirable to use as large a specific speed as possible since this results in a smaller-diameter impeller and hence a smaller and cheaper pump. In general the efficiency will also be higher.

In Figs. 4-9, 4-10, and 4-11 the capacity of the double-suction stages is taken as one-half the pump capacity, i.e., the plotted points are reduced to the equivalent of single-suction impellers, as explained in Section 4-3. The pumps include both single- and multistage machines and, although the efficiency of the multistage units is generally slightly

lower than the single-stage, the difference is neither very great nor consistent.

4-6 Model Tests. It is desirable to be able to predict the efficiency to be expected from large pumps on the basis of tests made on smaller homologous pumps. In designing large pumps, as for water supply systems, tests are sometimes made on models with the aim of securing the best design. If the larger pump or prototype is homologous with the model and if the two have the same proportionate degree of surface roughness, it has been found that the prototype will have a slightly higher efficiency than the model.

The same problem is met in hydraulic turbine design. Various formulas have been developed in this field, and these are applied to pumps. One of the earlier equations developed was the Camerer formula:

$$E = 1 - (1 - e) \frac{0.12 + \frac{0.015}{\sqrt{(A_2/U_2D)D}}}{0.12 + \frac{0.015}{\sqrt{(A_2/U_2D)d}}} \quad 4.3$$

where e is the efficiency of the model

E is the efficiency of the prototype

d is the runner diameter of the model

D is the runner diameter of the prototype

A_2/U_2D is the ratio of the outflow area, A_2 , of the runner to the product of the wetted perimeter and the runner diameter, i.e., the ratio of the hydraulic radius of the exit area to the runner diameter.

This equation is complicated; it requires a knowledge of the dimensions of the impeller to get the hydraulic radius; and in addition the coefficients change with the wheel type. Moreover it is based upon friction losses alone, neglecting turbulence.

Professor L. F. Moody* developed an equation which includes the turbulence. Because of its simplicity, it has largely replaced the Camerer formula. This equation is

$$E = 1 - (1 - e) \left(\frac{d}{D}\right)^a \left(\frac{h}{H}\right)^b \quad 4.4$$

the symbols being the same as above with the addition that h is the

* L. F. Moody, "The Propeller Type Turbine," *Trans. A.S.C.E.*, 1926, Vol. 89, pp. 625, 690.

head of the model and H is the head of the prototype. It may be noted that this equation does not involve actual dimensions since the diameters appear as a ratio.

The exponents a and b are based upon experimental evidence. Professor Moody found that if $a = 0.25$ and $b = 0.1$ fairly satisfactory results were obtained. The head ratio term has very little effect even with large ratios so that b might be made zero. Professor W. S. Pardoe,* on the basis of work done on venturi meters found that the a exponent depends considerably on the surface roughness, and suggests that if both model and prototype are very smooth the Moody value of 0.25 is correct. If both surfaces have the roughness of sand-cast pipe, the exponent may fall to 0.15. He suggests an average value of 0.20 for most cases. If the model is smooth and the prototype rough, there may be no increase in efficiency. In fact there may be a stepdown. Professor Pardoe uses 0.125 for the b exponent. Since this exponent has little effect in either case, it does not make much difference whether 0.10 or 0.125 is used.

Extreme care must be used to get accurate tests and to insure that both model and prototype have the same proportionate surface roughness. In some cases the results obtained have been quite satisfactory, whereas in others they have been rather disappointing.†

PROBLEMS

4.1 Determine the specific speeds of the following single-stage pumps and specify the type of pump which would probably be used for each.

Pump	R.p.m.	G.p.m.	Total Head — Feet
<i>a</i>	1,150	3,500	100
<i>b</i>	885	12,000	15
<i>c</i>	675	20,000	50
<i>d</i>	625	9,000	18

Ans. (a) 2155; (b) 12,710; (c) 5080; (d) 6800.

4.2 A six-stage pump delivers 1500 g.p.m. against a net pressure rise of 700 lb. per sq. in. What is the specific speed if it rotates at 1750 r.p.m.?

Ans. 1020.

* J. D. Scoville, "Comparative Characteristics of Fixed- and Adjustable-Blade Axial-Flow Pumps," *A.S.M.E. Trans.*, August, 1942, p. 599, and discussion by W. S. Pardoe, p. 603.

† R. W. Angus, "An improved Technique for Centrifugal-Pump-Efficiency Measurements," *A.S.M.E. Trans.*, January, 1941, p. 13, and discussions by Messrs. Babb, Pardoe, White, and Angus; L. M. Davis, "Model and Prototype Tests," *Trans. A.S.C.E.*, 1941, Vol. 106, p. 353, and ensuing discussions.

4-3 A pump is required to deliver 1200 g.p.m. against a head of 300 ft. at a motor speed of 1150 r.p.m. Would a two-stage pump probably be more efficient than a single-stage? Why?

Ans. Yes.

4-4 The following data on model and prototype water works single-stage pumps for the Victoria Park Station of the City of Toronto is taken from "An Improved Technique for Centrifugal-Pump-Efficiency Measurements," by Professor R. W. Angus, *A.S.M.E. Trans.*, January, 1941. Check the prototype efficiencies using both the Moody and Pardoe formulas.

Capacity m.g.d.	$\frac{D}{d}$	Head-Feet per Stage		Efficiency Per Cent	
		Prototype	Model	Prototype	Model
12	1.48	54	67.0	90.2	90.0
24	1.88	82	92.8	91.5	89.6
48	2.63	82	68.5	93.0	89.6
30	1.94	135	91.8	91.8	90.7

4-5 It is desired to pump 2800 g.p.m. of water against a head of 175 ft. What approximate operating speed would give the best efficiency?

Ans. About 2000 r.p.m.

4-6 A mixed-flow pump operating at 600 r.p.m. and delivering 15,000 g.p.m. has a specific speed of 4750 r.p.m. The suction flange is 24 in. in diameter and has an absolute pressure of 10 lb. per sq. in. The discharge flange is 22 in. in diameter, and its centerline is 1 ft. above the suction centerline. What discharge pressure in pounds per square inch absolute would you expect to find?

Ans. 26 lb. per sq. in.

4-7 Using the relationships of speed with the head and flow developed in Section 3-15 and substituting them in the specific speed formula, show that the specific speed of an impeller is unchanged if the speed of rotation is changed from n to n' r.p.m.

CHAPTER 5

PERFORMANCE CURVES AND CAVITATION OF PUMPS

5.1 Effect of Speed on Performance Curves. It is frequently desirable to be able to predict the performance of a pump when operating at speeds other than that at which it is tested. The basic relationships applicable to this were developed in Section 3.15. They are: (a) the capacity is proportional to the speed; (b) the developed head is proportional to the speed squared; (c) the brake horsepower is proportional to the cube of the speed; and (d) the efficiency remains approximately constant.

The top curve of Fig. 5.1 represents the characteristic curve of a pump operating at a speed n_a . If it is desired to predict the corresponding curve for a reduced speed of n_b , any point on the new curve has its head reduced as the speed squared, or $H_b = H_a \left(\frac{n_b}{n_a}\right)^2$; and its flow reduced directly with the speed, i.e., $Q_b = Q_a \frac{n_b}{n_a}$.

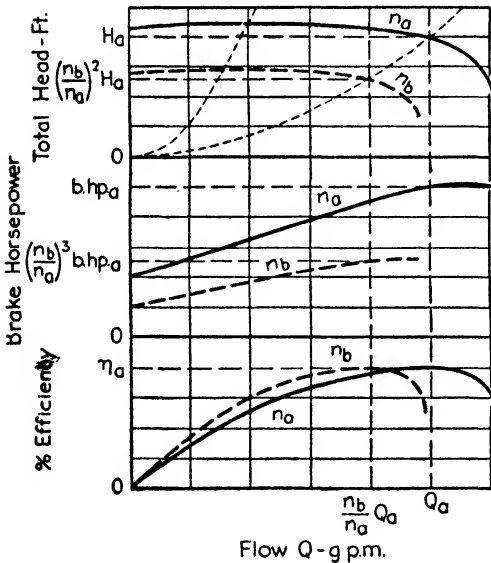


FIG. 5.1. Effect of speed changes on the head, horsepower, and efficiency.

These two values determine the corresponding point on the new curve for the speed n_b . It may be observed that corresponding points on the two curves will lie on parabolas passing through the zero head and zero capacity point. Two of these parabolas are shown in short dashes on the figure.

The actual head curves follow these relationships closely over a fairly wide speed range, but the varying losses must be considered if

The actual head curves follow these relationships closely over a fairly wide speed range, but the varying losses must be considered if

the change is large. It should be emphasized that it is the head or pressure *rise* and not the discharge pressure which follows the above relationships.

The upper brake horsepower curve of Fig. 5-1 is for a pump operating at a speed of n_a . To predict the corresponding curve for a reduced speed n_b , all points should have the horsepower reduced as the speed cubed, or $b.hp._b = b.hp._a \left(\frac{n_b}{n_a}\right)^3$, and the flow is reduced directly with the speed n_b/n_a as before. The horsepower curve $b.hp._b$ for the reduced speed n_b is shown on the figure.

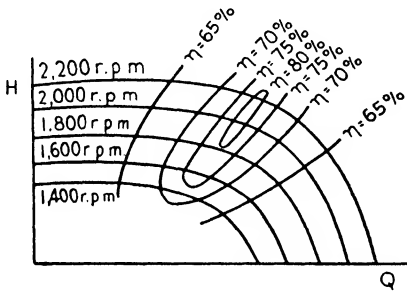


FIG. 5-2. Head-capacity curves for various speeds with curves of constant efficiency superimposed.

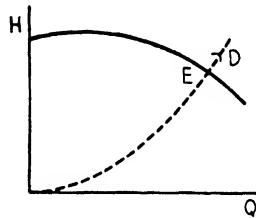


FIG. 5-3. Characteristic curve and design point D .

Since the efficiency remains practically constant for small speed changes, points on the efficiency curve for speed n_a move horizontally to the corresponding new values of Q for the lower speed n_b as shown in the lower portion of Fig. 5-1.

Figure 5-2 shows a series of head-capacity curves for several speeds with curves of points having the same efficiency superimposed. Curves of this type show the complete performance of the pump at any practical speed for a given suction lift.

Occasionally a pump on test may fail to develop sufficient head at the design capacity. If the pump is turbine driven, this shortcoming may be remedied by changing the setting of the turbine governor to increase the speed until the desired head is obtained. This may be done by trial but it may be necessary to know the approximate speed required in advance to be sure that stress limits are not exceeded.

Let the characteristic curve of Fig. 5-3 represent the test curve and the point D represent the design condition to be met. To estimate the required speed, the head of the point on the test curve corresponding to point D must be found. If a parabola similar to those shown

in the upper portion of Fig. 5.1 is drawn through point D it will intersect the test curve at point E . Since the heads at points D and E are known, the new speed is given by $n^2 = n_{\text{test}}^2 (H_D/H_E)$. The new efficiency will be that corresponding to point E and the new brake horsepower is given by $\text{b.hp.}_D = \text{b.hp.}_E (n^3/n_{\text{test}}^3)$.

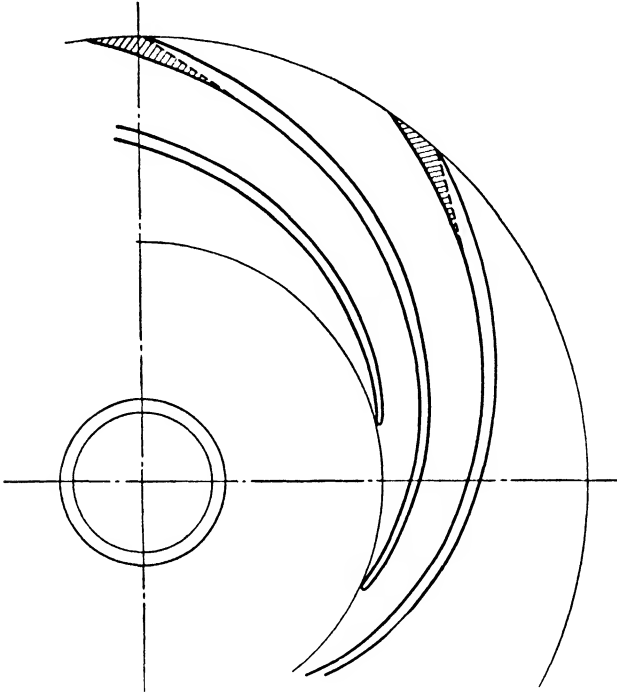


FIG. 5.4. Alteration of impeller vanes to increase head.

5.2 Effect of Impeller Changes on Performance Curves. Should the developed head at the design capacity be too high, either the speed of the unit may be reduced or the impeller diameter D_2 may be turned down as described in Section 8.5. When the impeller outside diameter is reduced the radial outlet area is decreased but, since the impeller inlet has not been altered, the flow through the impeller will be unchanged and the radial outlet velocity V_{r_2} is increased. The impeller tip speed u_2 is reduced, so the effect is to increase the absolute outlet angle α'_2 of the fluid. The drop in head is then due to the reduction in the tip speed and the change in the outlet angle of the fluid. The net result on the performance curves has been found to be similar to the relationships developed in the previous section if the

impeller diameter D_2 is substituted for the speed n , i.e., $Q' = Q \frac{D_2'}{D_2}$;
 $H' = H \left(\frac{D_2'}{D_2}\right)^2$; b.hp.' = b.hp. $\left(\frac{D_2'}{D_2}\right)^3$, and the efficiency remains approximately constant.

If the developed head is slightly deficient at the design capacity (2 or 3 per cent) it may be brought up to the required value by filing away the trailing side of the vane at the outlet as shown by the shaded area in Fig. 5-4. This alteration increases the average outlet angle β_2 , thereby increasing the tangential component of the absolute outlet velocity V'_{u_2} . It will be seen from Eq. 3-5 that this will increase the head. The change is usually accompanied by a slight increase in efficiency.

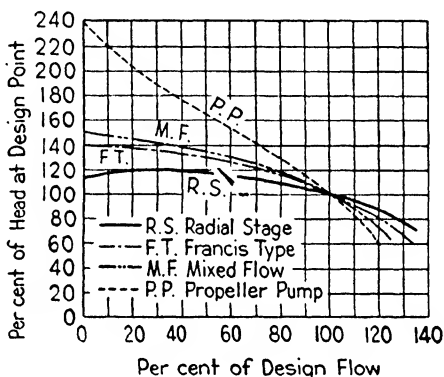


FIG. 5-5. Effect of impeller type on the characteristic curve shape.

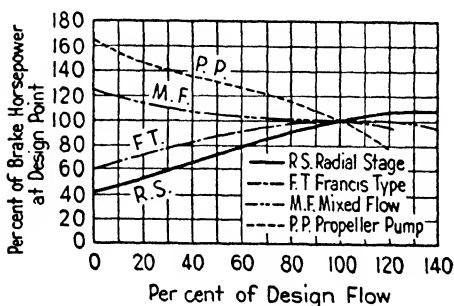


FIG. 5-6. Effect of impeller type on the brake horsepower curve shape.

5.3 Performance Curves for Various Types of Pumps. The various types of impellers discussed in Chapter 4, as built commercially, have

typically shaped performance curves when placed on a percentage basis. Figures 5-5, 5-6, and 5-7 show the head, brake horsepower, and efficiency respectively for these impellers plotted on this basis.

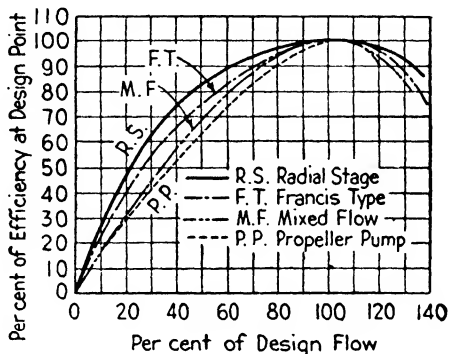


FIG. 5-7. Effect of the impeller type on the efficiency curve shape.

It should be realized that all the impellers of a particular class do not have exactly the percentage values shown for a given percentage flow, since the shape of the curve is dependent upon the vane angles, etc., but the general shape of the curves follows those shown.

The curves are interesting and of value in that they show comparatively the difference in performance of the various types. It should be noted that the higher specific speed impellers have steeper head curves and that the efficiency curves drop more rapidly on each side of the design point. This is due in part to the poor guidance given to the water in passing through the impellers.

5-4 Effect of Viscosity on Performance Curves. The great majority of pumps handle water. However, in the chemical industries many pumps are built to handle liquids whose viscosity is greatly different from water. Viscous fluids have high internal resistance to flow, so the frictional losses are increased and the disk friction is much greater. Hence, the developed head is reduced and the brake horsepower increased. There are very few published data* which may be used to evaluate the magnitude of the viscosity effect. However, Fig. 5-8

* A. J. Stepanoff, "Pumping Viscous Oils with Centrifugal Pumps," *Oil and Gas Journal*, May 9, 1940; M. D. Aisenstein, "Characteristics of the Centrifugal Oil Pump," *A.S.C.E. Trans.*, 1930, p. 425; R. L. Daugherty, "Investigation of the Performance of Centrifugal Pumps when Pumping Oil," *Goulds Pumps, Inc., Bulletin 126*; R. L. Daugherty, "A Further Investigation of the Performance of Centrifugal Pumps when Pumping Oil," *Goulds Pumps, Inc., Bulletin 130, 1926* (both *Goulds bulletins* out of print).

illustrates the effect of various viscosities on the characteristic and horsepower curves for one particular pump.

5-5 Cavitation. If the pressure at any point inside a pump drops below the vapor pressure corresponding to the temperature of the liquid, the liquid will vaporize and form cavities of vapor. The vapor

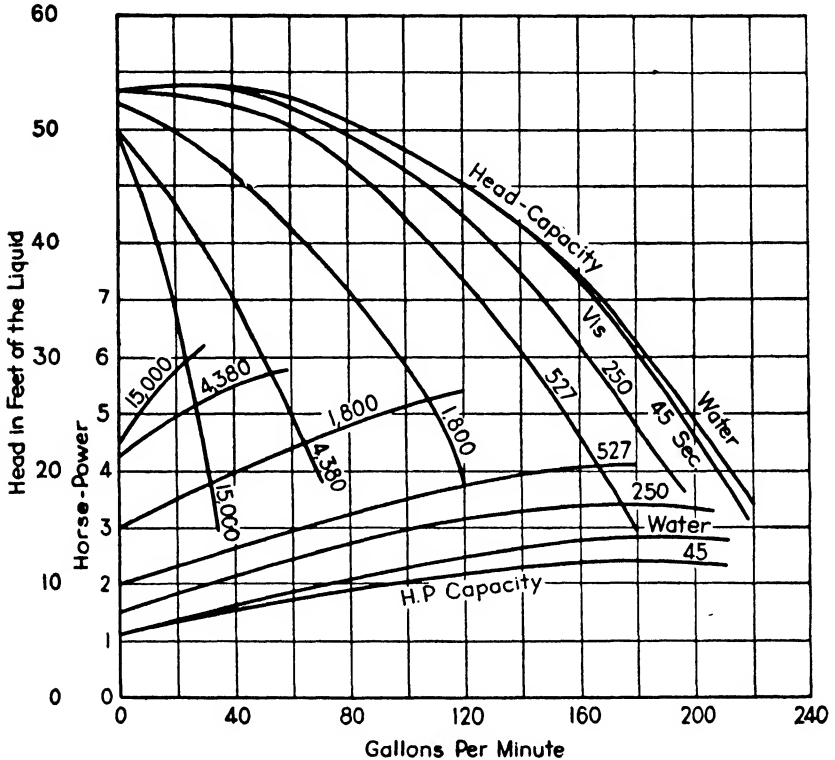


FIG. 5-8. Effect of viscosity on the head and horsepower curves for a pump handling oils at 1450 r.p.m. The numbers on the curves give the viscosity in Saybolt Universal Seconds. (Taken from Bulletin 401, "The Centrifugal Pump," Goulds Pumps, Inc.)

bubbles are carried along with the stream until a region of higher pressure is reached when they collapse or implode with a tremendous shock on the adjacent walls. This phenomenon is called cavitation.

The sudden inrush of liquid into the cavity created by the collapsed vapor bubbles causes mechanical destruction, sometimes apparent as a boring action which might be called erosion. Chemical reaction between the gases and metal also occurs and results in corrosion and additional destruction of the metal. Another undesirable feature is

the accompanying noise, varying in different units from low rumbling to loud knocks and a resultant heavy vibration of the unit.

The energy required for accelerating the water to the high velocity in suddenly filling the hollow spaces is a loss, and cavitation will therefore be accompanied by a reduced efficiency. Water at 70° F. increases in volume about 54,000 times when vaporized. Consequently it is not surprising that pumps operating with cavitation also show a reduction in capacity.

Cavitation will occur mainly at the vane inlet portion of the pump impeller, on both the vanes and the sidewalls. The erosion and wear due to cavitation will not occur at the point of lowest pressure where the gas pockets are formed, but farther upstream at the point where the implosion occurs.

5-6 Suction Head or NPSH. Since cavitation occurs when the absolute pressure of the liquid reaches its vapor pressure, it is obvious that the phenomenon is intimately related to the pump suction head. The suction head H_{sv} of a pump is the equivalent total head at the pump centerline corrected for vapor pressure.

The following four factors enter into its determination: (1) H_p is the head corresponding to the absolute pressure on the surface of the liquid from which the pump draws. This will be the atmospheric pressure corresponding to the altitude of the unit if the tank is open, or the absolute pressure in the heater or closed tank from which the pump takes liquid. (2) H_z is the height in feet of the fluid surface above or below the impeller centerline. (3) H_{vp} is the head corresponding to the vapor pressure of the liquid at the existing temperature. (4) H_f is the head lost because of friction and turbulence between the surface of the liquid and the pump suction flange.

The suction head is the algebraic sum of these factors. Any term which would tend to reduce the total suction head is considered to be negative. If the level of the surface is above the impeller centerline it is considered positive; if below, negative. The vapor pressure and loss due to friction and turbulence are always negative since they decrease the total suction head. Thus, the equation for the suction head is

$$H_{sv} = H_p \pm H_z - H_{vp} - H_f \quad 5-1$$

It may be noted that the suction velocity head $V_{su}^2/2g$ is not subtracted in Eq. 5-1. H_{sv} , which is the net suction head, will appear in two forms at the suction flange, i.e., as velocity and pressure heads.

Equation 5-1 gives the total head and not the static pressure head, so the $V_{su}^2/2g$ term is not subtracted.

In the chemical industries where liquids must be pumped in many instances at or near their boiling points, the term H_{sv} is known as the net positive suction head over the vapor pressure and designated by the letters *NPSH*.*

If a pump is handling cold water drawn from an open tank at sea level with no friction or turbulence losses, the maximum lift would approach 34 ft. These ideal conditions are never met in practice and the maximum lift will be much less than this.

In designing a pump installation and purchasing a pump there are two types of suction head or *NPSH* to be considered. One is the available suction head of the system and the other is the required suction head of the pump to be placed in the system. The former is determined by the plant designer and is based upon the condition of the liquid handled, the pump location, etc.; the latter is specified by the pump manufacturer, and is usually based upon test results of the actual pump or a similar one.

It is necessary that the available head of the system be equal to or greater than the required suction head in order to avoid cavitation difficulties. In many instances this requires close cooperation between the plant designer and the pump manufacturer, and may involve economic studies before a final solution is reached.

The factors upon which these two suction heads are based and the methods of determining them will now be considered.

5-7 Available Suction Head. The available suction head may be calculated by means of Eq. 5-1. Table 5-1 gives the vapor pressure and the specific gravity of water. More complete tables may be found in reference books. The head corresponding to a given pressure

is $\frac{P}{\gamma}$ or $\frac{144p}{62.34sg} = \frac{p \times 2.31}{sg}$, where the pressure p is in pounds per square inch. The atmospheric pressures corresponding to various altitudes may be taken from Fig. 11-4. The determination of the available suction head may best be illustrated by a few examples.

(a) The most common condition is that of pumping water from a sump, as illustrated diagrammatically in Fig. 5-9. Data: Water temperature 90° F., sea level, friction and turbulence loss in the suction line 1 ft., suction lift 8 ft. What is the available suction head?

From Table 5-1 the vapor pressure corresponding to 90° F. is 0.698 lb.

* L. H. Garnar, "NPSH and the Centrifugal Pump," *Refiner & Natural Gasoline Manufacturer*, July, 1942, p. 196.

TABLE 5-1

VAPOR PRESSURE, SPECIFIC WEIGHT, AND SPECIFIC GRAVITY OF WATER

Temperature, ° F.	Vapor Pressure		Specific Weight, lb. per cu. ft.	Specific Gravity
	in. Hg	lb. per sq. in.		
60	0.522	0.256	62.34	1.000
70	0.739	0.363	62.27	0.999
80	1.032	0.507	62.19	0.998
90	1.422	0.698	62.11	0.996
100	1.933	0.949	62.00	0.995
110	2.600	1.275	61.84	0.993
120	3.446	1.692	61.73	0.990
130	4.525	2.223	61.53	0.987
140	5.881	2.889	61.39	0.985
150	7.569	3.718	61.19	0.982
160	9.652	4.741	61.01	0.978
170	12.199	5.992	60.79	0.975
180	15.291	7.510	60.57	0.972
190	19.014	9.339	60.36	0.968
200	23.467	11.526	60.13	0.965
210	28.755	14.123	59.89	0.961
220	34.992	17.186	59.64	0.957
230	42.308	20.780	59.39	0.953
240	50.837	24.969	59.10	0.948
250	60.725	29.825	58.83	0.944

per sq. in. abs. and the specific gravity is 0.996. The terms for Eq. 5-1 then are:

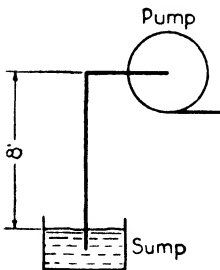


FIG. 5-9.

$$H_p = 14.7 \text{ lb. per sq. in. abs.}$$

$$= \frac{14.7 \times 2.31}{0.996} = 34.0 \text{ ft.}$$

$$H_z = -8 \text{ ft. (negative because it is a lift)}$$

$$H_{vp} = \frac{0.698 \times 2.31}{0.996} = 1.6 \text{ ft.}$$

$$H_f = 1 \text{ ft.}$$

$$\text{Available suction head } H_{sv} = H_p - H_z - H_{vp} - H_f$$

$$= 34.0 - 8.0 - 1.6 - 1.0 = 23.4 \text{ ft.}$$

(b) A condensate pump at sea level draws water from a condenser in which a 27.5-in. vacuum is maintained (Fig. 5-10). The friction

and turbulence loss in the piping between the two is estimated to be 4 ft. What minimum height of water level in the condenser above the pump centerline must be maintained if the required suction head of the pump is 12 ft. for the maximum capacity of the pump?

The condenser absolute pressure is $30.0 - 27.5 = 2.5$ in. of mercury or 1.227 lb. per sq. in. abs. The corresponding specific gravity taken from Table 5-1 is approximately 0.9933. Then

$$H_p = H_{vp} = \frac{1.227 \times 2.31}{0.9933} = 2.86 \text{ ft.}$$

$$H_f = 4 \text{ ft.} \quad H_{sv} = 12 \text{ ft.}$$

$$H_{sv} = H_p + H_z - H_{vp} - H_f = 12.0 = 2.86 + H_z - 2.86 - 4.0$$

$$H_z = 16 \text{ ft.}$$

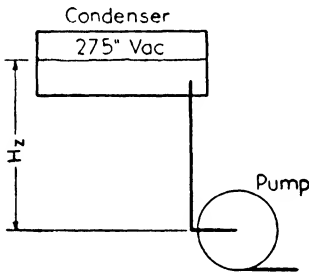


FIG. 5-10.

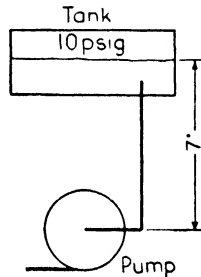


FIG. 5-11.

(c) Gasoline at 100°F. is being drawn from a closed tank having a pressure of 10 lb. per sq. in. ga. in a plant located 3000 ft. above sea level. The level of the gasoline in the tank is 7 ft. above the pump centerline, as shown in Fig. 5-11. The suction line friction and turbulence head losses amount to 2 ft. The vapor pressure of the gasoline is 7 lb. per sq. in. abs. and the specific gravity is 0.72. What is the available suction head of the system?

From Fig. 11-4 the atmospheric pressure for an altitude of 3000 ft. is 27 in., which corresponds to 13.22 lb. per sq. in. abs. The pressure at the surface of the gasoline is then $13.22 + 10.00$ or 23.22 lb. per sq. in. abs. Hence

$$H_p = \frac{23.22 \times 2.31}{0.72} = 74.5 \text{ ft.}$$

$$H_s = +7 \text{ ft. (plus because it is a positive head)}$$

$$H_{vp} = \frac{7 \times 2.31}{0.72} = 22.5 \text{ ft.} \quad H_f = 2 \text{ ft.}$$

Then

$$H_{av} = H_p + H_s - H_{vp} - H_f = 74.5 + 7.0 - 22.5 - 2.0 = 57.0 \text{ ft.}$$

In determining the available suction head it is imperative that the worst conditions be assumed in every case. The maximum liquid temperature expected, the maximum lift or the minimum level of the liquid above the pump, and a generous allowance for pipe friction and turbulence should be used. The responsibility of the plant designer ends at the suction flange. Any losses or pressure reductions occurring in the pump itself are taken care of by the required suction head as determined by the pump manufacturer.

Where the available head is less than that required for a pump of given size two alternatives are open. One is to change the plant layout, raising the tanks or heaters from which the liquid is drawn or decreasing the suction lift, thereby increasing the available suction head. This may involve considerable additional expense. The other alternative would be to use a pump of larger size and run it at partial loads or speeds because the required suction head would then be reduced. This involves a larger initial investment and increased operating costs due to a lowered efficiency. The final choice should be based upon an economic study of the two alternatives.

5-8 Required Suction Head. The required suction head of a pump includes the velocity head at the suction flange plus the head losses occurring between the suction flange and the impeller. It must also be large enough to care for the reduction in pressure due to sudden changes in velocity (either in magnitude or direction). A few of the factors upon which the required suction head depends will now be considered.

By the airfoil theory the pressure distribution on the two sides of an airfoil section moving through a fluid shows a pressure reduction on one side and a pressure rise on the other. The inlet edge of the impeller vanes acts in a manner similar to an airfoil giving a local pressure rise on the leading face and a pressure reduction on the trailing face (see Fig. 5-12). Owing to the pressure rise inside the impeller caused by the centrifugal action on the liquid, the pressure reduction will disappear in a short radial distance from the inlet edge.

Pressure reductions may also occur at points where sudden changes in the direction of flow occur. One point where this condition exists is at point *B* in Fig. 5-13; there the side plate of the impeller has a small radius near the inlet. The same action occurs at the vane inlet edge. The pressure at point *C* in Fig. 5-14, which is the stagnation point where the velocity is zero, will be relatively large, but at points

D and *E* it will be lower because of the flow of liquid past the edge. It should be realized that points *D* and *E* do not necessarily coincide

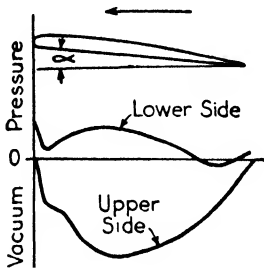


FIG. 5-12. Airfoil action and pressure distribution.

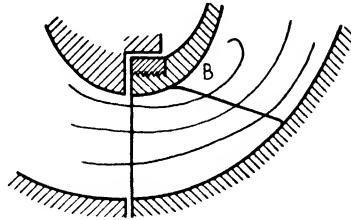


FIG. 5-13. Pressure reduction at impeller inlet.

with the point of lowest pressure owing to the airfoil action of the vane.

To the above factors affecting pressure reduction at the vane inlet must be added the effect of surface friction. It will be evident that a smoothly finished impeller will aid in reducing the pressure drop and hence the cavitation.

From this discussion it is evident that it is not easy to express the pressure reduction by a simple formula. The pressure reduction should have a definite relation to the relative inlet velocity v_1 for the following reasons.

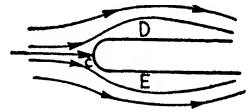


FIG. 5-14. Pressure reduction at vane inlet edge.

The total lift of an airfoil is given by

$$L = \delta \frac{\gamma}{g} \frac{v_1^2}{2} F$$

where δ is a coefficient dependent on the profile and the angle of attack

F is the area of the profile.

It is reasonable to assume then that the pressure reduction due to the airfoil action at the inlet of a given vane is proportional to v_1^2 , or the pressure reduction in feet of head equals $C' \frac{v_1^2}{2g}$. The pressure reduction in feet due to changes in direction equals $C'' \frac{v_1^2}{2g}$ and finally the friction loss follows the same law, equaling $C''' \frac{v_1^2}{2g}$. The total head re-

duction due to all these factors then may be taken as being equal to $C \frac{v_1^2}{2g}$. The actual value of C is dependent on so many factors, such as shape of the impeller, shape of vane tip, and smoothness of finish, that it cannot be predicted accurately, but some valuable conclusions may be drawn from the above equation.

For a particular pump v_1 increases with an increase in flow, both when it is operating at constant speed of rotation or when the speed is increased. Actual tests show that cavitation will occur for approximately the same value of v_1 when the operating conditions are varied.

The *NPSH* is measured at the pump by subtracting the gage vapor pressure head in feet corresponding to the temperature of the liquid at the point of measurement from the gage pressure head in feet taken at the suction flange, corrected to the pump centerline for horizontal shaft pumps or to the entrance eye of the suction impeller for vertical shaft pumps, and adding the velocity head at the point of measurement.

To illustrate this, assume a horizontal shaft pump handling water at 150° F. The suction nozzle is 1 ft. below the pump centerline, the pressure at this point being 32 lb. per sq. in. gage and the velocity 9 ft. per sec. What is the pump *NPSH*? From Table 5-1, the absolute vapor pressure of water at 150° F. is 3.718 lb. per sq. in. and the corresponding specific gravity is 0.982. Hence the gage vapor pressure head in feet is $\frac{2.31(3.718 - 14.7)}{0.982} = -25.8$ ft. The head corre-

sponding to the nozzle suction gage pressure is $\frac{2.31 \times 32}{0.982} = 75.3$ ft.

Correcting this latter value to the pump centerline gives 76.3 ft. The velocity head corresponding to a 9-ft.-per-sec. velocity is $V_{su.}^2/2g = \frac{9^2}{2 \times 32.2} = 1.26$ ft. Hence the *NPSH* = 76.3 - (-25.8) + 1.26 = 103.36 ft.

When cavitation occurs the flow through the pump is decreased as a result of the formation of the vapor bubbles. The efficiency also drops off sharply since energy is consumed in the formation of these bubbles. Hence the presence of cavitation considerably alters the shape of the performance curves.

Curve *AB* of Fig. 5-15 is a typical head-capacity curve of a pump as tested with a low suction lift. Curve *CD* is the corresponding efficiency curve. If the suction lift is increased (by throttling the suction

line) and the pump retested, the head curve from shut-off at *A* to a point *E* will be approximately the same as before. As the capacity is increased beyond *E* the head rapidly drops off to zero as shown by the broken line *EF*. When point *E* is reached cavitation has started, and at *F* it is complete. The dashed curve *GH* shows the effect on the efficiency curve. If the suction lift is again increased, a similar result is obtained at a lower capacity as shown by the dashed curves *JK* and *LM*.

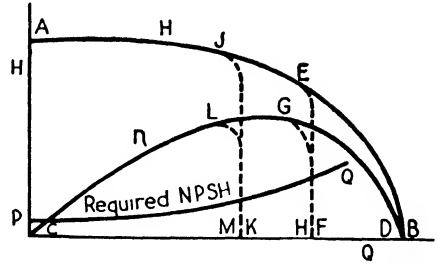


FIG. 5-15. Effect of cavitation on performance curves.

By plotting the suction heads as measured at the suction flange and corrected to the pump centerline against the flows at which cavitation starts, a curve *PQ* of required suction head against capacity for the particular pump is obtained. This curve should be used in connection with the available suction head to check whether the pump will operate satisfactorily, as outlined in the previous section. It is interesting to note that its shape is very nearly parabolic, i.e., the required suction head increases approximately with the square of the flow.

5.9 Factors Affecting Cavitation. To prevent cavitation the suction pressure must be kept above the critical pressure at which it starts. The following points should be kept in mind.

- (1) The barometric pressure at the point of installation has a definite influence on the suction lift that can be permitted and it must be considered for installations at high altitudes.
- (2) The liquid temperature should be as low as possible, as the vapor pressure increases with the temperature, thus decreasing the available suction lift.
- (3) The velocities in the suction line should be kept low and sharp bends should be avoided to keep friction and turbulence losses at a minimum.
- (4) The relative inlet velocity v_1 should be kept low. This means that the specific speed should be kept low when danger of cavitation is present. Francis-type impellers with the inlet vane edge brought close to the impeller hub will also help in reducing v_1 and the danger of cavitation.
- (5) Careful rounding of inlet edges to an airfoil shape, combined with a small inlet vane thickness, will also reduce cavitation.

(6) There should be a sufficient number of vanes to give good guidance to the water and to keep the fluid pressure on the vanes low.

(7) Sharp radii of the impeller shroud near the inlet (radius at B , Fig. 5-13) should be avoided.

(8) The impeller should have a smooth finish, particularly near the inlet.

(9) It has been found that the introduction of small amounts of air into the suction line will reduce the noise and erosion. This method of reducing cavitation should be used only if trouble develops in the field. Its beneficial effect is explained by the fact that the air acts as a cushion to soften the impact of the sudden collapse of the bubbles after they have formed and reached the point of higher pressure. This cure has been used on water turbines and does not seem to affect the efficiency measurably.

5-10 Cavitation Parameters. It is desirable to be able to predict the occurrence of cavitation and several relationships have been found to be quite satisfactory in this respect. The basis of these relationships is the Thoma-Moody Similarity Law which applies to both pumps and hydraulic turbines.* As pointed out in Section 5-8, cavitation is closely linked with the square of the relative inlet velocity, v_1^2 . The relative inlet velocity in turn is proportional to the r.p.m. or peripheral speed u_2 . Hence, cavitation is related to the peripheral speed squared, u_2^2 . As noted in Chapter 3, the total head H is also proportional to u_2^2 . Therefore, the suction head H_{sv} is related to the total head, and the ratio H_{sv}/H , designated as σ , may be used to predict cavitation in a given pump.

If a pump is tested with various suction heads, a curve of efficiency (or percentage drop in efficiency) may be plotted against σ as shown in Fig. 5-16. This figure illustrates the shape of curve obtained and shows the close agreement between σ and loss of efficiency for various operating speeds. Similar results will be obtained for a series of homologous pumps.

The point where the efficiency first begins to drop (at $\sigma = 0.175$ in Fig. 5-16) indicates the beginning of cavitation and is the minimum safe operating value of σ . The value of σ where the curve is vertical (at $\sigma = 0.09$ in Fig. 5-16) represents the absolute minimum value of σ at which it is possible to operate. Obviously, the pump should

* H. B. Taylor and L. F. Moody, "The Hydraulic Turbine in Evolution," *Engineers & Engineering*, Vol. 39, No. 7, July, 1922, pp. 241-259; D. Thoma, "Experimental Research in the Field of Water Power," First World Power Conference, London, 1924.

be operated continuously only when σ is above the minimum safe operating value.

When a new pump design is perfected, the value of σ at which cavitation starts must be found experimentally and this value may be applied to other similar pumps.

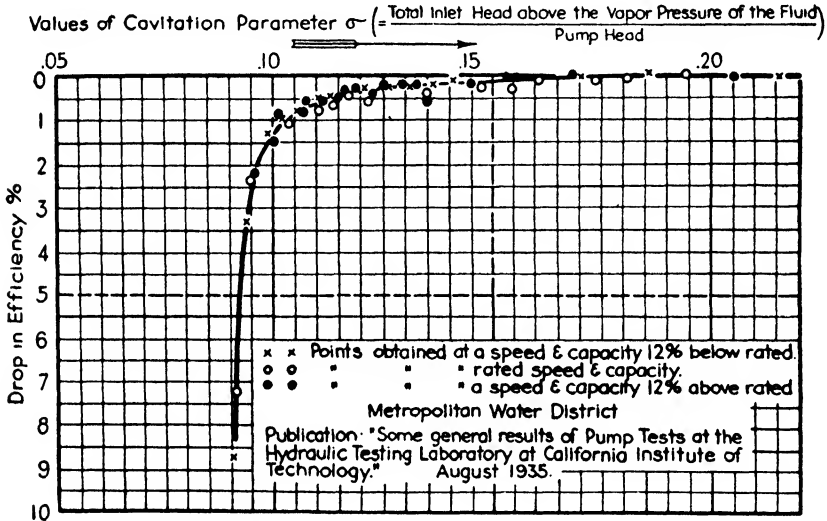


FIG. 5-16. Relationship between loss in efficiency and the cavitation parameter σ for a pump operating at various speeds.

Messrs. G. F. Wislicenus, R. M. Watson, and I. J. Karassik* develop a suction specific speed S which equals $\frac{n\sqrt{Q}}{H_{sv}^{3/4}}$ in order to correlate the minimum safe values of σ for similar operating conditions. Constant values of S indicate similar inlet flow conditions of pumps. They also show that the relationship between the minimum safe value of σ , specific speed, and S is $\sigma = \left(\frac{n_s}{S}\right)^{4/3}$. Figure 5-17 illustrates this relationship between σ , S , and n_s for pumps and the agreement with test results. Mr. G. F. Wislicenus† states:

The cavitation limits for safe operation of various types of centrifugal pumps, therefore, may be estimated by their respective S values in accordance with the following tabulation:

* "Cavitation Characteristics of Centrifugal Pumps Described by Similarity Considerations," *A.S.M.E. Trans.*, January, 1939, pp. 17-24.

† Marks Handbook, McGraw-Hill, 4th ed., pp. 1898-1900.

- Single suction pumps with overhung impeller $S \leq 7,500$ to $10,000$
- Single-stage pumps with shaft running through impeller inlet (for double-suction pumps use half capacity) $S \leq 6,500$ to $9,000$
- High-pressure multistage pumps (single suction) $S \leq 5,500$ to $7,500$
- High-pressure multistage pumps with special first-stage impeller (single suction) $S \leq 7,500$ to $9,000$

The higher values of these limits can be used only for specially designed pumps and favorable inlet flow conditions.

It is necessary to exercise caution in applying similarity considerations regarding cavitation outside the field of common experience.

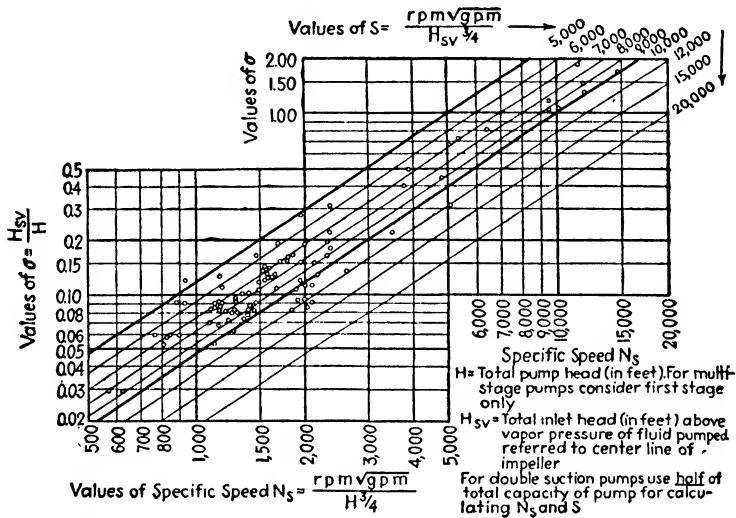


FIG. 5-17. Cavitation limits of pump operation. (Taken from Marks' *Mechanical Engineers' Handbook*, McGraw-Hill.)

The Standards of the Hydraulic Institute contain charts giving the maximum specific speeds that should be used for given total and suction heads or lifts. Head is plotted against specific speed and the curves cover a range from suction lifts (negative heads) of 20 or 25 ft. to positive heads of 15 ft. They are reproduced as Fig. 5-18 and 5-19. These curves are not to be considered as the maximum that can be obtained by careful design, but are a good guide in that they represent average results based on the experience of a large number of pump manufacturers.

The use of the charts is simple and may be illustrated with an example. A double-suction pump operating at 3560 r.p.m. delivers 1200 g.p.m. against a total head of 200 ft. What should be the maxi-

num suction head for satisfactory operation? The specific speed based on the total flow (rather than one-half the total since the impeller is double-suction) is:

$$n_s = \frac{n\sqrt{Q}}{H^{3/4}} = \frac{3560\sqrt{1200}}{(200)^{3/4}} = \frac{3560 \times 34.65}{53.2} = 2320 \text{ r.p.m.}$$

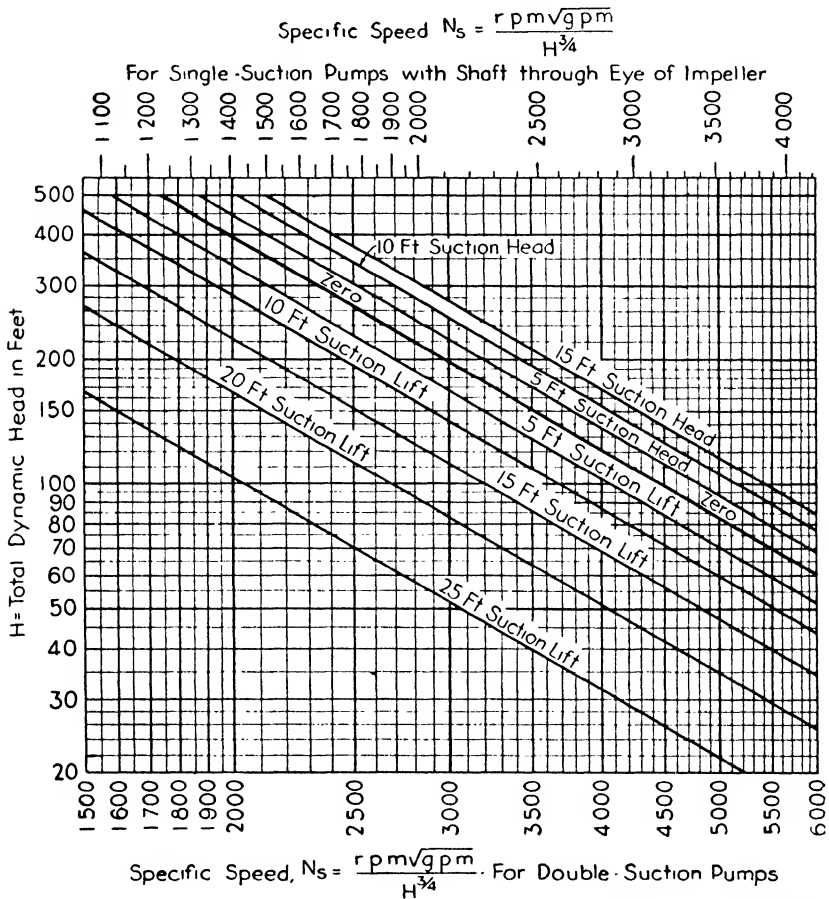


FIG. 5-18. Upper limits of specific speeds for single-stage pumps handling clear water at sea level at 85° F.

(This value could also be obtained from Fig. 4-1.) Referring to Fig. 5-18, the point corresponding to n_s equals 2320 for double-suction pumps and a total dynamic head of 200 ft. indicates about 12-ft. suction lift as the safe maximum. If the same conditions were applied

to a single-suction pump, the safe maximum suction condition would require at least a 7-ft. positive head (i.e., H_{sv} would have to be at least +7 ft. rather than -12 ft.).

These curves are based upon handling clear water at 85° F. and sea level barometric pressure. If the water temperature is higher, the difference in head corresponding to the differences in vapor pressures between 85° F. and the temperature of the water pumped should be subtracted from the suction lift or added to the suction head.

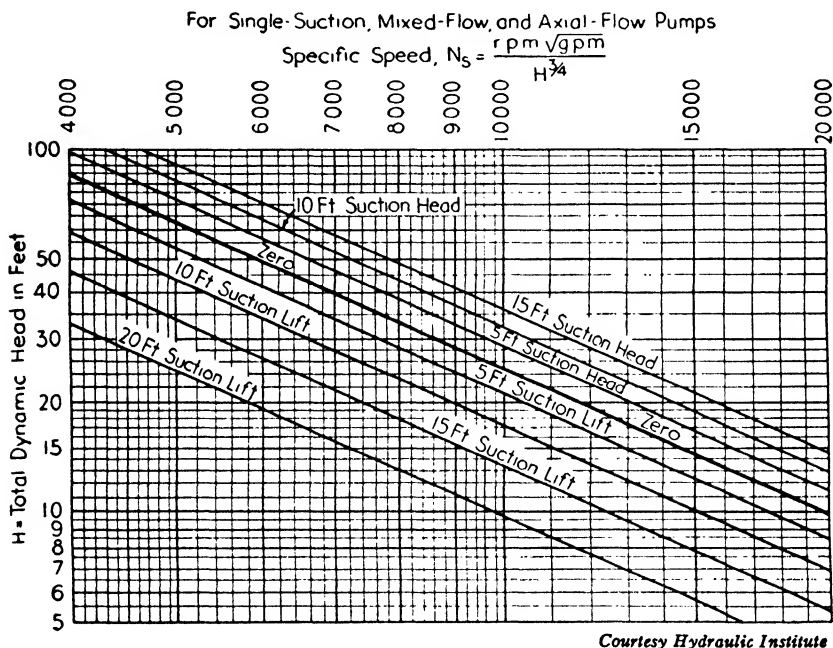


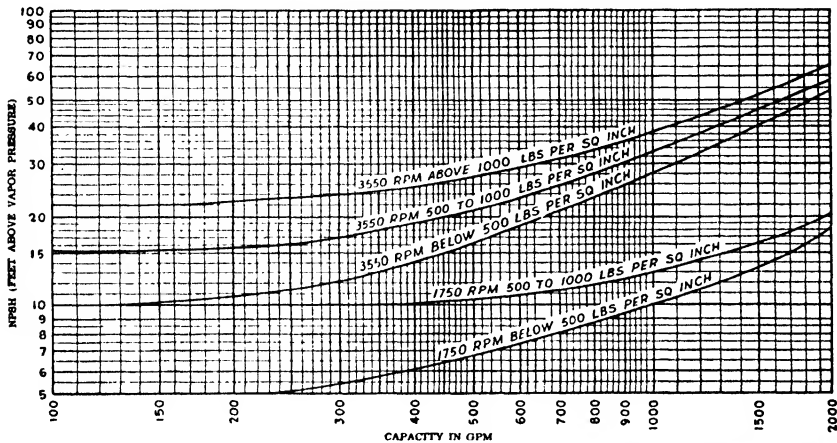
FIG. 5-19. Upper limits of specific speeds for single-stage pumps handling clear water at sea level at 85° F.

Also, if the unit is to be located above sea level, the difference in head corresponding to the difference in atmospheric pressures should be subtracted from the suction lift or added to the suction head.

Thus, in the example just used, if the water temperature is 150° F. and the plant is located at an altitude of 3000 ft., the correction for vapor pressure (see Table 5-1) will be $3.72 - 0.60 = 3.12$ lb. per sq. in., and for altitude (see Fig. 11-4) it will be $0.49 (30 - 27) = 1.47$ lb. per sq. in. The corresponding head change will be $\frac{2.31(3.12 + 1.47)}{0.982} = 10.8$ ft. For the double-suction pump the maximum suction lift

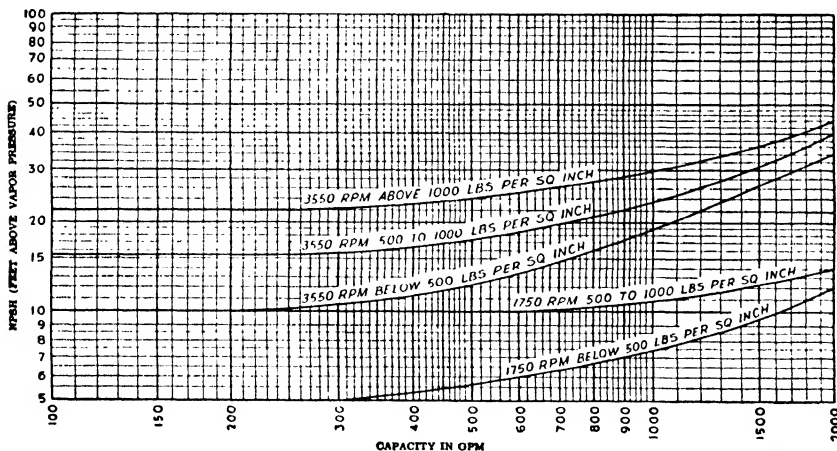
would be 12.0 – 10.8 or 1.2 ft., and for the single suction pump the positive suction head would have to be 7.0 + 10.8 or 17.8 ft.

The Hydraulic Institute has also prepared a series of charts to determine the required net positive suction head (*NPSH*) based upon



Courtesy Hydraulic Institute

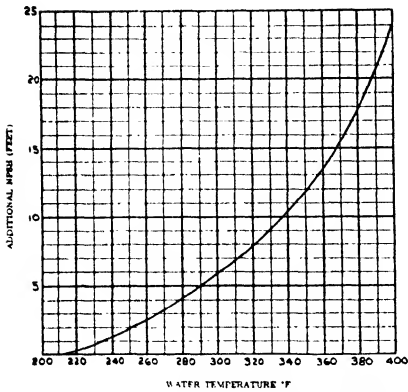
FIG. 5-20. Required net positive suction head of centrifugal single-suction hot water pumps.



Courtesy Hydraulic Institute

FIG. 5-21. Required net positive suction head of centrifugal double-suction, first-stage hot water pumps.

the flow, operating speed, and discharge pressure for hot water and condensate pumps which are reproduced as Figs. 5-20 to 5-23 inclusive. They may also be used to determine the maximum flow through a pump for a given available *NPSH*.

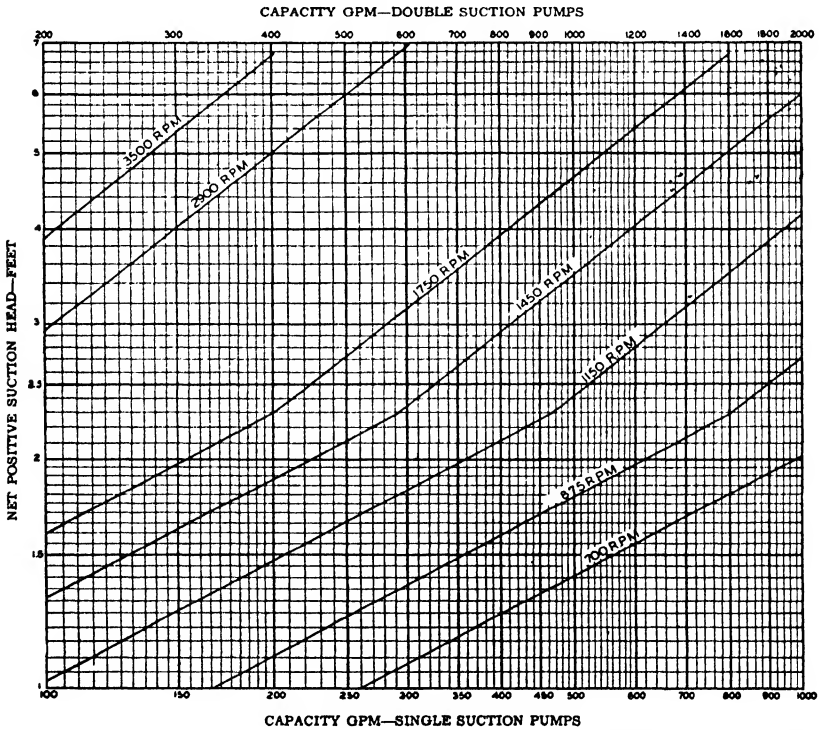


Courtesy Hydraulic Institute

FIG. 5-22. Temperature correction chart for centrifugal single- and double-suction hot water pumps. Additional suction head to be added to values given on basic charts.

Figures 5-20 and 5-21 give the required *NPSH* for single- and double-suction hot water pumps handling water with temperatures up to 212° F. For temperatures above 212° F. the *NPSH* as found from the figures is increased by the amount shown in Fig. 5-22. If the operating speed of the pump is within 25 per cent of those shown on Figs. 5-20 and 5-21, the flow through the pump is corrected according to the relationship r.p.m. $\sqrt{\text{g.p.m.}} = \text{a constant}$.

Figure 5-23 given the required *NPSH* for condensate pumps with a shaft passing through the eye of



Courtesy Hydraulic Institute

FIG. 5-23. Capacity and speed limitations for condensate pumps with a shaft through the eye of the impeller.

the impeller. It applies to pumps having a maximum of three stages, the lower scale representing single-suction pumps and the upper scale double-suction or a double-suction first stage impeller. The speed-capacity relationship given above may be applied to this curve also.

PROBLEMS

5-1 A test on a single-stage, double-suction radial-type pump operating at 1200 r.p.m. and designed for 7000 gallons of water per minute gives the following data:

G.p.m.	0	1600	3100	4300	5700	7000	7400	7900	8200
B.hp. input	197.5	237.5	270	305	345	377.5	390	400	395
Total head-feet	222.5	220	215	210	202.5	194	187.5	175	162.5

(a) Plot these curves and draw the efficiency curve. (b) On the same sheet draw the three performance curves for the pump operating at 1000 and 1400 r.p.m., checking a few points to see that the relations between the three curves are maintained.

5-2 Test results on a single-stage, single-suction mixed-flow-type pump operating at 575 r.p.m. and designed to deliver 6000 gallons of water per minute are given in curve form as follows:

G.p.m.	0	1000	2000	3000	4000	5000	6000	7000	7600
Total head-feet	39.5	37.2	35.0	32.5	30.0	27.0	23.5	19.2	16.2
Efficiency	0	23.0	45.0	62.0	75.5	84.0	88.0	86.0	81.0

(a) Plot these curves and draw the b.hp. curve. (b) On the same sheet draw the same three curves in dotted lines if the liquid pumped has a specific gravity of 0.9 but otherwise is the same as water. Give a brief discussion of your reasoning for each curve. (c) Plot on the same sheet the three performance curves for the pump operating at a speed of 500 r.p.m. with water.

5-3 A plant located at an altitude of 2500 ft. (atmospheric pressure = 27.5 in. Hg) has an open feedwater heater located 10 ft. above the pump centerline. The water in the heater has a temperature of 190° F. If the head loss in the line between the heater and pump is 1 ft., determine the available suction head at the pump.

Ans. 18.85 ft.

5-4 Determine the available suction head of a pump which is taking gas oil at a temperature of 400° F. from a closed tank in which the pressure is 85 lb. per sq. in. ga. The specific gravity of the oil is 0.78 and its vapor pressure is 90 lb. per sq. in. abs. The loss in the suction pipe is 2 ft. and the pump is located 12 ft. above the oil level in a plant at sea level.

Ans. 15 ft.

5-5 A single-stage pump is handling clear water at 85° F. at sea level. Determine from the Hydraulic Institute charts the maximum design capacity which may be delivered by a single-stage pump operating at 1750 r.p.m. and having a total head of 90 ft. and a positive dynamic suction head of 5 ft., if (a) the pump is single-suction mixed-flow; (b) the pump is single-suction with shaft through the impeller eye; (c) the pump is double-suction.

Ans. (a) 4950 g.p.m.; (b) 3630 g.p.m.; (c) 7300 g.p.m.

5-6 What would be the maximum design capacity of the pump in part (c) of Problem 5-5, if (a) the water has a temperature of 150° F.; (b) the altitude at which it operates is 2500 ft.

Ans. (a) 5730 g.p.m.; (b) 6700 g.p.m.

CHAPTER 6

DESIGN OF RADIAL-TYPE PUMP STAGE

6-1 Introduction. There is no rigorous procedure to be followed in designing a pump. Each company has developed its own approach and, although each has a slightly different method of calculation, the broad underlying principles of all are similar. The various companies have velocity limitations and proportions to which they attempt to adhere, but these may be exceeded in certain instances to meet competition with regard to cost or performance.

The general method of design will be considered in this chapter and the usual range of velocities, proportions, and coefficients will be given for present-day practice. It should be emphasized that these are average or usual values and may be altered or exceeded in accordance with the conditions imposed upon the designer.

The usual design is based upon a certain desired head and capacity at which the pump will operate most of the time and is specified by the purchaser. In addition, the type of driver (motor, turbine, etc.) may be specified.

6-2 Speed. The speed of the driver may be specified by the customer; it generally follows standard motor speeds such as 3560, 1760, etc., r.p.m. In such cases the specific speed is fixed, unless the head is high enough to use a multistage machine. Then the specific speed may be varied by using different numbers of stages.

If the operating speed is not given, it may be chosen to give a specific speed consistent with high pump efficiency (Section 4-5) and the prevailing suction conditions (Section 5-10). To reduce the cost of the pump the speed may be selected so that an impeller for which patterns are available may be used.

6-3 Pipe Connections and Velocities. To avoid cavitation difficulties the diameter of the suction pipe is usually made larger than the pump suction flange, and both are larger than the discharge flange and pipe. Standard pipe or flange inside diameters in inches are 1, $1\frac{1}{4}$, $1\frac{1}{2}$, 2, $2\frac{1}{2}$, 3, 4, 5, 6, 8, 10, 12, 14, 16, 18, 20, 24, 30, and 36. These sizes should be used to avoid the additional expense and delay caused by specifying odd sizes.

The diameter of the suction flange is selected to keep the liquid

velocity at the design point* in the neighborhood of 9 or 10 ft. per sec. This velocity depends upon the suction conditions and may range from about 4 to 18 ft. per sec.

The discharge flange diameter is generally based upon an average liquid velocity at the design point of 18 to 25 ft. per sec. with a range from about 12 to 40 ft. per sec.

6-4 Leakage Losses. The water which has been discharged from the impeller is at a higher pressure than the water in the eye of the impeller. Since clearance must be provided between the rotating impeller and the stationary casing, some of the water which has been discharged from the impeller will leak back to the suction side. The total flow through the impeller is the sum of the leakage plus the delivered flow. Thus the impeller is handling more water than is discharged by the pump. The leakage flow must be estimated because it must be added to the delivered flow for the determination of the impeller dimensions.

To reduce the amount of leakage, various types of close clearance wearing rings, one fixed to the impeller and the other to the casing, are provided. These rings are shown in Fig. 1-2 as items *O* and *P*. A. J. Stepanoff† made an extensive study of the leakage losses of various types of rings; he gives a method by which the leakage flow may be estimated.

The basic equation for calculating the leakage at each ring is: $Q_L = CA\sqrt{2gH_L}$, where C is a flow coefficient depending upon the ring type, A is the leakage area in square feet, H_L is the head across the ring, and Q_L is the leakage flow in cubic feet per second. Stepanoff found that the head across the ring is approximately $H_L = \frac{3}{4} \frac{u_2^2 - u_1^2}{2g}$,

although this may differ for impellers having proportions different from those used in his tests. Figure 6-1 gives the range of values of the flow coefficient C and the percentage of leakage loss when operating at the design condition based upon the pump tested by Stepanoff at various speeds, clearances, and ring types. These results are based upon a $4\frac{1}{8}$ -in.-diameter ring running at speeds from 1400 to 2500 r.p.m. The percentage of saving in leakage of various ring types as compared with plain rings of the same width and clearance may be summarized as follows:

* Throughout this book, the term design point refers to the point of maximum efficiency. It is usually the capacity at which the pump is expected to operate most of the time.

† A. J. Stepanoff, "Leakage Loss and Axial Thrust in Centrifugal Pumps," *A.S.M.E. Trans.*, HYD-54-5, 1932.

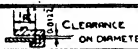
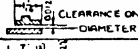
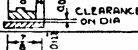
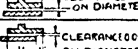
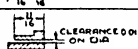
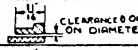
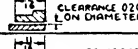
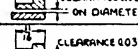
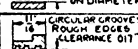
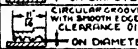
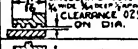
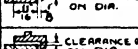
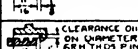
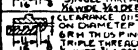
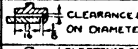
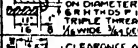
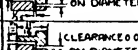
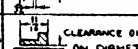
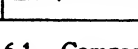
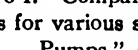


		SPEED R.P.M.								
		1400	1700	2000	2500	$Q_L = 2CA \sqrt{2gH_L}$				
CAPACITY AT MAXIMUM EFFICIENCY (NORMAL) G.P.M.		270	325	375	475	WHERE:				
TOTAL HEAD AT MAXIMUM EFFICIENCY (NORMAL) FEET		56	88	1175	184	Q_L IS LEAKAGE ON BOTH SIDES OF IMPELLER				
HEAD ON WEARING RING H_L IN FEET		35	55	74	116	C = COEFFICIENT OF DISCHARGE				
HEAD ON WEARING RING PER CENT OF TOTAL HEAD		62.5	630	630	630	A = CLEARANCE AREA				
						H_L = HEAD ON WEARING RING OVER SUCTION LEVEL				
No.	WEARING RINGS	LEAKAGE LOSS PER CENT AT SPEEDS R.P.M.				COEFFICIENT OF DISCHARGE AT SPEEDS R.P.M.				REMARKS
		1400	1700	2000	2500	1400	1700	2000	2500	
1	 CLEARANCE ON DIAMETER	1.52	1.80	2.00	2.18	0.176	0.200	0.220	0.244	LEAKAGE LOSS LESS FROM 41 TO 46 % AGAINST WEARING RING #2
2	 CLEARANCE ON DIAMETER	2.85	3.32	3.52	3.70	0.330	0.368	0.388	0.414	LEAKAGE LOSS GREATER FOR SMALLER OVERLAP THE PROJECTING OF RUNNER WEARING RING AGAINST CASE WEARING RING AND VICE VERSA, HAS VERY LITTLE IF ANY EFFECT ON COEFFICIENT OF DISCHARGE
3	 CLEARANCE ON DIA	3.08	3.60	3.86	4.17	0.356	0.400	0.424	0.468	
4	 CLEARANCE ON DIAMETER	3.16	3.62	3.87	4.07	0.366	0.402	0.426	0.456	
5	 CLEARANCE 0.002 ON DIAMETER	3.68	4.17	4.38	4.50	0.426	0.462	0.482	0.504	
6	 CLEARANCE 0.012 ON DIA	3.52	4.03	4.33	4.50	0.408	0.448	0.476	0.502	LEAKAGE INCREASES WITH LARGER CLEARANCE, DUE TO BOTH THE INCREASE OF CLEARANCE AREA AND INCREASE OF COEFFICIENT OF DISCHARGE
7	 CLEARANCE 0 ON DIAMETER	6.06	6.65	6.70	6.70	0.504	0.528	0.528	0.538	
8	 CLEARANCE 0.205 ON DIAMETER	7.92	8.62	8.66	8.60	0.542	0.574	0.573	0.578	
9	 CLEARANCE 0.025 ON DIAMETER	13.20	13.90	14.05	14.07	0.634	0.640	0.641	0.634	
10	 CLEARANCE 0.035 ON DIAMETER	18.72	19.65	19.85	20.00	0.678	0.682	0.684	0.700	
11	 CIRCULAR GROOVES WITH SMOOTH EDGES CLEARANCE 0.017 ON DIAMETER	3.91	4.28	4.31	4.48	0.325	0.340	0.340	0.360	LEAKAGE REDUCED FROM 32.2 TO 35.5 PER CENT AGAINST WEARING RING #7 MAXIMUM GAIN AT LOWER SPEED
12	 CIRCULAR GROOVES WITH SMOOTH EDGES CLEARANCE 0.017 ON DIAMETER	4.83	5.38	5.58	5.52	0.402	0.428	0.440	0.443	LEAKAGE REDUCED FROM 16.7 TO 20.7% AGAINST RING #7
13	 CIRCULAR GROOVES WITH SMOOTH EDGES CLEARANCE 0.034 ON DIA.	12.70	13.55	13.75	13.60	0.610	0.622	0.628	0.632	LEAKAGE DECREASED FROM 2.2 TO 4 PER CENT AGAINST RING #9
14	 CLEARANCE 0.017 ON DIA.	4.42	4.88	5.04	5.05	0.481	0.508	0.521	0.521	
15	 CLEARANCE 0.015 ON DIA.	3.18	3.68	3.94	4.08	0.390	0.432	0.460	0.485	CALCULATED
16	 CLEARANCE 0.015 ON DIAMETER WITH 3/16" SINGLE THREAD REVERSE SLOPE	2.52	2.88	2.92	2.98	0.309	0.338	0.342	0.354	LEAKAGE REDUCED FROM 20.8 TO 27 PER CENT AGAINST RING #15 MAX. GAIN AT HIGHER SPEED
17	 CLEARANCE 0.015 ON DIAMETER WITH 3/16" SINGLE THREAD REVERSE SLOPE	2.13	2.40	2.53	2.58	0.262	0.282	0.296	0.306	LEAKAGE REDUCED FROM 33 TO 36.8 PER CENT AGAINST RING #15 MAX GAIN AT HIGHER SPEED
18	 CLEARANCE 0.015 ON DIAMETER	8.53	9.04	9.15	9.19	0.560	0.568	0.572	0.584	CALCULATED
19	 CLEARANCE 0.015 ON DIAMETER WITH 3/16" SINGLE THREAD REVERSE SLOPE	6.24	6.68	6.89	6.82	0.410	0.420	0.430	0.432	LEAKAGE REDUCED FROM 24.7 TO 26.8 PER CENT AGAINST RING #18
20	 CLEARANCE 0.010 ON DIAMETER	1.94	2.18	2.27	2.40	0.274	0.295	0.305	0.328	LEAKAGE LESS THAN WITH RING #22 FROM 24 TO 33 PER CENT
21	 CLEARANCE 0.010 ON DIAMETER	2.07	2.34	2.45	2.52	0.292	0.316	0.328	0.344	
22	 CLEARANCE 0.010 ON DIAMETER	2.55	3.03	3.28	3.44	0.360	0.410	0.440	0.470	CALCULATED

FIG. 6-1. Comparative study of various ring types and corresponding flow coefficients for various speeds. (From "Leakage Loss and Axial Thrust in Centrifugal Pumps," A. J. Stepanoff, *Trans. A.S.M.E.*, HYD-54-5, 1932.)

	Clearance	Per Cent Saving
Single labyrinth	0.0122	41.0 to 46.6
Circular grooves, rough edges	0.0170	32.2 to 35.5
Circular grooves, smooth edges	0.0170	16.7 to 20.0
Circular grooves, smooth edges	0.0294	2.2 to 4.0
Spiral grooves, single-thread	0.0115	20.8 to 27.0
Spiral grooves, triple-thread	0.0115	33.0 to 36.8
Spiral grooves, triple-thread	0.0215	24.7 to 26.8
Stepped ring	0.0100	24.0 to 33.0

The clearance area, A , in square inches is given by $\frac{1}{2}\pi Ds$, where D is the mean clearance diameter and s is the *diametral* clearance. Stepanoff also states:

For the wearing-ring clearances the following values represent good practice: For rings of 6 in. diameter and smaller the clearance is made 0.010 in. on the diameter with 0.001 in. additional for every inch of the wearing ring diameter over 6 in., or $s = 0.010 + (D - 6)0.001$ in. where s and D are in inches. For small wearing rings on a pump with very exact machining and ball bearings, the minimum clearance may be reduced to 0.008 in.

6-5 Impeller Inlet Dimensions and Vane Angle. Before the impeller dimensions can be fixed, the shaft size must first be approximated. It should be large enough to care for the torque and bending moment, to avoid excessive lateral deflection, and to keep the critical speed a safe distance from the operating speed. The calculation of the critical speed is discussed in Chapter 19. The shaft diameter based upon torque alone is given by the well-known equation $D_s = \sqrt[3]{\frac{16T}{\pi s_s}}$, where T is the torque in pound-inches based upon the brake horsepower (found from the equation $T = \frac{63000 \text{ b.hp.}}{n}$), and s_s is the allowable shear stress. The maximum bending moment M is due to the impeller and shaft weights plus the unbalanced radial thrust acting on the impeller (Sections 3-16 and 8-11), all of which must be estimated at this stage in the design. The shaft diameter, based upon the bending strength alone, is $D_s = \sqrt[3]{\frac{32M}{\pi s_t}}$, where s_t is the allowable tensile or bending stress and M the maximum bending moment in inch-pounds. A more accurate check on the stresses and the deflection may be made after the impeller is designed and the loads are known. Then the maximum combined shear stress s'_s , due to the bending s_t and torsion stress s_s , is

$$s'_s = \frac{1}{2}\sqrt{4s_s^2 + s_t^2}$$

and the maximum combined tensile stress s'_t is

$$s'_t = \frac{1}{2}s_t + \frac{1}{2}\sqrt{4s_s^2 + s_t^2}$$

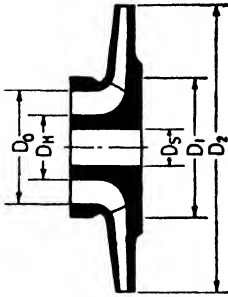


FIG. 6-2. Impeller dimension symbols.

For the preliminary steps, however, the diameter may be based upon shear and bending alone by using low allowable stresses to compensate for the uncertainties in the loads.

The hub diameter D_H (Fig. 6-2) is made from $\frac{5}{16}$ in. to $\frac{1}{2}$ in. larger than the shaft diameter, depending on the shaft size.

The inlet velocity through the eye of the impeller V_0 is usually slightly higher than the velocity in the suction flange, say 10 to 15 ft. per sec. average. Since the turbulence and friction losses are proportional to the velocity squared, the inlet velocity should be kept fairly low. On the other hand, very low values of V_0 result in large eye diameters and consequently poor impeller proportions. Having found or assumed values of D_H and V_0 , the eye diameter may be found from the continuity equation

$$\frac{\pi}{4} D_0^2 - \frac{\pi}{4} D_H^2 = \frac{144Q^*}{V_0}$$

or

$$D_0 = \sqrt{\frac{4}{\pi} \frac{144Q}{V_0} + D_H^2} \quad 6.1$$

The leakage loss usually ranges between 2 and 10 per cent of the delivered flow Q . Hence in applying Eq. 6.1 the total flow Q should be increased by this amount. After the outlet diameter of the impeller has been fixed, the leakage flow may be estimated according to Section 6.4.

The inlet vane edge diameter D_1 is usually made about the same as the eye diameter D_0 to insure smooth flow without excessive turbulence. If the inlet edge of the vane is sloped as shown in Fig. 6-2 an average value is used for D_1 .

Since slowing up a fluid is always more inefficient than speeding it up, the radial inlet velocity at the vane inlet V_r is usually made 5 to 10 per cent greater than V_0 . These assumed values of V_r and D_1 determine the width of the impeller at the inlet, b_1 . By the con-

* Throughout this chapter Q will have the units of cubic feet per second.

tinuity equation

$$b_1 = \frac{144Q}{\pi D_1 V_{r_1} \epsilon_1} \quad 6.2$$

The gross inlet area $\pi D_1 b_1$ is not available to the fluid, but is reduced by the vane thickness. This is accounted for by assuming a contraction factor ϵ_1 , which is generally between 0.8 and 0.9, in the preliminary calculation of the impeller inlet width b_1 . After the number of vanes and their inlet thickness have been determined, the exact value of the coefficient ϵ_1 may be found and, if necessary, the inlet width is corrected to give the required area.

The water is usually assumed to enter the vanes radially as discussed in Chapter 3, so that the absolute approach angle α_1 is 90° . Having determined V_{r_1} and u_1 , the vane inlet angle β_1 is found from

$$\tan \beta_1 = \frac{V_{r_1}}{u_1} \quad 6.3$$

This value of $\tan \beta_1$ is usually increased slightly to care for the contraction of the stream as it passes the inlet edges and the prerotation of the water (Section 3-11). It is increased more for high suction lifts and small ratios of D_2/D_1 (i.e., higher specific speed impellers). The inlet angle usually falls in the range from 10° to 25° .

Guide vanes could be placed before the impeller to give V_{u_1} a negative value and thus raise the head and overall efficiency at the design condition, but the head and efficiency would drop off more rapidly at partial capacities.

6-6 Flow in Impellers. Before proceeding with the impeller design it is important to consider the flow conditions existing in the fluid passage and at the impeller outlet.

The effect of the circulatory flow has already been discussed in Section 3-5. As noted there, the magnitude of this effect is very difficult to determine. Various experiments have been performed to determine the flow conditions existing in the impeller.

Fischer and Thoma* used an impeller having six vanes cast integral with the front shroud and a circular glass plate for a back shroud. They injected a dark-colored dye into the water and observed the flow by means of a "rotoscope" and camera. They found that the flow conditions, especially at low discharges, were entirely different from the ideal assumptions. The water passages were never completely filled with active flow, and the flow broke away from the vane surfaces.

* K. Fischer and D. Thoma, "Investigation of the Flow Conditions in a Centrifugal Pump," *A.S.M.E. Trans.*, HYD-54-8, 1932.

Dead water volumes formed in the passages on the low pressure side of the vanes. When the delivery was below the design point, the outward flow was no longer stable. The fluid in some instances even came out of the inlet of one passage and went into the next passage. At shut-off, instead of having one vortex for the impeller, there was a series of small vortices which resulted from the fluid friction. These conditions undoubtedly account for the curious breaks occurring in the head-capacity curves obtained on extremely accurate laboratory tests (see Figs. 3-18 and 3-19). As the result of careful measurements with a pitot tube T. Kasai,* R. C. Binder and R. T. Knapp† found similar conditions existed.

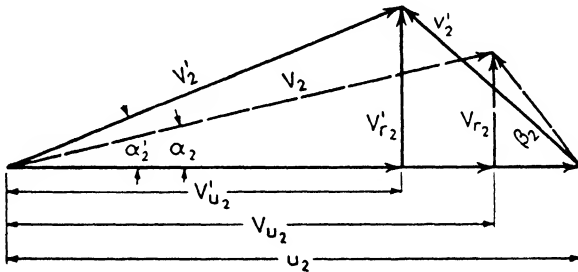


FIG. 6-3.

Since the passages may not be completely filled with active flow, the radial outlet velocity V_{r_2} may be greater than the calculated value. Hence, the actual outlet diagram will appear as shown in solid lines in Fig. 6-3. For comparison the ideal diagram uncorrected for circulatory flow is shown in dashed lines. As may be seen from the figure, the increase in the radial component of the absolute outlet velocity V_{r_2} decreases the absolute velocity V'_2 at which the liquid leaves the impeller and also increases the absolute outlet angle α'_2 . There are not sufficient data available to calculate the magnitude of this change on the outlet diagram.

6-7 Impeller Outlet Dimensions and Vane Angle. By Eq. 3-27 the virtual head $H_{vir.\infty}$ is

$$H_{vir.\infty} = \frac{1}{g} \left[u_2^2 - \frac{u_2 V_{r_2}}{\tan \beta_2} \right] \quad 3-27$$

* T. Kasai, "On the Exit Velocity and Slip Coefficient of Flow at the Outlet of the Centrifugal Pump Impeller," *Memoirs of Faculty of Engineering*, Kyushu Imperial University, 1926, Vol. 8, No. 1, pp. 1-89.

† R. C. Binder and R. T. Knapp, "Experimental Determinations of the Flow Characteristics in the Volute of Centrifugal Pumps," *A.S.M.E. Trans.*, HYD-58-4, 1936.

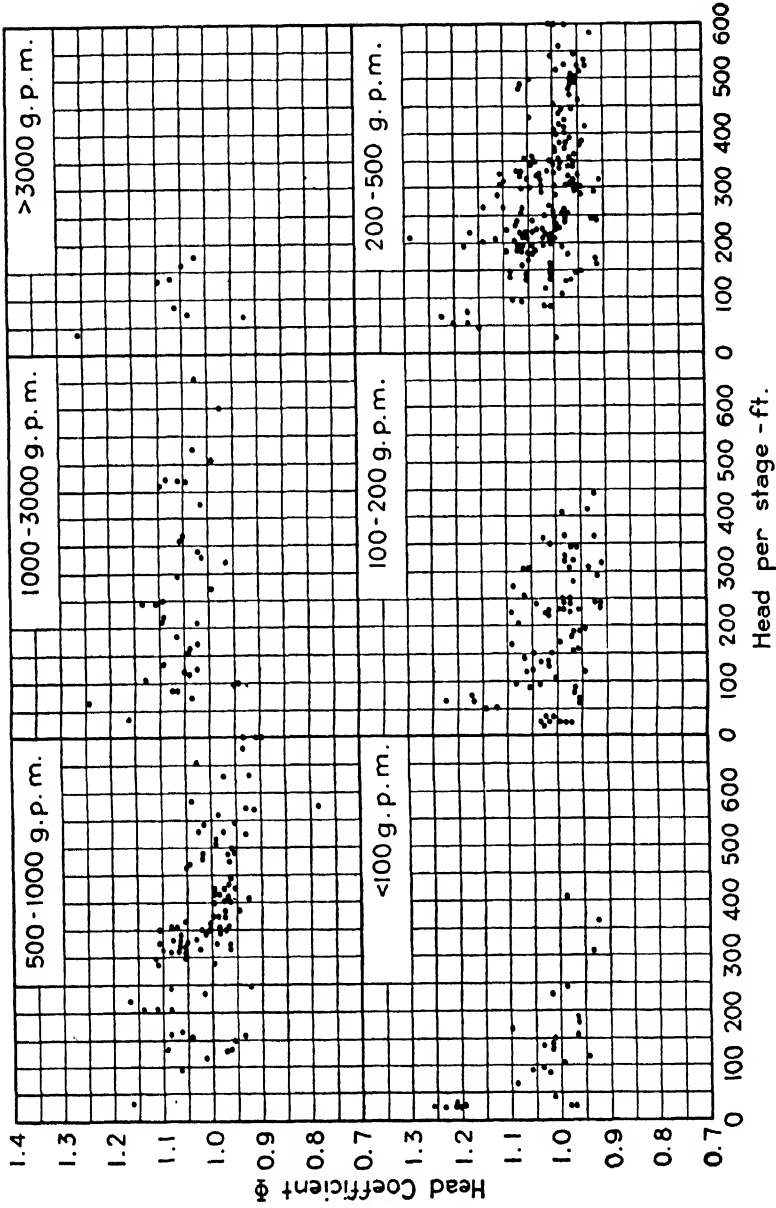


FIG. 6-4. Head coefficient ϕ -head points for various capacity ranges.

and by Eq. 3·15 the total head H is

$$H = K \frac{u_2 V_{u_2}}{g} = KH_{\text{vir.}\infty} \quad 3\cdot15$$

Combining these equations

$$\frac{Hg}{K} = u_2^2 - \frac{u_2 V_{r_2}}{\tan \beta_2}$$

or

$$u_2^2 - \frac{V_{r_2}}{\tan \beta_2} u_2 - \frac{Hg}{K} = 0$$

which is a quadratic equation in u_2 . Solving this for u_2 ,

$$u_2 = \frac{1}{2} \left[\frac{V_{r_2}}{\tan \beta_2} + \sqrt{\left(\frac{V_{r_2}}{\tan \beta_2} \right)^2 + \frac{4gH}{K}} \right]$$

Since $K = \eta_\infty \eta_{HY}$ this equation shows the effect of the various factors on u_2 . For radial-type impellers η_∞ varies between 0.65 and 0.75, and K varies between 0.6 and 0.7, the larger value applying to lower specific speed impellers.

The outlet diameter can be more easily obtained by means of the overall head coefficient Φ as developed in Section 3·12(d). By Eq. 3·17

$$D_2 = \frac{1840\Phi\sqrt{H}}{n}. \quad \text{The value of } \Phi \text{ varies between 0.9 and 1.20 with}$$

an average value very close to unity. Since it varies with the outlet angle and impeller dimensions, there will be a range of values for any given head, capacity, or specific speed. Figures 6·4, 6·5, and 6·6 show plots of Φ against these factors for the group of pumps cited in Section 4·5. These figures may be used to select a value of Φ for given operating conditions.

The outlet vane angle β_2 may be selected within fairly wide limits. The relationship between it and the characteristic curve was discussed in Section 3·14. In general, backward-curved vanes are used for pump impellers since, as illustrated in Fig. 3·15, the portion of the total head which is in the form of velocity is a minimum for backward-curved vanes. Because the velocity head is difficult to convert into pressure head efficiently, impellers having radial or forward-curved vanes are less efficient than the backward-curved type. Moreover, radial or forward-curved vanes have an undesirable passage shape between the vanes which is difficult for the liquid to follow; this results in eddy losses. The angle β_2 is usually made between 15° and

40°. It is usually made slightly larger than the inlet angle to obtain a smooth, continuous passage.

The radial outlet velocity V_{r_2} is ordinarily made equal to or slightly less (up to 15 per cent) than the radial inlet velocity V_{r_1} to avoid any sudden changes of velocity.

A contraction factor ϵ_2 , to compensate for the vane thickness at the outlet, is assumed subject to correction after the actual thickness and the number of vanes have been determined. This factor ϵ_2 is usually between 0.90 and 0.95. The approximate outlet width is then found from

$$b_2 = \frac{144Q}{V_{r_1} D_2 \pi \epsilon_2} \quad 6.4$$

6.8 Design of Vanes. The vane angles and diameters having been determined, the next step in the design of the stage is to construct the vane shape. There is no published information concerning the effect of the vane curvature between the inlet and exit on the pump efficiency, although it must have a great influence. The passage should not be too long because this would increase the frictional loss, and any change in cross-sectional area should be gradual in order to avoid turbulence losses. A total divergence of 10° to 12° (5° to 6° on each side) will give the best results according to tests made on stationary passages.

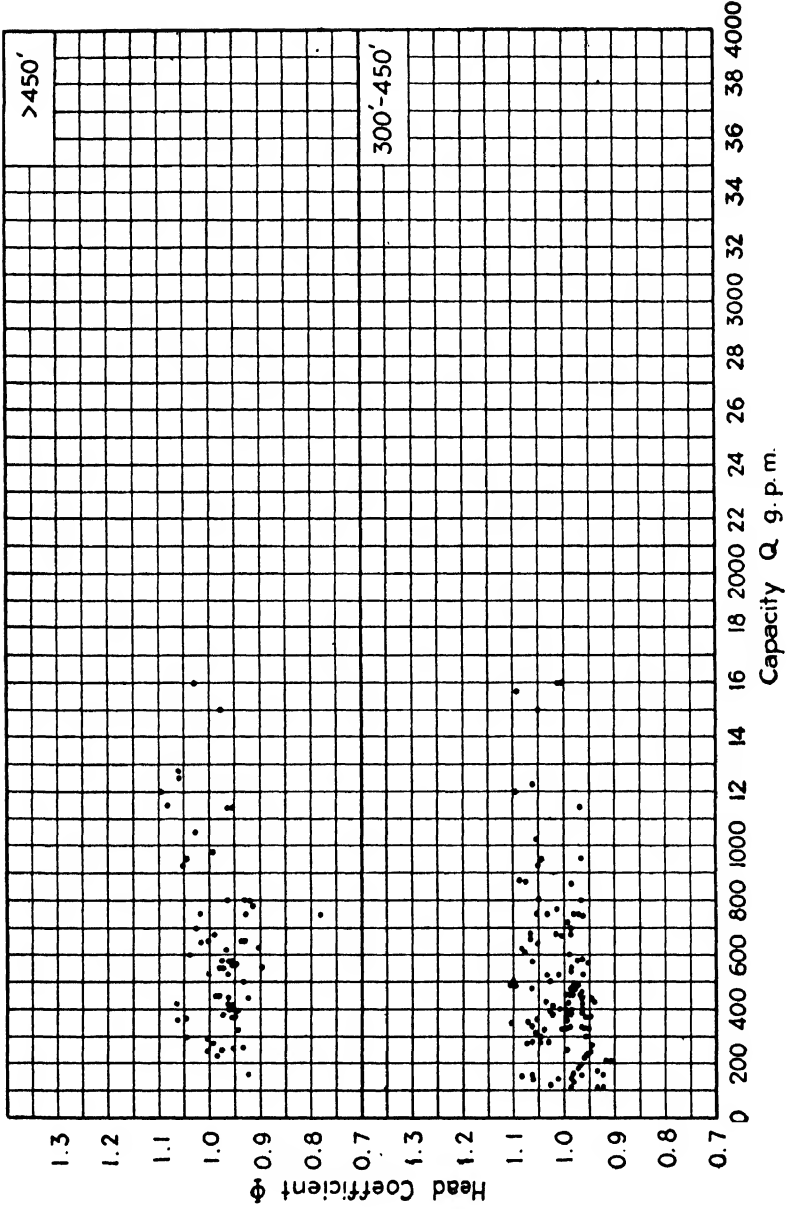
The velocity of the liquid relative to the impeller v and the radial component V_r of the absolute velocity V at both the inlet and outlet edges of the vanes are known and may be plotted against the impeller radius. If these two points are connected by a straight line or smooth curve (Fig. 6-10), intermediate values may be obtained which will not have any sudden changes to disrupt the flow. When the values of V_r and v are known, a curve of β may then be plotted against R , since $\sin \beta = V_r/v$.

There are two satisfactory methods of constructing the vane shape from these curves. One is to construct it of tangent circular arcs, and the other is to calculate and plot the shape by polar coordinates.

For the first method, the impeller is arbitrarily divided into a number of concentric rings between the radii R_1 and R_2 . The radius of the circular arc contained in any ring is given by

$$\rho = \frac{R_b^2 - R_a^2}{2(R_b \cos \beta_b - R_a \cos \beta_a)} \quad 6.5$$

where the subscripts a and b refer to the inner and outer rings respectively. This is illustrated in Fig. 6-7 where O is the center of rotation



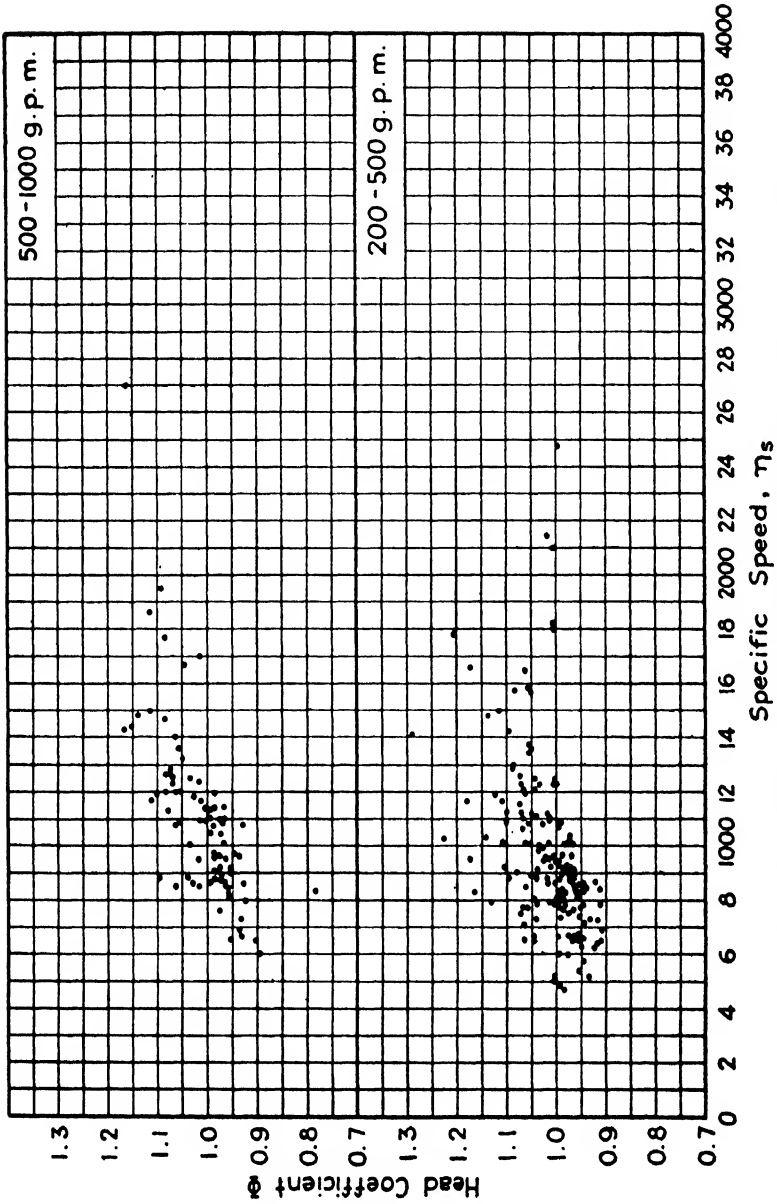


FIG. 6-6. Head coefficient ϕ -specific speed points for various capacity ranges.

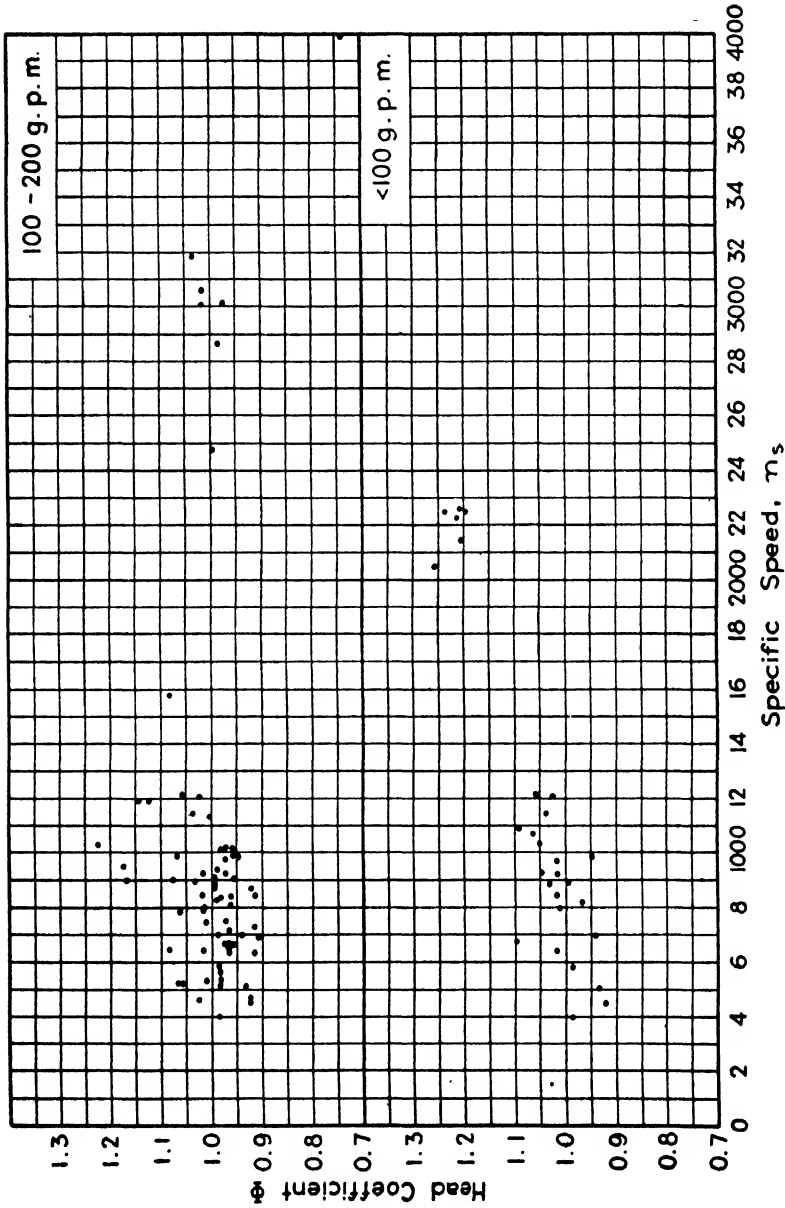
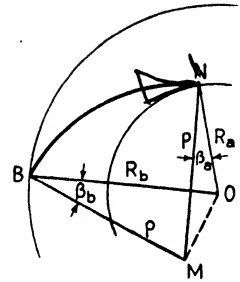


FIG. 6-6. Head coefficient ϕ -specific speed points for various capacity ranges. (Continued.)

of the impeller; and the circular arc NB , of radius ρ having its center at M , is the vane shape between the concentric rings of radii R_a and R_b . The angle ONM has one side perpendicular to u_a and the other one perpendicular to a tangent to the curve NB at N , hence ONM equals β_a . Similarly the angle OBM equals β_b . In the triangle MBO , by the law of cosines,



$$2\rho R_b \cos \beta_b = R_b^2 + \rho^2 - (OM)^2 \quad A$$

In the triangle MNO

$$2\rho R_a \cos \beta_a = R_a^2 + \rho^2 - (OM)^2 \quad B$$

FIG. 6-7. Vane construction by tangent circular arcs.

Combining Eqs. A and B,

$$2\rho R_b \cos \beta_b = R_b^2 + \rho^2 - R_a^2 - \rho^2 + 2\rho R_a \cos \beta_a$$

Collecting terms,

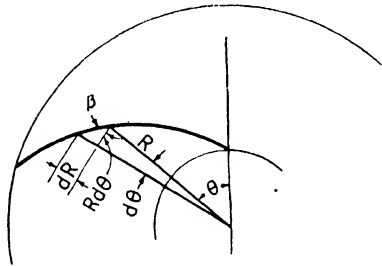
$$2\rho(R_b \cos \beta_b - R_a \cos \beta_a) = R_b^2 - R_a^2$$

or

$$\rho = \frac{R_b^2 - R_a^2}{2(R_b \cos \beta_b - R_a \cos \beta_a)} \quad 6.5$$

The vane angles at R_1 and R_b are taken from the curve. Therefore, the center for the first arc can be located. Since adjacent arcs are tangent to each other, both their centers will lie on the same line through the point of tangency as shown in Fig. 6-11.

In the second method, the points on the vane surface are plotted by polar coordinates. For any radius R the angle θ measured in degrees from an assumed radial line passing through the intersection of the vane surface with radius R_1 is given by the equation



$$\theta^\circ = \frac{180}{\pi} \int_{R_1}^R \frac{dR}{R \tan \beta} \quad 6.6$$

FIG. 6-8. Vane construction by polar coordinates.

Equation 6-6 is best solved by tabular integration, as illustrated in the example in the next section, since β may not vary in a simple mathematical manner with the radius. It is developed as follows (refer to Fig. 6-8). Let β be the vane angle at radius R . In the

infinitesimal triangle shown $\tan \beta = \frac{dR}{R d\theta}$, or $d\theta = \frac{dR}{R \tan \beta}$, where θ is measured in radians. Integrating from R_1 to any radius R , $\theta = \int_{R_1}^R \frac{dR}{R \tan \beta}$ or, if θ is measured in degrees,

$$\theta^\circ = \frac{180}{\pi} \int_{R_1}^R \frac{dR}{R \tan \beta} \quad 6.6$$

The impeller is usually cast with the vanes integral with the shrouds. They are made as thin as good casting practice will permit; in general this will give them sufficient strength. Vanes may be made constant in thickness, or the same curve shape may be used for both sides, allowing a certain thickness, say $\frac{1}{8}$ in., at the inlet edge. A thin vane edge at the inlet will give a high efficiency when the vane angle corresponds to the direction of fluid motion. Owing to the increased turbulence when the angles are not in agreement, the efficiency drops off rapidly. For rounded inlet edges, the efficiency does not reach the peak value of the sharp edge vane, but neither does it drop off as rapidly for incorrect angles.

The number of vanes z is based largely upon experience and is fixed after the vane shape has been determined. There should be enough vanes to secure proper guidance of the liquid. Too many vanes will result in excessive friction losses. A general rule is to make the cross section of the passage approximately square, as this will reduce the frictional resistance to a minimum. Pfeleiderer, in *Die Kreiselpumpen*, gives the following equation for the number of vanes:

$$z = 6.5 \frac{D_2 + D_1}{D_2 - D_1} \sin \beta_m \quad 6.7$$

where $\beta_m = \frac{\beta_1 + \beta_2}{2}$. As may be noted from Pfeleiderer's equation, large vane angles require more vanes in order to provide proper guidance to the liquid. The number of vanes generally used is between 5 and 12.

After the vane thickness and number of vanes have been decided upon, the contraction of the flow at any point due to the vanes may be found by

$$\epsilon = \frac{\pi D - \frac{zt}{\sin \beta}}{\pi D} \quad 6.8$$

where ϵ is the contraction factor, z the number of vanes, and t the normal vane thickness.

The width of the impeller passage b at any point may then be calculated from

$$\text{Area } A = \pi D b \epsilon = \frac{144Q}{V_r}$$

or

$$b = \frac{144Q}{\pi D \epsilon V_r} \quad 6.9$$

By means of Eqs. 6.8 and 6.9 the values of ϵ and b at points along the impeller may be found including those at the inlet and discharge.

6.9 Example of Impeller Design. To illustrate the general design procedure and to clarify the preceding sections, the design of an impeller for specified conditions will be considered. It should be kept in mind that the design will be greatly influenced in the interest of economy by previous impellers which have been made and for which the patterns are available. This factor must necessarily be neglected in the following example.

The pump will be designed to develop a head of 150 ft. and deliver 2500 g.p.m. of water. It is to be direct-connected to a motor operating at 1760 r.p.m.

As 1 gal. of water weighs 8.33 lb., the weight flow w is

$$w = \frac{\text{g.p.m.} \times 8.33}{60} = \frac{2500 \times 8.33}{60} = 347 \text{ lb. per sec.}$$

A gallon of water contains 0.134 cu. ft., hence

$$Q = \text{g.p.m.} \times 0.134 = 2500 \times 0.134 = 335 \text{ c.f.m.} = 5.58 \text{ c.f.s.}$$

Since water is practically incompressible, this volume of 5.58 c.f.s. remains constant at all points in the pump.

A pump operating under the given conditions could be made single-suction, but in order to make the example more general a double-suction impeller will be used. This means that each side of the inlet will handle 1250 g.p.m., and the impeller will discharge the total 2500 g.p.m. at the periphery. The specific speed is

$$n_s = \frac{n\sqrt{Q}}{H^{3/4}} = \frac{1760\sqrt{1250}}{150^{3/4}} = \frac{1760 \times 35.4}{43} = 1450$$

The water horsepower is

$$\text{w.hp.} = \frac{wH}{550} = \frac{347 \times 150}{550} = 94.6$$

From Fig. 4-9 for a head of 150 ft. and 1250 g.p.m. the overall efficiency will be between 75 and 88 per cent. From Fig. 4-10 it will be between 72 and 87 per cent and from Fig. 4-11 for a specific speed of 1450 the range is between 71 and 85 per cent. Probably 81 per cent would be a fair value to assume. The brake horsepower (from Eq. 3-20) is

$$\text{b.hp.} = \frac{\text{w.hp.}}{\eta} = \frac{94.6}{0.81} = 117$$

The shaft torque is

$$T = \frac{63000 \text{ b.hp.}}{n} = \frac{63000 \times 117}{1760} = 4190 \text{ lb.-in.}$$

Assume a shear stress of 4000 lb. per sq. in.; then the shaft diameter is

$$D_s = \sqrt[3]{\frac{16T}{\pi s_s}} = \sqrt[3]{\frac{16 \times 4190}{\pi 4000}} = 1.745 \text{ in.}$$

From the standpoint of torque alone a $1\frac{3}{4}$ -in.-diameter shaft would be satisfactory. It is difficult to predict the bending moment at this time but, to care for it and to keep the critical speed above the running speed, the shaft diameter will be increased to $2\frac{1}{8}$ in. The hub diameter D_H will then be made $2\frac{1}{2}$ in.

The suction flange passes 5.58 c.f.s. Assuming a velocity $V_{su.}$ of 10 ft. per sec. here, the diameter of the suction flange is

$$D_{su.} = \sqrt{\frac{4 \text{ } 144 Q}{\pi V_{su.}}} = \sqrt{\frac{4 \text{ } 144 \times 5.58}{\pi 10}} = 10.12 \text{ in.}$$

Use a 10-in.-diameter suction flange.

Velocity in suction line,

$$V_{su.} = \frac{Q}{A} = \frac{5.58}{\frac{\pi 10^2}{4 \text{ } 144}} = 10.22 \text{ ft. per sec.}$$

The velocity at the eye of the pump V_0 should be increased somewhat, to, say, 11 ft. per sec. A double-suction pump has a low percentage of leakage since the volume handled is relatively large compared to the leakage area. In this instance it will probably not exceed 2 per cent. The impeller is double-suction, so the total flow is divided

by 2 and the approximate eye diameter, by Eq. 6-1, will be

$$D_0 = \sqrt{\frac{4}{\pi} \frac{1.02Q144}{2V_0} + D_H^2} = \sqrt{\frac{4}{\pi} \frac{1.02 \times 5.58 \times 144}{2 \times 11} + 2.5^2}$$

$$= 7.33 \text{ in.}, \text{ say } 7\frac{5}{16} \text{ in.}$$

Wheel Inlet Dimensions and Angle. Assume an inlet diameter D_1 of $7\frac{5}{16}$ in.

Tangential inlet velocity

$$u_1 = \frac{\pi D_1 n}{12 \times 60} = \frac{\pi 7.31 \times 1760}{720} = 56.2 \text{ ft. per sec.}$$

The radial inlet velocity V_{r_1} should be slightly higher than V_0 . If it is made 12 ft. per sec. the increase is $12/11 = 1.09$ which is about right. The inlet area will be decreased by the vane thickness. Hence, a contraction factor ϵ_1 is assumed to obtain the approximate inlet width b_1 . When the vane thickness and number of vanes have been fixed, the final inlet width may be found.

Assume the inlet contraction factor $\epsilon_1 = 0.85$. Inlet width (from Eq. 6-2),

$$b_1 = \frac{144Q}{\pi D_1 V_{r_1} \epsilon_1} = \frac{144 \times 5.58 \times 1.02}{2\pi 7.31 \times 12 \times 0.85} = 1.748 \text{ in. per side}$$

Tangent of inlet angle is

$$\tan \beta_1 = \frac{V_{r_1}}{u_1} = \frac{12}{56.2} = 0.2137$$

Inlet angle $\beta_1 = 12^\circ 4'$.

The angle should be increased somewhat, say to 13° , to compensate for the stream contraction and prerotation. This angle is rather small and might be made somewhat larger by increasing V_{r_1} , i.e., by decreasing the inlet width b_1 .

Outlet Vane Angle and Dimensions. The outlet diameter of the impeller can be found by means of Eq. 3-17 after a suitable value of the overall head coefficient Φ has been selected. From Fig. 6-4 the range of Φ for a head of 150 ft. and 1250 g.p.m. is between 1.00 and 1.15; by Fig. 6-5 the range is from 1.00 to 1.10. For a specific speed of 1450 the range of Φ is between 0.98 and 1.10 according to Fig. 6-6. Probably a value of 1.05 would be obtained. Outside diameter of impeller (Eq. 3-17)

$$D_2 = \frac{1840\Phi\sqrt{H}}{n} = \frac{1840 \times 1.05\sqrt{150}}{1760} = 13.5 \text{ in.}$$

If there is any doubt concerning the correct value of Φ to be assumed, it is always advisable to use a higher value (which results in a larger D_2) to make certain that sufficient head is obtained. If the head is too high the outside diameter of the impeller can always be cut down, but material cannot be added if the head is found to be deficient.

The vane outlet angle β_2 is usually made larger than the inlet angle β_1 . For this case an outlet angle of 20° will be assumed.

The radial outlet velocity V_{r_2} is made the same as, or slightly less than, the radial inlet velocity V_{r_1} which is 12 ft. per sec.; 11 ft. per sec. would be a reasonable value. The outlet area should be based upon the total flow of 2500 g.p.m. plus the leakage. The net area required to make $V_{r_2} = 11$ ft. per sec. would be

$$A_2 = \frac{144Q}{V_{r_2}} = \frac{144 \times 5.58 \times 1.02}{11} = 74.6 \text{ sq. in.}$$

A contraction factor ϵ_2 to care for the vane thickness must be assumed in determining the gross outlet area and width b_2 . If this is tentatively taken to be 0.925, then by Eq. 6-4 the approximate outlet width is

$$b_2 = \frac{144Q}{V_{r_2}\pi D_2 \epsilon_2} = \frac{144 \times 5.58 \times 1.02}{11 \times \pi \times 13.5 \times 0.925} = 1.895 \text{ in.}$$

Outlet Velocity Diagram. To design correctly the volute or diffuser, the magnitude and direction of the absolute outlet velocity V_2 of the liquid leaving the impeller must be known. Sufficient data are now available to draw the outlet diagram.

For an outlet diameter D_2 of $13\frac{1}{2}$ in. and a speed of 1760 r.p.m. the tip speed is

$$u_2 = \frac{\pi D_2 n}{12 \times 60} = \frac{\pi 13.5 \times 1760}{720} = 103.7 \text{ ft. per sec.}$$

The virtual tangential component V_{u_2} of the absolute outlet velocity V_2 is

$$\begin{aligned} V_{u_2} &= u_2 - \frac{V_{r_2}}{\tan \beta_2} = 103.7 - \frac{11}{\tan 20^\circ} = 103.7 - 30.2 \\ &= 73.5 \text{ ft. per sec.} \end{aligned}$$

Assuming a value of $\eta_\infty = 0.7$, the actual tangential component V'_{u_2} of the absolute outlet velocity V'_2 is, by Eq. 3-11,

$$V'_{u_2} = V_{u_2} \eta_\infty = 73.5 \times 0.7 = 51.5 \text{ ft. per sec.}$$

The outlet diagram may now be drawn (Fig. 6-9). The tangent of the actual outlet angle α'_2 is $V_{r_2}/V'_{u_2} = 11/51.5 = 0.2137$ and $\alpha'_2 = 12^\circ 4'$. On account of the actual flow conditions, described in Sec-

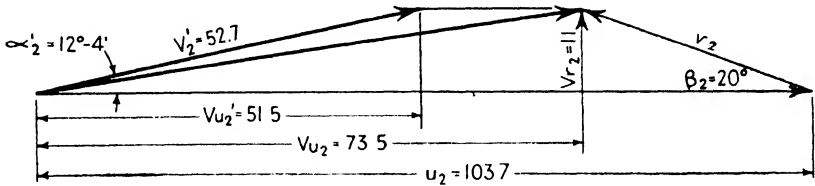


FIG. 6-9. Outlet velocity diagram.

tion 6-6, this angle is probably slightly larger, say 13° . The absolute outlet velocity is

$$V'_2 = \sqrt{V_{r_2}^2 + V'^2_{u_2}} = \sqrt{11^2 + 51.5^2} = 52.7 \text{ ft. per sec.}$$

This will also be slightly decreased although the increase of V_{r_2} will have a relatively minor effect, and V'_2 will probably not be less than 52.5 ft. per sec.

Leakage Loss. Sufficient data are now available to allow a closer approximation of the leakage in accordance with Section 6-4. From the impeller drawing (Fig. 6-13) the mean diameter of the clearance D is $8\frac{1}{2}$ in. The diametral clearance should be (Section 6-4)

$$s = 0.010 + (D - 6)0.001 = 0.010 + (8\frac{1}{2} - 6)0.001 = 0.013 \text{ in.}$$

The clearance area

$$A = \frac{1}{2}\pi Ds = \frac{1}{2}\pi \times 8\frac{1}{2} \times 0.013 = 0.174 \text{ sq. in.} = 0.00121 \text{ sq. ft.}$$

The head across the rings will be

$$H_L = \frac{3}{4} \frac{u_2^2 - u_1^2}{2g} = \frac{3}{4} \frac{(103.7^2 - 56.2^2)}{2 \times 32.2} = 88.6 \text{ ft.}$$

If the wearing rings are plain, similar to No. 3 of Fig. 6-1, the flow coefficient corresponding to a speed of 1760 r.p.m. and a clearance of 0.013 in. will be 0.410. The leakage then will be

$$Q_L = CA\sqrt{2gH_L} = 0.410 \times 0.00121\sqrt{2 \times 32.2 \times 88.6} = 0.0375 \text{ c.f.s.}$$

per side and the total leakage is 0.075 c.f.s. This amounts to $\frac{0.075}{5.58} \times 100$ or about 1.35 per cent, and is close enough to the assumed value of 2 per cent that no corrections need be made.

Design of Vanes. As pointed out in Section 6-8, there are two methods of laying out the vane shape. The vanes will be designed by each of these methods in turn.

The radial components V_{r_1} and V_{r_2} of the absolute velocity at the inlet and outlet are 12 and 11 ft. per sec. respectively. These are plotted against the corresponding radii of $3\frac{21}{32}$ in. and $6\frac{3}{4}$ in., respec-

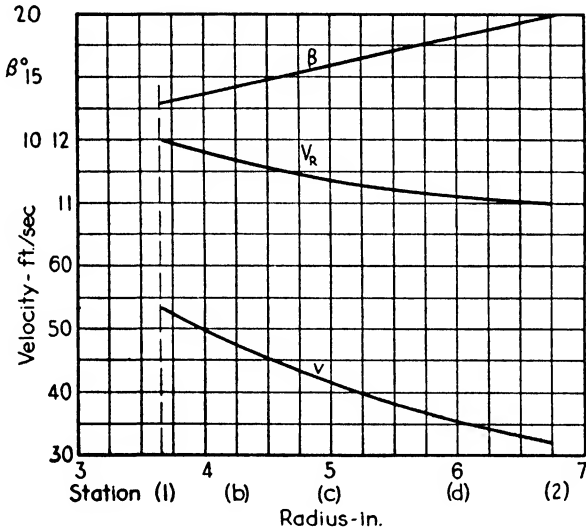


FIG. 6-10. Velocities and vane angle plotted against impeller radius.

tively, in Fig. 6-10 and may be connected by a straight line or by a smooth curve, as shown. The vane angles β_1 and β_2 at the inlet and outlet are 13° and 20° .

Since $v = \frac{V_r}{\sin \beta}$, the relative water velocities v

will be $\frac{12}{\sin 13^\circ} = 53.3$ ft. per sec. at the inlet, and $\frac{11}{\sin 20^\circ} = 32.2$ ft. per sec. at the outlet.

These values may also be plotted against the radius (Fig. 6-10) and connected by a straight line or smooth curve. Intermediate values of V_r and v may be read from these curves. The corresponding values for the vane angle β are computed from the relationship $\sin \beta = V_r/v$. The values of β thus found are plotted on the figure and will be used in each of the two methods.

(a) *Tangent Arcs.* When this method is used, the impeller is divided into a number of assumed concentric rings, not necessarily equally spaced, between R_1 and R_2 . The radius ρ of the arc defining the vane

shape between any two rings of radii R_b and R_a as given by Eq. 6-5 is

$$\rho = \frac{R_b^2 - R_a^2}{2(R_b \cos \beta_b - R_a \cos \beta_a)}$$

The values of ρ may be calculated conveniently in tabular form as follows:

Ring	R	R^2	β	$\cos \beta$	$R \cos \beta$	$R_b \cos \beta_b - R_a \cos \beta_a$	$R_b^2 - R_a^2$	ρ
<i>1</i>	3.66	13.39	13.00°	0.9744	3.56	0.56	4.67	4.17
<i>b</i>	4.25	18.06	14.25°	0.9692	4.12	0.69	6.94	5.03
<i>c</i>	5.00	25.00	15.92°	0.9617	4.81	0.89	11.00	6.18
<i>d</i>	6.00	36.00	18.33°	0.9492	5.70	0.64	9.55	7.46
<i>2</i>	6.75	45.55	20.00°	0.9397	6.34			

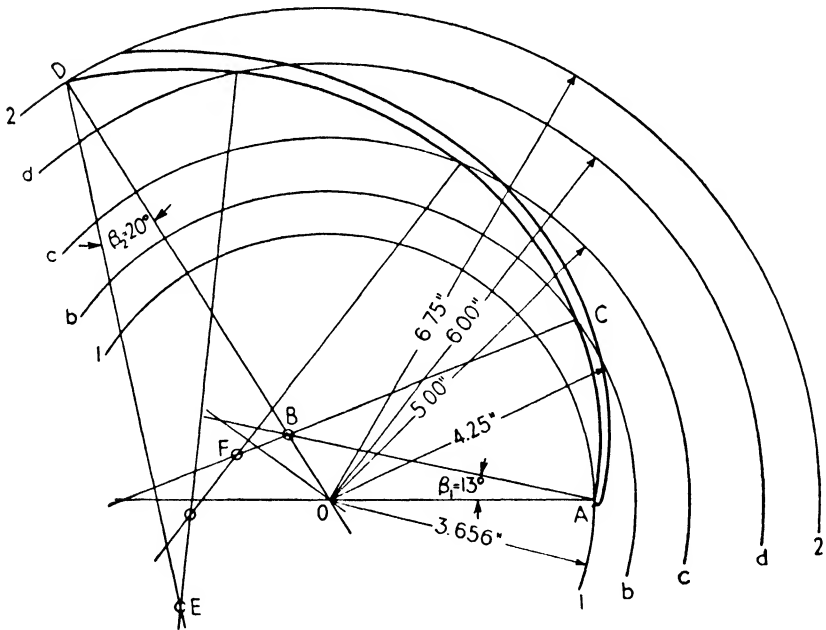


FIG. 6-11. Vane design using tangent arcs.

The values of ρ in the last column represent the radii of the circular arcs between the assumed rings or radii. A more accurate vane shape could be obtained by using more rings. Since the arcs are tangent to each other, the centers of adjacent arcs lie on a line with their point of tangency.

The layout of the vanes using these values is shown in Fig. 6-11. Any radial line OA from the center of rotation O to the radius R_1 is drawn. A line AB making an angle equal to β_1 (13°) with OA is next constructed. The center B for the first arc must lie on this line at a distance ρ of 4.17 in. from A . A line drawn through the intersection of this arc with the ring b of radius 4.25 in. (point C) and point B must contain the center for the second arc F . This process is repeated until the outside ring at radius R_2 is reached. As a check on the accuracy of the work the angle ODE , where E is the center of the last arc, must equal β_2 or 20° .

(b) *Polar Coordinates.* By this method points on the surface of the vane are calculated by using Eq. 6-6; they are plotted as polar coordinates.

$$\theta^\circ = \frac{180}{\pi} \int_{R_1}^R \frac{dR}{R \tan \beta} = \frac{180}{\pi} \sum_{R_1}^R \frac{\Delta R}{R \tan \beta} \quad 6-6$$

After the points have been calculated and plotted, they may be connected by a smooth curve or a series of tangent arcs. As mentioned in Section 6-8, this equation may best be solved by means of tabular integration (see the following table).

Ring	R	β	$\tan \beta$	$\frac{1}{R \tan \beta}$	$\frac{1}{R \tan \beta}$	ΔR	$\frac{\Delta R}{R \tan \beta}$	$\Delta \theta^\circ$	θ°
1	3.66	13.00°	0.2309	1.183					0
<i>b</i>	4.25	14.25°	0.2540	0.926	1.055	0.59	0.627	35.9	35.9
<i>c</i>	5.00	15.92°	0.2852	0.702	0.814	0.75	0.610	34.9	70.8
<i>d</i>	6.00	18.33°	0.3314	0.503	0.603	1.00	0.603	34.5	105.3
2	6.75	20.00°	0.3640	0.407	0.455	0.75	0.341	19.5	124.8

The same radii are used as before and the values of β are taken from Fig. 6-10. Since this is an integration more points should be taken, but the above table is sufficient to illustrate the method. The values of $\frac{1}{R \tan \beta}$ in the sixth column are found by averaging those in the fifth. The values of ΔR represent the difference between successive radii of the second column. In the ninth column $\Delta \theta^\circ$ is found by multiplying $\frac{180}{\pi}$ by $\frac{\Delta R}{R \tan \beta}$ of the eighth column. Integration is a summation, therefore θ° in the last column is found by successive additions of $\Delta \theta^\circ$ to obtain the angular position corresponding to the

radii. These points are plotted in Fig. 6-12 to give the vane shape.

The two methods just described give the trailing edge of the vane. The stress in the vanes due to the force exerted on the water is negligible, so the vane thickness is limited by casting difficulties rather than strength.

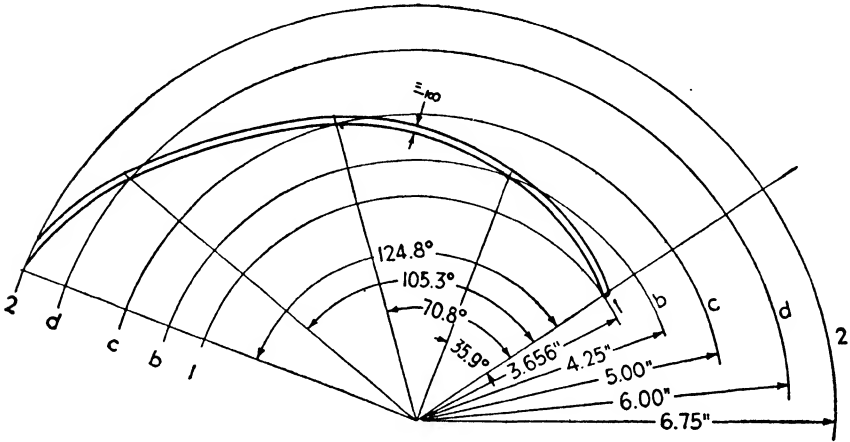


FIG. 6-12. Vane design using polar coordinates.

The front edge of the vane may be drawn with the same curvature as the back edge by rotating the impeller to obtain a definite thickness at the inlet, say $\frac{1}{8}$ in. The resulting vane will gradually increase in thickness toward the impeller rim as illustrated in Fig. 6-11; or the vane thickness perpendicular to the surface may be kept constant, as shown in Fig. 6-12,

The average value of the vane angle, $\beta_m = \frac{\beta_1 + \beta_2}{2} = \frac{13 + 20}{2} = 16.5^\circ$; therefore the number of vanes, according to Pfeleiderer (by Eq. 6-7), is

$$\begin{aligned} z &= 6.5 \frac{D_2 + D_1}{D_2 - D_1} \sin \beta_m = 6.5 \frac{13.5 + 7.312}{13.5 - 7.312} \sin 16.5^\circ \\ &= 6.5 \frac{20.812}{6.188} 0.284 = 6.21 \text{ or } 6 \text{ vanes} \end{aligned}$$

The circumferential pitch of the vanes then would be $\frac{\pi D_1}{z} = \frac{\pi 7.312}{6} = 3.83$ in. and the height of the passage perpendicular to the flow is equal to the circular pitch times the sine of the inlet angle or $3.83 \times \sin 13^\circ = 3.83 \times 0.225 = 0.863$ in. The approximate inlet width b_1 has been found to be 1.743 in. This is far from the desirable square

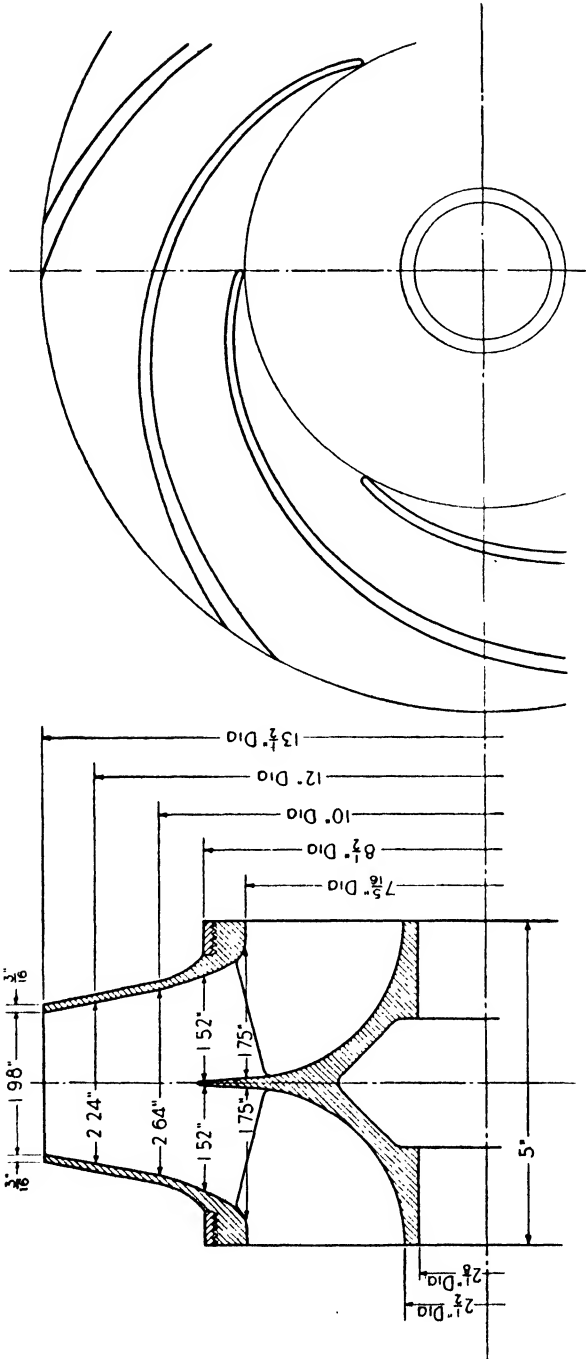


FIG. 6-13. Sketch of impeller designed in Section 6-9.

passage cross section. However, the passage height increases with the radius, hence the passage section tends to become more nearly square, and six vanes will be used.

Passage Width. To determine the width of the passage at various radii, the contraction factor ϵ must be first calculated at these radii by Eq. 6-8.

$$\epsilon = \frac{\pi D - \frac{zt}{\sin \beta}}{\pi D}$$

where t is the normal vane thickness and is scaled from the vane drawing (Fig. 6-11 will be used for illustration).

The width b is given by Eq. 6-9. The capacity Q is multiplied by the leakage factor and divided by the factor 2 because here the impeller is of the double-suction type. The values of V_r are taken from Fig. 6-10. The widths thus obtained from Eq. 6-9 represent those on each side of the impeller centerline $b/2$. The calculations in tabular form are as follows.

R	D	πD	t	$\sin \beta$	$\frac{zt}{\sin \beta}$	$\pi D - \frac{zt}{\sin \beta}$	ϵ	V_r	$b/2$	b
3.66	7.31	22.95	0.125	0.225	3.34	19.61	0.855	12.00	1.75	
4.25	8.50	26.69	0.150	0.246	3.66	23.03	0.864	11.68	1.52	
5.00	10.00	31.42	0.195	0.274	4.27	27.15	0.863	11.41	1.32	2.64
6.00	12.00	37.68	0.250	0.314	4.78	32.90	0.875	11.09	1.12	2.24
6.75	13.50	42.39	0.275	0.342	4.82	37.57	0.886	11.00	0.99	1.98

Summary. The calculated dimensions are summarized below, and Fig. 6-13 shows a sketch of the impeller.

- Diameter of suction flange, $D_{su.} = 10$ in.
- Velocity in suction flange, $V_{su.} = 10.22$ ft. per sec.
- Shaft diameter, $D_s = 2\frac{1}{8}$ in.
- Impeller hub diameter, $D_H = 2\frac{1}{2}$ in.
- Impeller eye diameter, $D_0 = 7\frac{5}{16}$ in.
- Velocity through impeller eye, $V_0 = 11$ ft. per sec.
- Diameter of inlet vane edge, $D_1 = 7\frac{5}{16}$ in.
- Velocity at inlet vane edge, $V_1 = V_{r_1} = 12$ ft. per sec.
- Passage width at inlet, $b_1 = 1.75$ in. per side
- Tangential velocity of inlet vane edge, $u_1 = 56.2$ ft. per sec.
- Vane angle at inlet, $\beta_1 = 13^\circ$
- Impeller outlet diameter, $D_2 = 13\frac{1}{2}$ in.
- Radial component of outlet velocity, $V_{r_2} = 11$ ft. per sec.
- Vane angle at outlet, $\beta_2 = 20^\circ$
- Total passage width at outlet, $b_2 = 1.98$ in.
- Tangential velocity of outlet vane edge, $u_2 = 103.7$ ft. per sec.
- Absolute velocity leaving impeller, $V'_2 = 52.5$ ft. per sec.
- Tangential component of V'_2 , $V'_{u_2} = 51.5$ ft. per sec.
- Angle of water leaving impeller, $\alpha'_2 = 13^\circ$
- Number of impeller vanes, $z = 6$

6-10 Design of Volute. The purpose of the volute, as outlined previously, is to convert the velocity head of the water leaving the impeller as efficiently as possible.

The water in the volute has very nearly the spiral flow described in Section 2-12(d), that is, $RV_u = C = \text{a constant}$, where C is determined from the relationship $R_2 V'_u = C$ for a given stage.

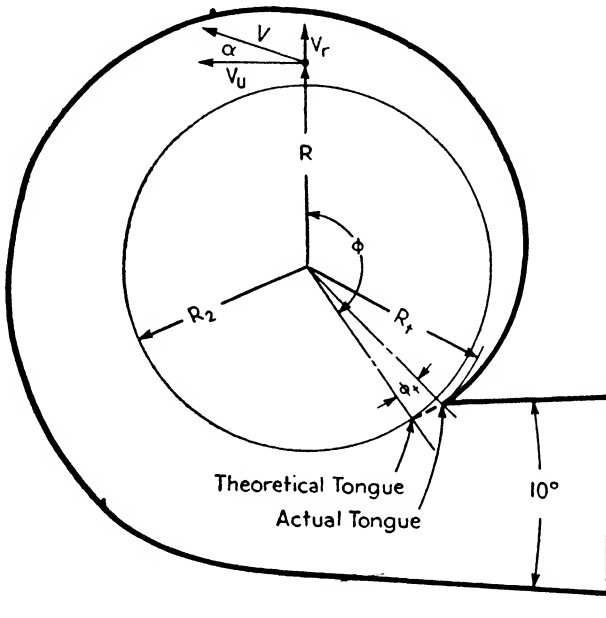


FIG. 6-14. Elevation of volute.

It may be assumed that the flow from the impeller is uniform about its periphery, so the flow past any section of the volute is $\phi/360$ of the total, where ϕ is the angle in degrees measured from the theoretical tongue of the volute as shown in Fig. 6-14.

In determining the cross-sectional area of the volute at any point, the problem consists in finding the area of the section that will pass the volume $Q\phi/360$ with a velocity $V_u = C/R$. It should be noted that the value of Q used is that of the delivered flow. It does not include the leakage flow which has now split off from the total impeller flow and returned to the suction through the wearing rings.

If friction is neglected, the flow through the differential section shown in Fig. 6-15 is

$$dQ_\phi = dA V_u = b dR V_u$$

But $V_u = C/R$, hence $dQ_\phi = b dR C/R$, and the total flow past the section becomes

$$Q_\phi = \int_{R_2}^{R_\phi} dQ = C \int_{R_2}^{R_\phi} \frac{b dR}{R}$$

where R_ϕ is the outer radius of a section at ϕ° from the theoretical tongue. Substituting for Q_ϕ the term $\phi Q/360$ there results

$$\phi^\circ = \frac{360C}{Q} \int_{R_2}^{R_\phi} b \frac{dR}{R} = \frac{360R_2 V'_{u2}}{Q} \int_{R_2}^{R_\phi} b \frac{dR}{R} \tag{6-10}$$

After the shape of the side walls of the volute has been decided upon, the integral can best be solved by tabular integration as illustrated in the next section.

The shape of the volute is generally similar to that shown on Fig. 6-15. The maximum total angle θ between the sides is usually about 60° . If made greater the water is unable to follow the sides and turbulence and inefficiency result. Volute with smaller θ angles and larger radii give better results, but then the casing diameter and weight of the pump are increased unduly. If the discharge angle from the impeller α'_2 is small, a larger angle between the sides may be used since the flow is then more nearly tangential.

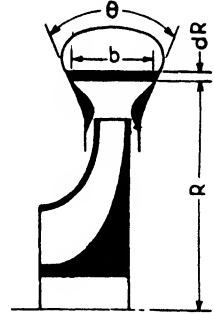


FIG. 6-15. Section through volute.

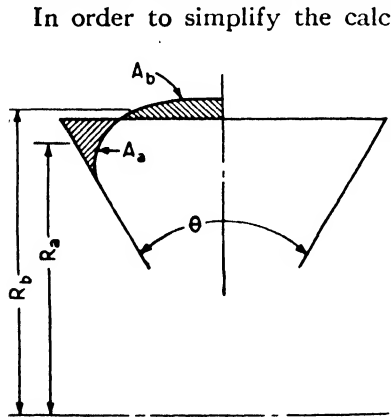


FIG. 6-16. Volute passage cross section.

In order to simplify the calculations it may be assumed that the top of the volute is parallel to the shaft axis. After the areas have been found on this basis, the top wall of the volute may be made of any desired shape by substituting equivalent areas for the original ones. Since RV_u is a constant and $V_u = dQ/A$ at each section, it may be seen that $dQ R/A$ must be constant also. Hence $R_a dQ/A_a = R_b dQ/A_b$, or $A_a/R_a = A_b/R_b$ and $A_b = A_a R_b/R_a$, where R_a and R_b are the distances from the shaft axis to the respective centers of gravity of the corresponding areas as shown in Fig. 6-16.

These corrections may, in most cases, be neglected since the ratio R_b/R_a is usually very near unity and inherent casting inaccuracies

destroy extreme refinements in calculation. It should also be remembered that the above calculations are based upon frictionless flow. Since the actual velocity is lower, the areas must be arbitrarily increased to care for this. This arbitrary increase in area may be much greater than the correction for the change of shape of passage.

To avoid shock losses the tongue angle should be made the same as the absolute outlet angle α'_2 of the water leaving the impeller. The radius R_t at which the tongue starts should be 5 to 10 per cent greater than the outside radius of the impeller to avoid turbulence and noisiness and to give the velocities of the water leaving the impeller a chance to equalize before coming into contact with the tongue.

The zero point of the volute or the point from which the angle ϕ is measured may be found by assuming that the flow follows a logarithmic spiral. The equation of a logarithmic spiral is:

$$R = R_2 e^{\tan \alpha'_2 \bar{\phi}}$$

where $\bar{\phi}$ is the angle measured in radians

α'_2 is the constant angle of the spiral or the angle at which the water leaves the impeller

e is the base of natural logarithms = 2.718.

Hence $R = R_2 2.718^{\tan \alpha'_2 \phi^\circ \frac{\pi}{180}}$, where ϕ° is the angle measured in degrees.

$$\log_{10} R = \log_{10} R_2 + \tan \alpha'_2 \left(\frac{\pi \phi^\circ}{180} \log_{10} 2.718 \right)$$

Hence

$$\phi^\circ = \frac{132 \log_{10} R/R_2}{\tan \alpha'_2} \quad 6.11$$

For the tongue radius $R = R_t$ and

$$\phi_t^\circ = \frac{132 \log_{10} R_t/R_2}{\tan \alpha'_2} \quad 6.12$$

In the passage between the volute and discharge flange further conversion of velocity into pressure may take place, especially with high head pumps, by making it divergent. In order to avoid turbulence the total divergence in this passage should not exceed 10° . The velocity here should never be greater than the minimum velocity in the volute, otherwise some of the pressure energy would be reconverted to velocity.

6.11 Example of Volute Design. A volute to fit the impeller designed in Section 6-9 will be used to illustrate Section 6-10.

The basic shape of the cross section will be a trapezoid as shown in Fig. 6-16, with walls at a 30° angle with radial lines ($\theta = 60^\circ$), and a base width at D_2 of $2\frac{5}{8}$ in. This base width is made up of the outlet width b_2 of 1.98 in. plus twice the shroud thickness ($2 \times \frac{3}{16}$ in.) plus clearances on each side of the impeller. Small pockets of inactive flow will be formed on each side of the impeller as shown by the black areas in Fig. 6-15. They have little effect on the efficiency and they adjust themselves to the flow. The width of the volute at any point may be scaled from a layout or calculated by the equation

$$b = b_3 + 2x \tan \frac{\theta}{2} = 2.625 + 2x \tan 30^\circ$$

where x = distance between any radius R and the impeller outside radius R_2 .

The volute is designed by determining the angle ϕ° measured from an assumed radial line by tabular integration of Eq. 6-10,

$$\phi^\circ = \frac{360R_2 V'_{u_2}}{Q} \int_{R_2}^{R_\phi} b \frac{dR}{R}$$

If R and b are expressed in inches, this equation becomes

$$\phi^\circ = \frac{360 \times 6.75 \times 51.5}{5.58 \times 144} \int_{R_2}^{R_\phi} b \frac{dR}{R} = 155.7 \int_{R_2}^{R_\phi} b \frac{dR}{R} = 155.7 \sum_{R_2}^{R_\phi} b \frac{\Delta R}{R}$$

The integration is best performed in tabular form.

R in.	ΔR in.	$R_{\text{ave.}}$ in.	$b_{\text{ave.}}$ in.	$\frac{b \Delta R}{R_{\text{ave.}}}$	$\Delta\phi^\circ$	ϕ°	ΔA sq. in.	A_ϕ sq. in.	Q_ϕ c.f.s.	$V_{\text{ave.}}$ ft. per sec.
6.75			2.625			0		0	0	
	1.25	7.375	3.346	0.568	88.5		4.18			
8.00			4.645	0.546	85.5	88.5	4.65	1.37	47.2	
	1.00	8.5	5.800	0.610	95.0	174.0	5.80	2.70	44.0	
9.00			6.955	0.662	103.0	269.0	6.95	4.17	41.1	
	1.00	10.5				372.0	21.58	5.76	38.4	
10.00										
11.00										

Radii equal to the impeller outside radius and greater are assumed in the first column to form rings having areas of $b_{\text{ave.}}(\Delta R)$. The average width of each ring is obtained from the equation

$$b = b_3 + 2x \tan \frac{\theta}{2} = 2.625 + 2(R_{\text{ave.}} - 6.75) \tan \frac{60}{2}$$

The values of $\frac{b \Delta R}{R_{\text{ave}}}$ are then calculated and multiplied by 155.7 to obtain the angle increments $\Delta\phi^\circ$ of the sixth column. These are integrated by successive addition in column 7 and the radii of column 1 are laid off at the corresponding ϕ° angles to obtain the top side of the volute.

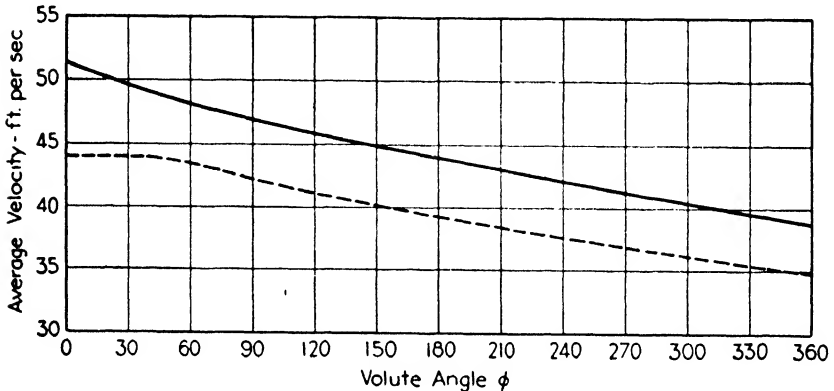


FIG. 6-17. Average velocities in volute around circumference.

The average velocity at these sections is found by dividing the flow past the section, $Q \frac{\phi^\circ}{360}$, by the total area at the section A_ϕ as found by the tabular integration of ΔA (the area increment $b \Delta R$). These values are listed in the last column and plotted in Fig. 6-17. These velocities should be reduced by about 10 per cent and the areas increased the same amount to allow for the friction loss in the volute. This is shown by the dotted curve of Fig. 6-17. The velocities near the tongue are decreased still further by increasing the area to avoid excessive losses due to the improper angle at capacities other than the design flow.

The base line from which ϕ is measured may be placed in any position. It is usual to have the discharge line horizontal. After the volute has been calculated, it is rotated about the shaft centerline until this condition is satisfied.

The volute is considered to begin at the assumed base line, but it actually begins at the tongue radius R_t which is 5 to 10 per cent greater than the impeller radius R_2 . This tongue radius is 1.05 to 1.10 times 6.75, or 7.09 to 7.42 in., hence $7\frac{1}{4}$ in. may be used. The tongue angle

is given by Eq. 6-12:

$$\phi_i^\circ = \frac{132 \log_{10} \frac{R_t}{R_2}}{\tan \alpha'_2} \tag{6-12}$$

Since $\alpha'_2 = 13^\circ$, $\tan \alpha'_2 = 0.231$. The ratio $\frac{R_t}{R_2} = \frac{7.25}{6.75} = 1.073$ and its log to the base 10 is 0.0306. Hence

$$\phi_i^\circ = \frac{132 \times 0.0306}{0.231} = 17.5^\circ$$

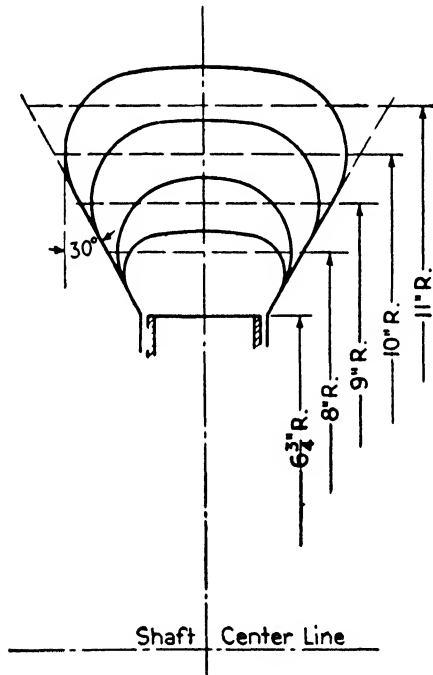


FIG. 6-18. Sections through volute passage at calculated angles.

After the volute with the trapezoidal shape has been determined the corners are rounded off as described in the previous section, with the aid of a planimeter to measure the areas.

The average velocity of the water leaving the volute is about 39 ft. per sec. According to Section 6-3 it would be desirable to have it leave the pump with a velocity of about 25 ft. per sec. A 6-in.-diameter flange has an area of 28.3 sq. in.; this corresponds to an average

velocity of $\frac{5.58 \times 144}{28.3} = 28.4$ ft. per sec. which will be satisfactory.

The section between the volute outlet and the discharge line, known as the discharge nozzle, would be made diverging to a 6-in. diameter.

Figure 6-18 shows sections of the volute passage at the calculated points with the areas increased approximately 10 per cent for friction, and Fig. 6-19 shows an elevation of the volute using the values as calculated in the table.

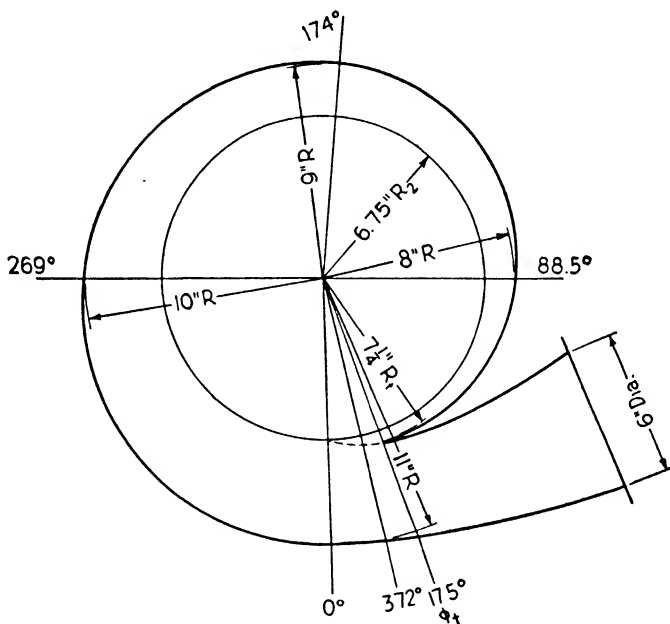


FIG. 6-19. Elevation of volute.

6-12 Design of Diffuser. As outlined in Section 3-16 a diffuser has essentially the same shape as a volute except that a number of passages are used rather than one. This permits the conversion of kinetic energy to pressure in a much smaller space, so a diffuser is frequently used for stages having high heads, as in multistage pumps.

The radial clearance between the impeller and diffuser vane tips should be fairly small for good efficiency. It varies between $\frac{1}{32}$ and $\frac{1}{8}$ in., depending upon the impeller size. The diffuser width b_3 may be made wider than the impeller outlet width. The water cannot follow this abrupt change; hence small pockets of inactive flow will be formed, as noted in the volute. For this reason the full throat area of the diffuser may not be effective.

The water traveling between the impeller and diffuser follows a logarithmic spiral of constant angle α'_2 as noted in Section 2-12(d). Neglecting friction and turbulence, the velocity of the water at the diffuser throat will be $V_3 = V'_2 \frac{D_2}{D_3}$.

Each passage is assumed to handle equal fractions of the total flow. The total throat area required, A_3 , is $\frac{144Q}{V_3}$ and if z' is the number of vanes or passages, the throat height, h_3 , is $\frac{A_3}{z' b_3}$.

The number of diffuser vanes z' should be a minimum consistent with good guidance of the water. In order to avoid vibration difficulties, the number of vanes should have no common factor with the number of impeller vanes. If possible the section of the passages in the diffuser are made nearly square, i.e., $b_3 = h_3$, since this will reduce the friction losses.

The shape of the passage should be diverging. Experiments indicate that this divergence angle should be between 10° and 12° for best results. If the velocity or viscosity of the liquid is high, the angle must be made smaller. General practice is to keep the angle small near the throat where the velocity is high and gradually increase it as the velocity decreases. The losses in the diffuser are rather high. The percentage of kinetic energy that is converted to pressure ranges from 75 to 90 per cent.

The velocity of the water leaving the diffuser is made slightly greater than the velocity in the discharge line from the pump. The mouth area $A_4 = \frac{144Q}{V_4}$ and $h_4 = \frac{A_4}{z' b_4}$.

The mouth width b_4 may be made greater than the throat width b_3 to increase the area ratio by securing divergencies in both directions. This would shorten the passage length required to secure a given conversion of velocity to pressure energy and hence reduce the size and weight of the pump. It is seldom done because of the increased cost.

6-13 Example of Diffuser Design. To illustrate the discussion in the previous section the design of a diffuser to operate with the impeller of Section 6-9 will be outlined. As the head is low a diffuser is not required, but the design is discussed to illustrate the procedure.

A radial clearance between the impeller and vane tips of $\frac{1}{16}$ in. will be assumed. As a preliminary estimate an approximate mean throat diameter of $14\frac{1}{2}$ in. will be used. The width of the diffuser will be taken as $2\frac{5}{8}$ in., which is the same as that used for the volute.

The velocity of the water at the throat $V_3 = V_2' \frac{D_2}{D_3} = 52.5 \frac{13.5}{14.5} = 48.9$ ft. per sec. Reducing this about 15 per cent for losses and width ratio b_2/b_3 makes $V_3 = 42$ ft. per sec. The total throat area required is $A_3 = \frac{144Q}{V_3} = \frac{144 \times 5.58}{42} = 19.1$ sq. in. If 11 vanes are used, the throat height $h_3 = \frac{A_3}{z'b_3} = \frac{19.1}{11 \times 2.625} = 0.661$ in. As noted in the previous section the number of diffuser vanes should not have any common factor with the number of impeller vanes. There should be enough vanes to give good guidance to the water. Eleven vanes will satisfy these requirements.

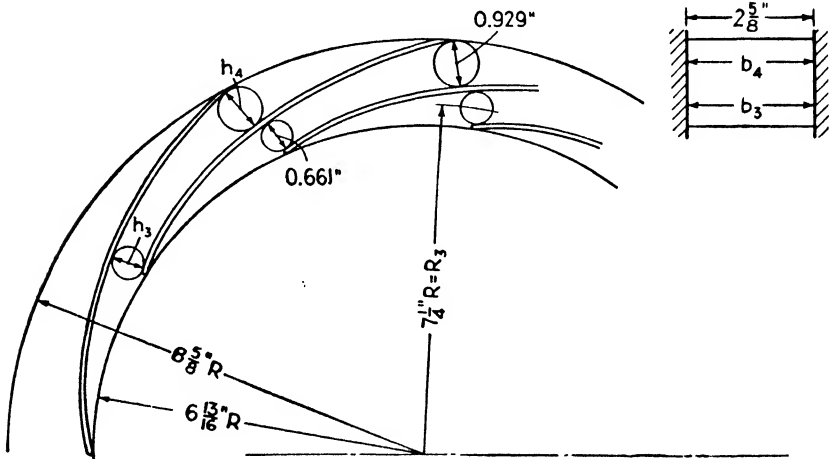


FIG. 6-20. Diffuser of Section 6-13.

As the velocity in a 6-in.-diameter discharge line is 28.4 ft. per sec. the velocity leaving the diffuser may be made slightly higher, say 30 ft. per sec. The corresponding total area at the diffuser mouth will be $A_4 = \frac{144Q}{V_4} = \frac{144 \times 5.58}{30} = 26.8$ sq. in. and the mouth height will be $h_4 = \frac{A_4}{z'b_4} = \frac{26.8}{11 \times 2.625} = 0.929$ in.

The vanes may be made constant in thickness or varying in thickness. This varies widely with different manufacturers depending upon experimental test results and individual preference. A satisfactory passage shape is based largely upon experience and may require many trials. The curve of the vane from the tip to the throat should approx-

imate a logarithmic spiral (Eq. 6-11 may be used for this) with the corrected absolute outlet angle ($\alpha'_2 = 13^\circ$) to avoid turbulence.

The divergence should be low just after the throat and should increase gradually as the water velocity is reduced. As pointed out previously, an average value of 10° to 12° will produce satisfactory results. After the ideal shape has been found by using a French curve, it may be approximated by a series of tangent circular arcs for shop use. A sketch of this diffuser is shown in Fig. 6-20.

6-14 Disk Friction. The theory underlying the power loss due to disk friction was discussed in Section 3-8 and it will be recalled that the loss is proportional to $D^2 u^3 \gamma$ or to $D^5 n^3 \gamma$.

For water, the two most commonly used equations are those of Pfleiderer and Gibson which are based upon experiment. Pfleiderer's equation is

$$\text{hp}_{.DF} = 1.83 \left(\frac{u_2}{100} \right)^3 \left(\frac{D_2}{10} \right)^2 \quad 6-13$$

where u_2 is the rim velocity in feet per second and D_2 is the rim diameter in inches. This equation seems to give rather high values for high peripheral speeds (high u_2).

The second equation, given by A. H. Gibson, is

$$\text{hp}_{.DF} = \frac{\left(\frac{D_2}{12} \right)^{4.83} n^{2.83}}{8.75 (10)^8} \quad 6-14$$

where n is the speed in revolutions per minute and D_2 is the rim diameter in inches.

To illustrate their application, consider the impeller calculated in Section 6-9. By Pfleiderer's equation,

$$\text{hp}_{.DF} = 1.83 \left(\frac{103.7}{100} \right)^3 \left(\frac{13.5}{10} \right)^2 = 1.83 \times 1.12 \times 1.82 = 3.73 \text{ hp.}$$

By Gibson's equation,

$$\text{hp}_{.DF} = \frac{\left(\frac{13.5}{12} \right)^{4.83} (1760)^{2.83}}{8.75 (10)^8} = \frac{1.765 \times 15.3(10)^8}{8.75 (10)^8} = 3.09 \text{ hp.}$$

6-15 Multistaging. Multistaging is the mounting of two or more impellers on the same shaft so that they act in series. Although they run at the same r.p.m. and handle the same flow as a single stage, the developed head and, consequently, the diameter of each impeller are smaller.

If the total head to be developed by a pump is too large for a single stage to handle, multistaging is resorted to. It may also be used when not absolutely required by head considerations in order to secure better performance or design. By varying the head per stage a specific speed corresponding to higher efficiency may be obtained. If the head per stage is lowered less leakage will result. The use of smaller diameter impellers reduces the total disk friction because the disk friction is proportional to the cube of the diameter whereas the head is proportional to the square of the diameter. The smaller impeller size will decrease the induced stresses due to centrifugal force. There will be some additional loss due to friction and turbulence in transmitting the fluid from the diffuser to the eye of the next stage impeller, which often balances the advantages mentioned above.

Usually all the impellers of a multistage pump have the same diameter, so each stage develops the same head. The total head of the pump then is the product of the head per stage and the number of stages. The design procedure for each stage will be the same as outlined in this chapter for a single stage.

The water leaving a diffuser has a tangential component as well as a radial one. Hence, it may be assumed that its path in the return passage between the stages approximates that of a logarithmic spiral having RV_u equal a constant. As the water approaches the eye of the following stage R is decreasing, so V_u must increase. To avoid this condition guide vanes are placed in this passage to receive the water and cause it to enter the succeeding stage radially.

PROBLEMS

6-1 A centrifugal pump is required to develop a pressure of 30 lb. per sq. in. at 2000 r.p.m. when delivering 1000 g.p.m. What is the approximate impeller diameter and pump efficiency?

6-2 Estimate the impeller diameter of the pump in Problem 4-5.

6-3 A 700-g.p.m. single-suction radial-type pump handling water rotates at 2500 r.p.m. and develops a head of 250 ft. If $D_0 = D_1$, $D_H = 3$ in., $V_0 = 15$ ft. per sec., $V_1 = 17.5$ ft. per sec., $V_r = 11.5$ ft. per sec., $\epsilon_1 = 0.92$, $\epsilon_2 = 0.90$, $\Phi = 1.030$, determine (a) approximate outside diameter of impeller, D_2 ; (b) approximate eye diameter, D_0 ; (c) vane inlet angle, β_1 ; (d) vane inlet width, b_1 ; (e) vane outlet width, b_2 .

Ans. (a) 12 in.; (b) 5.3 in.; (c) 16.8°; (d) 0.840 in.; (e) 0.576 in.

6-4 Given the following data on a single-stage, double-suction, radial-type pump handling water and having radial inlet flow ($\alpha_1 = 90^\circ$):

1750 r.p.m.	$D_1 = 4$ in.	$b_1 = 1$ in. per side	$H = 100$ ft.
1000 g.p.m.	$D_2 = 11\frac{1}{2}$ in.	$b_2 = 15/16$ in. total	$\beta_2 = 27^\circ$

Overall efficiency = 83 per cent. Leakage loss = 30 g.p.m. Horsepower losses:

disk friction 1.4; bearings and packing 0.5. Inlet and outlet contraction factor for vane thickness = 0.87.

Determine: (a) Correct vane inlet angle, β_1 , (b) the factors K and η_∞ , (c) hydraulic efficiency, η_{HY} , (d) actual absolute velocity leaving the impeller, V_2' , (e) actual angle at which the water leaves the wheel, α_2' , (f) the overall head factor Φ .

Ans. (a) $26^\circ 25'$; (b) 0.557, 0.611; (c) 91.1 per cent; (d) 41.8 ft. per sec.;
(e) $15^\circ 40'$; (f) 1.097

CHAPTER 7

OTHER PUMP IMPELLER TYPES

7.1 Introduction. The radial-type stage designed in the previous chapter is used for the majority of pumps manufactured today. Francis, mixed-flow, and propeller stages are used for higher specific speeds and may be used in either single-stage or multistage pumps.

7.2 Francis-Type Impeller. Francis-type impellers are used for lower heads and higher capacities than the radial-type stage, i.e., for specific speeds in the range from 1500 to 4500. They may be made single- or double-suction depending upon the flow to be handled. The outlet edge of the vanes is parallel to the shaft axis, but the inlet edge curves from the impeller eye radius inward almost to the hub radius (Fig. 4-4).

As the peripheral speed u_1 of points along the inlet edge of the vane increases with the radius while the absolute inlet velocity of the liquid V_1 remains practically constant, it is obvious from the inlet triangle that the vane inlet angle β_1 varies inversely with the radius. Since the vane itself is curved (as for a radial-type impeller) the vane surface at the inlet is doubly curved or warped.

The resultant angles of the vanes are gradually changed to a common value at some chosen radius. Beyond this radius the vane is singly curved and is similar to the conventional radial-type impeller. If the impeller outside diameter is small relative to the eye diameter, the radius at which the vane angle is made uniform may be that of the impeller rim.

The general design procedure is similar to that of the radial-type impeller. It may best be outlined by means of an example which will deal chiefly with the determination of the vane shape and method of specifying it. For this example consider the design of a 20,000-g.p.m., 80-ft. head, double-suction stage operating at 600 r.p.m. and handling water.

(a) *Determination of the Chief Impeller Dimensions.* Since the impeller is double suction its specific speed is based upon one-half the

total flow or $n_s = \frac{n\sqrt{Q}}{H^{3/4}} = \frac{600\sqrt{10000}}{80^{3/4}} = 2240$. The total flow $w = \frac{\text{g.p.m.} \times 8.33}{60} = \frac{20000 \times 8.33}{60} = 2775$ lb. per sec., and the volume

flow $Q = \frac{20,000 \times 0.134}{60} = 44.67$ c.f.s. The water horsepower is
 w.hp. = $wH/550 = 2775 \times 80/550 = 403$.

An examination of Figs. 4-9, 4-10, 4-11, and 4-12 reveals that an efficiency of 85 per cent could be expected. The brake horsepower required to drive the unit is $\frac{w.hp.}{\eta} = \frac{403}{0.85} = 475$ b.hp.

The shaft torque $T = \frac{63000 \text{ b.hp.}}{\text{r.p.m.}} = \frac{63000 \times 475}{600} = 49900$ lb.-in.

For a torsional stress of 5000 lb. per sq. in. the shaft diameter $D_s = \sqrt[3]{\frac{16T}{\pi s_s}} = \sqrt[3]{\frac{16 \times 49900}{5000\pi}} = 3.70$ in. This value will be increased to 4 in. to care for the bending stress and to avoid excessive lateral deflection. The hub diameter D_H may then be made 5 in.

The absolute velocity of the water in the impeller eye V_0 and at the vane inlet V_1 will be taken as 11 ft. per sec. in accordance with the discussion in Section 6-5. Since the flows are large the leakage past the wearing rings will be rather small. A value of 1 per cent will be assumed and checked later. Remembering that this is a double-suction impeller and that one-half the flow enters each side, the impeller eye diameter as given by Eq. 6-1 is

$$D_0 = \sqrt{\frac{4}{\pi} \frac{144Q}{V_0} + D_H^2} = \sqrt{\frac{4}{\pi} \frac{144 \times 1.01 \times 44.67}{11 \times 2} + 5^2} = 20.1 \text{ in.}$$

A diameter of 20 in. may be used.

It is not desirable to have the minimum vane inlet angle too small (less than about 10°), hence it would be wise to check roughly this value before proceeding. The vane peripheral speed for a diameter of 20 in. is $\frac{\pi 20 \times 600}{720} = 52.4$ ft. per sec. The tangent of the vane inlet angle is $\tan \beta_1 = V_1/u_1 = 11/52.4 = 0.21$, hence β_1 at the eye will be about 12° , which is satisfactory.

The data given on Figs. 6-4, 6-5, and 6-6 are rather meager for use in selecting a value of Φ for determining the impeller outside diameter, but a value of 1.08 probably would not be far out of line. By Eq. 3-17,

$$D_2 = \frac{1840\Phi\sqrt{H}}{n} = \frac{1840 \times 1.08\sqrt{80}}{600} = 29.65 \text{ in.}$$

To be on the safe side the outside diameter will be made 30 in.

The leakage loss may now be checked roughly by the method de-

scribed in Section 6-4. A mean clearance diameter of 21 in. will be assumed, and the diametral clearance will be

$$s = 0.010 + (D - 6)0.001 = 0.010 + (21 - 6)0.001 = 0.025 \text{ in.}$$

The clearance area $A = \frac{1}{2}\pi Ds = \frac{1}{2}\pi 21 \times 0.025 = 0.825 \text{ sq. in.} = 0.00573 \text{ sq. ft.}$ The impeller tip speed $u_2 = \frac{\pi 30 \times 600}{720} = 78.5 \text{ ft. per}$

sec., and the maximum inlet edge speed u_1 is 52.4 ft. per sec. The head across the ring is

$$H_L = \frac{3}{4} \frac{u_2^2 - u_1^2}{2g} = \frac{3}{4} \left[\frac{78.5^2 - 52.4^2}{2 \times 32.2} \right] = 39.8 \text{ ft.}$$

It is rather difficult to estimate the flow coefficient C for this case from Fig. 6-1 on account of the low speed. For plain rings of type No. 8 or 9 of Fig. 6-1, a speed of 600 r.p.m., and a diametral clearance of 0.025 in. the coefficient will probably be about 0.575.

The leakage flow per side is

$$Q_L = CA\sqrt{2gH_L} = 0.575 \times 0.00573\sqrt{2 \times 32.2 \times 39.8} = 0.167 \text{ c.f.s. per side}$$

The per cent leakage = $\frac{Q_L \times 2}{Q} = \frac{0.167 \times 2}{44.67} = 0.0075 = 0.75 \text{ per cent,}$ which is close to the assumed value of 1 per cent.

The radial velocity at the outlet V_{r_1} is made equal to or slightly less than the inlet velocity V_1 (Section 6-5). Here 10 ft. per sec. will be assumed. If a contraction factor at the outlet ϵ_2 is assumed to be 0.925, one-half the impeller rim width, by Eq. 6-4, is

$$\frac{b_2}{2} = \frac{144Q}{V_{r_1}D_2\pi\epsilon_2} = \frac{144 \times 1.0075 \times 44.67}{10 \times 30 \times \pi \times 0.925 \times 2} = 3.72 \text{ in.}$$

From these dimensions the impeller shape may be drawn as shown in Fig. 7-1. Throughout this section only one-half of the impeller will be considered, since it is symmetrical about a radial centerline. As may be seen in the figure, the sides of the passages are made smooth curves which gradually converge with increasing radius. The inner portion of the passage near the radial centerline is not extended to the rim. It is made large enough to give good guidance to the water and to give strength to the vanes, but beyond that it is not necessary. The center portion of the impeller is frequently made hollow to decrease the weight. This is easily done since the impeller is cast and this portion may be cored.

(b) *Determination of Streamlines.* After the impeller shape has

been determines, the next step is to sketch in three to five (depending upon the impeller shape and size) streamtubes of flow (Section 2.12). In this case four streamtubes will be used. The edges of the passages fix two of the streamlines and the other three must be determined.

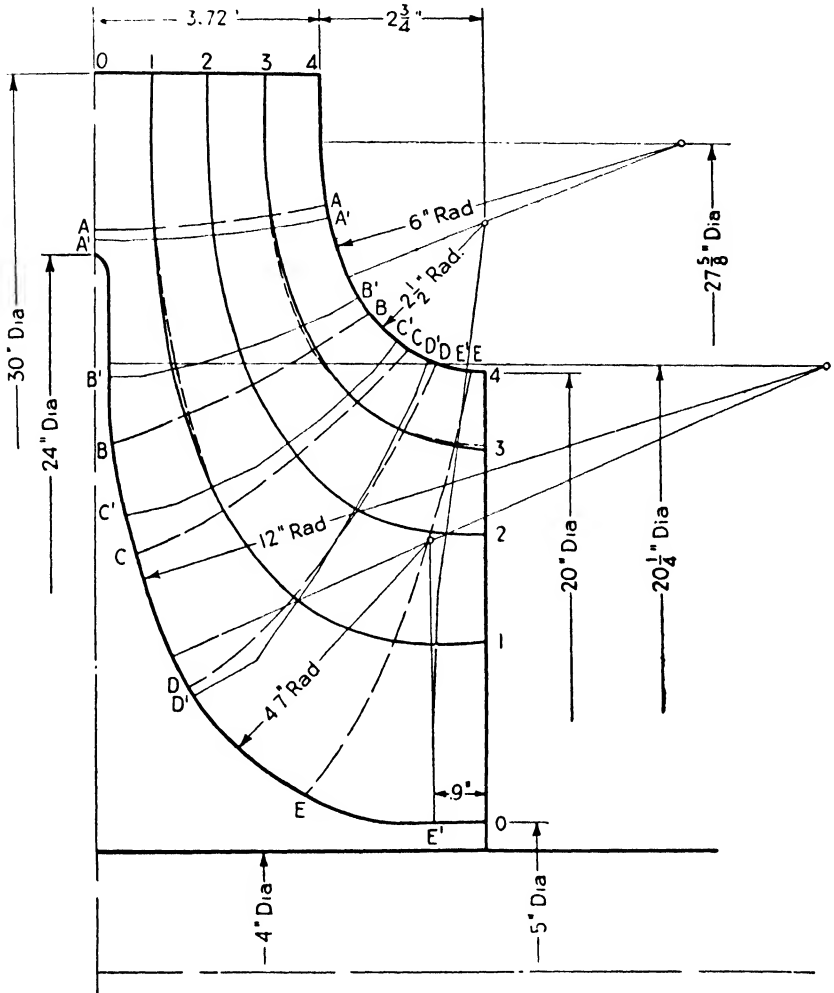


FIG. 7.1 Determination of impeller shape and streamlines.

This may be done by assuming the dashed lines AA , BB , etc., shown in Fig. 7.1. These lines are drawn as nearly perpendicular to the direction of flow as can be estimated by eye. Each line is then divided into four lengths, each having equal flow areas, i.e., the product bR_m is the same for each length, where b is the length of the section meas-

ured along the assumed normal line and R_m is the mean radius of the length. This division of the normal lines to form the rings of equal area may be done mathematically, or a graphical method may be used.

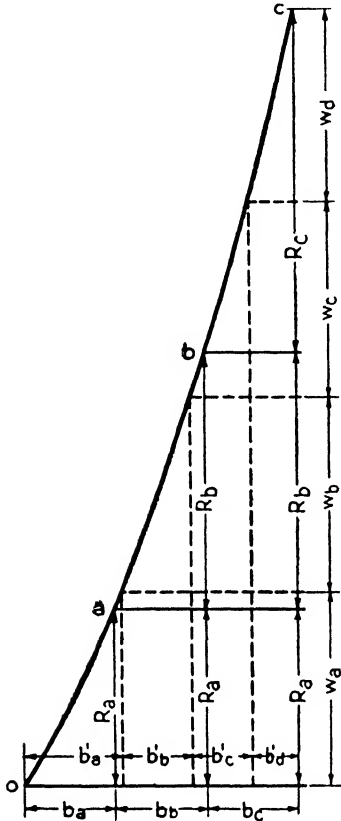


FIG. 7-2. Graphical division of normal lines.

The graphical method will be explained with the aid of Fig. 7-2. The assumed normal line (such as AA , BB , etc., of Fig. 7-1) is divided into a convenient number of equal lengths b_a , b_b , etc. (in Fig. 7-2, three are used), and the mean radius of each length (R_a , R_b , etc.) is found. The lengths b_a , b_b , and b_c are laid off successively as abscissas on Fig. 7-2. At the end of the first b length an ordinate equal to the first mean radius R_a is erected; at the end of the second b length an ordinate equal to $R_a + R_b$, and so on. The points o , a , b , and c thus located are joined by a smooth curve which represents a plot of a function of the normal flow area against path length, since $A = 2\pi R_m b$ or $A = CR_m$ for each equal b length. The maximum ordinate, which is a function of the total area, is then divided into the desired number of equal parts w_a , w_b , etc., equal to the number of streamtubes desired (in this instance, four) and the corresponding lengths b'_a , b'_b , etc., are found as shown by the dotted lines of Fig. 7-2. The lengths b'_a , b'_b , etc., will divide the assumed normal line into lengths of equal area.

After the boundary points of the streamtubes have been located on Fig. 7-1 they should be joined with smooth curves to give the approximate streamlines. Unless the assumed normal lines were very well drawn, they will not be perpendicular to all the streamlines. To bring the two into agreement a new set of normal lines $A'A'$, $B'B'$, etc., is drawn perpendicular to the preliminary streamlines and the process of locating a new set of boundary points is repeated. If care is taken in the original assumption of normal lines, the revised set of streamlines will generally be sufficiently accurate for design purposes. It may be

observed that the second approximation (shown dotted in Fig. 7-1) does not differ greatly from the first.

(c) *Vane Shape.* The impeller shape with the final streamlines taken from Fig. 7-1 is redrawn in Fig. 7-3. The inlet edge of the vane is curved as shown in Fig. 7-3 in order to shorten the "inner" streamline length (0-0) and make it more nearly equal to the "outer" (4-4). This is done to give the water in each streamtube approximately the same amount of guidance. However, it is desirable to keep the vane inlet diameter small in order to keep the peripheral speed u_1 and the absolute water velocity V_1 low at the inlet without reducing the inlet angle β_1 too much. These two factors must be balanced to secure a satisfactory design.

The points where the streamlines cut the inlet edge are numbered 0, 1, 2, 3, and 4. Normal lines labeled *AA*, *BB*, *CC*, *DD*, and *EE* are drawn through each of these points respectively and the total area of each surface represented by these lines is found. Since these surfaces have different areas but the flow passing each is the same, the absolute water velocity V_1 varies along the inlet edge of the vane. The value at any streamline may be found by dividing the fluid flow by the surface area of the normal line passing through the point. Knowing the impeller speed and the water speed at the points along the inlet edge, the corresponding vane angles may be found. This calculation is shown in the table below. A vane thickness factor ϵ_1 of 0.85 is assumed subject to a later correction when the number of vanes, their thickness, and shape have been fixed. The tangent of the inlet angle is increased somewhat (here 10 per cent) to care for the prerotation of the water and the contraction of the flow at the inlet.

Pt.	D_1 in.	u_1 ft. per sec.	$A_{1\infty}$ sq. in.	ϵ_1	$A_{1act.}$ sq. in.	$V_{1act.}$ ft. per sec.	$\tan \beta_1 = \frac{V_{1act.}}{u_1}$	$1.1 \tan \beta_1$	β_1
0	10.0	26.2	314	0.85	267	12.13	0.463	0.509	27.0°
1	12.2	32.0	315	0.85	268	12.10	0.378	0.416	22.6°
2	14.9	39.0	312	0.85	265	12.23	0.314	0.346	19.1°
3	17.6	46.1	300	0.85	255	12.70	0.275	0.302	16.8°
4	20.0	52.4	295	0.85	251	12.90	0.246	0.270	15.1°

The diameters D_1 are scaled from Fig. 7-3. The areas $A_{1\infty}$ are found by breaking the normal lines *AA*, *BB*, etc., into sections and adding the areas of each section to find the total. $A_{1act.}$ equals $A_{1\infty}$ times ϵ_1 .

$$\text{The actual velocity } V_{1act} = \frac{Q}{A_{1act.}} = \frac{1.0075 \times 44.67 \times 144}{A_{1act.} \times 2} = \frac{3240}{A_{1act.}}$$

In general, the outlet angle β_2 is made equal to or slightly larger than the maximum inlet angle to keep the flow smooth and to avoid

turbulence. It is seldom made much greater than 30° because the absolute outlet velocity would be too large. Since the inlet angle varies between 15° and 27° an outlet angle of 27° may be used. The

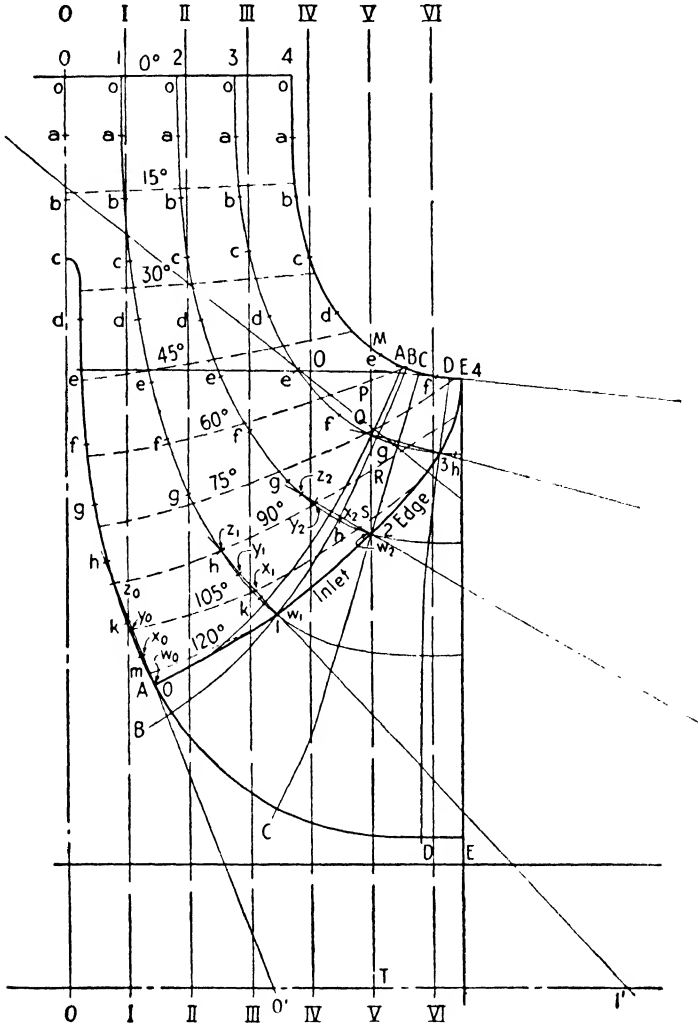


FIG. 7-3. Impeller section.

vane angle of each streamline will gradually increase from its value at the inlet to 27° at the rim.

It is not necessary to have the vane angle become uniform at the rim. Any other radius may be selected, but sufficient path length

must be allowed for the transformation to take place gradually without undue turbulence.

(d) *Construction of End View.* Starting at the rim in Fig. 7-3 equally spaced points *a, b, c, etc.*, are marked off and labeled on each streamline (in this example 1-in. spacing is used). This procedure

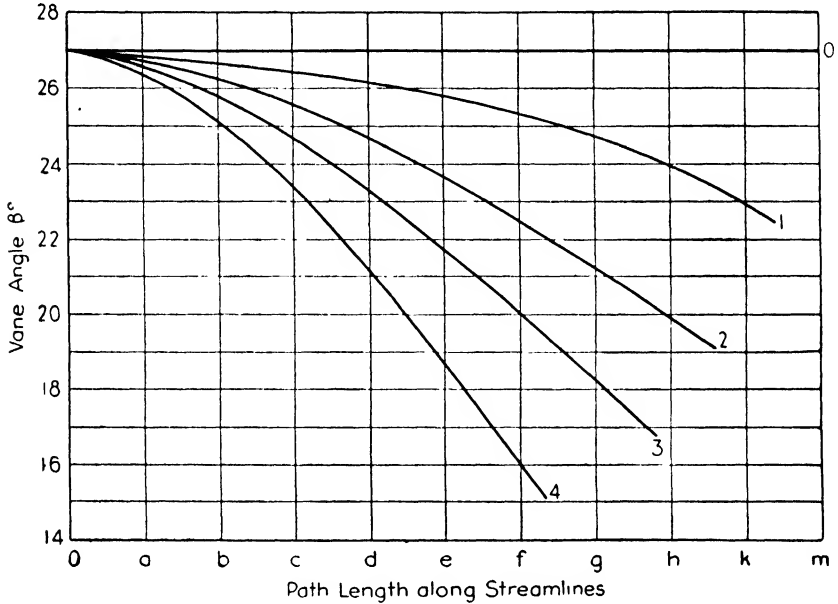


FIG. 7-4. Variation of vane angle with streamline length.

gives distances measured along each streamline from the rim. The values of the vane angle at the inlet taken from the above table are plotted at the corresponding distance from the rim in Fig. 7-4. The vane angle at the rim β_2 is 27° for all the streamlines, and is plotted at zero path length. These points are joined by smooth curves as shown in the figure to give the angle at any point along any streamline. The next step in the design is to draw the end view of the vanes.

Equation 6-6, which was used in designing the vanes of the radial-type impeller, is $\phi^\circ = \frac{180}{\pi} \int_{R_2}^{R_\phi} \frac{dR}{R \tan \beta}$. It may be modified to the form

$\phi^\circ = \frac{180}{\pi} \sum_0^x \frac{\Delta x}{R \tan \beta}$ by substituting Δx for dR in the derivation to make it suitable for tabular integration similar to that used in Section 6-9. The values of the vane angle β are taken from Fig. 7-4 and the intervals along the streamline are used for Δx . The method of

solving the equation is similar to that used in Section 6-9; it is illustrated in Table 7-1 for streamline 3-3. The procedure is similar for the other four lines.

TABLE 7-1
DETERMINATION OF VANE SHAPE ALONG STREAMLINE 3-3

Point	Δx	β	$\tan \beta$	R	$\frac{1}{R \tan \beta}$	$\frac{\Delta x}{R \tan \beta}$	$\Delta \phi^\circ$	ϕ_{TOT}°
0		27.0	0.510	15.0	0.1307			0
a	1.0	26.6	0.501	14.0	0.1424	0.1365	7.81	7.81
b	1.0	25.8	0.483	13.0	0.1590	0.1507	8.62	16.43
c	1.0	24.7	0.460	12.0	0.1811	0.1701	9.74	26.17
d	1.0	23.3	0.431	11.1	0.2088	0.1950	11.16	37.33
e	1.0	21.7	0.398	10.2	0.2460	0.2274	13.02	50.35
f	1.0	20.1	0.366	9.4	0.2902	0.2681	15.36	65.71
g	1.0	18.3	0.331	9.0	0.3354	0.3128	17.91	83.62
j	0.8	16.8	0.302	8.8	0.3760	0.2846	16.29	99.91

After these calculations have been made, the values of ϕ_{TOT}° and the corresponding values of R may be plotted as polar coordinates to obtain the axial view of the streamlines. This is illustrated in Fig. 7-5, the streamlines being numbered 0, 1, 2, 3, and 4; and the points on them being lettered *a*, *b*, *c*, etc., to correspond with those of Fig. 7-3.

To determine if the vane shape is satisfactory, radial lines are drawn at regular intervals (every 15° here) on Fig. 7-5. The radial distance from the shaft axis to each of the streamlines is then laid off from the impeller centerline to the corresponding streamline in Fig. 7-3. In this manner the dotted lines labeled 15° , 30° , etc., are obtained in Fig. 7-3. If these lines make small angles with the impeller walls, the frictional losses will be high and the efficiency poor. When this condition exists, it may be necessary to shift the streamlines in Fig. 7-5 relative to each other to secure an outlet edge which is not parallel to the shaft axis, i.e., change to a mixed flow impeller.

(e) *Pattern Maker's Sections.* The vane shape is now fixed, and the next step is to find sections which will enable the pattern maker to construct this warped surface correctly. The procedure is similar to that employed by naval architects in specifying hull shapes. Par-

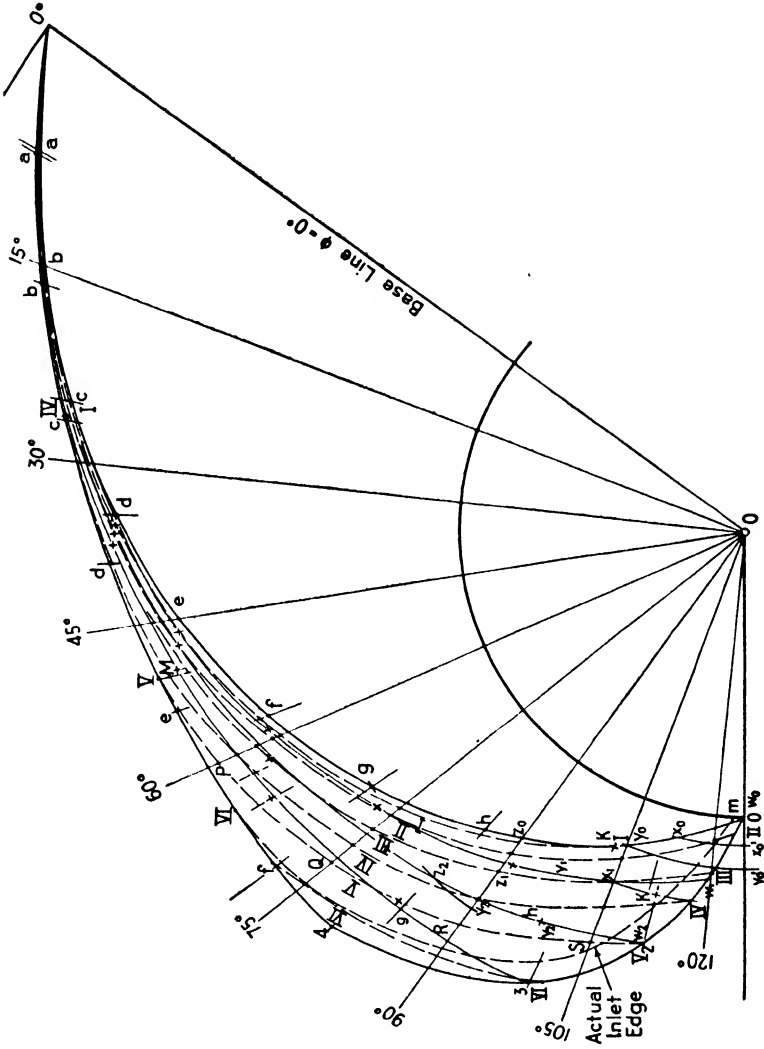


FIG. 7-5. End view of impeller. Pattern maker's sections shown.

allel planes perpendicular to the shaft axis are passed through the impeller and their line of intersection with the vane surface is found. These curves are transferred to boards, having thicknesses equal to the distances between the planes, by the pattern maker and the boards are cut to this shape. They are then located properly and glued together to approximate the surface. After the edges have been cut away and the surface smoothed, the exact surface may be obtained.

A series of planes, equally spaced 1 in. apart, are passed through the impeller perpendicular to the shaft axis. These are labeled I, II, III, etc., in Fig. 7-3. The section cut from the vane by any of these planes is found in Fig. 7-5 by laying off the radius from the shaft centerline to the intersection of the plane with the various radial lines at the 15° angles previously drawn on Figs. 7-3 and 7-5. The resulting curves are labeled I-I, II-II, etc., on Fig. 7-5, and are similar to the curves on a contour map.

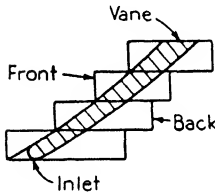


FIG. 7-6. Method of securing vane shape from boards on which pattern maker's sections have been pricked. Cross-hatched portion is finished vane section.

To clarify the procedure consider the intersection of plane V with the vane surface. The plane V intersects the shaft axis at T , and the 60° , 75° , 90° , and 105° lines at points P , Q , R , and S respectively. Hence the radius PT as found from Fig. 7-3 is laid off on the 60° line of Fig. 7-5, the radius QT on the 75° line, etc. This locates the points P , Q , R , and S on curve V of Fig. 7-5. This curve is extended until it strikes the bounding curve at a radius TM to locate point M , and at a radius of $T2$ to locate point 2. The lines for planes I, II, . . . , VI are found in a similar manner.

These curves are transferred to pieces of wood having a thickness equal to the distance between the planes, and each piece is then cut along these curves. After the pieces have been aligned in their correct position, they are glued together and the surface is smoothed by cutting the steps away and sandpapering, as shown in Fig. 7-6. The resulting surface is that of one side of the vane. Figure 7-7 is an isometric drawing showing the boards cut to shape and glued together, before the steps have been removed. This drawing is taken from Figs. 7-3 and 7-5 for one side of the impeller.

When determining these lines for the pattern maker, the proper shrink scale for the metal to be used in casting must be employed, since the usual procedure is for the designer to lay out the lines on heavy drawing paper. The pattern maker transfers the lines to the wood by pricking through the paper with a sharp point. Hence the

designer's lines are used directly by the pattern maker, and the designer must care for the casting shrinkage.

(f) *Vane Thickness and Inlet Edge.* The vane thickness is usually based upon casting difficulties rather than strength. It is generally made fairly thin at the inlet and increased with the radius. Here

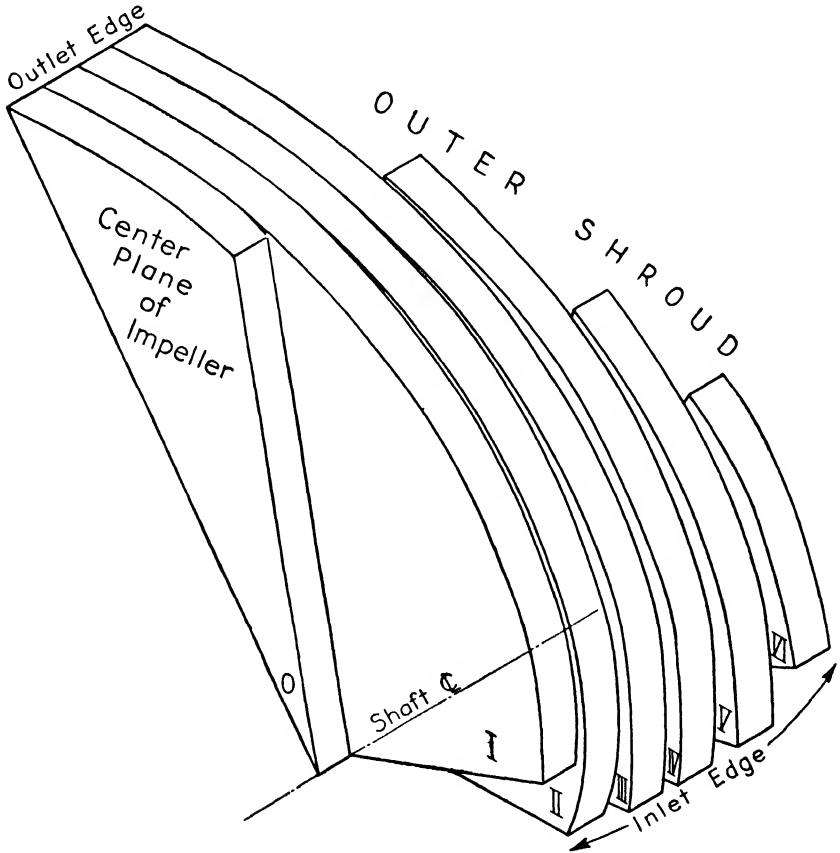


FIG. 7-7. Isometric view of one-half of impeller, showing boards in place ready for surfacing.

the inlet edge will be made $\frac{1}{4}$ in. thick and this thickness will be gradually increased to $\frac{1}{2}$ in. at the outlet. The tip is well rounded to reduce the turbulence loss at this point, as shown in Fig. 7-6.

To show the pattern maker how the rounding is to be done and to check the inlet angle graphically, developed views of the inlet edge for each streamline may be drawn. An imaginary cone, having its apex on the shaft centerline and its surface approximately tangent to

the streamline at the vane inlet edge, is developed. The procedure is described for the 0-0 streamline, and is similar for the other four.

The limiting element of the imaginary cone is shown in Fig. 7-3 and labeled as 0-0', the 0' point being on the shaft centerline whereas the 0 point is at the inlet edge of the streamline 0-0. The line 0-0' is approximately tangent to the streamline at point 0. Four points, w_0 , x_0 , y_0 , and z_0 , which may be considered to lie on both the streamline 0-0 and its tangent cone are shown on Fig. 7-3 and also located on Fig. 7-5.

The development of this cone is shown on Fig. 7-8(c). A series of concentric circular arcs of radii $0'w_0$, $0'x_0$, $0'y_0$, $0'z_0$ (taken from Fig. 7-3) and a radial reference line $0'w_0$ are drawn. The distances measured along concentric circular arcs from the reference line $0'w_0$ in Fig. 7-5 are then laid off on Fig. 7-8(c) on the corresponding arcs to locate the points w_0 , x_0 , y_0 , and z_0 , i.e., $y'_0 y_0$ on Fig. 7-5 equals $y'_0 y_0$ of Fig. 7-8 measured along the arcs, etc. The procedure is correct because the distances measured on both figures are on circles cut from the cone by planes perpendicular to the shaft centerline. The points are joined by a smooth curve to form the leading side of the vane. The trailing side of the vane is drawn with desired thicknesses from the leading surface and the inlet edge is rounded off as shown. Figures 7-8(a) and 7-8(b) show similar sketches for streamlines 2-2 and 1-1 respectively and the others could be obtained in the same manner. The inlet angles are indicated on the sketches as perpendiculars to the path of motion and the vane surface.

Since the vanes are cut back, the surface does not actually extend to the full line of Fig. 7-5, but is set back to the heavy dashed line located from Fig. 7-8.

The remainder of the impeller design is similar to that outlined in Chapter 6 and will not be repeated here. Volute are usually used with impellers of this type. Their design is similar to that outlined in Sections 6-10 and 6-11.

7-3 Mixed-Flow Impeller. The mixed-flow impeller is similar to the Francis type, except that the outlet edge is sloping and the outlet angle varies across it. Since each streamtube has a different path length and different angles, the efficiency along each will be different. Therefore each streamline may be considered to be a separate impeller, the outer ones having lower efficiencies than the inner ones. The design procedure is similar to that of the Francis impeller.

Since the outlet angle and the absolute outlet water velocity vary along the outlet edge, a diffuser is not practical and a volute is always used.

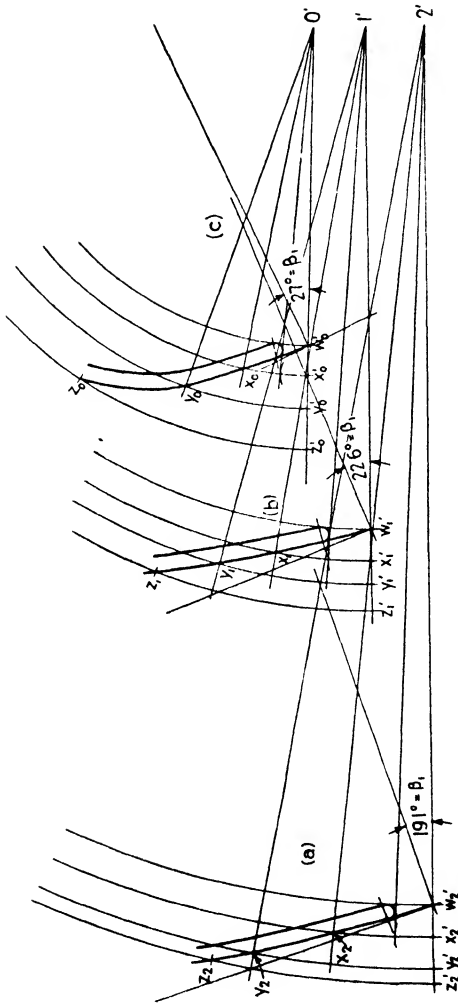


FIG. 7-8. Developed views of vane inlet edge at various streamlines.

7-4 Propeller Pump. The flow in propeller pumps is purely axial, so no centrifugal action is present. The blade sections are airfoils and that theory forms the basis for design. As this is entirely different from the theory upon which the other types are based and as it is highly dependent upon experimental data, the procedure will not be considered.*

*Information concerning these pumps may be found in "Die Krieselpumper," by Pfeleiderer, "Propeller Pumps," by M. P. O'Brien and R. G. Folsom *A.S.M.E. Trans.*, HYD-57-3, July, 1935, and "The Design of Propeller Pumps and Fans" by M. P. O'Brien and R. G. Folsom, University of California Press, 1939.

CHAPTER 8

PUMP DETAILS AND MATERIALS

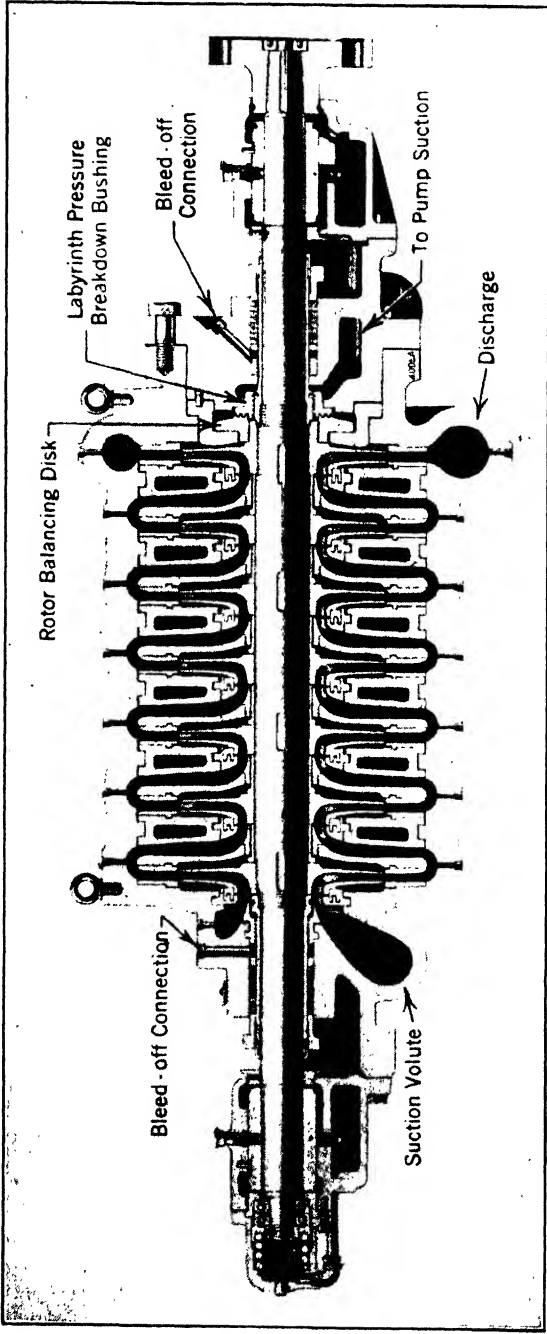
8.1 Introduction. The method of calculating the dimensions of the fluid passages has been covered in Chapters 6 and 7. In this chapter the accepted practice regarding construction details and materials will be considered. To illustrate the various points Figs. 8-1, 8-2, 8-3, and 8-4, showing sections through typical pumps, are given here and will be referred to throughout the chapter.

8.2 Shaft and Sleeves. The determination of the shaft diameter was discussed in Section 6.5. The shaft is stepped with its greatest diameter near the center. The diameter at the bearings is larger than at the coupling and the diameter at the impellers is still greater. This construction aids in assembling the pump as the various fittings may be slid on from the end. Another advantage is to give greater strength at the center where the bending moment is large.

Before the shaft size is finally fixed and after the impeller and casing have been designed the critical speed must be determined. Single-stage machines usually operate below the lowest critical speed, whereas multistage machines may run above it because of the greater suspended weight and the correspondingly longer distance between the bearings. In any event the running speed should be 20 to 30 per cent removed from the critical to prevent excessive vibration and possible rubbing of the wearing rings. Owing to the damping effect of the relatively dense liquid this effect is not so serious for pumps as for blowers. The method of determining the critical speed is described in Chapter 19.

The shaft is usually protected by sleeves, particularly where it passes through the packing boxes, to prevent scoring and corrosion. If the liquid is very corrosive stainless steel or Monel metal shafts may be used, but they are more expensive than ordinary steel. The sleeves fit close to the shaft and are threaded to it, as shown in Figs. 8-1 to 8-4. The direction of the thread is counter to the direction of rotation of the impeller and the sleeve is locked in place.

8.3 Bearings. Both sleeve or journal bearings and anti-friction bearings are used for pumps. Journal bearings are more commonly used for multistage machines which have higher bearing loads and rubbing speeds. Ball bearings are extensively used for single-stage

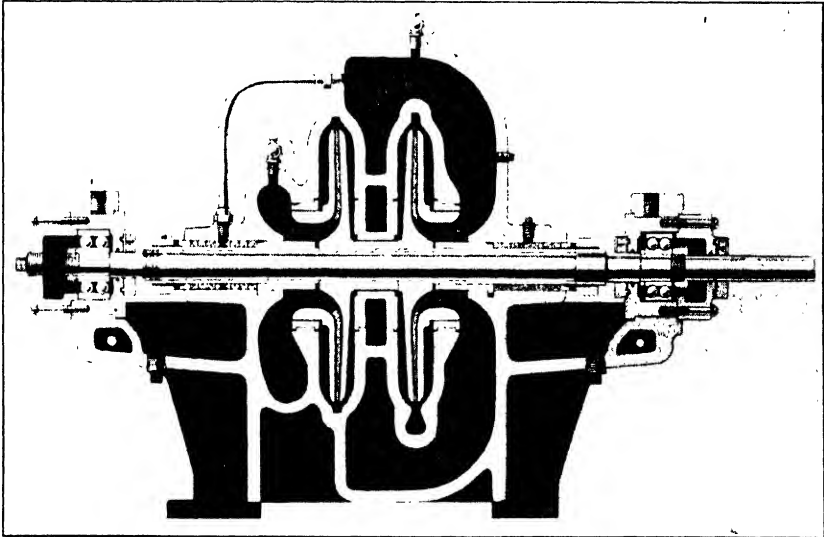


Courtesy De Laval Steam Turbine Co.

Fig. 8-1. Seven-stage pump with journal bearings.

units because the lubrication problem is simplified and they maintain more accurate alignment. If the liquid temperature is above about 250° F. the bearings are usually water cooled.

Journal bearings are usually babbitt-lined with a cast iron or steel shell horizontally split to facilitate removal without disturbing the rotating element. Generally speaking, the bearing pressure for ring oil lubrication should not exceed 25 lb. per sq. in. of projected area,



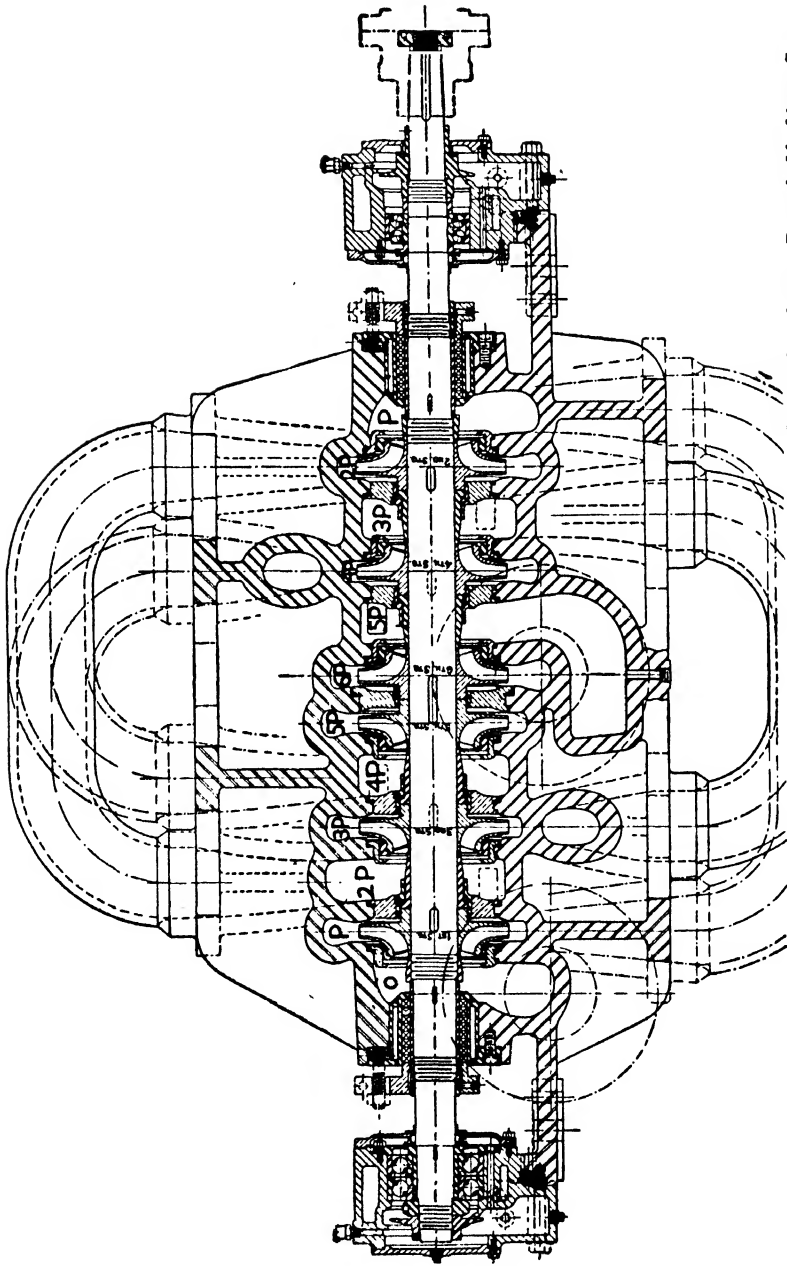
Courtesy Goulds Pumps, Inc.

FIG. 8-2. Two-stage pump with opposed impellers.

the projected area being the product of the bearing diameter and length. For large units force-feed lubrication may be used, with bearing pressures of 100 lb. per sq. in. or more. For most applications oil-ring bearings are quite satisfactory (see Figs. 1-2 and 8-1).

Ball bearings are usually grease-lubricated and require very little attention, the bearing being packed with the proper amount of grease and requiring no further maintenance for a month or more. Although the shaft must be removed to replace the bearings they are easily mounted and readily obtainable. As in mounting any pair of anti-friction bearings, one is held fixed in place by the housing to absorb minor thrust loads and to hold the shaft in the correct axial position and the other is free to move axially with temperature changes. This is illustrated in Figs. 8-2, 8-3, and 8-4.

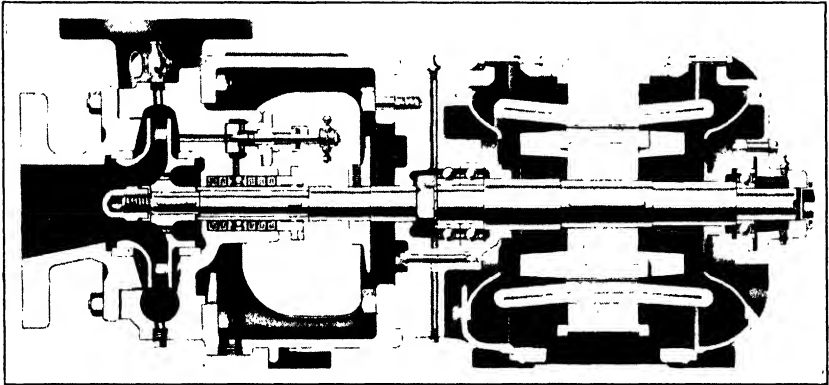
8-4 Packing Boxes. Where the shaft enters the pump casing, packing or stuffing boxes are provided to prevent leakage. These boxes



Courtesy Worthington Pump & Machinery Corp

Fig. 8-3. Multistage pump with interstage loops.

are filled with a soft packing which is compressed against the shaft by a gland. The gland is usually split as illustrated in Fig. 8-5(b) and held in place by swivel eye bolts as shown in Fig. 8-5(a). Sufficient space should be provided between the box and bearing to replace the packing without disturbing any parts of the pump other than the gland. The glands should be tightened only lightly to allow some water to leak to the outside to lubricate and cool the packing.



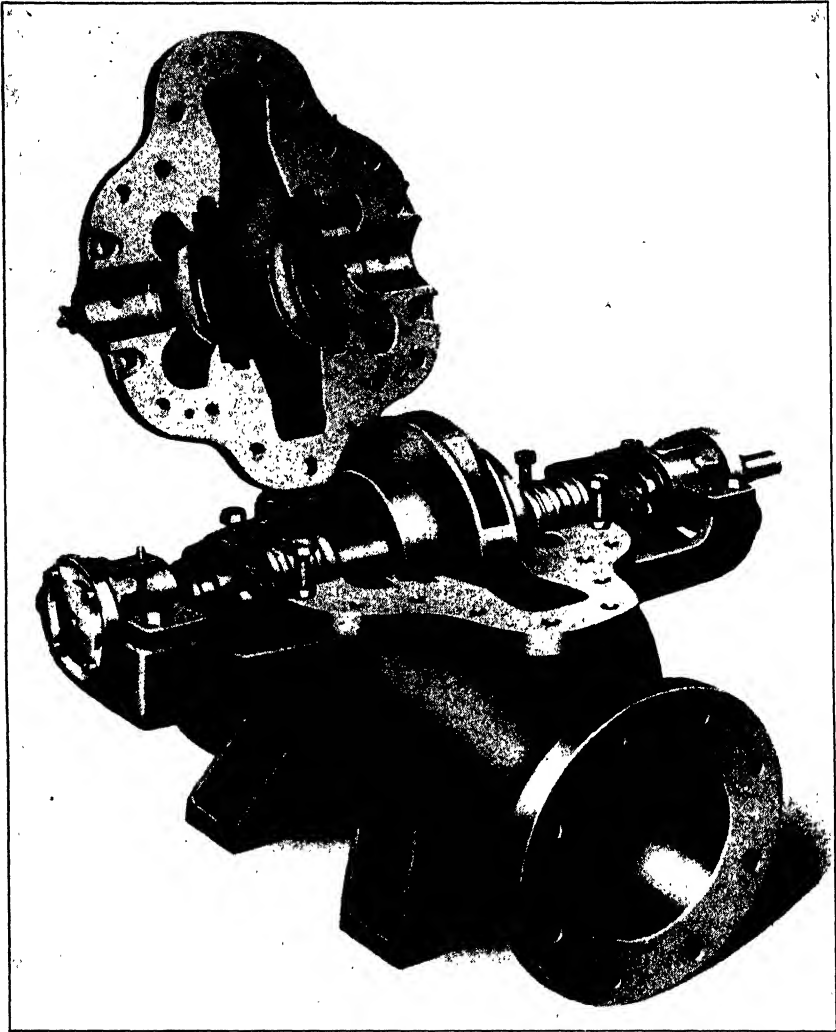
Courtesy Ingersoll-Rand Co.

FIG. 8-4. End-suction, single-stage pump.

The packing has a square section and is cut into separate rings, each having a butt joint. These joints should be staggered to minimize the leakage. For cold water service graphited asbestos packing is commonly used; for hot water service metallic packing may be employed. For special applications involving other liquids a multitude of special packing materials are on the market. On account of the higher rubbing speeds usual in multistage pumps, the material of the shaft sleeve and type of packing must receive special consideration. As the packing may wear rapidly and hence be replaced frequently it is common practice to specify that an extra complete set be furnished with each new pump.

Pumps operating under a suction lift have the packing divided into two parts by means of a lantern ring (item *Q*, Fig. 1-2) which is H-shaped. Water from the pump discharge or other pressure source is introduced into the ring to prevent air from entering the pump. The pump shown in Fig. 1-2 has both boxes equipped with these rings whereas the pump illustrated in Fig. 8-2 has the ring only in the left box. The water on the right box is above atmospheric pressure so no air can leak into the casing. These lantern rings may also be used

to bleed off leakage past a labyrinth as shown in Fig. 8-1. The liquid connections to the boxes should be large enough to insure sufficient



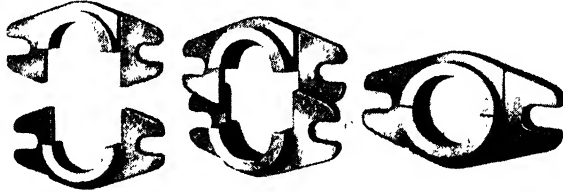
Courtesy Ingersoll-Rand Co.

FIG. 8-5(a). Double-suction pump with cover lifted showing construction details.

flow even when the pipe has aged. The minimum pipe size is usually taken to be $\frac{1}{2}$ in.

Pumps handling gritty materials which may become embedded in the packing and score the shaft sleeves usually have provision for

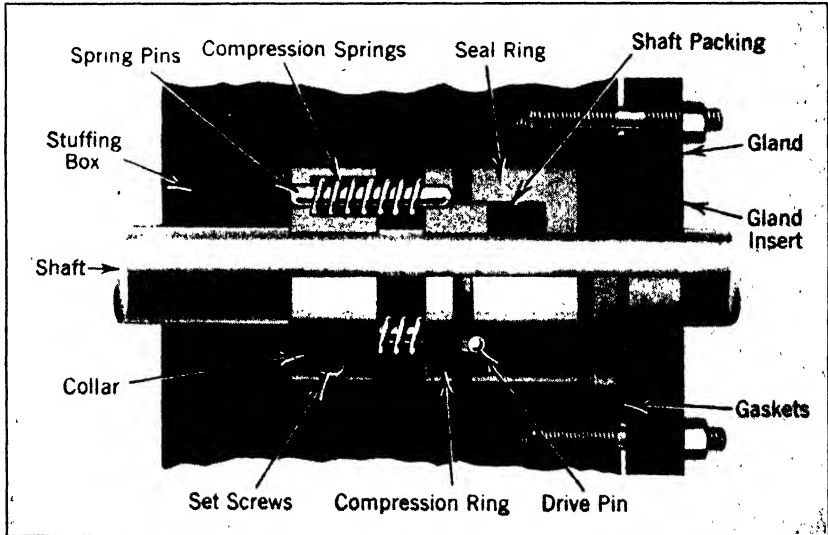
flushing the inner part of the box with clean water to prevent the grit from entering. This is illustrated in Figs. 9-4, and 9-9. If the temperature of the liquid is greater than about 250° F., the packing boxes are usually water cooled.



Courtesy Ingersoll-Rand Co.

FIG. 8-5(b). Split-gland detail.

If the pump operates under high pressures, ordinary packing may not be satisfactory and some form of mechanical seal must be used. One type of these seals is illustrated in Fig. 8-6. A collar is fixed to



Courtesy Durametallic Corp.

FIG. 8-6. Section through mechanical seal.

the shaft by means of a setscrew. This collar, because of its position, causes the compression springs to exert a force through the shaft packing to a seal ring. All the parts so far mentioned rotate with the shaft. The gland insert is fixed to the gland which is stationary,

hence rubbing takes place between this insert and the seal ring, the action being similar to a collar-type thrust bearing. By varying the number of gaskets between the gland and the box the best setting and corrections for wear can be obtained. The materials used for the various parts will depend somewhat on the liquid being pumped.

8-5 Impellers. The impeller is usually cast in one piece and made of cast iron or bronze. For special liquids it may be made of stainless steel, lead, glass, or other suitable material. It is fixed to the shaft with a light press fit, keyed, and securely locked in place. After assembling the rotating parts, the shaft should be balanced both statically and dynamically. In order to realize the high efficiencies usual with modern pumps, the surface should be made as smooth as possible, both in the vane passage and on the outside.

The wall and vane thickness is usually made a minimum consistent with good foundry practice. The stresses due to centrifugal force and the fluid pressure are quite low for average applications. For high pressure pumps operating at high speeds, it may be necessary to calculate the centrifugal stresses as outlined in Chapter 18.

The impeller may be "open" with no shrouds, "semi-open" or "semi-enclosed" with a shroud only on one side away from the inlet (Fig. 9-7) or "enclosed" with both a front and back shroud. Open and semi-enclosed impellers have no wearing rings and the leakage is relatively greater unless a very close axial clearance between the impeller and casing is maintained. They are cheaper to manufacture because no cores are required for casting and the castings can be cleaned easier. The enclosed impeller is by far the most common type and, in general, it maintains higher efficiencies for longer periods of time.

Pump manufacturers have a standard line of impellers and casings which may be modified to meet the particular conditions applying to any purchase order. The outside diameter of the impeller D_2 is cut down to meet the required head. It may be reduced as much as 15 to 20 per cent without affecting the efficiency greatly. With diffuser pumps the shrouds are usually left on, only the vanes being cut away. Although this does not reduce the disk friction loss, the better guidance of the liquid into the diffuser more than offsets the disk friction. On volute pumps the shrouds may or may not be cut away, depending upon the position of the impeller rim relative to the volute. If the impeller is close to the volute, the shrouds are usually cut away. If not they may be left on to secure better guidance. Some manufacturers have two sizes of casings to be used with a given impeller. A small casing is used with an impeller having a reduced diameter and a larger casing is used with a full-size impeller.

8-6 Wearing Rings. Wearing rings operate with close clearances, generally in the neighborhood of 0.015 in. on the diameter, as discussed in Section 6-4. Because there is danger of rubbing between the rings as a result of sudden temperature variations, vibrations, etc., it is wise to make the two rings of different materials such as cast iron and bronze to prevent seizure. If made of the same material it is well to have the surface hardness at least 50 Brinell numbers different. They are usually made as separate parts of the pump so that they may be replaced if seizure or excessive wear occurs. The impeller wearing rings are commonly threaded on the impeller counter to the direction of rotation and secured by a pin. Casing wearing rings may be prevented from rotating by making the seats of the upper and lower halves of different cross-sectional shapes. The shapes of the rings vary with different manufacturers. Figure 6-1 shows a number of these shapes with information concerning their effectiveness. To cut down the wearing action in pumps handling gritty materials the wearing rings may be continually flushed with clear water as illustrated in Fig. 9-9.

8-7 Casing. Practically all pumps having their impellers between the bearings are split horizontally on the shaft centerline so the upper half or cover can be easily removed for inspection or repair. The suction and discharge nozzles are located in the base in order that they do not have to be disconnected when the cover is removed. The suction flange of pumps with overhung impellers (Fig. 8-4) forms an end plate for inspection and repair; therefore for this form the suction line must first be disconnected.

Pumps having the suction line connected to the base (Figs. 1-2, 8-1, 8-2, and 8-3) require a suction volute which conducts the water to the eye of the impeller. In general this suction volute area is made proportional to the impeller circumference, i.e., one-half the area at the horizontal split, and so on. From an ideal standpoint the area of this volute at the top is zero but actually a collection chamber is required to insure a proper distribution of flow into the impeller eye. In double-suction pumps, the suction line is split into two volutes, one on each side of the impeller, as shown in Fig. 8-5(a). To prevent a whirling action from building up, a radial stop plate is usually located at the top of the volute. The discharge line leaving the pump is usually horizontal, but it may be shifted around to any position desired. Manufacturers generally standardize on even 45° positions, as illustrated in Fig. 8-7.

For cold water service the casing is usually made of cast iron for low pressures and of semi-steel for discharge pressures exceeding

100 lb. per sq. in. Semi-steel is a high grade cast iron having a minimum tensile strength of 30,000 lb. per sq. in. or higher. For corrosive liquids with acid reactions, such as salt water, the casing material should be bronze. For corrosive liquids having an alkaline reaction bronze is not suitable, so stainless steel may be used. The latter is so expensive and difficult to machine that in many such installations cheap cast iron is used and the casing is renewed periodically. In such installations the casing is made $\frac{1}{4}$ to $\frac{3}{4}$ in. thicker than is required on the basis of strength or stiffness. The casing thickness is checked

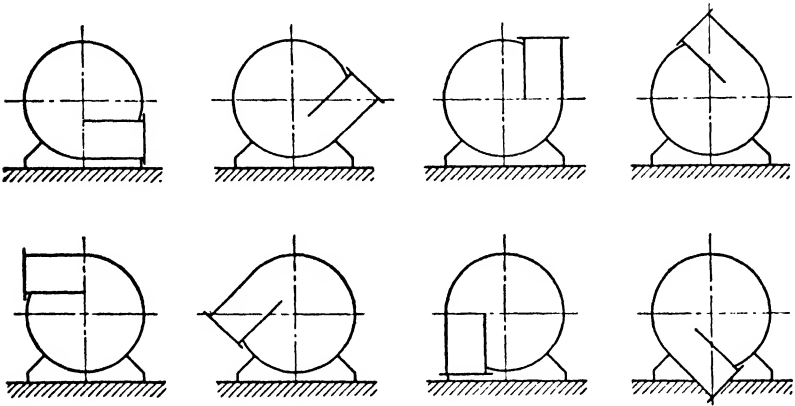


FIG. 8-7. Conventional positions of discharge flange.

periodically and when this surplus metal (known as corrosion allowance) has been eaten or worn away by the action of the liquid, the casing is replaced. Multistage casings are made of high grade cast iron for pressures up to about 750 lb. per sq. in. and of cast steel for higher pressures. A further discussion of materials appears in the next section.

The casing thickness for low head pumps is usually made as thin as is consistent with good foundry practice. Owing to the complicated shape of the castings it is very difficult to calculate the required wall thickness for high heads. It is usually based upon experience and test data. As a rough check, the stress in the section may be found by the simple equation $s = pA/A'$, where p equals the approximate pressure in pounds per square inch; A equals the projected area on which the pressure p acts in square inches; A' equals the area of metal resisting the force pA , in square inches.

The actual stress will be increased by a bending action due to the shape and movement of the side walls; therefore these walls should be

made as stiff as possible. This can be done without increasing the thickness by making them "dished" or "conical" as shown in Fig. 8-8. The larger the angle θ is, the lower the stress. If radial walls are used, they may be reinforced with ribs. The general practice is to subject the entire casing to a hydrostatic pressure test for at least 30 minutes with a pressure 50 per cent greater than the design discharge pressure before it leaves the factory.

In Europe it is common practice to split multistage pumps vertically. They are more expensive because they require more machining and they are more difficult to maintain and repair. It is only for pressures above about 1500 lb. per sq. in. that American manufacturers have used this "barrel type"

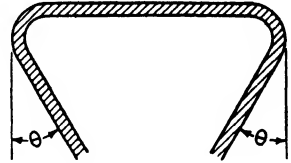
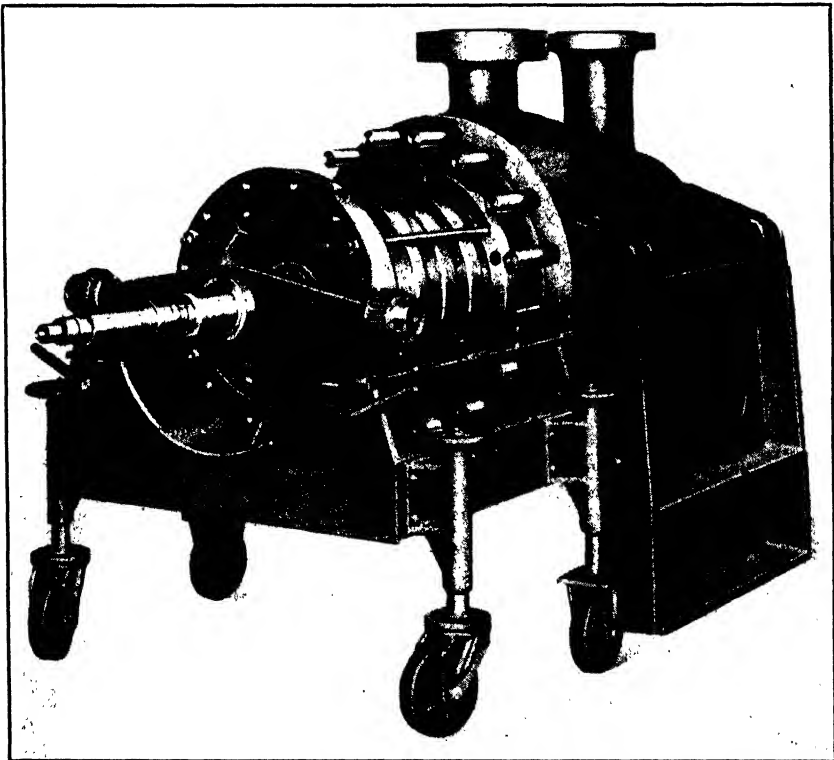


FIG. 8-8. Section through outer portion of pump casing.



Courtesy Worthington Pump & Machinery Corp.

FIG. 8-9. High pressure solid forged-steel diffuser-type pump with rotor assembly withdrawn onto portable assembly truck.

design. The hydraulic construction is similar to that of horizontally split pumps. Each stage forms a unit, and when these are assembled they are slid into the casing as shown in Fig. 8-9. As the higher pressures are usually accompanied by high temperatures the casing is supported on feet located on the level of the shaft centerline. This avoids misalignment difficulties which result from temperature changes.

8-8 Selection of Materials. To aid in the selection of the proper materials to be used when pumping various liquids, the Standards of the Hydraulic Institute list over 200 liquids and give the materials suitable for the parts which come into contact with the liquid (casing, impeller, wearing rings, etc.). This table is too extensive for inclusion here.

Materials may also be selected on the basis of their pH number. The pH number is a measure of the relative acidity or alkalinity of the liquid being pumped. The numbers range from 0.0 to 14.0. The number 7.0 indicates a neutral fluid. Numbers ranging down from 7.0 indicate increasing acidity; those ranging up from 7.0 represent increasing alkalinity. The pH value is a characteristic of the liquid, its concentration and temperature, and the presence of other substances. The following table* may be used as a guide in selecting materials according to the pH value of the fluid handled:

pH Range	Material
Under 3.5	Corrosion-resistant steels
3.5 to 6.0	All bronze
6.0 to 8.0	Bronze, iron, or a combination of the two
Over 8.0	All iron or steel

Care must be taken to avoid electrolytic action when dissimilar materials are used in the same pump. Thus, although salt water has little effect on cast iron or bronze when they are used separately, it will corrode the cast iron if the two metals are used in the same pump.

8-9 Diffuser. Diffuser vanes are usually made of bronze or steel. If they are of the thick type they may be cast and machined separately and then bolted to finished side plates; or one side plate may be cast integral with the vanes and, then, after the surfaces have been finished the second side plate is bolted on. If they are of the thin type they may be cut from sheets; then, after being bent to the correct shape, they are fastened to the side plates by pins or by welding.

* Taken from J. B. Godshall, " pH Guides Selection of Feed Pump Materials," *Power*, August, 1939.

8-10 Axial Thrust.* A single-suction impeller is subjected to an axial thrust which is the result of two opposing forces. The smaller of these forces is due to the change in momentum of the fluid entering the wheel. As the liquid approaches the impeller axially it has a velocity V_0 (see Fig. 8-10), hence its change of momentum or force is $\frac{w}{g} V_0$. This force tends to move the impeller away from the suction side and acts on the area bounded by the rings of diameters D_0 and D_H .

The fluid discharged from the impeller is at a higher pressure than that on the suction side. The resulting forces are balanced between D_2 and D_0 as they are equal and opposite on the two shrouds. However, between D_0 and D_H there is a force equal to $(P_T - P_0) \frac{\pi}{4} (D_0^2 - D_H^2)$

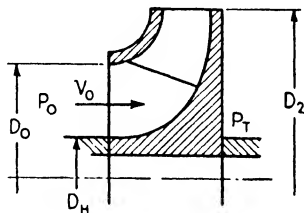


FIG. 8-10. Section through impeller.

which tends to move the impeller toward the suction. As noted in Section 6-4 the magnitude of $P_T - P_0$ may be estimated from the equation

$$P_T - P_0 = \frac{3}{4} \frac{u_2^2 - u_1^2}{2g} \gamma$$

To illustrate the magnitude of these effects assume that the impeller of Section 6-9 is single suction instead of double but that it has the calculated dimensions and velocities, i.e., handles one-half the total flow of 347 lb. per sec. The momentum force then will be $\frac{w}{g} V_0 = \frac{347 \times 1.02 \times 11}{2 \times 32.2} = 60$ lb. The pressure difference $P_T - P_0 = H_L \gamma = 88.6 \times 62.4 = 5500$ lb. per sq. ft. or 38.3 lb. per sq. in.; therefore the pressure thrust will be

$$(p_T - p_0) \frac{\pi}{4} (D_0^2 - D_H^2) = 38.3 \frac{\pi}{4} (7.313^2 - 2.5^2) = 1420 \text{ lb.}$$

The net thrust toward the suction will be $1420 - 60 = 1360$ lb. On a multistage pump with all the impellers facing the same direction this force is proportional to the number of stages. From these figures it

* J. H. Polhemus and J. Healy, "Dredge Pump Pressures and Thrust Loads," *A.S.M.E. Trans.*, HYD-51-4, 1929; A. J. Stepanoff, "Leakage Loss and Axial Thrust in Centrifugal Pumps," *A.S.M.E. Trans.*, HYD-54-5, 1932

may be noted that for practical purposes the momentum force may be neglected and that the axial thrust can become very large, particularly with multistage machines.

Since a double-suction impeller is symmetrical about its centerline no axial thrust exists. On multistage pumps such as Figs. 8-2 and 8-3 the impellers are faced in opposite directions in order to balance out the thrust forces. In Fig. 8-3 it should be noted that the stages are placed along the shaft in an order which keeps the packing box pressures low and at the same time keeps the pressure difference between adjacent stages low. This arrangement reduces the interstage leakage and the length of packing box.

For single-stage single-suction pumps two methods of overcoming the thrust are sometimes used. The first is illustrated in Fig. 8-4, where wearing rings have been placed on the back shroud at the impeller eye diameter and holes have been drilled through the impeller, thus equalizing the pressure on the two sides. An alternative method is to use wearing rings, as in Fig. 8-4, but instead of drilling through the impeller this space is connected by piping to the pump suction, thereby equalizing the pressure.

In any of the above arrangements there are bound to be some inequalities which will produce small amounts of thrust which are largely indeterminant and are taken either by the ball bearings or by a collar thrust bearing when journal bearings are employed.

When a multistage pump with all impellers facing in the same direction is used some form of balance disk is required. One type is illustrated in Fig. 8-1. The resultant force exerted on the impeller is a thrust toward the left having a magnitude approximating $\frac{\pi}{4}(D_0^2 - D_H^2)(p_d - p_s)$ where p_d and p_s are the pump discharge and suction pressures respectively. To balance out this force a rotor-balancing disk is keyed to the shaft after the last stage (see Fig. 8-1). In back of this disk is a labyrinth pressure breakdown bushing followed by a chamber connected by a pipe to the pump suction. The left side of the balancing disk is subjected to a pressure approximating that of the pump discharge, and the right side pressure approximates that of the pump suction. The force exerted on the disk and hence on the shaft acts to the right; therefore it balances out the impeller thrust. If for any reason the impeller thrust should temporarily decrease, the force on the balancing disk, because it is greater, causes the shaft to move slightly to the right, thus increasing the clearance between the disk and the casing balancing ring. This allows the high pressure water to flow to the right side of the disk where it is temporarily held

by the labyrinth breakdown bushing, and reduces the load on the balancing disk. Thus the shaft will always assume a position by varying the clearances where the axial impeller and balancing disk forces are equal and opposite. As wear gradually takes place between the balancing disk and the ring the shaft moves slightly to the left.

8-11 Radial Thrust. In designing a volute the assumption was made that the flow was uniform around the impeller circumference. Careful tests* made with a pitot tube on the pressures existing in volutes at various flows show variations which indicate that this assumption is not true, especially at partial flows. The pressure distribution is such that there is a radial force acting towards the volute tongue. This force is markedly reduced if a double volute (the tongues being diametrically opposite) is used, and is negligible with a diffuser. There is not sufficient information available to calculate the magnitude of the force, but it is sufficient in many cases to deflect the shaft sufficiently to cause rubbing of the wearing rings. On multistage volute pumps the effect can be balanced by staggering the position of the volute tongues in successive stages.

✓ **8-12 Couplings.** A flexible coupling should be used between driver and pump to care for small misalignments. Rubber-bushed couplings are frequently used. Although this type is inexpensive and satisfactory for most installations, the rubber is subject to deterioration, especially if oil is present. All-metal couplings of the Falk or Fast type are now being used extensively. If the casing is split vertically the coupling should be of the spacer type to facilitate repairs.

8-13 Priming. Before the pump will operate, the eye of the impeller must be submerged and the suction line filled. The pump should never be run unless the impeller is filled with liquid because the wearing rings may rub and seize; also, the packing must be lubricated by the liquid leaking past it. If air is allowed to leak into the suction line or pump, the unit may become airbound and lose its prime, i.e., cease delivery. Then it is necessary to stop the machine and start up again after priming.

If the impeller is submerged below the water level, it is only necessary to open a petcock leading from the volute to release any entrapped air and insure that the pump is primed. In the majority of installations the pump is not submerged, so some other provision must be made to prime it.

* R. T. Knapp, "Centrifugal Pump Performance as Affected by Design Features," *A.S.M.E. Trans.*, April, 1941; R. C. Binder and R. T. Knapp, "Experimental Determination of the Flow Characteristics in the Volute of Centrifugal Pumps," *A.S.M.E. Trans.*, HYD-58-4, November, 1936.

There are three general systems of priming a pump. These are (a) admitting water to the suction line until the eye of the impeller is covered, (b) exhausting air from the suction line and pump so that water is forced into the pump by atmospheric pressure, and (c) designing the pump to be self-priming (i.e., so that the impeller eye and suction line are always filled with water) or have some means of removing the air incorporated into the design.

Water may be admitted to the pump and suction line from a reservoir, city water supply, or some other outside source. The volute petcocks should be open while the water is introduced to allow the pump to be completely filled.



Courtesy Buffalo Pumps, Inc.

FIG. 8-11. Medium-size foot valve.

Where the discharge line remains filled with water after the pump is stopped, a by-pass line around the gate valve may be used to supply the necessary water (shown dotted in Fig. 10-1). In order to hold the water in the suction line and pump a check or foot valve is placed at the bottom of the suction line. These foot valves are made large to keep the velocity through them low (about 2 ft. per sec.) and have a strainer or screen placed before them to filter out any objects which would tend to clog them. They are usually leather- or rubber-lined; for small sizes ($\frac{3}{4}$ in. to 6 in. diameter) they are made single flap, for medium sizes (7 in. to 16 in. diameter) double flap (see Fig. 8-11),

and for large sizes of the disk type with individual springs behind each disk.

By the second method the pump discharge valve is closed and the air is ejected from the highest point on the pump casing so that the water is forced up into the pump impeller. An ejector using high pressure water, steam, or compressed air and operating on the principle of an injector may be employed (Fig. 10-1), or a wet vacuum pump may be used.

There are many automatic priming systems and types of self-priming pumps. They are rather specialized and will not be described here. For further information concerning them, manufacturers catalogs may be consulted.*

* Many are described in Chapter XI of *Pumps*, by Kristal and Annett, McGraw-Hill, 1940.

CHAPTER 9

PUMP APPLICATIONS AND SELECTION

9.1 Pumping Arrangements. When the pumping requirements are variable, it may be more economical to install several small pumps in parallel rather than a single large one. When the demand drops, one or more smaller pumps can be shut down, thus allowing the remainder to operate at or near the peak efficiency. If a single pump is used with lowered demand, the discharge must be throttled and it will operate at reduced efficiency. Moreover, when smaller units are used opportunity is provided during the slack demand periods for repairing and maintaining each pump in turn and avoiding plant shut-downs which would be required with a single unit.

Similarly, multiple pumps in series may be used when large quantities of liquid must be delivered at high heads. In planning such installations the first step is to construct a head-capacity curve for the system. The head required by the system is the sum of the static head (difference in elevation and/or its pressure equivalent) plus the variable head (friction and turbulence in the pipe, bends, heaters, etc.). The former is usually constant for a given installation whereas the latter increases approximately with the square of the flow as discussed in Chapter 2. This system head requirement is represented by the curve *AB* in Figs. 9.1 and 9.2.

Pumps in Parallel. For units to operate satisfactorily in parallel, they must be working on the stable part of their characteristic curves, i.e., to the right of the pulsation point. This may be illustrated by assuming that two "identical" pumps are operating at a low capacity on the unstable portion of the curve. One pump will discharge against a slightly lower resistance than the other on account of small differences in the piping arrangement and the turbulence and friction losses. For a slight increase in the system demand, the pump with the lower discharge head will deliver more liquid. This will cause its discharge pressure to rise as the operating point moves to the right on the characteristic curve. The other pump, discharging at a lower pressure, reduces its delivery and so throws more burden on the first pump. The result is that the pump having the larger system resistance stops delivery while the other handles the entire system demand. This

does not happen if both pumps are operating on the stable part of the curve when a slight increase in demand occurs. The pump with the lower system resistance will take more liquid as before, but its discharge pressure will decrease as the operating point moves to the right. This automatically throws more flow to the pump with the higher discharge pressure. Thus the total flow will be shared by the two pumps.

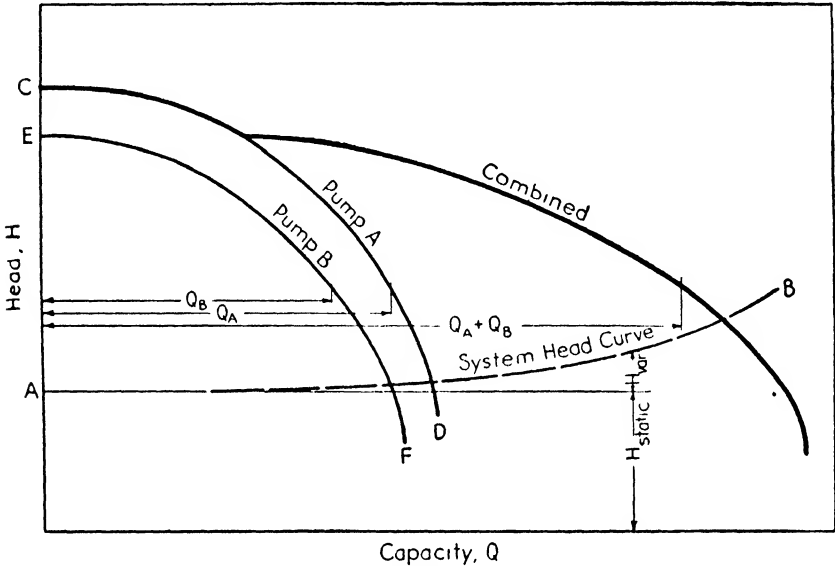


FIG. 9-1. Head-capacity curves of pumps operating in parallel.

If one pump is delivering liquid at a pressure greater than the shut-off pressure of the second pump, the second pump cannot deliver liquid, since the higher system pressure keeps the check valve shut. To place the second unit on the line, it may be necessary to decrease the speed of the first pump or by-pass the flow of the second until its discharge pressure builds up to a value greater than that of the first; then the check valve will automatically open. The same result could be obtained by speeding up the second pump.

Consider the action of two pumps of different sizes operating in parallel. The system head-capacity curve *AB* shown in Fig. 9-1 starts at H_{st} , when the flow is zero and rises parabolically with increased flow. Curve *CD* represents the head-capacity curve of pump *A* operating alone; the similar curve for pump *B* is represented by *EF*. Pump *B* will not start delivery until the delivery pressure of pump *A* falls below that of the shut-off head of *B* (point *E*). The

combined delivery for a given head is equal to the sum of the individual capacities of the two pumps at that head. For a given combined delivery head, the capacity is divided between the pumps as noted on the figure by Q_A and Q_B . The combined characteristic curve shown on the figure is found by plotting these summations.

The combined brake horsepower curve can be found by adding the brake horsepower of pump *A* corresponding to Q_A to that of pump *B* corresponding to Q_B , and plotting this at the combined flow. The efficiency curve of the combination may be determined by dividing the combined fluid horsepower, $\frac{\gamma(Q_A + Q_B)H}{550}$, by

the corresponding combined brake horsepower (Q taken as cubic feet per second).

Pumps in Series. If two pumps are operated in series, the combined head for any flow is equal to the sum of the individual heads, as illustrated in Fig. 9-2. The combined brake horsepower curve may be found by adding the horsepowers given by the curves for the individual pumps. Points on the combined efficiency curve are

found by dividing the combined fluid horsepower, $\frac{(H_A + H_B)Q\gamma}{550}$, by

the combined brake horsepower; Q is again in cubic feet per second.

It may be noted in both figures that the combined and system curves coincide at only one point. This should be the point of maximum flow for the system. For operating conditions to the left of this point the discharge head must be throttled to meet the system head; this involves a loss of power. If the unit is driven by a steam turbine, or if a variable speed transmission is used between the pump and the driver, the system head for any flow may be met by varying the pump

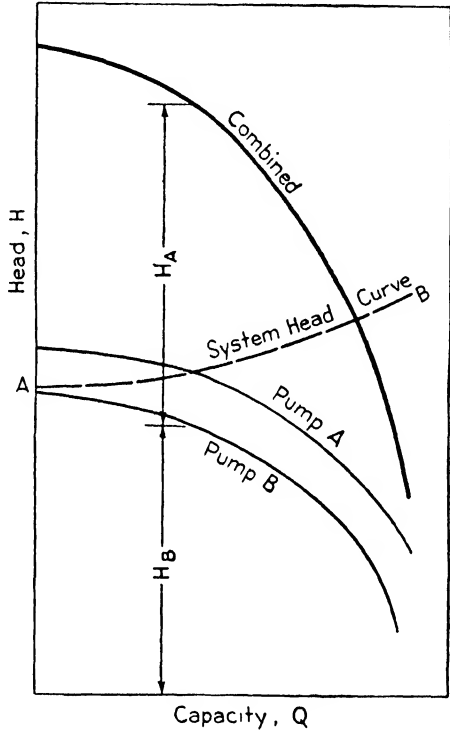


FIG. 9-2. Head-capacity curves of pumps operating in series.

speed. This latter arrangement involves a greater initial investment but lower operating costs because power is not wasted by throttling.

9-2 Prime Movers. Electric motors, steam turbines, or internal combustion engines are the common forms of drivers used for centrifugal pumps. The selection of the type to be used will depend mainly upon the kind of power available and the size of the pump.

The majority of pumps are driven by 60-cycle alternating-current motors. These operate at or somewhat below the standard synchronous speeds of 3600, 1800, 1200, 900, 720, 600, etc., r.p.m. The amount of slip depends upon the motor size and line voltage and may be obtained from the motor manufacturer for a given installation. These speeds are also frequently used with other types of drives. For lower horsepowers, squirrel-cage induction motors are usually used; for the larger horsepowers, synchronous motors are commonly employed.

Steam turbines are frequently geared to larger pumps when wide speed variations are desired or if the exhaust steam may be used for heating or process work.

Pumps located in isolated positions or to be used for emergency service, such as fire pumps, may be driven by gasoline or Diesel engines. They usually operate at relatively low speeds and may require a speed-up gear.

9-3 Economic Considerations. The final selection of the pumping arrangement to be used in a given installation and the particular bid to select in accordance with this arrangement usually depend upon an economic study of the various alternatives available. Such a study may also dictate the replacement of an existing pump or pumping arrangement which appears to be giving satisfactory service.

It is beyond the scope of this volume to consider fully load factors, replacement, depreciation, etc., although they must be understood in making an intelligent selection on an economic basis.*

The total cost of the pump and driver is made up of the initial purchase price plus the annual charges required to keep them in operation. These annual charges include the cost of power, taxes, interest on the investment, depreciation, insurance, and maintenance. For comparison, the calculation of the annual charges of operation, in which the initial cost is included in the form of straight-line depreciation, is generally satisfactory. The total annual cost is the sum of the power cost (total power consumed per year times the unit cost), plus maintenance (repairs and replacements averaged over the pump life), plus depreciation (initial cost of pump and driver divided by

* This subject is well covered in books on engineering economics, such as *Principles of Engineering Economy*, by E. L. Grant, Ronald Press.

the estimated life in years), plus taxes, plus interest on the initial investment, plus insurance. In comparing competitive bids on an annual basis, it is convenient to include maintenance, depreciation, taxes, interest, and insurance as a fixed percentage of the initial cost. If this is designated as x per cent, the annual cost = x per cent \times initial cost + b.hp. \times hours of operation per year \times cost of power per b.hp.-hr.

To illustrate the above, assume that the annual fixed charges are 20 per cent of the initial price and that power costs 1.5 cents per kw.-hr. Competitive bids from three companies for a water-circulating pump to handle 500 g.p.m. of water with a head of 150 ft. and operate 8 hours per day, 300 days per year are as follows:

Company	A	B	C
Price	\$235	\$415	\$265
Efficiency	71%	77%	73%

$$\text{The water horsepower, w.hp.} = \frac{\text{g.p.m.} \times H \times 8.33}{33,000} = \frac{500 \times 150 \times 8.33}{33,000} =$$

18.92 hp. As a horsepower is 0.746 kw., the cost of power is 1.5×0.746 or 1.12 cents per b.hp.-hr. The bids may best be analyzed in tabular form which requires no particular explanation.

Company	A	B	C
B.hp. = $\frac{\text{w.hp.}}{\eta}$	26.63	24.58	25.93
B.hp.-hr. per yr.	64,000	59,000	62,200
Power cost per year	\$717	\$661	\$697
Fixed charges per year	\$47	\$83	\$53
Total annual cost	\$764	\$744	\$750

It may be noted from this tabulation that there is little actual difference between the three bids even though their initial prices are quite different. If they operate continuously (24 hours per day, 365 days a year) the yearly operating time will be 8760 hours. The total annual costs will then be \$2667, \$2498, and \$2598 respectively for pumps A, B, and C; this indicates an advantage for pump B over the other two.

The above analysis may be used to determine if it is economically sound to pay a higher price for a pump to secure additional efficiency. It may also be applied to an existing installation to decide if the savings resulting from replacing it with a new higher efficiency pump are justifiable.

Points of efficiency are frequently evaluated in terms of first cost in preparing specifications for proposals. In order to evaluate bids

for comparison, a penalty of so many dollars is added to the bid price for each point the bid efficiency is below a stated amount. After the contract has been awarded a similar penalty may be deducted from the contract price for each point the efficiency is below the guaranteed figure. In one pump for the Victoria Park Pumping Station of the City of Toronto* this penalty was \$4450 a point, which was $12\frac{1}{2}$ per cent of the contract price. These values may be found by equating the increased annual power costs for each point to the annual percentage fixed charge times the penalty. This will make the total annual charge the same as if the pump had the guaranteed efficiency. To illustrate, assume a pump is to operate 2400 hours a year with a guaranteed efficiency of 75 per cent. The water horsepower is 50, annual fixed charges are 20 per cent of the contract price, and power costs 2 cents per b.hp.-hr. What penalty should be invoked for each point that the efficiency is below the guaranteed value? The guaranteed brake horsepower will be $50/0.75 = 66.7$ and each point of efficiency below this represents $66.7/75 = 0.89$ b.hp. Then $2400 \times 0.89 \times 0.02 = 0.2P$, or the penalty P will be \$214 per point.

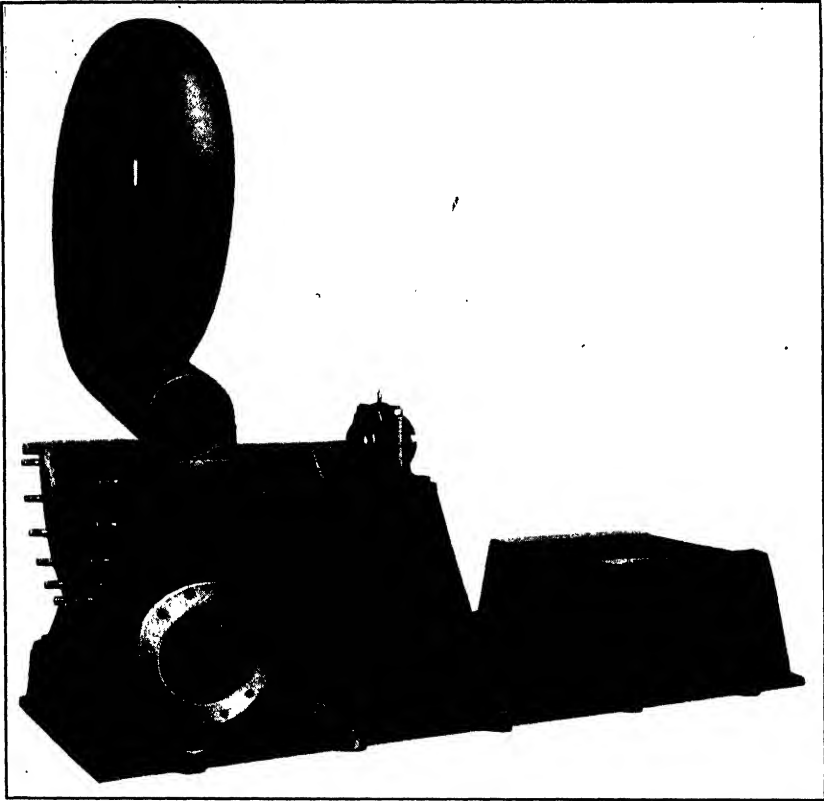
It is possible that the brake horsepowers required may range over two standard motor or turbine sizes, and thus result in higher initial costs for the drivers of less efficient pumps. Hence, it is wise to include the price of the driver in the above tabulations. Bids submitted should be based upon delivery at the town of installation rather than FOB the town where the pump is manufactured in order to obtain true comparative prices.

9.4 Fire Pumps. Pumps for fire protection may be single-stage, single- or double-suction (Figs. 1-2 or 8-4), or two-stage units with opposed impellers (Fig. 8-2). They develop a pressure of about 100 lb. per sq. in. and are generally made in standard capacities of 500, 750, 1000, and 1500 g.p.m. They are commonly motor driven with speeds ranging from 1350 to 2500 r.p.m. and are usually bronze fitted. For most applications they must meet the specifications and tests of the National Board of Fire Underwriters. The efficiency is not particularly important as they are used only occasionally and the flows are not large. Reliability and low cost are more important.

9.5 Dredge Pumps. These pumps have to handle sand and gravel, so they are made very rugged and simple with large clearances. This generally results in a sacrifice in efficiency. Since wear is rapid, the clearances may be checked weekly. The casing is usually provided with replaceable manganese steel liners to lower maintenance costs,

* R. W. Angus, "An Improved Technique for Centrifugal Pump Efficiency Measurements," *A.S.M.E. Trans.*, January, 1941.

as shown in Fig. 9-3. The impellers are generally single-suction and may be of the semi-enclosed type, frequently without wearing rings.

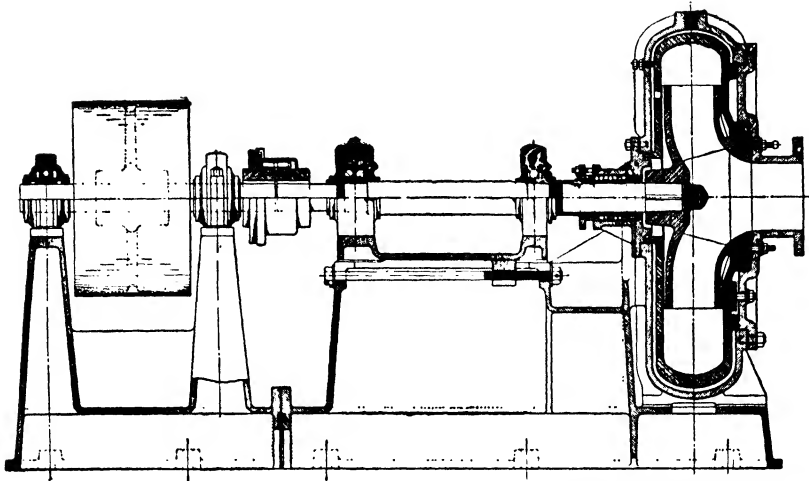


Courtesy Morris Machine Works

FIG. 9-3. Heavy-duty lined dredging pump showing steel liner being put in place.

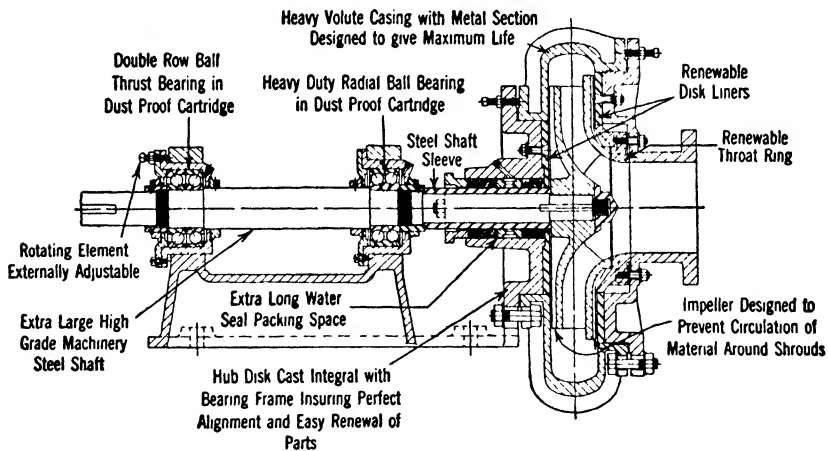
To prevent sand from getting in the packing box, it is flushed continually with clear water. Figure 9-4 shows a typical dredge pump in section.

9-6 Slurry Pumps. Centrifugal pumps are frequently used to handle slurries, which are liquids with finely divided suspended solid matter. They have packing boxes flushed with clear water and may not use wearing rings. If wearing rings are used they should be flushed also. Figure 9-5 illustrates a typical pump of this class. The impeller is made of simple construction and abrasive-resistant material. The back shroud has a series of radial ribs to prevent the slurry from packing in back of the impeller. The case thickness is proportioned to the expected wear at the various points.



Courtesy Morris Machine Works

FIG. 9-4. Heavy-duty lined dredging pump.

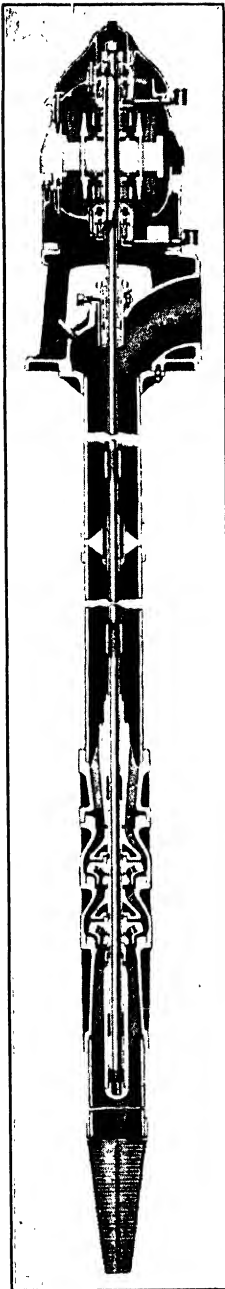


Courtesy Morris Machine Works

FIG. 9-5. Section through slurry pump showing general construction.

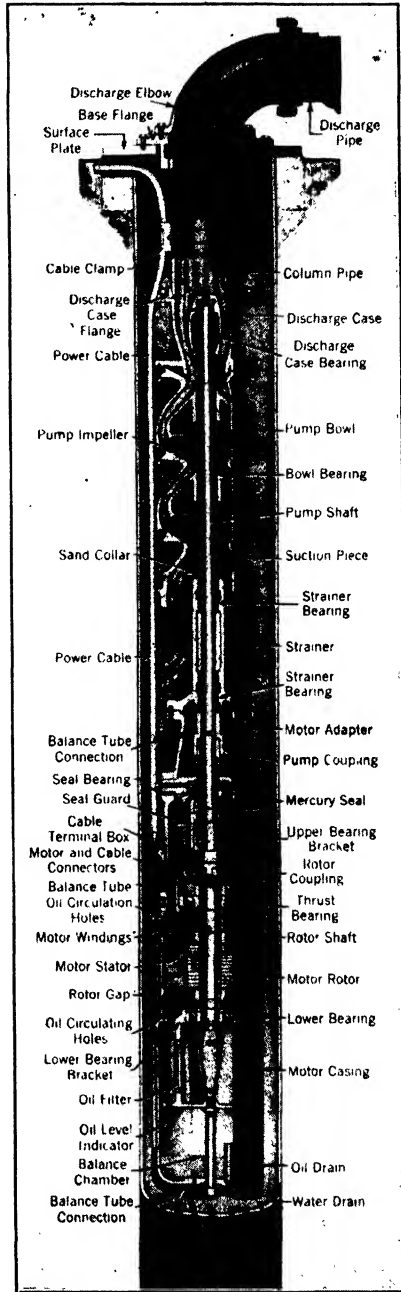
9-7 Deep Well Pumps.* When pumping water from deep wells, the pump is lowered into the well and operated close to the water level. They are usually motor driven, the motor being at ground level and connected to the pump by a long vertical line shaft as shown in Fig. 9-6.

* R. G. Folsom, "Some Performance Characteristics of Deep Well Turbine Pumps," *A.S.M.E. Trans.*, April, 1941, p. 245.



Courtesy Fairbanks, Morse & Co.

FIG. 9-6. Deep well pump with rubber bearings.



Courtesy Byron Jackson Co., Los Angeles, Calif.

FIG. 9-7. Deep well pump.

Bearings are spaced along the shaft to prevent excessive vibration, and, if metallic, are enclosed in a shaft tube. They may also be made of rubber with the water serving as a lubricant as shown in the figure. Another type avoids the use of the long line shafting by placing the motor below the pump in a watertight case (Fig. 9-7). The motor is lubricated by means of an oil tube running beside the power line. A novel feature of this pump is the use of a mercury seal to prevent water leakage into the motor.

The outside diameter of the pump must be kept small to reduce the size of the well hole required. This necessitates the use of small-diameter impellers and multistaging. The impellers are generally of mixed-flow type, either fully enclosed (Fig. 9-6) or semi-enclosed (Fig. 9-7), although axial-flow impellers are also used. The diffuser and return guide passages are combined to save space.

9-8 Waterworks, Irrigation, and Drainage Pumps. Pumps for these applications generally operate at a constant head and handle large capacities. For higher heads they are of the standard radial double-suction type; for lower heads they may be mixed-flow or propeller pumps. For heads above 150 ft. two pumps may be used in series, and for large capacities they may be placed in parallel.

The head is found by adding the frictional resistance to the difference in elevation. The pumps may be directly connected to motors operating at speeds anywhere from 300 to 1750 r.p.m. For large power consumptions they are commonly driven by geared turbines, usually at a speed of about 800 r.p.m. High efficiency is very important since they operate almost continuously, so a specific speed which gives good efficiencies is desirable. A high specific speed pump generally gives good efficiency and will also have a lower initial cost on account of the smaller size for a given flow.

9-9 Circulating Pumps. The conditions under which condenser circulating pumps operate are quite similar to those for waterworks pumps since the capacity and head are practically constant. The flow requirement is determined by the inlet water temperature and the amount of heat to be removed from the steam. This may be expressed by

$$\text{g.p.m.} = \frac{W(xL + t_1 - t_2)}{500(T_2 - T_1)}$$

where W = pounds of steam per hour

t_1 = temperature of steam entering condenser, ° F.

t_2 = temperature of condensate leaving condenser, ° F.

L = latent heat at condenser pressure, B.t.u.

- x = quality of steam entering condenser, per cent
- T_1 = circulating water inlet temperature, ° F.
- T_2 = circulating water outlet temperature, ° F.

The pump may be either a double-suction radial, mixed-flow, or propeller type. For marine service, where space and weight are important, propeller-type pumps are frequently used.

The head developed is usually quite low (about 25 to 30 ft.) since the water in the discharge pipe from the condenser usually balances that in the inlet pipe, as shown in Fig. 9-8. Hence practically all of the head is used to overcome friction and turbulence in the condenser and pipe lines. These pumps are usually motor driven. Since the capacity is large and the head is low the specific speed is high.

9-10 Boiler Feed Pumps.* As the water capacity of a modern boiler is only great enough to supply steam to the prime mover for one or two minutes when operating at full load, a dependable uninterrupted water supply to the boilers is vital. To meet this condition there must not be any cavitation and there must be sufficient flow to prevent the water from flashing into steam while passing through the pump. The cavitation problem has already been discussed in Chapter 5. To increase the suction head of high speed units a feed booster pump may be placed before the feed pump if a closed feed water system is being used.

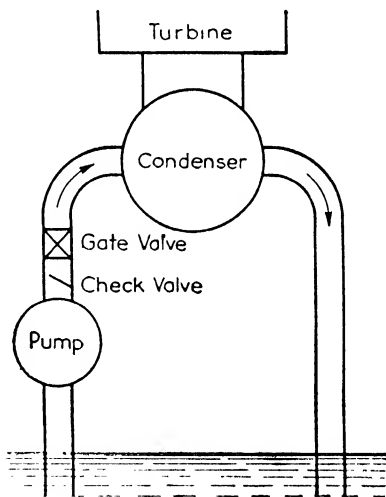


FIG. 9-8. Typical arrangement of circulating pump.

The difference between the brake and water horsepowers in any centrifugal pump represents lost energy which is converted into heat. A small percentage is removed from the pump by radiation but most of it is absorbed by the water. Under normal operating conditions the temperature rise is small and does not cause difficulties. At reduced capacities or for zero discharge the temperature of the water in the

* A. Peterson, "Centrifugal Boiler Feed Pumps for High Pressures," *Combustion*, May, 1935; Hans Gartmann, "Operation of Centrifugal Boiler-Feed Pumps," *Combustion*, January, 1941; A. H. Richards, "Feed Pump Troubles — How to Avoid Them," *Power*, February, 1936, p. 86; "Instructions for the Operation and Maintenance of Pumps," U. S. Navy Department, 1941, pp. 14-37 to 14-50.

pump will rise rapidly. The stationary parts of the pump will heat up more slowly than the rotating parts since they have larger masses and have one side exposed to the atmosphere. This uneven expansion may cause rubbing or even seizing of the wearing rings. In addition, the already hot feed water may flash into steam and interrupt the flow to the boiler. To avoid this condition it is customary to have a by-pass line which for low capacities will allow about 5 per cent of the design flow to be recirculated back to the feed heater.

For pressures below about 400 lb. per sq. in. the pump may be made single-stage whereas above this it is usually multistage. To keep the number of stages low, each stage should develop the largest possible head; this means that the specific speed will be relatively low. Standard radial-type wheels are used. Since several pumps are usually operated in parallel the characteristic curve should be stable, as outlined in Section 9-1.

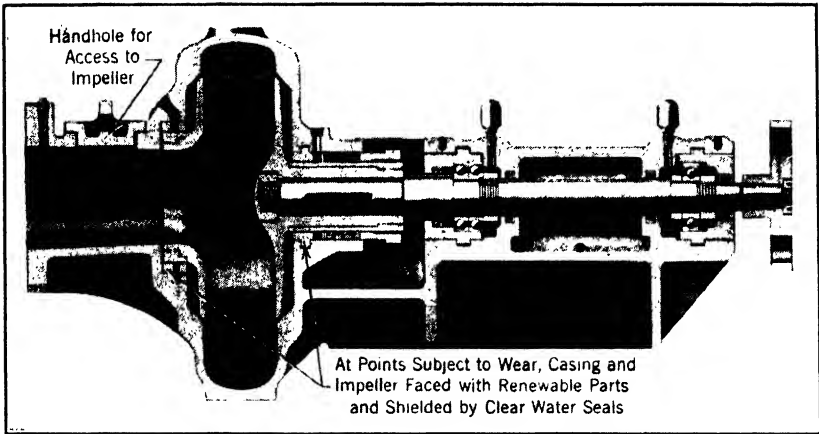
These pumps are usually motor driven at a speed of 3500 r.p.m. Frequently they have a dual drive with a steam turbine to be used for emergency operation if the current fails. As noted in Section 9-1 a variable speed turbine drive will give a material saving in power cost by running the pump at reduced speeds to meet the lower head requirements at small capacities. However, the initial cost is greater.

The flow through the pump is generally regulated by a water level control which throttles the flow to the boiler. A check valve is placed in the discharge line to prevent backflow into the pump.

9-11 Condensate Pumps. Condensate pumps operate under a nearly constant suction head. The capacity is based upon the steam flow to the condenser. The impeller is usually of the Francis wheel type and is motor driven at a constant speed between 1000 and 1750 r.p.m., depending upon the capacity and submergence. Since the temperature of the condensate is very close to its boiling point (at the suction pressure) the available suction head must be very carefully investigated for each installation. The pump should be kept as low as possible relative to the condenser to reduce the suction lift, and the suction pipe should be made large to reduce the velocity losses before the impeller.

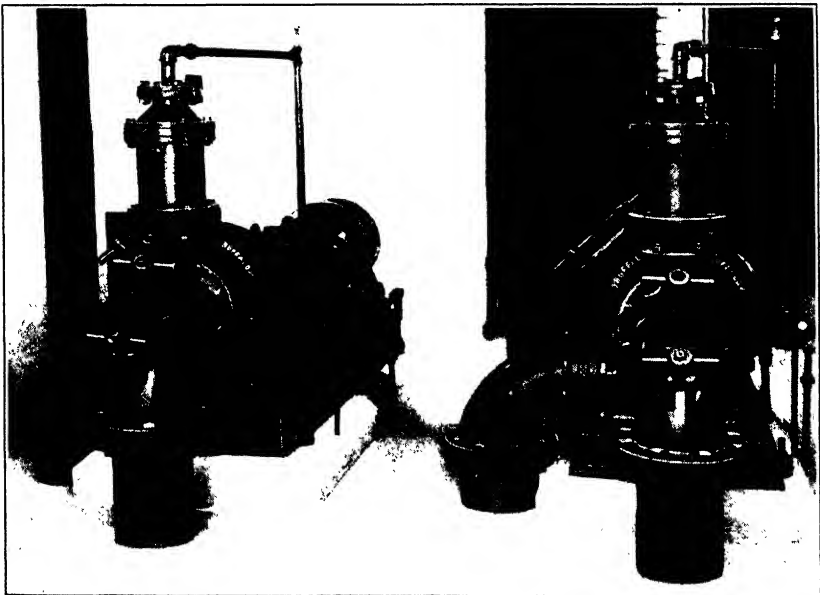
9-12 Clogless Pumps.* Pumps included in this classification are those used to handle sewage, bilge water, and fluids containing solids such as paper pulp. Their chief feature is that they must be able to pass a sphere whose diameter is the same or slightly smaller than

* A. Peterson, "Sewage Pumps," *Municipal Sanitation*, April, 1938; V. J. Mill, "Things to Consider in Selecting Sewage Pumps," *Waterworks & Sewerage*, March, 1936, p. 93.



Courtesy De Laval Steam Turbine Co.

FIG. 9-9. Section through clogless pump.



Courtesy Buffalo Pumps, Inc.

FIG. 9-10. Self-priming sewage pumps.

the suction pipe diameter. In very large pumps this diameter is usually limited to 8 in. A bar screen is placed before the inlet to filter out any objects whose diameter is greater than that for which the pump is designed.

The impeller is extra wide and has few vanes (2 to 4, depending upon the pump size). This results in relatively low efficiencies as the liquid cannot be given much guidance, but efficiency must be sacrificed for the non-clogging feature. The impeller is made of cast iron and may be made either semi-enclosed or fully enclosed. The speeds range up to 1750 r.p.m. with a specific speed range from about 1200 to 3000. They generally operate under low heads (20 to 40 ft.). To prevent the packing box and impeller rings from being packed with dirt, provision is made to flush them with clear water as illustrated in Fig. 9-9.

The suction lift should be quite low because the liberated gases tend to cause cavitation difficulties. For this reason the inlet portion is well rounded to decrease flow resistance, and often the shaft is vertical so the impeller may be placed closer to the sewage level without flooding the driver.

It is necessary to provide easy access to the impeller to clean out wire and rags which may become wrapped around it. Generally a large hand hole with a plate held in place with wing nuts is provided on either suction elbow or a convenient place on the casing or both (see Fig. 9-10).

PROBLEMS

9-1 Competitive bids from three companies for a chemical pump to develop 255 water horsepower are as follows:

Company	A	B	C
Price	\$3584	\$6113	\$3912
Efficiency	76%	81%	79%

Determine the annual costs based upon a power cost of 2 cents per b.hp.-hr. and an annual fixed charge of 15 per cent of the initial price if (a) the pump is to operate 2400 hours per year; (b) the pump is to operate 8760 hours per year.

<i>Ans.</i> Company	A	B	C
(a)	\$16,643	\$16,028	\$16,080
(b)	\$59,322	\$56,073	\$57,139

9-2 What penalty should be invoked for each point that the efficiency is below that guaranteed for pump B for conditions (a) and (b) in Problem 9-1?

Ans. (a) \$1250; (b) \$4555.

9-3 A pump operating continuously (8760 hours a year) has an efficiency of 70 per cent and develops 300 w.hp. A new pump costing \$1000 and having an

efficiency of 80 per cent can be purchased. If power costs 2 cents per kw.-hr. and the annual fixed charges are 20 per cent of the initial cost, would you advise purchasing the new pump?

Ans. Annual charges: Old \$56,056; new \$49,250; buy new pump.

9·4 It is desired to operate the pump of Problem 5·2 in parallel with the pump tested in Chapter 10. Using the data given in Fig. 10·5 with that of Problem 5·2 plot the combined head, horsepower, and efficiency curves.

9·5 Same as Problem 9·4 except that the pumps are to be operated in series.

CHAPTER 10

PUMP INSTALLATION, OPERATION, AND TEST

10-1 Installation. Certain precautions must be observed in planning a pump installation and during the erection period. Some of these points will now be considered.

Piping. Both the suction and discharge lines should be independently supported so no strains will be thrown on the casing; such strains may cause distortions and rubbing.

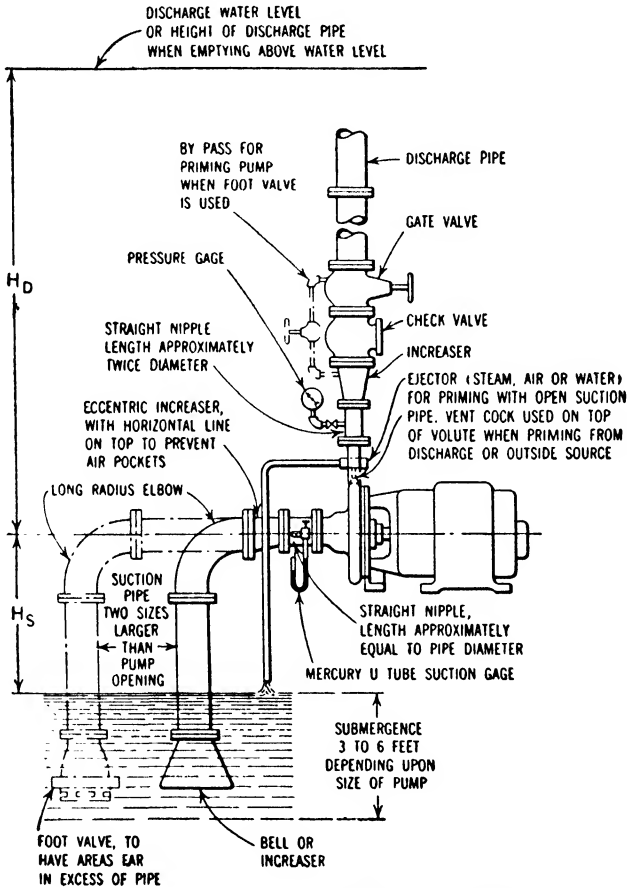
The suction line should be as short and straight as possible. Any elbows should have large radii. For pumps operating with suction lifts no valves other than a foot-valve should be placed in it. Generally, the diameter is made one or two sizes larger than the pump flange size. All these precautions insure the maximum available suction head on the pump. When an oversize line is used an eccentric reducer is placed between it and the pump flange as illustrated in Fig. 10-1.

It is very important to have the suction line airtight and to avoid high spots at which dissolved gases or air might separate out and destroy the vacuum. After the piping is installed and the pump is running all joints should be inspected with a flame, as air leakage will draw the flame to the opening. The same method can be used to determine leakage through the packing box. (The eccentric reducer is used at the suction flange to avoid high spots at which the air might collect. The inlet end of the suction line should be 3 to 6 ft. below the minimum water level of the sump to prevent air from being drawn into the pipe with the water.

It is desirable to have as long a length of straight piping between the elbow and suction flange as possible to even out the flow of the water as it enters the pump. The pump should be placed to secure the greatest possible suction head and yet be available for inspection and repair work.

A check valve and a gate valve are usually placed in the discharge line. The gate valve is used to regulate the flow and the check valve prevents backflow into the pump which might cause it to operate like a turbine and perhaps be damaged on account of overspeed. The check valve is placed between the gate valve and the pump so that it may be inspected or repaired without emptying the discharge line.

Foundation. The foundation should be heavy to reduce vibrations and should be rigid enough to avoid any twisting or misalignment. A space of $\frac{3}{4}$ to $1\frac{1}{2}$ in. is allowed between the base plate and top of the foundation which is filled with grouting to secure a uniform load distribution.



Courtesy De Laval Steam Turbine Co.

FIG. 10-1. Diagram of typical pump installation and methods of priming pump.

When the grouting has dried the base plate should be drawn down evenly to avoid springing it. After this has been done the shaft is finally aligned both radially and axially with the driver by means of shims or wedges so that it turns freely. If the shaft is not properly aligned there will be vibration and excessive wear on the bearings, packing, and wearing rings.

10-2 Operation. The operation of centrifugal pumps is quite simple and safe. There are relatively few valves and the pump will not be damaged even if the discharge valve is closed for short periods of time.

Starting. The pump must be primed before it will deliver any fluid. Failure to prime the pump may cause the wearing rings to seize or the shaft may be scored at the packing boxes. A discussion and description of the methods of priming is given in Section 8-13. During starting it is wise to have the petcock in the casing open slightly to remove any dissolved air in the water.

It is best to have the discharge valve set so that the least load is thrown on the driver when the pump is started. Reference to Fig. 5-6 shows that for impellers of the radial or Francis types this occurs when the discharge valve is closed, i.e., zero delivery. The valve should be opened gradually to avoid throwing a large sudden load on the driver and to prevent a sudden surge in the discharge line. The discharge valve should be fully open when starting mixed-flow or propeller pumps because the brake horsepower will then be a minimum as shown in Fig. 5-6.

Running. When the unit is running it requires very little attention beyond occasionally checking to see that (a) the journal and thrust bearings are running cool and have a sufficient supply of oil, (b) the packing is adjusted to permit a slight leakage to cool and lubricate it, and (c) the water is flowing to the water seal of the suction gland to prevent air from leaking in.

Shutting Down. When shutting down, the discharge valve should be in the same position as when starting up so that less power is dropped from the line and any sudden pressure surges in the pipe system are avoided.

*Inspection and Maintenance.** Manufacturers supply instruction books which give directions for the operation and maintenance of each pump, so the following information is general.

The wearing ring clearances should be checked as they will increase with time and thus cause a decrease in efficiency. The frequency of the inspection will depend upon the liquid handled. If the liquid contains gritty materials or is corrosive inspection may be made monthly, but if clear water is pumped it may be sufficient to check them annually. A general rule is to replace the rings when the clearance has increased 100 per cent above the original.

The packing should be replaced after it becomes hard and tends to score the shaft. When the packing is being replaced the finish of the

* "Instructions for the Operation and Maintenance of Pumps," U. S. Navy Department, 1941, pp. 14-66 to 14-75.

shaft sleeves should be examined for smoothness. It is essential that the lantern ring be placed directly under the water inlet when putting in the new packing to insure a circulation of the water and a satisfactory seal. The packing should be gradually compressed with the pump running. It should not be compressed too much as local heating of the shaft and consequent misalignment will result. A slight leakage will insure proper lubrication and cooling.

If the base is not too rigid the shaft alignment should be checked occasionally when the pump is at a temperature corresponding to running conditions. This must be done with the packing removed. At the same time the clearances of the journal bearings should be checked for wear.

The oil should be changed as required and at that time inspected for the presence of water. If water appears in the oil the pump casing should be examined to find the leak.

The entire pump should be dismantled periodically and examined for excessive wear or corrosion.

Operating Difficulties. Probably the chief source of trouble in operating centrifugal pumps is insufficient available suction head. It may be satisfactory when the pump is installed but may decrease with age or changes in the operating conditions. The foot-valve may become jammed so that it cannot open fully, or its strainer may become clogged with leaves, paper, or brush. The suction line may become clogged, particularly when repairs are being made. Gradual changes may take place in the water temperature which will reduce the available head. In addition the water level may decrease; this not only increases the lift but also may permit air to be drawn into the suction line as a result of the decreased immersion of the inlet. Under these conditions the flow through the pump may be reduced or stop entirely on account of cavitation and the discharge pressure will be reduced as discussed in Chapter 5. The cures are obvious.

Another common difficulty is caused by air leakage into the suction line or pump casing. This may occur at the various joints or at the packing boxes, as the packing ages, or if the lantern rings are not in line with the water connections. These leaks may be located by holding a flame near the joints and packing boxes while the pump is operating. If the inlet is not sufficiently submerged, air may be drawn into the suction line. If the water contains much dissolved air or gas it will be released at the low suction pressures. When sufficient air has collected the pump may lose its prime or at least operate unevenly and the capacity and pressure will be reduced.

Besides the above-mentioned causes of reduced capacity and pres-

sure, mechanical defects such as worn wearing rings, partially clogged or damaged impellers or diffusers may produce the same results.

If the pump does not deliver any liquid it may be because it is not primed. Also, the impeller or diffuser may be clogged or damaged or they may be mounted for the wrong direction of rotation. It may also be caused by a low speed of rotation or by the discharge head being too high (on account of too high a line pressure or an obstruction in the discharge line) as discussed in Section 9-1.

Lowered efficiency may be caused by excessive rubbing of the parts due to tightening the packing too much or binding resulting from a bent shaft. It may also be caused by worn wearing rings or an increase in the specific gravity or viscosity of the liquid being pumped.

10-3 Pump Test. Before a pump is accepted by the purchaser it is subjected to a test to make sure that it meets the guaranteed head, capacity, and efficiency. Smaller pumps are tested in the manufacturer's shop generally with a representative of the purchaser present to witness the test; larger pumps are usually tested after they have been installed. Frequently tolerances may be specified for the head, horsepower, and efficiency; for example, the head may have tolerances from minus zero to plus 3 to 5 per cent, the horsepower plus 2 per cent, and the efficiency minus $\frac{1}{2}$ per cent. While the performance test is being run the unit may be observed for mechanical defects such as bearing temperatures, vibration, etc.

The tests are usually conducted according to procedure outlined by the Standards of the Hydraulic Institute which are similar to the American Society of Mechanical Engineers Test Code.

For the test to have significance accuracy is essential. All instruments should be of an approved type and should be calibrated both before and after the test. The test set-up should be designed to give the greatest flexibility of operation and yet secure steady conditions for each setting. Figure 10-2 illustrates a typical set-up with notes indicating points to be observed. The dimensions given on the figure apply to the sample test considered in Section 10-5.

Performance tests are used to supply two kinds of information. The first is to establish the performance curves of head, brake horsepower, and efficiency. The most important point on these curves is the one corresponding to the design condition, hence this point should be more accurately determined than the rest of the curve. A common procedure is to take several instrument readings at equal time intervals at this point, and then average the values obtained. Other points are found by varying the discharge valve setting to establish the curve

shape, allowing sufficient time between readings to establish steady conditions.

The pump should be run at full speed before the test is started in order to warm up the bearings and establish operating conditions. It is wise to operate it with the discharge valve closed since air inleakage may then be detected by a loss of prime or gradually increasing noisiness of operation. When the test starts, the curve may be established by running at various points between shut-off and maximum capacity and then at the design point as outlined above.

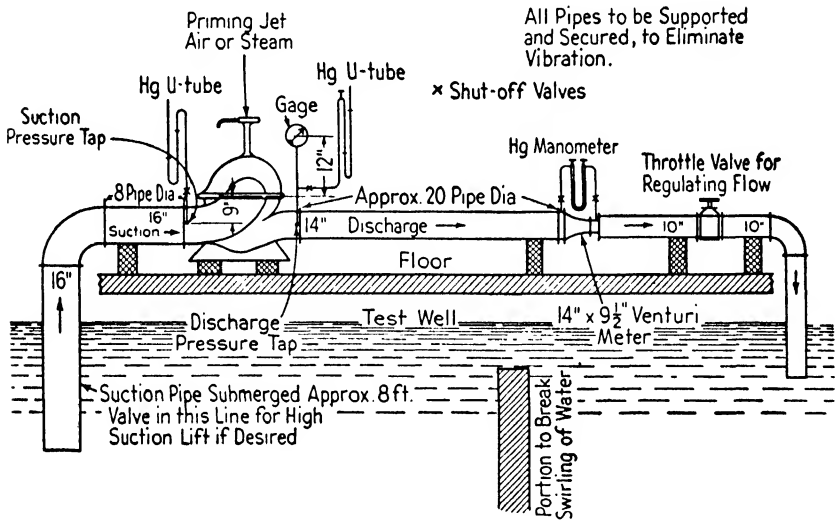


FIG. 10-2. Typical pump test arrangement.

The second type of test is to establish the required suction head of a pump. This may be done for the design point only or for the full range of capacities. It is done only if there is a possibility that the available head is insufficient, as when the unit has a high suction lift or when it is handling hot water, etc. This test is accomplished by placing a gate-valve in the suction line. By regulating the setting of this valve any given suction head referred to the pump centerline can be established. For a given suction head values of total head and efficiency can be found for various capacities. The flow at which the head drops to zero will represent the maximum capacity corresponding to this required suction head. By repeating this process several times for different suction heads a curve of required suction head against capacity may be obtained (curve *PQ* of Fig. 5-15).

10-4 Test Instruments and Apparatus. It is not the purpose of this section to discuss in detail the theory and give tables of coefficients for the apparatus and instruments used in pump testing. They are well covered in books on experimental engineering,* hydraulics, and the Test Codes. The methods of measurement will be considered briefly.

Measurement of Head. The values of head are always referred to the pump shaft centerline. For heads above about 30 ft. a calibrated pressure gage is generally used. For low heads a water column or U-tube filled with a substance heavier than water is commonly used. The U-tube should be self-draining and it usually has no water on the pipe side of the manometer.

The fluid most commonly used in the U-tube is mercury, which has a specific gravity of 13.6. Other fluids such as carbon tetrachloride (specific gravity 1.595), acetylene tetrabromide (specific gravity 2.96), and kerosene (specific gravity 0.81) are also used.

The Test Codes give illustrations and formulas for finding the heads with different arrangements of tubes and gages to which the interested reader may refer.

The velocity head $\frac{V^2}{2g}$ may be expressed in the form $\frac{0.002594(\text{g.p.m.})^2}{D^4}$, where D is the pipe size in inches. This may be written $H_v = A \left(\frac{\text{g.p.m.}}{1000} \right)^2$; the values of A for standard pipe sizes are given in Table 10-1. When the change in velocity head is required the constant for any combination of pipe sizes may be found by subtracting the value of A for the discharge flange from that for the suction flange. For example, for the combination of a 10-in.-diameter suction flange and an 8-in.-diameter discharge flange the coefficient A will be $0.63333 - 0.2594$ or 0.3739 and the difference in velocity head for a flow of 2000 g.p.m. is 1.5 ft.

Measurement of Capacity. The most obvious method of measuring the capacity would be to draw liquid from or discharge it into a tank where the change of volume or weight may be found for a given time interval. This may also be done with large pumps by using a reservoir of known size and calculating the volume handled in a given time interval by the change in water level.

The most common method, however, is a venturi meter, illustrated diagrammatically in Fig. 10-3. As the fluid approaches the throat or narrowest section its velocity is increased and static pressure is de-

* Diederichs and Andrae, *Experimental Mechanical Engineering*, Vol. I, Wiley, 1930.

TABLE 10·1

Diameter	Coefficient <i>A</i>
1	2594.
1¼	1062.6
1½	512.43
2	162.14
2½	66.41
3	32.027
4	10.137
5	4.156
6	2.0017
8	0.63333
10	0.25940
12	0.12510
14	0.067526
15	0.051244
16	0.039583
18	0.024712
20	0.016214

creased. The flow is measured by an equation based upon Bernoulli's theorem and the continuity equation. If the meter is horizontal, so that there is no change in elevation, Bernoulli's equation may be written

$$\frac{V_m^2}{2g} + \frac{P_m}{\gamma} = \frac{V_t^2}{2g} + \frac{P_t}{\gamma}$$

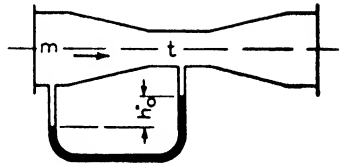


FIG. 10·3. Section through venturi meter.

where the subscripts *m* and *t* denote mouth and throat respectively. The manometer connecting these two points indicates $P_m/\gamma - P_t/\gamma$. Hence,

$$h = \frac{P_m}{\gamma} - \frac{P_t}{\gamma} = \frac{V_t^2 - V_m^2}{2g}$$

By the continuity equation, the flow $Q = V_m A_m = V_t A_t$, so that

$$2gh = V_t^2 - V_m^2 = \frac{Q^2}{A_t^2} - \frac{Q^2}{A_m^2} = Q^2 \left(\frac{1}{A_t^2} - \frac{1}{A_m^2} \right) = \frac{Q^2}{A_m^2} \left(\frac{A_m^2}{A_t^2} - 1 \right)$$

As the area is proportional to the diameter squared, the equation may be written $2gh = \frac{Q^2}{A_m^2} \left(\frac{D_m^4}{D_t^4} - 1 \right)$. If the diameter ratio D_m/D_t is

designated by the symbol *R*, the equation becomes $Q = A_m \frac{\sqrt{2gh}}{\sqrt{R^4 - 1}}$.

A flow coefficient C of about 0.99 must be included. The final equation may be written:

$$Q = 3.117C \frac{A_m}{\sqrt{R^4 - 1}} \sqrt{2gh} \quad 10-1$$

where Q is in gallons per minute, A_m is in square inches, and h is measured in feet of the liquid being handled. For a given venturi,

$\frac{3.117CA_m\sqrt{2g}}{\sqrt{R^4 - 1}}$ is a constant, hence $Q = k\sqrt{h}$, where k includes the

flow coefficient. The manometer connecting the mouth and throat is usually filled with mercury, and when it is displaced it is partially balanced by a water leg. Then,

$$h = h_0'' \frac{(13.6 - 1.0)}{12} = 1.05h_0''$$

where h_0'' is the manometer reading in inches of mercury.

There are other methods of measuring the flow, such as weirs, nozzles, pitot tubes, current meters, the Gibson or Allen salt velocity method, and orifice plates. These are described in the Test Code Section of the Hydraulic Institute Standards and will not be included here.

Measurement of Speed. The test speed is very important since all other measurements are based upon it in making corrections to the rated speed. These corrections are made in accordance with the principles developed in Section 3-15. Moreover, changes in the impeller diameter may be made on the basis of the test. After the impeller has been cut down the diameter cannot be increased again. The speed may be measured by a calibrated tachometer, or a revolution counter may be used.

Measurement of Power. The brake horsepower input may be determined by using a calibrated electric motor to drive the pump. Another method is to use an electric dynamometer, which will probably give the most accurate results.

One of the most common types of transmission dynamometers is the torsion meter. This is illustrated diagrammatically in Fig. 10-4. It is placed between the driver and the pump. The angular twist of the bar A , which is due to the power being transmitted between sections B and C , is measured on the flanges D and E . Flange D has a thin radial slit cut in it; opposite this slit on flange E is a celluloid scale marked off in degrees and having a vernier. By placing a light behind flange E and sighting through the rotating slit on D , the angular deflection

may be read quite accurately. The torque in inch-pounds is then given by $20,550 \frac{\alpha d^4}{L}$ for a steel bar A , where α is the angle of twist in

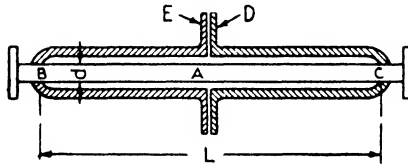


FIG. 10.4. Section through torsion meter.

degrees, L is the distance between B and C in inches, and d is the diameter of the bar A in inches. This will reduce to a coefficient times α for a particular meter. The coefficient should be determined by calibration before the meter is used for test work.

10.5 Sample Pump Test. It is impracticable to illustrate all the possible testing arrangements and types of instruments which might be used. Figure 10.5 shows a typical data and calculation sheet for the test set-up illustrated in Fig. 10.2. The dimensions given on Fig. 10.2 apply to this particular test.

The sample test is for a single-stage double-suction pump with a 16-in. suction line and a 14-in. discharge line. The pump is designed to deliver 5000 g.p.m. of water with a total head of 30 ft. at 860 r.p.m. and an efficiency of 80 per cent. The capacity is measured with a 14-in. \times 9½-in. venturi meter, the suction lift with a mercury U-tube; the discharge head with a mercury U-tube for the lower heads, and a pressure gage reading in feet of water for the higher heads, and the speed with a calibrated tachometer. The pump is driven by a 50-hp., 230-v., 900-r.p.m. direct-current compound-wound motor, with a field rheostat for speed regulation. The motor efficiency for various loads is taken from a certified test curve. Certain corrections applying to the test instruments will be given when the calculations are discussed.

The pump was run for a half hour at the design point and readings were taken every five minutes. These values were averaged in determining the design point. Seven other points ranging from maximum flow to shut-off were then taken at five-minute intervals to determine the curve shape.

The first seven columns are the test readings and the other columns are the calculations dependent upon these readings. The calculation procedure will now be outlined, the average readings at the design point

and those at shut-off being used as examples. These will be considered in order by columns.

Column 8. The kilowatt input to the motor is found by multiplying the volts and amperes of columns 2 and 3 and dividing by 1000.

$$\text{Design: } \frac{225 \times 174}{1000} = 39.15 \quad \text{Shut-off: } \frac{225 \times 95}{1000} = 21.38$$

Customer: <u>A B C Company, Philadelphia, Penn</u>													Serial No. <u>186214</u>									
Date: <u>8-23-43</u>													Type: <u>Double Suction, Single Stage 16"14"</u>		R.P.M. <u>860</u>							
Design Conditions: B.H.P. <u>47.3</u> H <u>30</u> ft. Q <u>5000</u> G.P.M. Suction lift <u>6</u> ft. Eff. <u>80%</u>													Driver <u>50 H.P., 250 V, 900 R.P.M., DC Compound Wound</u>					Venturi <u>14" x 9 1/2"</u>				
①	②	③	④	⑤	⑥	⑦	⑧	⑨	⑩	⑪	⑫	⑬	⑭	⑮	⑯	⑰						
Time of Test	V	A	Tach Read	Suct *Hg	Disch *Hg	Vent Man *Hg	Motor KW	Motor η	B.H.P	Suct Lift Ft	Disch Head Ft	G.P.M	ΔH _{vel} Ft	Total Head Ft	W.H.P	η %						
9:30	224	174	860	5.1	20.4	6.25																
9:35	"	175	"	5.1	20.4	6.25																
9:40	"	174.5	"	5.0	20.3	6.20																
9:45	226	173.5	"	5.0	20.35	6.25																
9:50	"	174	"	5.1	20.35	6.15																
9:55	225	173	"	5.1	20.4	6.20																
10:00	226	174	"	5.1	20.4	6.10																
Ave	225	174	860	5.07	20.37	6.20	39.15	0.907	47.60	6.50	23.2	5060	0.72	30.42	38.85	81.6						
10:10	225	114.3	860	6.2	1.65	9.2	25.75	0.899	31.0	7.78	2.80	61.60	1.06	11.64	18.09	58.3						
10:15	"	140.2	"	5.8	8.0	8.4	31.55	0.904	38.2	7.33	9.73	58.90	0.97	18.03	26.80	70.1						
10:20	224	161.6	"	5.4	14.5	7.3	36.2	0.906	44.0	6.87	16.82	54.90	0.84	24.53	34.00	77.3						
10:25	"	179.2	"	4.1	8.4	3.95	40.15	0.907	48.8	5.40	33.0	40.40	0.46	38.86	39.60	81.2						
10:30	225	164.3	"	3.8	40.2	2.1	37.0	0.906	45.0	5.05	41.0	29.40	0.24	46.29	34.35	76.3						
10:35	"	132.2	"	2.9	49.1	6	29.75	0.903	36.0	4.04	49.9	15.73	0.07	54.01	21.40	59.5						
10:40	"	95.0	"	2.5	55.5	0	21.38	0.890	25.5	3.59	56.3	0	0	59.89	0	0						

FIG. 10-5. Pump test data and calculation sheet.

Column 9. The motor efficiencies are read from a certified test curve for the motor.

$$\text{Design: } 90.7\% \quad \text{Shut-off: } 89.0\%$$

Column 10. The brake horsepowers are obtained by multiplying the kilowatt input by the motor efficiency and dividing by 0.746.

$$\text{Design: } \frac{39.15 \times 0.907}{0.746} = 47.6 \quad \text{Shut-off: } \frac{21.38 \times 0.890}{0.746} = 25.5$$

Column 11. The suction pressure tap is located 9 in. below the pump centerline and both sides of the tube are filled with air; hence, there is no water leg correction.

$$H_s = \frac{13.6h''}{12} + \frac{9}{12}$$

Design: $\frac{13.6 \times 5.07}{12} + \frac{9}{12} = 6.5$ ft. Shut-off: $\frac{13.6 \times 2.5}{12} + \frac{9}{12} = 3.59$ ft.

Column 12. The center of the U-tube and the centerline of the pressure gage are both 12 in. above the pump centerline. The manometer and gage are filled with water on the pump side. The pressure gage records feet of water, but calibration shows that it reads 0.2 ft. high.

$$H_D = \frac{13.6}{12} (\text{in. Hg}) - \frac{1}{12} \frac{\text{in. Hg}}{2} + 1$$

Design: $H_D = \frac{13.6}{12} \times 20.37 - \frac{1}{12} \frac{20.37}{2} + 1 = 23.2$ ft.

Shut-off: $55.5 - 0.2 + 1 = 56.3$ ft.

Column 13. The venturi flow coefficient is 0.99 and the ratio of the diameters is $14/9\frac{1}{2} = 1.472 = R$. The mouth area is

$$A_m = \frac{\pi}{4} D_m^2 = \frac{\pi}{4} 14^2 = 154 \text{ sq. in.}$$

hence the venturi constant is

$$k = \frac{3.117 C A_m \sqrt{2g}}{\sqrt{R^4 - 1}} = \frac{3.117 \times 0.99 \times 154 \sqrt{2 \times 32.2}}{\sqrt{1.72^4 - 1}} = 1978$$

The head across the venturi in feet of water is $\frac{13.6 - 1}{12}$ or 1.05 times the manometer reading in inches Hg, h_0'' .

Flow in g.p.m.: $1978 \times \sqrt{1.05} \times \sqrt{h_0''} = 2027 \sqrt{h_0''}$

Design g.p.m.: $2027 \sqrt{6.20} = 5060$ Shut-off: g.p.m. = 0

Column 14. By Table 10.1 the velocity head coefficient A for a 16-in. suction and a 14-in. discharge line is $0.067526 - 0.039583 = 0.027943$. This coefficient multiplied by $(\text{g.p.m.}/1000)^2$ gives the difference in velocity head between the discharge and suction lines.

Design: $0.027943 \left(\frac{5060}{1000} \right)^2 = 0.716$ ft. Shut-off: 0

Column 15. The total head is the sum of the suction head, discharge head, and difference in velocity heads of columns 11, 12, and 14.

Design: $H_T = 6.5 + 23.2 + 0.72 = 30.42$ ft.

Shut-off: $H_T = 3.59 + 56.3 + 0 = 59.89$ ft.

Column 16. The water horsepower is the product of the total head and weight flow in pounds per minute divided by 33,000 (1 gal. weighs 8.33 lb.).

$$\text{Design: w.hp.} = \frac{5060 \times 30.42 \times 8.33}{33,000} = 38.85 \quad \text{Shut-off: } 0$$

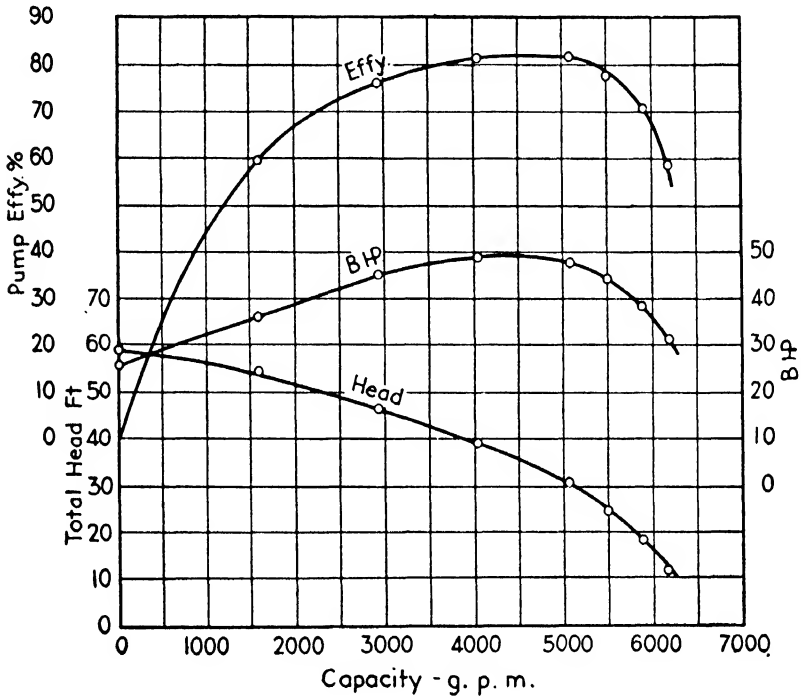


FIG. 10-6. Performance curves of pump test.

Column 17. The pump efficiency is the ratio of the water horsepower to the brake horsepower.

$$\text{Design: } \eta = \frac{38.85}{47.60} = 81.6\% \quad \text{Shut-off: } \eta = \frac{0}{25.5} = 0\%$$

The calculated values are plotted on Fig. 10.6 and connected by smooth curves.

CHAPTER 11

THERMODYNAMIC PRINCIPLES

11·1 Introduction. The principles of thermodynamics which apply to blower design will be reviewed briefly. More complete discussions may be found in standard textbooks on the subject.*

11·2 Characteristic Equation. Boyle's Law states that the absolute pressure of an ideal or perfect gas at constant temperature is inversely proportional to the volume, or $PV = C_1$. Charles' Law states that the absolute pressure of an ideal or perfect gas at constant volume is directly proportional to the absolute temperature, or $P = C_2T$. Also, the volume of an ideal or perfect gas at constant pressure is directly proportional to the absolute temperature, or $V = C_3T$. These three relationships may be combined into one equation:

$$PV = WRT \qquad 11\cdot1$$

which is known as the characteristic equation of a gas. P is the absolute pressure in pounds per square foot; V is the volume in cubic feet; W is the weight of gas in pounds; R is a constant depending upon the composition of the gas; and T is the absolute temperature in degrees. If only 1 lb. of gas is considered, $W = 1$, and the equation becomes

$$P\bar{V} = RT \qquad 11\cdot2$$

where \bar{V} is the specific volume in cubic feet per pound.

Equations 11·1 and 11·2 are very useful in thermodynamic work in determining the complete condition of the gas, or in finding the weight of a given volume when its temperature and pressure are specified.

A perfect or ideal gas is one which meets the requirements of the above laws. Actual gases do not do so exactly, but the error is usually small and may be neglected in engineering work. It must be remembered that the equation applies only to gases, or vapors such as steam with an extremely high superheat. If the superheat is low (on account of reduced pressure or temperature), vapor charts must be substituted for the equation.

* For example, Barnard, Ellenwood, and Hirshfeld, *Heat-Power Engineering*, Part I, Wiley, 1926, and Faires, *Applied Thermodynamics*, Macmillan, 1938.

The specific volume \bar{V} or its reciprocal, specific weight γ , depends only upon the static pressure. If the gas is flowing past a point, the velocity head must be subtracted from the total head to determine the static pressure. This static pressure is used to find the specific weight or specific volume.

11.3 Specific Heat. The specific heat of a gas is defined as the amount of heat required to raise the temperature of a unit weight of gas one degree. Its value depends upon the method by which the heat is added. If the volume is kept constant while the heat is added, all the heat is used in increasing the internal energy, i.e., in raising its temperature. The amount of heat required is known as the specific heat at constant volume and is denoted as c_v . If the pressure is kept constant and the volume allowed to vary while the heat is added, more heat will be required than in the previous instance. In addition to increasing the internal energy or raising the temperature, the gas expands and external work equal to $\int AP dV$ is done, where A is the mechanical equivalent of heat (in English units $A = 1/778$). This amount of heat is known as the specific heat at constant pressure, and is denoted as c_p . The specific heats are not constant, but vary with the temperature. For the usual conditions met in centrifugal blower work this variation may be neglected, or average values may be used for the temperature range considered.

The ratio of the specific heat at constant pressure to that at constant volume is known as k ; it occurs frequently in thermodynamic relations.

$$k = \frac{c_p}{c_v} \quad 11.3$$

It has been found that the gas constant R in Eqs. 11.1 and 11.2 when multiplied by the molecular weight of the gas equals 1544 or a value very close to it. This fact is very useful in finding R for gas mixtures, as will be shown later. R represents the work done in foot-pounds when a unit weight of gas is heated one degree at constant pressure. If A is the mechanical equivalent of heat,

$$c_p = c_v + AR = c_v + \frac{R}{778} \quad 11.4$$

Now $k = \frac{c_p}{c_v}$, so

$$c_p - \frac{c_p}{k} = c_p \left(1 - \frac{1}{k} \right) = AR$$

or

$$c_p = \frac{ARk}{k-1} = \frac{R}{778} \frac{k}{k-1} \quad 11.5$$

and

$$c_v \left(\frac{c_p}{c_v} - 1 \right) = c_v(k-1) = AR$$

or

$$c_v = \frac{R}{778} \frac{1}{k-1} = \frac{AR}{k-1} \quad 11.6$$

The value of R for air having 36 per cent relative humidity at 68° F. (which approximates usual conditions) is generally taken to be 53.34 and that of k as 1.3947. Hence, $\frac{k-1}{k} = 0.283$ which is the value used in the A.S.M.E. Test Code for Centrifugal Compressors.

11.4 Enthalpy. The total heat energy contained in a pound of gas, known as its enthalpy, H , is the sum of its internal energy, I , plus the external energy APV due to its pressure and volume:

$$H = I + APV \quad 11.7$$

There is no definite condition at which the enthalpy is zero. This makes no difference since in dealing with processes it is the change in heat energy rather than its absolute value which is important. Thus the heat added or removed during the process is

$$\Delta H = \Delta I + \Delta(APV) = \text{change in internal energy} + \text{external work done} \quad 11.8$$

Joule's experiment showed that the internal energy of a gas depends only upon its temperature. If a gas is subjected to a constant volume process, $\Delta(APV)$, which is the work done, is zero, and

$$\Delta H = \Delta I = Wc_v \Delta T \quad 11.9$$

Hence for any process the change in internal energy is equal to

$$\Delta I = Wc_v \Delta T$$

11.5 Entropy. An intangible but highly important property of a gas is its entropy, S . It cannot be measured by instruments, but like moment of inertia it is quite real, and very useful in thermodynamic calculations. Like heat it has no definite value, but is measured above an arbitrarily chosen datum. The absolute value is of no importance, the change during a given process being the quantity which is of interest.

The change in entropy during a process is

$$dS = \int_a^b \frac{dQ}{T} \quad 11-10$$

where dQ is the amount of heat transferred, $Wc dT$, during the process. It can be shown that it will be the same amount for given temperature limits regardless of the process involved. In the English system, the units of entropy are B.t.u. per ° F., but they are not usually named as they are given merely as a number.

11-6 "Standard" Air and "Free" Air. It is convenient to refer gases at various conditions to some standard for comparison, hence the term "standard" air. Unfortunately this term has been variously defined by different engineering societies. They agree that the pressure is atmospheric at sea level, but the temperature is taken as 60° F., 68° F., or 70° F., with various amounts of humidity. In blower work standard air is generally assumed to be air at 68° F., a pressure of 14.7 lb. per sq. in. abs., and a relative humidity of 36 per cent. However, blowers are usually designed on the basis of a 60° F. inlet temperature and 14.7 lb. per sq. in. inlet pressure, and the performance curves specified for this condition.

Another commonly used term is "free" air which should not be confused with standard air. Free air is air at the pressure and temperature existing in the surrounding atmosphere. It may happen to be the same as standard air but usually will differ in both temperature and pressure.

11-7 Compression of Gases. The design of blowers is usually based upon either an adiabatic or an isothermal compression. The thermodynamic relations occurring during each of these processes will now be reviewed. The subscript a indicates the condition before, and b the condition after the compression. All the terms are in absolute units of feet, pounds, and degrees Fahrenheit.

(a) *Adiabatic Compression.* If no heat is added to or removed from the gas during the compression, the process is called adiabatic. There are two types of adiabatic processes, reversible and irreversible. During a reversible adiabatic process the entropy remains constant. Throughout this book the term adiabatic will refer to this isentropic process, which is in accordance with standard practice.

During the adiabatic process the relationship between the pressure and volume for a given weight of gas is

$$PV^k = C = \text{constant} \quad 11-11$$

where k is the ratio of the specific heats c_p/c_v . Hence,

$$P_b = P_a \left(\frac{V_a}{V_b} \right)^k = \frac{WRT_b}{V_b} \quad 11\cdot12$$

$$V_b = V_a \left(\frac{P_a}{P_b} \right)^{\frac{1}{k}} = \frac{WRT_b}{P_b} \quad 11\cdot13$$

$$T_b = T_a \left(\frac{V_a}{V_b} \right)^{k-1} = T_a \left(\frac{P_b}{P_a} \right)^{\frac{k-1}{k}} = \frac{P_b V_b}{WR} \quad 11\cdot14$$

Since no heat is transferred, the entropy must remain constant, and the process is said to be isentropic.

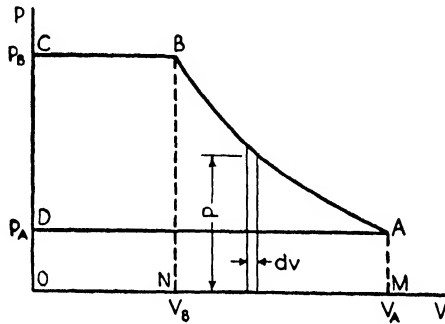


FIG. 11·1. Pressure-volume diagram of compression.

The work done on the gas is $W \int P dV$ (see Fig. 11·1); it equals

$$Wk = \frac{P_b V_b - P_a V_a}{k - 1} \quad 11\cdot15$$

or, from Eq. 11·1,

$$Wk = \frac{WR(T_b - T_a)}{k - 1} \quad 11\cdot16$$

This may be written

$$Wk = \frac{WRT_a}{k - 1} \left(\frac{T_b}{T_a} - 1 \right)$$

and since $\frac{T_b}{T_a} = \left(\frac{P_b}{P_a} \right)^{\frac{k-1}{k}}$,

$$Wk = \frac{WRT_a}{k - 1} \left[\left(\frac{P_b}{P_a} \right)^{\frac{k-1}{k}} - 1 \right] \quad 11\cdot17$$

Equations 11-15, 11-16, and 11-17 represent only the work done during the actual compression, as shown by the area $ABNM$ in Fig. 11-1. After the gas has been compressed, it must be removed from the compressor; this will require an amount of work equal to the area $BCON$ or $P_b V_b$. On account of the suction at the inlet, gas will be forced in which represents work equal to the area $ADOM$ or $P_a V_a$.

The net work of compression then is the area $ABCD$ or

$$Wk = P_b V_b + \frac{P_b V_b - P_a V_a}{k - 1} - P_a V_a$$

$$Wk = (P_b V_b - P_a V_a) \left(1 + \frac{1}{k - 1} \right) = \frac{k}{k - 1} (P_b V_b - P_a V_a) \quad 11-18$$

This also may be written

$$Wk = \frac{k}{k - 1} WRT_a \left[\left(\frac{P_b}{P_a} \right)^{\frac{k-1}{k}} - 1 \right] = \frac{k}{k - 1} P_a V_a \left[\left(\frac{P_b}{P_a} \right)^{\frac{k-1}{k}} - 1 \right] \quad 11-19$$

Combining Eq. 11-19 with Eqs. 11-3 and 11-6,

$$Wk = 778 c_p WT_a \left[\left(\frac{P_b}{P_a} \right)^{\frac{k-1}{k}} - 1 \right] \quad 11-20$$

Equations 11-18, 11-19, and 11-20 represent the amount of work done in compressing one pound of gas adiabatically if W is taken equal to 1. By definition, this work per pound is the same as the head measured in feet of gas. Hence, these equations also give the head developed on an adiabatic basis when W equals one.

If the weight flow of the gas is w lb. per sec. the adiabatic horsepower is given by $\frac{H_{ad} w}{550}$ which may be written in any of the following forms:

$$\text{hp}_{ad} = \frac{k}{k - 1} \frac{wRT_a}{550} \left[\left(\frac{P_b}{P_a} \right)^{\frac{k-1}{k}} - 1 \right] \quad 11-21$$

$$\begin{aligned} \text{hp}_{ad} &= \frac{k}{k - 1} \frac{P_a Q_a}{550} \left[\left(\frac{P_b}{P_a} \right)^{\frac{k-1}{k}} - 1 \right] \\ &= \frac{k}{k - 1} \frac{w P_a \bar{V}_a}{550} \left[\left(\frac{P_b}{P_a} \right)^{\frac{k-1}{k}} - 1 \right] \end{aligned} \quad 11-22$$

$$\text{hp}_{ad} = \frac{1}{550} \frac{k}{k - 1} (P_b Q_b - P_a Q_a) = \frac{w}{550} \frac{k}{k - 1} (P_b \bar{V}_b - P_a \bar{V}_a) \quad 11-23$$

It should be observed from Eq. 11-21 that the head, and, hence, the horsepower required for a given pressure ratio are increased for a higher initial temperature.

If the work required to compress 1 lb. of gas is divided by the initial volume a mean effective pressure P_m is obtained:

$$P_m = \frac{P_a}{k-1} \left[\left(\frac{P_b}{P_a} \right)^{\frac{k-1}{k}} - 1 \right] \quad 11-24$$

This term, though having no physical significance in centrifugal blower work, is simple to use since the head equals $\bar{V}_a P_m$ and the horsepower is $Q_a P_m / 550$ or $\bar{V}_a P_m w / 550$.

(b) *Isothermal Compression.* If the air is cooled during the compression, so that its temperature remains constant, the process is called isothermal. The relation between the pressure and volume for a given weight of gas is

$$PV = C = \text{constant} \quad 11-25$$

Hence

$$P_b = P_a \frac{V_a}{V_b} = \frac{WRT}{V_b} \quad 11-26$$

and

$$V_b = V_a \frac{P_a}{P_b} = \frac{WRT}{P_b} \quad 11-27$$

Obviously,

$$T_a = T_b = \frac{P_b V_b}{WR} = \frac{P_a V_a}{WR} \quad 11-28$$

The work done on the gas is again $W \int P dV$ (Fig. 11-1), and for this case it will be

$$Wk = P_a V_a \log_e^* \frac{V_a}{V_b} = WRT \log_e \frac{V_a}{V_b} \quad 11-29$$

or

$$Wk = P_a V_a \log_e \frac{P_b}{P_a} = WRT \log_e \frac{P_b}{P_a} \quad 11-30$$

As in the previous case, this represents only the actual work of compression. The net work is the area $ABCD$ of Fig. 11-1 and it equals

$$P_b V_b + P_a V_a \log_e \frac{V_a}{V_b} - P_a V_a$$

* $\log_e = 2.3026 \log_{10}$.

but since $P_a V_a = P_b V_b$, the $Wk = P_a V_a \log_e \frac{V_a}{V_b}$ or any of its forms given above in Eqs. 11-29 and 11-30.

The gain in entropy during the process will be

$$\Delta S = WAR \log_e \frac{V_a}{V_b} = WAR \log_e \frac{P_b}{P_a} \quad 11-31$$

The amount of heat to be removed in keeping the temperature constant is

$$\Delta H = WART \log_e \frac{V_a}{V_b} = WART \log_e \frac{P_b}{P_a} \quad 11-32$$

The head is again equal to the work done per pound of fluid, hence it is given by Eqs. 11-29 and 11-30 if $W = 1$. The corresponding equations for isothermal horsepower may be found by multiplying these equations by w , the weight flow in pounds per second, and dividing by 550.

11-8 Notes on the Compression of Gases. Since the specific weight of a liquid remains practically constant, the head is relatively easy to visualize. With gases, however, the specific weight varies considerably during compression and is dependent upon the process (adiabatic or isothermal) considered. This explains why the process must be specified when the head is given.

The actual compression curve rarely follows either the adiabatic or isothermal shape but rather a relationship of the form $PV^n = \text{constant}$. For an uncooled blower handling air the value of n is greater than 1.3947. If two points can be located on the curve, the value of n may be found from

$$n = \frac{\log \frac{P_b}{P_a}}{\log \frac{V_a}{V_b}} \quad 11-33$$

since

$$P_a V_a^n = P_b V_b^n \quad \text{or} \quad \frac{P_b}{P_a} = \left(\frac{V_a}{V_b} \right)^n$$

The corresponding work per pound of gas, or head, is given by

$$\bar{V}_a P_a \frac{n}{n-1} \left[\left(\frac{P_b}{P_a} \right)^{\frac{n-1}{n}} - 1 \right]$$

Pressure-volume curves for isothermal, adiabatic, and uncooled compressions are shown in Fig. 11-2.

The actual temperature rise is greater than the ideal rise because of the losses occurring during the compression. These losses are due to friction and turbulence and appear in the form of heat which raises the temperature of the gas being compressed. The actual horsepower put into the shaft is greater than that required by the ideal compression. Hence, the efficiency is the ratio of the ideal horsepower to the actual horsepower. A blower may have two efficiencies depending upon the process by which it is calculated.

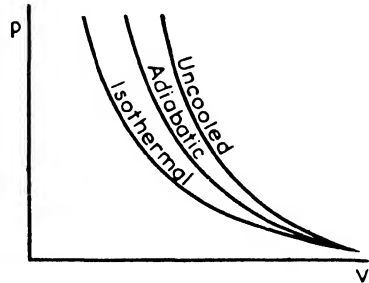


FIG. 11-2. Pressure-volume curves for various types of compression.

Usually blowers are uncooled and are designed on an adiabatic basis. Occasionally the efficiency may be given on an isothermal basis, so the relationship between the two efficiencies may be desired.

$$\frac{\eta_{ad.}}{\eta_{iso.}} = \frac{Wk_{ad.}}{Wk_{act.}} \times \frac{Wk_{act.}}{Wk_{iso.}} = \frac{Wk_{ad.}}{Wk_{iso.}} = f$$

or

$$\frac{\eta_{ad.}}{\eta_{iso.}} = \frac{k}{k-1} \frac{ART_a \left[\left(\frac{P_b}{P_a} \right)^{\frac{k-1}{k}} - 1 \right]}{T_a AR \log_e \frac{P_b}{P_a}} = \frac{\left(\frac{P_b}{P_a} \right)^{\frac{k-1}{k}} - 1}{\frac{k-1}{k} \log_e \frac{P_b}{P_a}} = f \quad 11-34$$

Figure 11-3 shows the relation between f and P_b/P_a for air, where $k = 1.3947$. Since f is also the ratio of the adiabatic work to the isothermal, the figure shows the additional work required for various pressure ratios if the gas is compressed adiabatically rather than isothermally.

The losses occurring in a blower are (a) turbulence, (b) friction in the fluid passages, (c) leakage, (d) disk friction, and (e) packing and bearing friction. The gas horsepower plus the horsepower representing the losses listed above equals the shaft or brake horsepower.

Of these losses all except the last appear as heat in the gas and tend to raise its temperature. A close approximation of the efficiency can, therefore, be found by taking the ratio of the adiabatic temperature rise to the actual rise. This is designated as Y and is the adiabatic efficiency when the mechanical losses in the bearings and packing are

TABLE 11-1. VALUES OF X FOR NORMAL

$$X = \epsilon_p^{0.283} - 1$$

ϵ_p	0	1	2	3	4	5	6	7	8	9	ϵ_p	0	1	2	3	4	5	6	7	8	9			
1.00	.00	000	028	057	085	113	141	169	198	226	254	1.50	.12	159	180	201	222	243	264	286	307	328	349	
1.01		282	310	338	366	394	422	450	478	506	534	1.51		370	391	412	433	454	475	496	517	538	559	
1.02		562	590	618	646	673	701	729	757	785	812	1.52		580	601	622	643	664	685	706	726	747	768	
1.03		840	868	895	923	951	978		006	034	061	089	1.53		789	810	831	852	872	893	914	935	956	977
1.04	.01	116	144	171	199	226	253	281	308	336	363	1.54		997	018	039	060	080	101	122	142	163	184	
1.05		390	418	445	472	500	527	554	581	608	636	1.55	.13	205	225	246	266	287	308	328	349	370	390	
1.06		663	690	717	744	771	798	825	852	879	906	1.56		411	431	452	472	493	513	534	554	575	595	
1.07		933	960	987	014	041	068	095	122	148	175	1.57		616	636	657	677	698	718	739	759	780	800	
1.08	.02	202	229	255	282	309	336	362	389	416	442	1.58		820	841	861	881	902	922	942	963	983	003	
1.09		469	495	522	549	575	602	628	655	681	708	1.59	.14	024	044	064	085	105	125	145	165	186	206	
1.10		734	760	787	813	840	866	892	919	945	971	1.60		226	246	267	287	307	327	347	367	387	408	
1.11		997	024	050	076	102	129	155	181	207	233	1.61		428	448	468	488	508	528	548	568	588	608	
1.12	.03	259	285	311	337	363	389	415	441	467	493	1.62		628	648	668	688	708	728	748	768	788	808	
1.13		519	545	571	597	623	649	675	700	726	752	1.63		828	848	868	888	908	928	948	968	988	007	
1.14		778	804	829	855	881	906	932	958	983	009	1.64	.15	027	047	067	087	107	126	146	166	186	206	
1.15	.04	035	060	086	111	137	162	188	213	239	264	1.65		225	245	265	284	304	324	344	363	383	403	
1.16		290	315	341	366	391	417	442	467	493	518	1.66		423	442	462	481	501	521	540	560	580	599	
1.17		543	569	594	619	644	670	695	720	745	770	1.67		619	638	658	678	697	717	736	756	775	795	
1.18		796	821	846	871	896	921	946	971	996	021	1.68		814	834	853	873	892	912	931	951	970	990	
1.19	.05	046	071	096	121	146	171	196	221	245	270	1.69	.16	009	028	048	067	087	106	125	145	164	184	
1.20		295	320	345	370	394	419	444	469	493	518	1.70		203	222	242	261	280	299	319	338	357	377	
1.21		543	567	592	617	641	666	691	715	740	764	1.71		396	415	434	454	473	492	511	531	550	569	
1.22		789	813	838	862	887	911	936	960	985	009	1.72		588	607	626	646	665	684	703	722	741	760	
1.23	.06	034	058	082	107	131	155	180	204	228	253	1.73		780	799	818	837	856	875	894	913	932	951	
1.24		277	301	325	350	374	398	422	446	470	495	1.74		970	989	008	027	046	065	084	103	122	141	
1.25		519	543	567	591	615	639	663	687	711	735	1.75	.17	160	179	198	217	236	255	274	292	311	330	
1.26		759	783	807	831	855	879	903	927	951	974	1.76		349	368	387	406	425	443	462	481	500	519	
1.27		998	022	046	070	094	117	141	165	189	212	1.77		538	556	575	594	613	631	650	669	688	706	
1.28	.07	236	260	283	307	331	354	378	402	425	449	1.78		725	744	762	781	800	818	837	856	874	893	
1.29		472	496	520	543	567	590	614	637	661	684	1.79		912	930	949	968	986	005	023	042	061	079	
1.30		708	731	754	778	801	825	848	871	895	918	1.80	.18	098	116	135	153	172	191	209	228	246	265	
1.31		941	965	988	011	035	058	081	104	128	151	1.81		283	302	320	339	357	376	394	412	431	449	
1.32	.08	174	197	220	243	267	290	313	336	359	382	1.82		468	486	505	523	541	560	578	596	615	633	
1.33		405	428	451	474	497	520	543	566	589	612	1.83		652	670	688	707	725	743	762	780	798	816	
1.34		635	658	681	704	727	750	773	795	818	841	1.84		835	853	871	890	908	926	944	962	981	999	
1.35		864	887	910	932	955	978	001	023	046	069	1.85	.19	017	035	054	072	090	108	126	144	163	181	
1.36	.09	092	114	137	160	182	205	228	250	273	295	1.86		199	217	235	253	271	289	308	326	344	362	
1.37		318	341	363	386	408	431	453	476	498	521	1.87		380	398	416	434	452	470	488	506	524	542	
1.38		543	566	588	611	633	655	678	700	723	745	1.88		560	578	596	614	632	650	668	686	704	722	
1.39		767	790	812	834	857	879	901	923	946	968	1.89		740	758	776	794	811	829	847	865	883	901	
1.40		990	012	035	057	079	101	123	145	168	190	1.90		919	937	954	972	990	008	026	044	061	079	
1.41	.10	212	234	256	278	300	322	344	366	389	411	1.91	.20	097	115	133	150	168	186	204	221	239	257	
1.42		433	455	477	499	521	542	564	586	608	630	1.92		275	292	310	328	345	363	381	399	416	434	
1.43		652	674	696	718	740	761	783	805	827	849	1.93		452	469	487	504	522	540	557	575	593	610	
1.44		871	892	914	936	958	979	001	023	045	066	1.94		628	645	663	681	698	716	733	751	768	786	
1.45	.11	088	110	131	153	175	196	218	239	261	283	1.95		804	821	839	856	874	891	909	926	944	961	
1.46		304	326	347	369	390	412	433	455	476	498	1.96		979	996	013	031	048	066	083	101	118	135	
1.47		520	541	562	584	605	627	648	669	691	712	1.97	.21	153	170	188	205	222	240	257	275	292	309	
1.48		734	755	776	798	819	840	862	883	904	925	1.98		327	344	361	379	396	413	431	448	465	482	
1.49		947	968	989	010	032	053	074	095	116	138	1.99		500	517	534	552	569	586	603	620	638	655	

* Reprinted from "Engineering Computations for Air

AIR AND PERFECT DIATOMIC GASES*

$$X = \frac{0.283}{\epsilon_p} - 1$$

ϵ_p	0	1	2	3	4	5	6	7	8	9	ϵ_p	0	1	2	3	4	5	6	7	8	9		
2.00	.21	672	689	707	724	741	758	775	792	810	827	2.50	.29	604	618	633	647	662	677	691	706	721	735
2.01		844	861	878	895	913	930	947	964	981	998	2.51		750	765	779	794	808	823	838	852	867	881
2.02	.22	015	032	049	066	084	101	118	135	152	169	2.52		896	911	925	940	954	969	984	998	013	027
2.03		186	203	220	237	254	271	288	305	322	339	2.53	.30	042	056	071	085	100	114	129	144	158	173
2.04		356	373	390	407	424	441	458	474	491	508	2.54		187	202	216	231	245	260	274	289	303	318
2.05		525	542	559	576	593	610	627	644	660	677	2.55		332	346	361	375	390	404	419	433	448	462
2.06		694	711	728	745	762	778	795	812	829	846	2.56		476	491	505	520	534	548	563	577	592	606
2.07		863	879	896	913	930	946	963	980	997	013	2.57		620	635	649	663	678	692	707	721	735	750
2.08	.23	030	047	064	080	097	114	130	147	164	181	2.58		764	778	793	807	821	836	850	864	879	893
2.09		197	214	231	247	264	281	297	314	331	347	2.59		907	921	936	950	964	979	993	007	021	036
2.10		364	380	397	414	430	447	463	480	497	513	2.60	.31	050	064	079	093	107	121	136	150	164	178
2.11		530	546	563	579	596	613	629	646	662	679	2.61		193	207	221	235	249	264	278	292	306	320
2.12		695	712	728	745	761	778	794	811	827	844	2.62		335	349	363	377	391	405	420	434	448	462
2.13		860	877	893	909	926	942	959	975	992	008	2.63		476	490	505	519	533	547	561	575	589	603
2.14	.24	024	041	057	074	090	106	123	139	155	172	2.64		618	632	646	660	674	688	702	716	730	744
2.15		188	204	221	237	253	270	286	302	319	335	2.65		759	773	787	801	815	829	843	857	871	885
2.16		351	368	384	400	416	433	449	465	481	498	2.66		899	913	927	941	955	969	983	997	011	025
2.17		514	530	546	563	579	595	611	627	644	660	2.67	.32	039	053	067	081	095	109	123	137	151	165
2.18		676	692	708	724	741	757	773	789	805	821	2.68		179	193	207	221	235	249	262	276	290	304
2.19		838	854	870	886	902	918	934	950	966	983	2.69		318	332	346	360	374	388	402	416	429	443
2.20		999	015	031	047	063	079	095	111	127	143	2.70		457	471	485	499	513	527	540	554	568	582
2.21	.25	159	175	191	207	223	239	255	271	287	303	2.71		596	610	624	637	651	665	679	693	707	720
2.22		319	335	351	367	383	399	415	431	447	463	2.72		734	748	762	776	789	803	817	831	845	858
2.23		479	495	511	526	542	558	574	590	606	622	2.73		872	886	900	913	927	941	955	968	982	996
2.24		638	654	669	685	701	717	733	749	765	780	2.74	.33	010	023	037	051	065	078	092	106	119	133
2.25		796	812	828	844	859	875	891	907	923	938	2.75		147	161	174	188	202	215	229	243	256	270
2.26		954	970	986	001	017	033	049	064	080	096	2.76		284	297	311	325	338	352	366	379	393	407
2.27	.26	112	127	143	159	175	190	206	222	237	253	2.77		420	434	448	461	475	488	502	516	529	543
2.28		269	284	300	316	331	347	363	378	394	409	2.78		556	570	584	597	611	624	638	651	665	679
2.29		425	441	456	472	488	503	519	534	550	566	2.79		692	706	719	733	746	760	773	787	801	814
2.30		581	597	612	628	643	659	675	690	706	721	2.80		828	841	855	868	882	895	909	922	936	949
2.31		737	752	768	783	799	814	830	845	861	876	2.81		963	976	990	003	017	030	044	057	070	084
2.32		892	907	923	938	954	969	984	000	015	031	2.82	.34	097	111	124	138	151	165	178	191	205	218
2.33	.27	046	062	077	092	108	123	139	154	169	185	2.83		232	245	259	272	285	299	312	326	339	352
2.34		200	216	231	246	262	277	292	308	323	338	2.84		366	379	393	406	419	433	446	459	473	486
2.35		354	369	384	400	415	430	446	461	476	492	2.85		500	513	526	540	553	566	580	593	606	620
2.36		507	522	538	553	568	583	599	614	629	644	2.86		633	646	660	673	686	700	713	726	739	753
2.37		660	675	690	705	721	736	751	766	781	797	2.87		766	779	793	806	819	832	846	859	872	886
2.38		812	827	842	857	873	888	903	918	933	948	2.88		899	912	925	939	952	965	978	991	005	018
2.39		964	979	994	009	024	039	054	070	085	100	2.89	.35	031	044	058	071	084	097	110	124	137	150
2.40	.28	115	130	145	160	175	190	205	220	236	251	2.90		163	176	190	203	216	229	242	255	269	282
2.41		266	281	296	311	326	341	356	371	386	401	2.91		295	308	321	334	347	361	374	387	400	413
2.42		416	431	446	461	476	491	506	521	536	551	2.92		426	439	452	466	479	492	505	518	531	544
2.43		566	581	596	611	626	641	656	671	686	701	2.93		557	570	584	597	610	623	636	649	662	675
2.44		716	730	745	760	775	790	805	820	835	850	2.94		688	701	714	727	740	753	767	780	793	806
2.45		865	879	894	909	924	939	954	969	984	998	2.95		819	832	845	858	871	884	897	910	923	936
2.46	.29	013	028	043	058	073	087	102	117	132	147	2.96		949	962	975	988	001	014	027	040	053	066
2.47		162	176	191	206	221	235	250	265	280	295	2.97	.36	079	092	105	118	131	144	157	169	182	195
2.48		309	324	339	353	368	383	398	412	427	442	2.98		208	221	234	247	260	273	286	299	312	324
2.49		457	471	486	501	515	530	545	559	574	589	2.99		337	350	363	376	389	402	415	428	440	453

and Gases" by Moss and Smith, *Trans. A.S.M.E., APM-52-8, 1930.*

TABLE 11-1.

$$X = \epsilon_p^{0.283} - 1$$

ϵ_p	0	1	2	3	4	5	6	7	8	9
3.0	0.3647	0.3659	0.3672	0.3685	0.3698	0.3711	0.3723	0.3736	0.3749	0.3761
3.1	0.3774	0.3786	0.3799	0.3811	0.3824	0.3836	0.3849	0.3861	0.3874	0.3886
3.2	0.3898	0.3911	0.3923	0.3935	0.3947	0.3959	0.3971	0.3984	0.3996	0.4008
3.3	0.4020	0.4032	0.4044	0.4056	0.4068	0.4080	0.4091	0.4103	0.4115	0.4127
3.4	0.4139	0.4150	0.4162	0.4174	0.4186	0.4197	0.4209	0.4220	0.4232	0.4244
3.5	0.4255	0.4267	0.4278	0.4290	0.4301	0.4313	0.4324	0.4335	0.4347	0.4358
3.6	0.4369	0.4380	0.4392	0.4403	0.4414	0.4425	0.4437	0.4448	0.4459	0.4470
3.7	0.4481	0.4492	0.4503	0.4514	0.4525	0.4536	0.4547	0.4558	0.4569	0.4580
3.8	0.4591	0.4602	0.4612	0.4623	0.4634	0.4645	0.4656	0.4666	0.4677	0.4688
3.9	0.4698	0.4709	0.4720	0.4730	0.4741	0.4752	0.4762	0.4773	0.4783	0.4794
4.0	0.4804	0.4815	0.4825	0.4835	0.4846	0.4856	0.4867	0.4877	0.4887	0.4898
4.1	0.4908	0.4918	0.4928	0.4939	0.4949	0.4959	0.4970	0.4980	0.4990	0.5000
4.2	0.5010	0.5020	0.5030	0.5040	0.5050	0.5060	0.5070	0.5080	0.5090	0.5100
4.3	0.5110	0.5120	0.5130	0.5140	0.5150	0.5160	0.5170	0.5179	0.5189	0.5199
4.4	0.5209	0.5219	0.5228	0.5238	0.5248	0.5258	0.5267	0.5277	0.5287	0.5296
4.5	0.5306	0.5316	0.5325	0.5335	0.5344	0.5354	0.5363	0.5373	0.5382	0.5392
4.6	0.5401	0.5411	0.5420	0.5430	0.5439	0.5449	0.5458	0.5467	0.5477	0.5486
4.7	0.5495	0.5505	0.5514	0.5523	0.5533	0.5542	0.5551	0.5560	0.5570	0.5579
4.8	0.5588	0.5597	0.5606	0.5616	0.5625	0.5634	0.5643	0.5652	0.5661	0.5670
4.9	0.5679	0.5688	0.5697	0.5706	0.5715	0.5724	0.5733	0.5742	0.5751	0.5760
5.0	0.5769	0.5778	0.5787	0.5796	0.5805	0.5814	0.5822	0.5831	0.5840	0.5849
5.1	0.5858	0.5867	0.5875	0.5884	0.5893	0.5902	0.5910	0.5919	0.5928	0.5936
5.2	0.5945	0.5954	0.5962	0.5971	0.5980	0.5988	0.5997	0.6006	0.6014	0.6023
5.3	0.6031	0.6040	0.6048	0.6057	0.6065	0.6074	0.6082	0.6091	0.6099	0.6108
5.4	0.6116	0.6125	0.6133	0.6142	0.6150	0.6159	0.6167	0.6175	0.6184	0.6192
5.5	0.6200	0.6209	0.6217	0.6225	0.6234	0.6242	0.6250	0.6258	0.6267	0.6275
5.6	0.6283	0.6291	0.6300	0.6308	0.6316	0.6324	0.6332	0.6340	0.6349	0.6357
5.7	0.6365	0.6373	0.6381	0.6389	0.6397	0.6405	0.6413	0.6421	0.6430	0.6438
5.8	0.6446	0.6454	0.6462	0.6470	0.6478	0.6486	0.6494	0.6502	0.6509	0.6517
5.9	0.6525	0.6533	0.6541	0.6549	0.6557	0.6565	0.6573	0.6581	0.6588	0.6596
6.0	0.6604	0.6612	0.6620	0.6628	0.6635	0.6643	0.6651	0.6659	0.6666	0.6674
6.1	0.6682	0.6690	0.6697	0.6705	0.6713	0.6721	0.6729	0.6736	0.6744	0.6752
6.2	0.6759	0.6767	0.6774	0.6782	0.6789	0.6797	0.6805	0.6812	0.6820	0.6827
6.3	0.6835	0.6843	0.6850	0.6858	0.6865	0.6873	0.6880	0.6888	0.6895	0.6903
6.4	0.6910	0.6918	0.6925	0.6933	0.6940	0.6948	0.6955	0.6963	0.6970	0.6978
6.5	0.6985	0.6992	0.7000	0.7007	0.7014	0.7021	0.7028	0.7036	0.7043	0.7050
6.6	0.7058	0.7065	0.7073	0.7080	0.7087	0.7095	0.7102	0.7110	0.7117	0.7124
6.7	0.7131	0.7138	0.7145	0.7153	0.7160	0.7167	0.7174	0.7181	0.7189	0.7196
6.8	0.7203	0.7210	0.7217	0.7224	0.7232	0.7239	0.7246	0.7253	0.7260	0.7267
6.9	0.7274	0.7281	0.7288	0.7295	0.7302	0.7309	0.7316	0.7323	0.7330	0.7338
7.0	0.7345	0.7352	0.7359	0.7366	0.7373	0.7380	0.7386	0.7393	0.7400	0.7407
7.1	0.7414	0.7421	0.7428	0.7435	0.7442	0.7449	0.7456	0.7463	0.7470	0.7477
7.2	0.7483	0.7490	0.7497	0.7504	0.7511	0.7518	0.7524	0.7531	0.7538	0.7545
7.3	0.7552	0.7559	0.7565	0.7572	0.7579	0.7586	0.7592	0.7599	0.7606	0.7613
7.4	0.7620	0.7626	0.7633	0.7640	0.7646	0.7653	0.7660	0.7666	0.7673	0.7680
7.5	0.7687	0.7693	0.7700	0.7706	0.7713	0.7720	0.7726	0.7733	0.7740	0.7746
7.6	0.7753	0.7760	0.7766	0.7773	0.7779	0.7786	0.7792	0.7799	0.7806	0.7812
7.7	0.7819	0.7825	0.7832	0.7838	0.7845	0.7851	0.7858	0.7864	0.7871	0.7877
7.8	0.7884	0.7890	0.7897	0.7903	0.7910	0.7916	0.7923	0.7929	0.7936	0.7942
7.9	0.7949	0.7955	0.7961	0.7968	0.7974	0.7981	0.7987	0.7993	0.8000	0.8006

Continued

$$X = \epsilon_p^{0.283} - 1$$

ϵ_p	0	1	2	3	4	5	6	7	8	9
8.0	0.8013	0.8019	0.8025	0.8032	0.8038	0.8044	0.8051	0.8057	0.8063	0.8070
8.1	0.8076	0.8082	0.8089	0.8095	0.8101	0.8108	0.8114	0.8120	0.8126	0.8133
8.2	0.8139	0.8145	0.8151	0.8158	0.8164	0.8170	0.8176	0.8183	0.8189	0.8195
8.3	0.8201	0.8207	0.8214	0.8220	0.8226	0.8232	0.8238	0.8245	0.8251	0.8257
8.4	0.8263	0.8269	0.8275	0.8281	0.8288	0.8294	0.8300	0.8306	0.8312	0.8318
8.5	0.8324	0.8330	0.8336	0.8343	0.8349	0.8355	0.8361	0.8367	0.8373	0.8379
8.6	0.8385	0.8391	0.8397	0.8403	0.8409	0.8415	0.8421	0.8427	0.8433	0.8439
8.7	0.8445	0.8451	0.8457	0.8463	0.8469	0.8475	0.8481	0.8487	0.8493	0.8499
8.8	0.8505	0.8511	0.8517	0.8523	0.8529	0.8535	0.8541	0.8547	0.8552	0.8558
8.9	0.8564	0.8570	0.8576	0.8582	0.8588	0.8594	0.8600	0.8605	0.8611	0.8617
9.0	0.8623	0.8629	0.8635	0.8641	0.8646	0.8652	0.8658	0.8664	0.8670	0.8676
9.1	0.8681	0.8687	0.8693	0.8699	0.8705	0.8710	0.8716	0.8722	0.8728	0.8734
9.2	0.8739	0.8745	0.8751	0.8757	0.8762	0.8768	0.8774	0.8779	0.8785	0.8791
9.3	0.8797	0.8802	0.8808	0.8814	0.8819	0.8825	0.8831	0.8837	0.8842	0.8848
9.4	0.8854	0.8859	0.8865	0.8871	0.8876	0.8882	0.8888	0.8893	0.8899	0.8905
9.5	0.8910	0.8916	0.8921	0.8927	0.8933	0.8938	0.8944	0.8949	0.8955	0.8961
9.6	0.8966	0.8972	0.8977	0.8983	0.8989	0.8994	0.9000	0.9005	0.9011	0.9016
9.7	0.9022	0.9028	0.9033	0.9039	0.9044	0.9050	0.9055	0.9061	0.9066	0.9072
9.8	0.9077	0.9083	0.9088	0.9094	0.9099	0.9105	0.9110	0.9116	0.9121	0.9127
9.9	0.9132	0.9138	0.9143	0.9149	0.9154	0.9159	0.9165	0.9170	0.9176	0.9181
10.0	0.9187	0.9192	0.9198	0.9203	0.9208	0.9214	0.9219	0.9225	0.9230	0.9235
10.1	0.9241	0.9246	0.9252	0.9257	0.9262	0.9268	0.9273	0.9278	0.9284	0.9289
10.2	0.9295	0.9300	0.9305	0.9311	0.9316	0.9321	0.9327	0.9332	0.9337	0.9343
10.3	0.9348	0.9353	0.9358	0.9364	0.9369	0.9374	0.9380	0.9385	0.9390	0.9396
10.4	0.9401	0.9406	0.9411	0.9417	0.9422	0.9427	0.9432	0.9438	0.9443	0.9448
10.5	0.9453	0.9459	0.9464	0.9469	0.9474	0.9480	0.9485	0.9490	0.9495	0.9500
10.6	0.9506	0.9511	0.9516	0.9521	0.9526	0.9532	0.9537	0.9542	0.9547	0.9552
10.7	0.9558	0.9563	0.9568	0.9573	0.9578	0.9583	0.9589	0.9594	0.9599	0.9604
10.8	0.9609	0.9614	0.9619	0.9625	0.9630	0.9635	0.9640	0.9645	0.9650	0.9655
10.9	0.9660	0.9665	0.9671	0.9676	0.9681	0.9686	0.9691	0.9696	0.9701	0.9706
11.0	0.9711	0.9716	0.9721	0.9726	0.9732	0.9737	0.9742	0.9747	0.9752	0.9757
11.1	0.9762	0.9767	0.9772	0.9777	0.9782	0.9787	0.9792	0.9797	0.9802	0.9807
11.2	0.9812	0.9817	0.9822	0.9827	0.9832	0.9837	0.9842	0.9847	0.9852	0.9857
11.3	0.9862	0.9867	0.9872	0.9877	0.9882	0.9887	0.9892	0.9897	0.9902	0.9907
11.4	0.9912	0.9916	0.9921	0.9926	0.9931	0.9936	0.9941	0.9946	0.9951	0.9956
11.5	0.9961	0.9966	0.9971	0.9975	0.9980	0.9985	0.9990	0.9995	1.0000	1.0005
11.6	1.0010	1.0015	1.0019	1.0024	1.0029	1.0034	1.0039	1.0044	1.0049	1.0054
11.7	1.0058	1.0063	1.0068	1.0073	1.0078	1.0083	1.0087	1.0092	1.0097	1.0102
11.8	1.0107	1.0112	1.0116	1.0121	1.0126	1.0131	1.0136	1.0140	1.0145	1.0150
11.9	1.0155	1.0160	1.0164	1.0169	1.0174	1.0179	1.0184	1.0188	1.0193	1.0198
12.0	1.0203	1.0207	1.0212	1.0217	1.0222	1.0226	1.0231	1.0236	1.0241	1.0245

neglected.

$$Y = \frac{\Delta T_{\text{ad.}}}{\Delta T_{\text{act.}}} = \frac{T_a \left[\left(\frac{P_b}{P_a} \right)^{\frac{k-1}{k}} - 1 \right]}{\text{actual temperature rise}} \quad 11.35$$

To simplify the calculations, values of $\epsilon_p^{0.283} - 1$, which represents $\left(\frac{P_b}{P_a} \right)^{\frac{k-1}{k}} - 1$ for air, are given in Table 11·1.

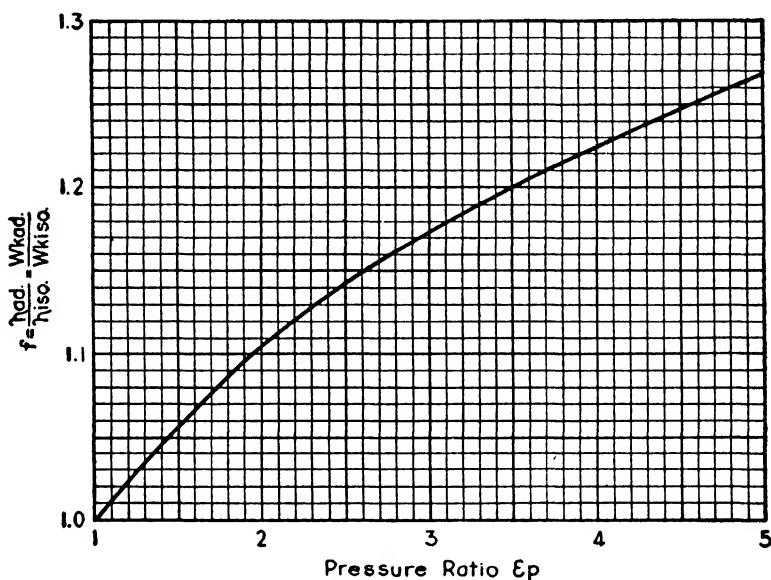


FIG. 11-3. Ratio, f , of $\frac{\eta_{\text{ad.}}}{\eta_{\text{iso.}}}$ or $\frac{Wk_{\text{ad.}}}{Wk_{\text{iso.}}}$ for air with various pressure ratios p_b/p_a or ϵ_p .

11·9 Properties of Gas Mixtures. Frequently it is desired to design a blower to handle a gas mixture whose chemical composition is known. To do this, the thermodynamic properties of the gas must be determined. This involves relations already given in Section 11·3:

$$R = 778(c_p - c_v) = \frac{1544}{M} \quad \text{but} \quad k = \frac{c_p}{c_v} \quad 11.4 \text{ and } 11.3$$

Hence

$$\frac{R}{778} = c_p - \frac{c_p}{k} = c_p \left(1 - \frac{1}{k} \right)$$

or

$$\frac{1544}{M} = 778(c_p - c_v) \quad \text{or} \quad \frac{1544}{778M} = \frac{1.985}{M} = c_p - c_v \quad 11-36$$

Two laws are of use in determining the properties. Avogadro's Law states that equal volumes of all gases having the same temperature and pressure contain an equal number of molecules. Dalton's Law states that each constituent of a gas mixture acts as if the other constituents were not present.

From these laws, the following mathematical expressions are apparent:

$$MV = m_1v_1 + m_2v_2 + m_3v_3 + \text{etc.} \quad 11-37$$

$$\frac{G}{M} = \frac{g_1}{m_1} + \frac{g_2}{m_2} + \frac{g_3}{m_3} + \text{etc.} \quad 11-38$$

$$CG = c_1g_1 + c_2g_2 + c_3g_3 + \text{etc.} \quad 11-39$$

where M is the molecular weight of the mixture

$m_1, m_2, \text{etc.}$, are the molecular weights of the constituents

G is the weight of the mixture

$g_1, g_2, \text{etc.}$, are the weights of the constituents

V is the total volume considered

$v_1, v_2, \text{etc.}$, are the volumes of the constituents

C is the specific heat of the mixture

$c_1, c_2, \text{etc.}$, are the specific heats of the constituents.

The specific gravity of air is taken as unity, and its molecular weight is 28.95. Hence the specific gravity of any gas or mixture is $M/28.95$.

The chemical composition is customarily given on a volumetric basis, and may be so considered unless otherwise specified.

The physical properties of the more common gases and average composition of industrial gases are given in Tables 11-2 and 11-3. More complete tables may be found in handbooks.

The properties of mixtures may best be found by a tabular calculation, as illustrated by the two examples below.

(a) Find the properties of flue gas having the following volumetric percentage composition: 15 per cent CO_2 , 4 per cent O_2 , and 81 per cent N_2 .

Gas	v % Vol.	m Mol.Wt.	$v \times m$	$\% G = \frac{v \times m}{M}$	c_p	$\% Gc_p$
CO_2	0.15	44	6.60	0.216	0.203	0.04385
O_2	0.04	32	1.28	0.042	0.217	0.00911
N_2	0.81	28	22.68	0.742	0.244	0.18105
	<u>1.00</u>		<u>$M = 30.56$</u>	<u>1.000</u>		<u>$c_p = 0.23401$</u>

The values of molecular weight m and the specific heat at constant pressure c_p of the constituents are taken from Table 11-2.

$$\text{Molecular weight} = 30.56$$

$$\text{Mixture specific heat at constant pressure } c_p = 0.234$$

$$\text{Specific gravity} = \frac{M}{28.95} = \frac{30.56}{28.95} = 1.056$$

$$R = \frac{1544}{M} = \frac{1544}{30.56} = 50.52$$

$$c_v = c_p - \frac{R}{778} = 0.234 - \frac{50.52}{778} = 0.234 - 0.065 = 0.169$$

$$\frac{k-1}{k} = \frac{R}{778c_p} = \frac{50.52}{778 \times 0.234} = 0.2775$$

TABLE 11-2
PHYSICAL PROPERTIES OF GASES

Substance	Chemical Formula	Molecular Weight	c_p	c_v
Carbon dioxide	CO ₂	44	0.203	0.156
Carbon monoxide	CO	28	0.244	0.174
Ethane	C ₂ H ₆	30	0.397	0.325
Ethylene	C ₂ H ₄	28	0.404	0.340
Hydrogen	H ₂	2	3.410	2.420
Methane	CH ₄	16	0.593	0.450
Nitrogen	N ₂	28	0.244	0.173
Oxygen	O ₂	32	0.217	0.155
Saturated water vapor 212° F.	H ₂ O	18	0.470	0.360

(b) Find the properties of atmospheric air saturated with water vapor at 170° F., and having a total pressure of 14.7 lb. per sq. in. abs.

This mixture consists of nitrogen, oxygen, and water vapor. For a temperature of 170° F. the vapor pressure is 6.0 lb. per sq. in. (from Table 5-1), and from steam tables the specific weight of the vapor is 0.0161 lb. per cu. ft.

The pressure due to the air is $14.7 - 6.0 = 8.7$ lb. per sq. in. of which $0.79 \times 8.7 = 6.87$ lb. per sq. in. is due to the nitrogen and $0.21 \times 8.7 = 1.83$ lb. per sq. in. is due to the oxygen.

$$\begin{aligned} \text{Specific weight of nitrogen} &= \frac{P}{RT} = \frac{MP}{1544T} = \frac{28 \times 6.87 \times 144}{1544(460 + 170)} = \\ &0.0285 \text{ lb. per cu. ft., and specific weight of oxygen} = \frac{32 \times 1.83 \times 144}{1544(460 + 170)} \\ &= 0.0087 \text{ lb. per cu. ft.} \end{aligned}$$

Gas	Spec. Wt.	% G	c_p	c_v	% Gc_p	% Gc_v
H ₂ O	0.0161	0.302	0.470	0.360	0.142	0.109
N ₂	0.0285	0.535	0.244	0.173	0.131	0.093
O ₂	0.0087	0.163	0.217	0.155	0.035	0.025
	<u>0.0533</u>	<u>1.000</u>			<u>$c_p = 0.308$</u>	<u>$c_v = 0.227$</u>

$$k = \frac{c_p}{c_v} = \frac{0.308}{0.227} = 1.357$$

$$R = 778(c_p - c_v) = 778(0.308 - 0.227) = 63$$

$$M = \frac{1544}{R} = \frac{1544}{63} = 24.51$$

$$\text{Specific gravity} = \frac{M}{28.95} = \frac{24.51}{28.95} = 0.847$$

$$\frac{k - 1}{k} = \frac{1.357 - 1.0}{1.357} = 0.263$$

TABLE 11-3

AVERAGE COMPOSITION OF INDUSTRIAL GASES BY VOLUME

	H ₂	C ₂ H ₄	C ₂ H ₆	CH ₄	CO	CO ₂	O ₂	N ₂	Misc. H.C.
Air	—	—	—	—	—	—	0.21	0.79	—
Natural gas	—	—	0.14	0.85	—	—	—	0.01	—
Coal gas	0.49	0.04	0.03	0.29	0.08	0.01	0.03	0.03	—
Coke oven gas	0.56	—	0.005	0.30	0.06	0.015	0.005	0.025	0.03
Coke producer gas	0.13	—	—	—	0.26	0.05	0.01	0.55	—
Anthracite producer gas	0.12	—	—	0.01	0.26	0.03	0.01	0.57	—
Bituminous producer gas	0.14	—	—	0.03	0.20	0.05	0.01	0.57	—
Blast furnace gas	0.03	—	—	0.02	0.25	0.12	—	0.58	—
Carbureted water gas	0.38	—	0.03	0.10	0.30	0.03	—	0.03	0.13
Water gas	0.48	—	—	0.01	0.40	0.05	0.01	0.05	—
Flue gas	—	—	—	—	—	0.15	0.04	0.81	—

11-10 Effect of Altitude on Atmospheric Conditions. As the altitude increases the temperature and pressure of the atmosphere decrease. Figure 11-4 shows these variations, and may be used to secure average values under which a blower will work when operating above sea level.

PROBLEMS

11-1 It requires 55 hp. to compress 1000 c.f.m. of air at 60° F. and 14.7 lb. per sq. in. to a pressure of 10 lb. per sq. in. ga. The temperature of the air leaving the blower is 184° F. (a) What is the flow in cubic feet per minute from the blower

discharge? (b) What is the head of the blower in feet on an adiabatic basis? (c) What is the head of the blower in feet on an isothermal basis? (d) What is the value of n of the compression? (e) What horsepower would be required if the compression were adiabatic? (f) What horsepower would be required if the compression

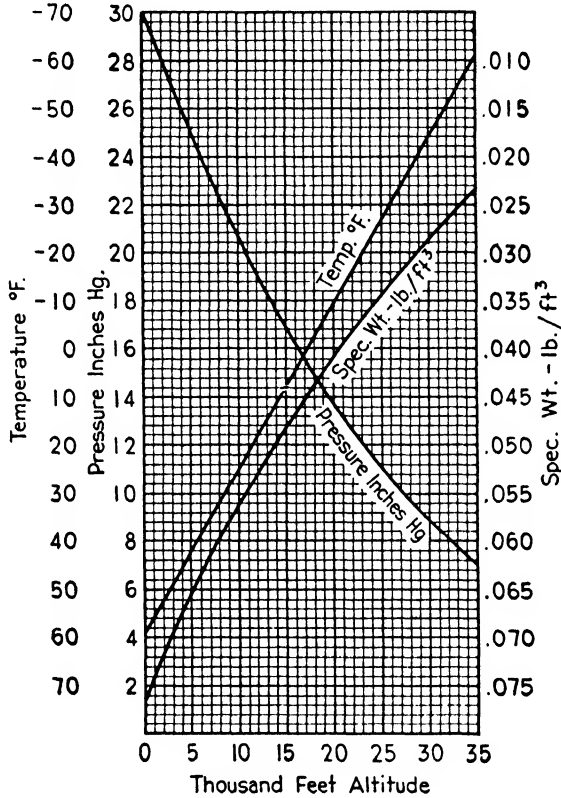


FIG. 11-4. Variation of pressure, temperature, and specific weight with altitude in a "standard" atmosphere.

were isothermal? (g) What is the adiabatic efficiency? (h) What is the isothermal efficiency? (i) Check the ratio of (g) and (h) by Eq. 11-34. (j) What is the adiabatic temperature rise ratio? (k) Why is (j) not the same as (g)?

Ans. (a) 738; (b) 15,500; (c) 14,400; (d) 1.708; (e) 35.8; (f) 33.2; (g) 65.1; (h) 60.4; (i) 1.078; (j) 0.663.

11-2 Determine the thermodynamic properties (c_p , c_v , R , etc.) of blast furnace gas whose chemical composition is given in Table 11-3.

Ans. $R = 53.6$; $c_p = 0.244$; $c_v = 0.175$; $\frac{k-1}{k} = 0.282$.

11-3 A blower draws 3000 c.f.m. of air through a duct 12 in. in diameter with a suction of 3 in. of water. The air is discharged through a duct 10 in. in diameter

against a pressure of 2 in. of water. The air is measured at 70° F. and 30.2 in Hg. Calculate the air horsepower.

Ans. 2.83 hp.

11-4 A booster blower takes 12,000 c.f.m. of natural gas having a volumetric chemical composition of 15 per cent C_2H_6 and 85 per cent CH_4 at a gage pressure of 2 lb. per sq. in. and a temperature of 70° F. and compresses it to 10 lb. per sq. in. ga. What horsepower is required if the adiabatic efficiency of the booster is 60 per cent?

Ans. 592 hp.

CHAPTER 12

CLASSIFICATION AND PERFORMANCE CURVES OF BLOWERS

12.1 Classification. Centrifugal machines may be divided into three general classes which, like the classes of pumps, have no sharp lines of demarcation between them. These classes are known as fans, blowers, and compressors.

(a) *Fans.* Fans are used where low pressures (from a few inches of water to 1 lb. per sq. in.) and comparatively large volumes are required. They run at relatively low speeds, the casing and impeller usually being built up of sheet iron.

(b) *Blowers (or Turbo-Blowers).* A blower, according to the Compressed Air Institute, is a machine to compress air or gas by centrifugal force to a final pressure not exceeding 35 lb. per sq. in. ga. It is not water cooled as the added expense of the cooling system is not justified in view of the relatively slight gain at these pressures.

When used for special applications, blowers are sometimes given other names. In gas service, a blower used to remove gases from a coke oven is known as an *exhauster*. If the pressure at the suction is above atmospheric (as sometimes used in the chemical industry where sufficient head must be developed to circulate the gases through the process) the blower is known as a *booster* or *circulator*.

(c) *Compressors (or Turbo-Compressors).* The Compressed Air Institute defines a centrifugal compressor as a machine to compress air or gas to a final pressure above 35 lb. per sq. in. and also states that such compressors are invariably water cooled. The term is sometimes applied to multistage machines in general regardless of final pressures or cooling. Although compressors have been built for pressures exceeding 100 lb. per sq. in., reciprocating machines are commonly used for pressures above 50 lb. per sq. in.

12.2 Specific Speed. The specific speed term may be applied to blowers or compressors by using Eq. 4.1, i.e., $n_s = \frac{n\sqrt{Q}}{H^{3/4}}$, where Q now is the flow measured in cubic feet per minute and H is the static head calculated on an adiabatic basis. This has been done to some extent, although the term has not been generally used or accepted.

12-3 Head of Blowers and Compressors. It is essential to have a clear understanding of what is meant by the head of a blower before proceeding. For uncooled blowers, the head is based upon an adiabatic compression whereas if cooling is employed the isothermal basis is frequently used. It is generally based only upon the static pressure developed. The velocity head is negligible compared to the pressure head for blowers and compressors. The following expressions for the head, based upon an adiabatic compression, have been given previously but are collected here for convenience and reference:

$$H = \frac{\Delta P}{\gamma_m} = (\Delta P)\bar{V}_m = \frac{P_m}{\gamma_1} = \frac{P_0\bar{V}_0}{k-1} \left[\left(\frac{p_4}{p_0} \right)^{\frac{k-1}{k}} - 1 \right]$$

$$= \frac{RT_0}{k-1} \left[\left(\frac{p_4}{p_0} \right)^{\frac{k-1}{k}} - 1 \right] = K \frac{u_2 V_{u_2}}{g}$$

where the subscript m indicates a mean value. Since the specific volume does not remain constant during a compression as it does for liquids, the head is not proportional to the pressure rise as it is in pumps.

Another expression for the head at the design point, which uses a factor similar to the overall head coefficient Φ for pumps, is frequently employed. This is

$$H = K' \frac{u_2^2}{g} \quad 12.1$$

where K' is known as the overall pressure coefficient and equals K for shut-off conditions (when $V_{u_2} = u_2$). The factor K' may be calculated from tests since

$$K' = \frac{Hg}{u_2^2} = \frac{RT_0 g}{k-1} \frac{1}{u_2^2} \left[\left(\frac{p_4}{p_0} \right)^{\frac{k-1}{k}} - 1 \right]$$

or for air,

$$K' = \frac{6088T_0 \left(\frac{p_4}{p_0} \right)^{0.283} - 1}{u_2^2} \quad 12.2$$

The relationship between Φ and K' may be found by equating the head equations:

$$H = \frac{u_2^2}{\Phi^2 2g} = K' \frac{u_2^2}{g} \quad \text{or} \quad K' = \frac{1}{2\Phi^2}$$

12.4 Performance Curves. The basic principles underlying performance curves were discussed in Chapter 3. It is customary to plot the flow in cubic feet of air or gas per minute at some constant inlet conditions of pressure and temperature. The conditions may be those applying to the particular installation or may be those of standard air (68° F. and 14.7 lb. per sq. in. abs.). In either event, the inlet density is constant and the abscissa of the curve, which is in cubic feet per minute, is a measure of the weight flow. The changes in the performance curves for various operating conditions will be considered in the following sections. By plotting curves of pressure coefficient K' and temperature ratio Y against Q/n , characteristic curves are obtained which are independent of the speed and operating conditions of pressure and temperature.

12.5 Change of Speed — Other Factors Constant. If the temperature and pressure of a gas at the inlet are held constant but the speed of the impeller is varied, the capacity Q and weight flow w will be directly proportional to the speed. (See Section 3.15.)

As the head $H = K \frac{V_{u_2} u_2}{g}$, it must be proportional to the speed squared as for pumps. In terms of pressure ratio, ϵ_p (where $\epsilon_p = p_4/p_0$) the head $H = \frac{P_0 \bar{V}_0}{k-1} \left(\epsilon_p^{\frac{k-1}{k}} - 1 \right)$. Hence $\frac{H_b}{H_a} = \frac{\epsilon_{p_b}^{\frac{k-1}{k}} - 1}{\epsilon_{p_a}^{\frac{k-1}{k}} - 1} = \left(\frac{n_b}{n_a} \right)^2$.

For a given single stage, the efficiency is approximately the same for a given flow per revolution, Q/n , as the velocity diagrams for both the inlet and outlet will be homologous. As the capacity Q is proportional to the r.p.m., Q/n is constant, and the flow corrected for the new speed will have the same efficiency as it had before. Since the brake horsepower is proportional to the product of flow and head, it must be proportional to the cube of the speed, i.e., $b.hp._b = b.hp._a \left(\frac{n_b}{n_a} \right)^3$.

As noted for pumps, the above relationships hold true under test conditions if the speed change is not too great.

To illustrate the above, assume a blower operating at 4000 r.p.m. compressing air from 68° F. and 14.7 lb. per sq. in. abs. to 8.5 lb. per sq. in. ga., handling 16,000 c.f.m. at the design point with an efficiency of 70 per cent. It is desired to find the operating conditions at 3600 r.p.m.

The inlet pressure is $14.7 \times 144 = 2117$ lb. per sq. ft. abs., and the absolute inlet temperature = $460 + 68 = 528^\circ$ F. The inlet

specific volume then is $\frac{RT_0}{P_0} = \frac{53.34 \times 528}{2117} = 13.3$ cu. ft. per lb.

The weight flow at the design point is $\frac{16,000}{60 \times 13.3} = 20$ lb. per sec.

The pressure ratio $\epsilon_p = \frac{14.7 + 8.5}{14.7} = \frac{23.2}{14.7} = 1.578$ at the design point.

The static head at the design point is $H = \frac{P_0 \bar{V}_0}{0.283} (\epsilon_p^{0.283} - 1) =$

$$\frac{RT_0}{0.283} (\epsilon_p^{0.283} - 1) = \frac{2117 \times 13.3}{0.283} \times 0.1378 = \frac{528 \times 53.34}{0.283} \times 0.1378$$

$$= 99,500 \times 0.1378 = 13,700 \text{ ft. of air.}$$

The air horsepower developed is $\frac{wH}{550} = \frac{20 \times 13,700}{550} = 498$. The

brake horsepower required equals $\frac{\text{a.hp.}}{\eta} = \frac{498}{0.70} = 711$ b.hp.

Having determined the above values, the corresponding points for the new speed may be found. The speed ratio is $3600/4000 = 0.9$, so the new flow will be $0.9 \times 16,000 = 14,400$ c.f.m. The new head will be $(0.9)^2 \times 13,700 = 11,100$ ft. The corresponding pressure ratio is found from

$$(\epsilon_p^{0.283} - 1) = \frac{H}{\frac{RT_0}{0.283}} = \frac{11,100}{99,500} = 0.1116 \quad \text{and} \quad \epsilon_p = 1.453$$

The absolute discharge pressure = $1.453 \times 14.7 = 21.4$ lb. per sq. in., and the gage pressure will be $21.4 - 14.7 = 6.7$ lb. per sq. in. The new brake horsepower required will be $(0.9)^3 711 = 518$ b.hp. The efficiency at the new flow will be 70 per cent as it was at the former flow with higher speed.

12.6 Constant Speed — Inlet Conditions Changed. (a) General.

Consider changing the specific weight of the inlet gas from γ_{0a} to γ_{0b} , while keeping the speed of the blower constant. The volume of gas drawn into the blower per minute does not change, but the weight flow is varied: $w_b = w_a \frac{\gamma_{0b}}{\gamma_{0a}}$. As noted in Section 12.4, the capacity Q ,

on which the performance curves are plotted, is based upon a constant specific weight of gas at the inlet and therefore the abscissa is really a measure of weight flow, w . When this weight flow changes, it is

equivalent to changing the referred volume flow, hence the relationship

$$Q_b = Q_a \frac{\gamma_{0b}}{\gamma_{0a}}.$$

If the speed of the impeller is constant, the head will be unchanged, but the discharge pressure will vary as discussed later for each of the special cases.

Since the actual volumetric flow in cubic feet per minute and the speed do not change, Q/n and hence the efficiency remain constant.

The weight flow is proportional to the inlet specific weight and as the head remains constant: $\text{b.hp.}_b = \text{b.hp.}_a \frac{\gamma_{0b}}{\gamma_{0a}}$.

(b) *Throttling (Constant T_0 , Altered p_0)*. It is sometimes necessary or desirable to throttle the suction by placing a regulating valve before the blower. As the gas passes the valve, its pressure and temperature are reduced and the velocity is increased. After passing the valve the kinetic energy due to the velocity is destroyed by eddying and is converted into heat, so the temperature returns approximately to the value it had before the throttling. Thus, the gas enters the impeller with the same temperature it had before the valve, but at a reduced pressure.

The volume flow in cubic feet of gas per minute at a specified specific weight is proportional to the inlet density γ_0 . As the specific weight equals P_0/RT_0 and T_0 is approximately constant, $Q_b = Q_a \frac{\gamma_{0b}}{\gamma_{0a}} = Q_a \frac{p_{0b}}{p_{0a}}$.

Although the capacity in terms of weight flow is changed, the actual volume flow in cubic feet per minute remains constant as the r.p.m. is unchanged, i.e., the blower is taking in the same number of cubic feet per minute, but fewer pounds per minute. Since Q/n is constant, the efficiency will be approximately constant, i.e., the efficiency curve is moved horizontally to the new Q .

The head is constant since the impeller speed is unchanged, and it equals $\frac{RT_0}{k-1} \left(\epsilon_p^{\frac{k-1}{k}} - 1 \right)$. Since R , T_0 , and $\frac{k-1}{k}$ are all constant for

this case, the pressure ratio will also be constant.

The horsepower is proportional to $H\gamma_0$ and, as the head remains constant, $\text{b.hp.}_b = \text{b.hp.}_a \frac{\gamma_{0b}}{\gamma_{0a}}$. Since the temperature is also constant

this may be written $\text{b.hp.}_b = \text{b.hp.}_a \frac{p_{0b}}{p_{0a}}$.

To illustrate this, consider the example of Section 12.5 and assume that the speed and inlet temperature remain the same, but that the inlet pressure at the point considered drops to 10 lb. per sq. in. abs. and that the abscissa is plotted in terms of standard air.

The new Q in terms of standard air then will be

$$Q_b = Q_a \frac{p_{0b}}{p_{0a}} = 16,000 \frac{10}{14.7} = 10,880 \text{ c.f.m.}$$

The new efficiency will be the same as before, or 70 per cent. The pressure ratio, which was 1.578, will remain the same, so the new absolute discharge pressure will become 15.78 lb. per sq. in. and the gage discharge pressure will be $15.78 - 14.7 = 1.08$ lb. per sq. in. The new brake horsepower will be $711 \times 10/14.7 = 484$.

(c) *Constant Inlet Pressure — Altered Inlet Temperature.* The volume flow of gas at the specified specific weight in cubic feet per minute is again proportional to the inlet density γ_0 . Since γ_0 is given by P_0/RT_0 , and P_0 is constant, the flow is expressed as $Q_b = Q_a \frac{\gamma_{0b}}{\gamma_{0a}} = Q_a \frac{T_{0a}}{T_{0b}}$. Hence, the new flow will be inversely proportional to the absolute temperatures.

The head is again constant and equals $\frac{RT_0}{k-1} (\epsilon_p^{\frac{k-1}{k}} - 1)$. Since

$$\frac{k-1}{k} \text{ and } R \text{ are constant, it may be seen that } \frac{H_a}{H_b} = \frac{T_{0a}(\epsilon_{pa}^{\frac{k-1}{k}} - 1)}{T_{0b}(\epsilon_{pb}^{\frac{k-1}{k}} - 1)}$$

or $\epsilon_{pb}^{\frac{k-1}{k}} - 1 = \frac{T_{0a}}{T_{0b}} (\epsilon_{pa}^{\frac{k-1}{k}} - 1)$. From this relationship, the pressure ratios and, hence, discharge pressures for altered conditions may be found and plotted at the corresponding new values of Q .

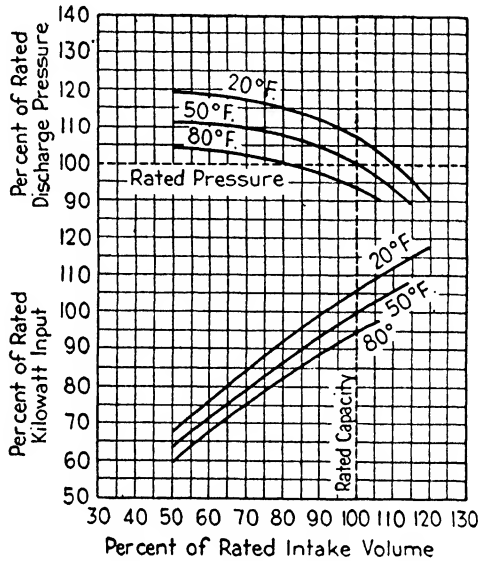
Since the head is constant, the brake horsepower relationship is $b.hp._b = b.hp._a \frac{\gamma_{0b}}{\gamma_{0a}}$. As the inlet pressure is unchanged, this equation

$$\text{may be written } b.hp._b = b.hp._a \frac{T_{0a}}{T_{0b}}$$

As noted previously, the volumetric flow remains unchanged, so Q/n and the efficiency are constant, and points on the efficiency curve are moved horizontally to the new flow.

To illustrate this, consider the example of Section 12.5 and assume that the speed and inlet pressure remain the same, but that the inlet temperature rises to 100° F. (560° F. abs.) and that the abscissa is plotted in terms of standard air.

The new Q in terms of standard air will be: $Q_a \frac{T_{0a}}{T_{0b}} = 16,000 \frac{528}{560} = 15,100$ c.f.m. The new efficiency will be the same as before, or 70 per cent. The original pressure ratio was 1.578 and $\epsilon_p^{0.283} - 1$ was 0.1378. The new $\epsilon_p^{0.283} - 1$ is $\frac{T_{0a}}{T_{0b}} (\epsilon_p^{0.283} - 1) = \frac{528}{560} \times 0.1378 = 0.1298$, and



Courtesy Elliott Co.

FIG. 12-1. Influence of inlet temperature on blower performance for a unit operating at constant speed. (Taken from "Selection of Centrifugal Blowers for Sewage Works," R. T. Regester, *Powerfax*, Summer, 1940.)

the new ϵ_p then equals 1.539. The new absolute discharge pressure is $1.539 \times 14.7 = 22.6$ lb. per sq. in., and the gage discharge pressure is 7.9 lb. per sq. in. The new brake horsepower is $b.hp_b = b.hp_a \frac{T_{0a}}{T_{0b}} = 711 \times \frac{528}{560} = 670$.

Figure 12-1 shows the variation of discharge pressure and kilowatt input plotted on a percentage basis from test data for suction temperatures of 20, 50, and 80° F. for a blower operating at constant speed. It should be remembered that the values apply to a particular installation and are not general, but the graph is of interest because it shows the magnitude of the changes for a typical case.

12·7 Summary. The relationships for correcting the performance curves described in Sections 12·5 and 12·6 may be summarized by the following equations.

Volume flow $Q_b = Q_a \frac{n_b}{n_a}$ 12·3

Weight flow $w_b = w_a \frac{n_b \rho_{0b} T_{0a}}{n_a \rho_{0a} T_{0b}}$ 12·4

Head $H_b = H_a \left(\frac{n_b}{n_a}\right)^2$ 12·5

Pressure ratio $\epsilon_{p_b}^{\frac{k-1}{k}} - 1 = (\epsilon_{p_a}^{\frac{k-1}{k}} - 1) \left(\frac{n_b}{n_a}\right)^2 \frac{T_{0a}}{T_{0b}}$ 12·6

Efficiency $\eta_b = \eta_a$ 12·7

Brake horsepower $b.hp._b = b.hp._a \left(\frac{n_b}{n_a}\right)^3 \frac{\rho_{0b} T_{0a}}{\rho_{0a} T_{0b}}$ 12·8

$$= b.hp._a \frac{\rho_{0b} Q_b \epsilon_{p_b}^{\frac{k-1}{k}} - 1}{\rho_{0a} Q_a \epsilon_{p_a}^{\frac{k-1}{k}} - 1}$$
 12·9

PROBLEMS

12·1 A blower operating at 15,000 r.p.m. compresses air from 68° F. and 14.7 lb. per sq. in. abs. to 10 lb. per sq. in. ga. The design flow is 1350 c.f.m. and at this point the b.hp. is 80. Determine the efficiency of the blower at the design point.

Ans. 60.5 per cent.

12·2 It is desired to increase the discharge pressure of the blower of Problem 12·1 to 12 lb. per sq. in. ga. Find the new speed and corresponding values of Q and b.hp.

Ans. 16,200 r.p.m.; 1458 c.f.m.; 100.5 b.hp.

12·3 If the suction of the blower of Problem 12·1 is throttled to 12 lb. per sq. in. abs., determine the head and discharge pressure in pounds per square inch gage, the flow (referred to 68° F. and 14.7 lb. per sq. in. abs.) and the brake horsepower.

Ans. 15,750 ft., 5.47 lb. per sq. in. ga., 1102 c.f.m., 65.3 b.hp.

12·4 If the temperature of the inlet air of the blower of Problem 12·1 is reduced to 40° F. (winter operation) determine the head and discharge pressure in pounds per square inch gage, the flow (referred to 68° F. and 14.7 lb. per sq. in. abs.) and the brake horsepower.

Ans. 15,750 ft., 10.7 lb. per sq. in. ga., 1425 c.f.m., 84.5 b.hp.

12·5 The outside diameter D_2 of the radial blower impellers of Section 12·5 are reduced 5 per cent. If it is run at 4000 r.p.m. and handles air at standard conditions, what is the probable discharge pressure in pounds per square inch? Assuming that the efficiency remains 70 per cent what will be the probable brake horsepower?

Ans. 7.5 lb. per sq. in. ga.; 610 b.hp.

12-6 A two-stage radial-type airplane supercharger is designed to deliver 175 lb. of air per minute at a pressure of 31.5 in. Hg abs. when operating at an altitude of 20,000 ft. where the temperature is -10° F. and the pressure is 13.7 in. Hg abs. It rotates at 20,000 r.p.m. and is to have an adiabatic efficiency of 70 per cent. It is to be tested at sea level (30 in. Hg and 70° F.) at a speed of 12,000 r.p.m. Assuming that the efficiency at the design point does not change, determine for the design point under test conditions: (a) the cubic feet of air taken in per minute; (b) the discharge pressure in inches of mercury absolute; (c) the horsepower required for driving.

Ans. (a) 2600 c.f.m. at 30 in. Hg and 70° F.; (b) 39.6 in. Hg; (c) 68.6 b.hp.

12-7 A blower is designed to compress 5000 c.f.m. of air from 60° F. and atmospheric pressure to 4 lb. per sq. in. ga. If the speed and inlet temperature remain unchanged what suction pressure can be maintained if the discharge pressure is 3 lb. per sq. in. ga.?

Ans. 13.9 lb. per sq. in. abs.

12-8 A blower is designed to draw in 1000 c.f.m. of carbon dioxide at 90° F. and 3 lb. per sq. in. ga. and compress it to 5 lb. per sq. in. ga. when operating at 4000 r.p.m. It is to be tested with air at 14.7 lb. per sq. in. abs. and 70° F. and driven by a motor running at 3550 r.p.m. Determine the flow and discharge pressure which the machine should deliver at the design point on test to be acceptable.

Ans. 888 c.f.m., 0.85 lb. per sq. in. ga.

12-9 A two-stage radial-type airplane supercharger is designed to deliver 10,000 lb. of air per hour at a pressure of 31.5 in. Hg abs. when operating at an altitude of 15,000 ft. where the temperature is 5° F. and the pressure is 16.9 in. Hg abs. It rotates at 18,000 r.p.m. and is to have an adiabatic overall efficiency of 72 per cent. It is to be tested at sea level (30 in. Hg abs. and 80° F.) at a speed of 14,000 r.p.m. Assuming that the efficiency at the design point does not change, determine for the design point under test conditions: (a) the cubic feet of air taken in per minute; (b) the discharge pressure in inches of mercury absolute; (c) the horsepower required to drive it.

Ans. (a) 2690; (b) 42.1; (c) 85.5.

12-10 A sewage aeration blower running at 3500 r.p.m. is designed to deliver 20,000 c.f.m. of air from 68° F. and 14.7 lb. per sq. in. abs. to a discharge pressure of 7.5 lb. per sq. in. ga. with an adiabatic efficiency of 65 per cent. On a hot summer day the atmospheric temperature rises to 110° F. but the barometric pressure does not change. It is desired to vary the blower speed to maintain the same discharge pressure. Determine: (a) blower speed for the summer operation; (b) corresponding flow in cubic feet per minute of standard air with the new speed; (c) brake horsepower required, assuming that the efficiency remains constant.

Ans. (a) 3640; (b) 19,270; (c) 896.

CHAPTER 13

DESIGN OF RADIAL-TYPE BLOWER STAGE

13·1 Introduction. The general design procedure for blowers is similar to that for pumps, except that it is complicated by the compressibility of the gas. This compressibility effect is considered in Section 13·3.

The design is based upon the capacity and pressure rise to be developed as specified by the purchaser. The type of driver and the speed may also be given.

Many of the formulas used in the design of blowers are the same as for pumps, and many of the discussions presented in Chapter 6 apply equally well to this chapter. These are not repeated here, so the corresponding sections of Chapter 6 should be referred to when this chapter is being read.

13·2 Speed. The desired speed of rotation may be specified by the purchaser and may be based upon a standard motor speed. Since air or gas has a relatively low density the speed is higher than for pumps and may require the use of speed-up gears. These higher speeds may induce dangerous stresses in the impeller which are due to the centrifugal force, hence the stresses should be investigated as outlined in Chapter 18.

13·3 Effect of Compressibility on Design. The weight flow of gas per unit of time passing any point in a blower is constant when the flow is steady. The volume flow will not be constant since the specific weight varies with changes in the temperature and pressure of the gas. The dimensions of the gas passages must be calculated in accordance with these variations in the volume flow.

The specific volume at any point in the blower may be found from the head existing at that point by the relationships developed in Chapters 3 and 11. It should be remembered that the head and the work done per pound of fluid are the same and may be used interchangeably. Throughout this discussion adiabatic (isentropic) processes will be assumed. The condition of the gas as it passes through the blower will be outlined.

Usually the gas or air is initially at rest and is drawn into the eye of the impeller with a velocity V_0 . The impeller, on account of its

rotation, removes the gas or air from the eye. The gas in a receiver or the air in the atmosphere expands to fill this void. In so doing, the pressure drops and the velocity V_0 is attained. During this process the total head remains constant, so, by Bernoulli's theorem (neglecting elevation changes),

$$H = \frac{V_0^2 - V_a^2}{2g} = \frac{P_a - P_0}{\gamma_m} \quad 13.1$$

where the subscript a refers to the condition of the gas before the suction or to the condition of the air in the atmosphere. Usually V_a is zero so that $H = V_0^2/2g$. The velocity head $V_0^2/2g$ is acquired at the expense of pressure head $\frac{P_a - P_0}{\gamma_m}$, and represents a change in the form of the energy but not of the total energy before the impeller.

By assuming a mean or average specific weight during the small pressure drop while the air is being expanded, the pressure of the gas in the impeller eye can be found from Eq. 13.1. A more direct method would be to use Eq. 11.19 in the form

$$\epsilon_{p_{a-0}}^{\frac{k-1}{k}} - 1 = \frac{k-1}{k} \frac{H}{RT_a} \quad 13.2$$

where H is the head or work per pound of gas obtained from Eq. 13.1. The pressure ratio may be found from Eq. 13.2 and, since this is an expansion, $P_0 = P_a/\epsilon_p$. The corresponding absolute temperature at the eye may be found from Eq. 11.14:

$$T_0 = T_a \left(\frac{P_0}{P_a} \right)^{\frac{k-1}{k}} \quad 13.3$$

The specific weight or specific volume of the gas may be found by Eq. 11.2: $P\bar{V} = RT$.

As the velocity at the inlet edge of the vane, V_1 , and in the impeller eye, V_0 , are not greatly different, the specific volume is about the same at both points.

The total virtual head for an infinite number of vanes is given by Eq. 3.3:

$$H_{\text{vir.}\infty} = \frac{u_2^2 - u_1^2}{2g} + \frac{v_1^2 - v_2^2}{2g} + \frac{V_2^2 - V_1^2}{2g} \quad 13.3$$

where $\frac{u_2^2 - u_1^2}{2g}$ is the head due to centrifugal action

$\frac{v_1^2 - v_2^2}{2g}$ is the head due to the change in relative velocity

$\frac{V_2^2 - V_1^2}{2g}$ is the head due to the change in the absolute velocity.

The first two terms represent the pressure head which is developed in the impeller; the last term is the velocity head developed in the impeller and converted into pressure in the volute or diffuser. The pressure head developed in the impeller at any radius R may be expressed by

$$H_{p_{vir.\infty}} = \frac{u_R^2 - u_1^2}{2g} + \frac{v_1^2 - v_R^2}{2g} \tag{13.4}$$

The pressure at points within the impeller can be found by applying Eq. 13.2:

$$\epsilon_{p_{R-0}}^{\frac{k-1}{k}} - 1 = \frac{k-1}{k} \frac{H_R}{RT_0} = \frac{k-1}{k} \frac{u_R^2 - u_1^2 + v_1^2 - v_R^2}{RT_0 2g} \tag{13.5}$$

and the corresponding temperature from Eq. 11.14:

$$T_R = T_0 \epsilon_{p_{R-0}}^{\frac{k-1}{k}} \tag{13.6}$$

To secure the pressure, temperature, and specific weight at the impeller outlet, the subscript 2 may replace the subscript R in Eqs. 13.5 and 13.6.

$$\epsilon_{p_{2-0}}^{\frac{k-1}{k}} - 1 = \frac{k-1}{k} \frac{u_2^2 - u_1^2 + v_1^2 - v_2^2}{RT_0 2g} \tag{13.7}$$

$$T_2 = T_0 \epsilon_{p_{2-0}}^{\frac{k-1}{k}} \tag{13.8}$$

As the term $\frac{u_2^2 - u_1^2 + v_1^2 - v_2^2}{2g}$ represents the pressure head and not the total head developed in the impeller, it is not necessary to subtract the velocity head in determining the specific weight. The velocity head term is separate and equals $\frac{V_2^2 - V_1^2}{2g}$.

It is possible that the entire velocity head $\frac{V_2^2 - V_1^2}{2g}$ generated by the impeller may not be converted into pressure. If the velocity of the

gas leaving the volute or diffuser V_4 is greater than the inlet velocity V_1 , the difference will not appear as pressure. Hence the pressure rise between the impeller outlet and the volute or diffuser outlet is $\frac{V_2^2 - V_4^2}{2g}$.

It may be calculated by the equation

$$\epsilon_{p_{4-2}} - 1 = \frac{k-1}{k} \frac{H}{RT_2} = \frac{k-1}{k} \frac{V_2^2 - V_4^2}{RT_2 2g} \quad 13.9$$

and the temperature by

$$T_4 = T_2 \epsilon_{p_{4-2}}^{\frac{k-1}{k}} \quad 13.10$$

Losses. The above discussion neglects the circulatory flow and the losses due to turbulence, friction, and leakage which occur within the machine. As developed in Chapter 3, the virtual head with an infinite number of vanes, $H_{\text{vir.}\infty}$, as given by Eq. 3-3, is reduced to the virtual head $H_{\text{vir.}}$ when a finite number of vanes is used. This virtual head is further reduced to the actual head H by the friction and turbulence of the gas.

The losses will reduce the pressures and increase the temperatures and hence increase the specific volume as calculated by the above formulas. The magnitudes of these losses are difficult to determine but will be a function of the various velocities squared. A list of the losses and the velocities to which they are related follows.

Friction and turbulence in impeller eye	V_0^2
Turbulence at impeller vane inlet	v_1^2
Friction and turbulence in vane passages	v_{1-2}^2
Friction and turbulence between impeller outlet and diffuser inlet	V_{2-3}^2
Friction and turbulence in diffuser or volute	V_{3-4}^2
Friction and turbulence in discharge passages	V_4^2

As noted above, it is practically impossible to evaluate the magnitude of these losses so that overall coefficients must be used in designing the fluid passages.

Of the virtual pressure head developed by the impeller at the design point and given by the first two terms of Eq. 3-3, about 80 to 90 per cent will actually appear as pressure. A good portion of the difference will be transformed into heat and raise the temperature of the gas. Hence, the actual developed pressure head at the design point may be assumed to be 80 to 90 per cent of the virtual head with an infinite number of vanes. However, the actual temperature of the gas leaving

the impeller will approximate the adiabatic temperature based upon the entire virtual pressure head for an infinite number of vanes.

Between the impeller and diffuser outlets the losses will be much greater because the turbulence of the gas leaving the impeller and entering the volute or diffuser is very great. Also slowing up a gas, i.e., converting from kinetic energy to pressure energy, is a relatively inefficient process. About 40 to 60 per cent of the velocity head, represented by $\frac{V_2^2 - V_4^2}{2g}$, will appear as pressure, the remainder being lost in turbulence and friction. Again the temperature of the gas leaving the blower or stage will approximate the adiabatic temperature based upon a complete conversion from V_2 to V_4 , i.e., upon the head given by $\frac{V_2^2 - V_4^2}{2g}$.

13.4 Pipe Connections and Velocities. Frequently the blower takes the gas or air from a large tank or the atmosphere, so no suction line is required. The standard pipe sizes listed in Section 6-3 also apply to blower flanges and pipes handling gases. The velocity in the pipes for the design condition is usually between 60 and 100 ft. per sec., whereas the velocity at the flanges generally lies in the range from 100 to 200 ft. per sec. Standard pipe sizes which give velocities in this range are used.

13-5 Impeller Inlet Dimensions and Vane Angle. The diameter of the shaft D_s is based upon the strength and critical speed as outlined for pumps (see Section 6-5). Since the operating speeds are higher for blowers the critical speed becomes more important. The unit may operate below the first critical speed or between the first and second criticals. Because the speed of a blower may frequently be variable in order to meet the system demands, it is usually designed to operate below the first critical, and the shaft diameter is proportionally greater for a given brake horsepower than the corresponding pump shaft.

The hub diameter D_H is made from $\frac{3}{4}$ in. to 2 in. greater than the shaft diameter. The inlet velocity through the impeller eye V_0 is made slightly greater than the suction flange velocity. The eye diameter D_0 is given by Eq. 6-1, $D_0 = \sqrt{\frac{4}{\pi} \frac{144Q_0}{V_0} + D_H^2}$, where Q_0 is the volume flow in cubic feet per second as corrected for the velocity head.

The mean diameter of the vane inlet is made slightly greater than the impeller eye diameter, and it may be sloped slightly. The velocity of the gas at the vane inlet is made somewhat greater than V_0 and the

inlet width b_1 is found from the expression $b_1 = \frac{144Q'_0}{\pi D_1 V_1 \epsilon_1}$, where Q'_0 equals Q_0 increased by the leakage flow, and ϵ_1 is an assumed vane thickness factor (0.85 to 0.95). The width may be corrected later after the number of vanes and their thickness have been fixed.

It is usually assumed that the gas enters the vanes in a radial direction ($V_1 = V_{r1}$). The impeller inlet speed $u_1 = \frac{\pi D_1 n}{720}$. The tangent of the inlet angle is $\tan \beta_1 = V_1/u_1$, which may be increased somewhat to care for the contraction of the gas stream as it enters the vane passages.

13-6 Flow Conditions in the Impeller. As in pumps, accurate tests reveal breaks in the characteristic curves. These indicate sudden changes in the flow conditions in the impeller as well as departure from the ideal assumptions upon which the theory is based.

Professor W. J. Kearton investigated these conditions and has presented his findings in a very interesting paper.* He measured the magnitude of the absolute outlet velocity V'_2 with a pitot tube, and its direction α'_2 with a swinging vane. He found that the breaks were accompanied by abrupt changes in the angle α'_2 and in the velocity distribution of the gas leaving the impeller. This sudden change always occurred at the same value of Q/n . Below the critical flow the velocity distribution was fairly symmetrical and resembled the velocity distribution obtained with turbulent flow in a pipe. Above the critical flow the velocity distribution was not symmetrical, but much greater on the side of the impeller away from the inlet.

His measurements indicate that the flow is far from uniform, and that on the trailing face of the vane there is an area of "inactive flow." This area increases as the capacity is reduced. The effect of this inactive flow is equivalent to increasing the vane thickness and reducing the passage area. This becomes apparent in the outlet diagram by an increased radial component V_r^2 , a larger absolute outlet angle α'_2 , and a smaller absolute outlet velocity V_2 (Fig. 6-3).

Kearton's theory concerning the formation of these "dead pockets" seems logical. When the flow through the impeller is small and the relative velocity v is low, the gas will stay in the impeller for a longer period. This permits the impeller to give it a greater angular acceleration. Owing to this greater acceleration the gas is crowded against the leading face of the vane, and the less dense gas in contact with the

* W. J. Kearton, "Influence of the Number of Impeller Blades on the Pressure Generated in a Centrifugal Compressor and on its General Performance," *Proc. Inst. Mech. Engrs.*, Vol. 124, pp. 481-568.

trailing face of the vane becomes "inactive." In addition, at low flows the relative angle of the entering gas β_1 is less than the vane angle, since the impeller speed u_1 is constant but the gas inlet velocity V_1 is decreased. This causes the gas to crowd against the leading face of the vane.

The gas enters the impeller eye axially and must be turned through a right angle before entering the vane. For large flows the air is crowded against the back shroud as a result of its greater momentum. This results in the poor velocity distribution of the gas leaving the impeller at high capacities.

As noted above the gas changes from one type of flow to the other instantaneously and always at the same value of Q/n for a given blower. It is difficult to predict the point of change or the magnitude of the effects on the performance of the blower and to incorporate them into the impeller design. Hence overall coefficients based upon experience and test results must be used until more complete information is available.

13-7 Impeller Outlet Dimensions and Vane Angle. The outlet diameter may be found by the use of Eq. 12-1 by inserting $\pi D_2 n / 720$ for u_2 . The equation then reduces to

$$D_2 = 1300 \frac{\sqrt{H}}{n \sqrt{K'}} \quad 13-11$$

where H is the adiabatic head of the stage in feet, n is the r.p.m., and K' is the pressure coefficient which has a value between 0.50 and 0.65, depending on the type of impeller.

The vane outlet angle β_2 may be between 45° and 90° although for most blowers it is between 60° and 70° . From a stress standpoint a 90° angle is more satisfactory because the bending stresses are then eliminated. Most supercharger impellers, which have high tip speeds, have the vanes radial at the outlet. It is more difficult for the gas to follow the larger change in vane angle from the inlet to the outlet; moreover, a higher absolute outlet velocity V_2 will result. This latter fact places a greater load on the diffuser or volute where the conversion is relatively inefficient. For these reasons impellers with a 90° outlet angle will not have as high an efficiency as may be obtained with backward-curved vanes.

The radial component V_{r_2} of the outlet gas velocity is made less than the absolute inlet velocity V_1 . The losses occurring in the impeller and their approximate magnitude have been discussed in Section 13-3. The specific volume or weight may be found by the method outlined there.

When the volume of gas leaving the impeller and the radial component of the absolute outlet velocity V_{r_2} are known, the outlet width is $b_2 = \frac{144Q_2}{D_2 V_{r_2} \pi \epsilon_2}$. The outlet vane thickness factor ϵ_2 may be assumed to be about 0.95 to 0.99. The width b_2 may be corrected when the number of vanes and their thickness have been fixed.

Outlet Diagram. Sufficient data are now available to draw the virtual outlet diagram. The actual radial component will be greater because of the "inactive" flow mentioned in Section 13-6. The circulatory flow effect reduces the tangential component, V_{u_2} , by an amount equal to W_z . Stodola* states that the value of W_z equals $u_2 \frac{\pi \sin \beta_2}{z}$ for large numbers of vanes, but for fewer vanes (about 12) its value is about 0.6 times the value calculated by this equation. Kearton, in his experiments mentioned in Section 13-6, found good agreement with Stodola's equation. With this correction to the tangential component the actual outlet diagram may be drawn.

13-8 Leakage Losses. Labyrinths are extensively used in blowers and compressors to prevent leakage where the shaft enters the casing, between stages, and past the impeller from the discharge to the suction.

The leakage flow past labyrinths may be calculated by the method outlined by Egli.† This method was developed to measure the leakage of superheated steam through steam turbine labyrinths, but may be

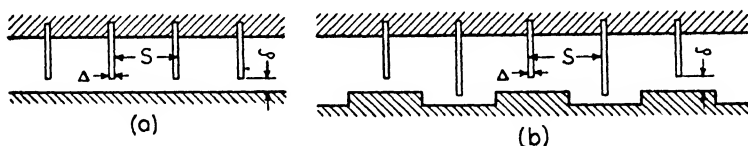


FIG. 13-1. Labyrinth types: (a) straight-through type; (b) staggered type.

applied to air and gases. There are two general types of labyrinths, the straight-through, Fig. 13-1(a), and the staggered, Fig. 13-1(b). The leakage through the labyrinth will depend upon many factors and may be found from the equation

$$w_L = A\alpha\phi\gamma\sqrt{g\frac{P_i}{V_i}} \quad 13-12$$

where w_L = leakage flow through the labyrinth in pounds per second

* Stodola-Loewenstein, *Steam and Gas Turbines*, p. 1259.

† A. Egli, "The Leakage of Steam Through Labyrinth Seals," *A.S.M.E. Trans.*, FSP-57-5, April, 1935.

$$A = \text{leakage area in square feet} = \frac{\pi D \delta}{144}$$

δ = radial clearance in inches

D = clearance diameter in inches

α = contraction factor due to throttling, taken from curve 13·2(a)

ϕ = overall labyrinth pressure ratio factor, taken from curves 13·2(b) or 13·2(c)

γ = carry-over correction factor for straight-through labyrinths, taken from curve 13·2(d) = unity for staggered-type labyrinths

g = acceleration due to gravity = 32.2 ft. per sec.²

P_i = absolute pressure before labyrinth in pounds per square foot

P_f = absolute pressure after labyrinth in pounds per square foot

Δ = strip thickness at the tip in inches

s = pitch of strips of straight-through labyrinth in inches

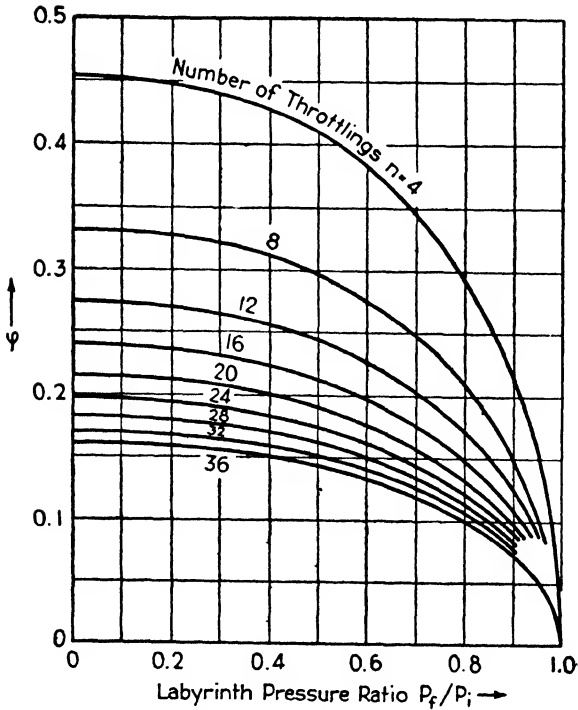
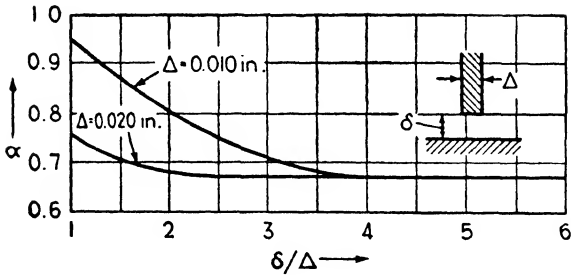
\bar{V}_i = specific volume before labyrinth in cubic feet per pound

When the factors α , ϕ , and γ have been taken from the curves of Fig. 13-2 and inserted in Eq. 13-12 with the other terms the leakage flow may be determined.

As the specific weight and viscosity of gases is much lower than those of liquids, the damping effect on the impeller and shaft vibration is less, and the clearances must be made larger. Satisfactory values may be obtained by doubling those given in Section 6-4 for pumps.

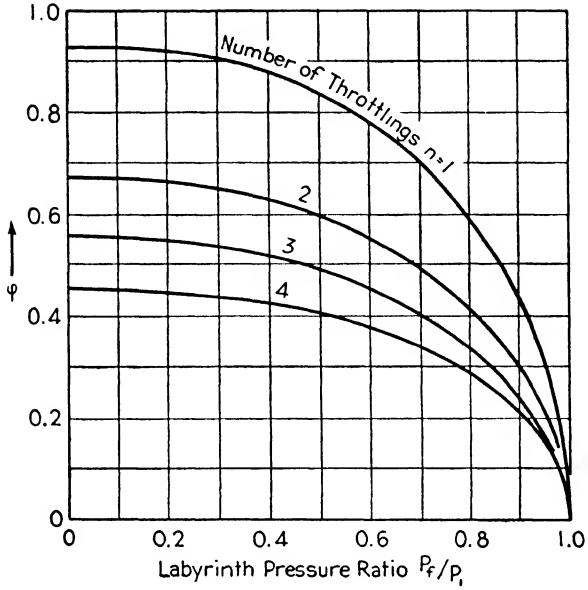
13-9 Design of Vanes. As in pumps, very little is known about the effect of the vane shape on the efficiency and head. Since gases are more elastic than liquids, the effects are probably not so pronounced. After the diameters and vane angles at the inlet and outlet have been determined, the vane surfaces are generally made with a single arc or perhaps two arcs connected with a straight line. The method of manufacture is discussed in Section 14-6.

The usual number of vanes used varies between 15 and 30. A greater number will reduce the circulatory flow effect but will increase the friction. Kearton found that an impeller with 32 vanes had a higher peak efficiency than one with 16 vanes, but that the efficiency dropped off more rapidly at partial loads. Partial vanes have been placed between the main vanes in the outer portion of the impeller,

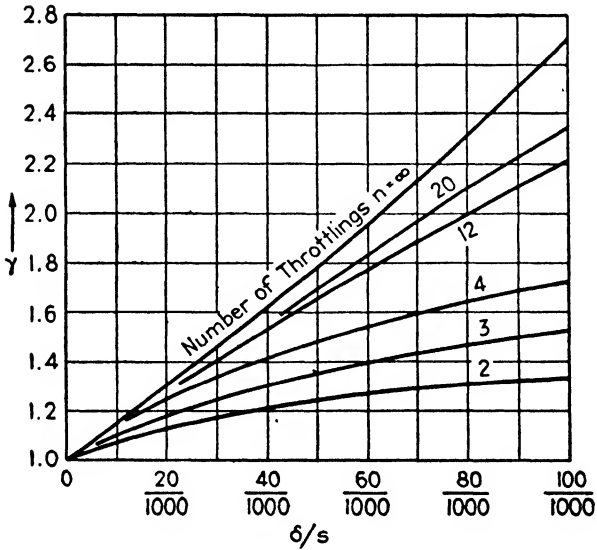


(b)

FIG. 13.2. Factors influencing leakage of air or gas through labyrinths: (a) flow or more throttlings; (c) leakage factor, ϕ , for labyrinths with one to four



(c)



(d)

coefficient, α , or contraction factor; (b) leakage function, ϕ , for labyrinths with four throttlings; (d) carry-over correction factor, γ , for straight-through labyrinths.

but generally they seem to throttle the flow without much gain in efficiency.

13·10 Example of Impeller Design. The general design procedure may be illustrated and clarified by an example in which an impeller is designed for specified conditions. For this purpose the first-stage impeller of a two-stage blower will be considered. This blower is to run at 3600 r.p.m. and handle 16,000 c.f.m. of air at 60° F. and 14.7 lb. per sq. in. abs. with a discharge pressure of 8.5 lb. per sq. in. ga.

General.

$$\text{Overall pressure ratio: } \epsilon_p = \frac{14.7 + 8.5}{14.7} = 1.578; \epsilon_p^{0.283} - 1 = 0.1378.$$

$$\begin{aligned} \text{Total adiabatic head: } H_{\text{ad.}} &= \frac{RT_a}{0.283} (\epsilon_p^{0.283} - 1) \\ &= \frac{53.34 \times 520 \times 0.1378}{0.283} = 13,500 \text{ ft.} \end{aligned}$$

$$\text{Adiabatic head per stage: } H_{\text{ad.}} = \frac{13,500}{2} = 6750 \text{ ft.}$$

$$\text{Specific weight of air: } \gamma_a = \frac{P_a}{RT_a} = \frac{144 \times 14.7}{53.34 \times 520} = 0.0763 \text{ lb. per cu. ft.}$$

$$\text{Weight flow: } w = \frac{Q\gamma_a}{60} = \frac{16,000 \times 0.0763}{60} = 20.35 \text{ lb. per sec.}$$

$$\begin{aligned} \text{Adiabatic air horsepower: a.hp.} &= \frac{wH_{\text{ad.}}}{550} = \frac{20.35 \times 6750}{550} \\ &= 249.7 \text{ hp. per stage.} \end{aligned}$$

$$\text{Total air horsepower: } 2 \times 249.7 = 499.4.$$

Inlet Dimensions and Vane Angle. Assume a velocity through the impeller eye V_0 of 175 ft. per sec.

$$\text{Velocity head: } \frac{V_0^2}{2g} = \frac{175^2}{2 \times 32.2} = 476 \text{ ft.}$$

$$\text{By Eq. 13-2: } \epsilon_p^{0.283} - 1 = \frac{0.283H}{RT_a} = \frac{0.283 \times 476}{53.34 \times 520} = 0.00486.$$

$$\epsilon_p = 1.0173 \text{ and } p_0 = \frac{14.7}{1.0173} = 14.45 \text{ lb. per sq. in. abs.}$$

$$T_0 = \frac{T_a}{\epsilon_p^{0.283}} = \frac{520}{1.00486} = 517.5^\circ \text{ F. abs.}$$

The specific weight of the air in the impeller eye:

$$\gamma_0 = \frac{P_0}{RT_0} = \frac{144 \times 14.45}{53.34 \times 517.5} = 0.0754 \text{ lb. per cu. ft.}$$

Volume flow through impeller eye: $Q_0 = \frac{w}{\gamma_0} = \frac{20.35}{0.0754} = 270$ c.f.s.

The shaft diameter D_s is based upon the critical speed and deflection. It will be amply strong in torsion and bending if it is made 8 in. in diameter. The hub diameter D_H may then be made 9 in.

The impeller eye diameter: $D_0 = \sqrt{\frac{4}{\pi} \frac{144Q_0}{V_0} + D_H^2} =$

$$\sqrt{\frac{4144 \times 270}{\pi \cdot 175} + 9^2} = 19.08 \text{ in.}, \text{ so } 19 \text{ in. may be used.}$$

The vane inlet diameter D_1 may be made slightly greater than the eye diameter, say $19\frac{1}{2}$ in.

$$\text{Inlet tip speed: } u_1 = \frac{\pi D_1 n}{720} = \frac{\pi 19.5 \times 3600}{720} = 306 \text{ ft. per sec.}$$

The inlet velocity is assumed to be radial, i.e., $V_1 = V_{r1}$, and is made slightly greater than V_0 , say 185 ft. per sec.

The tangent of the inlet angle: $\tan \beta_1 = \frac{V_1}{u_1} = \frac{185}{306} = 0.605$. This should be increased by about 3 per cent to care for the contraction of the stream at the inlet: $1.03 \times 0.605 = 0.624$. Then $\beta_1 = 32^\circ 0'$.

Relative inlet velocity: $v_1 = \sqrt{u_1^2 + V_1^2} = \sqrt{306^2 + 185^2} = 358$ ft. per sec.

In calculating the impeller areas, the flow must be increased because of leakage past the impeller. This leakage may be assumed to be about $2\frac{1}{2}$ per cent of the flow, subject to correction after the impeller dimensions have been established.

$$\text{Impeller inlet area: } A_1 = \frac{1.025Q_0 \times 144}{V_1} = \frac{1.025 \times 20.35 \times 144}{185 \times 0.0754} = 215 \text{ sq. in.}$$

Assuming a vane thickness factor ϵ_1 of 0.925, the impeller inlet width: $b_1 = \frac{A_1}{\pi D_1 \epsilon_1} = \frac{215}{\pi 19.5 \times 0.925} = 3.80$ in. This width will be checked later when the number of vanes and their thickness have been fixed.

Impeller Outlet Vane Angle and Dimensions. The outside diameter of the impeller is found from Eq. 13-11 after assuming a value of K' . Since this is a multistage machine, K' will be lower than it would be for a single-stage unit on account of the friction and turbulence occurring in the return passages between the stages. A value of K' equal to

$$0.55 \text{ would be reasonable. } D_2 = 1300 \frac{\sqrt{H}}{n\sqrt{K'}} = \frac{1300\sqrt{6750}}{3600\sqrt{0.55}} = 40 \text{ in.}$$

The impeller tip speed: $u_2 = \frac{\pi D_2 n}{720} = \frac{\pi 40 \times 3600}{720} = 628$ ft. per sec.

The vane outlet angle, β_2 , of 65° , 20 vanes, and a radial outlet velocity V_{r_2} of 100 ft. per sec. will be assumed. With these assumptions the virtual and actual outlet diagrams (Fig. 13-3) may be drawn.

$$V_{u_1} = u_2 - \frac{V_{r_2}}{\tan \beta_2} = 628 - \frac{100}{2.145} = 581.5 \text{ ft. per sec.}$$

$$W_z = u_2 \frac{\pi \sin \beta_2}{z} = \frac{628\pi \times 0.907}{20} = 89.5 \text{ ft. per sec.}$$

$$V'_{u_1} = V_{u_1} - W_z = 581.5 - 89.5 = 492 \text{ ft. per sec.}$$

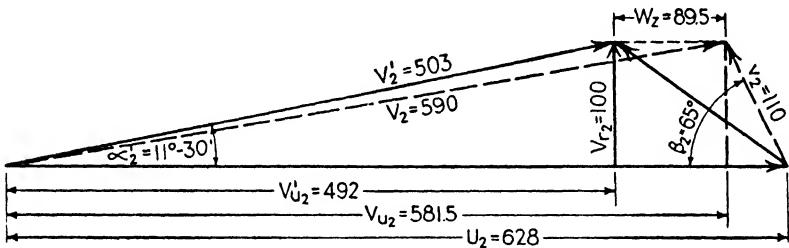


FIG. 13-3. Outlet velocity diagram.

$$V_2 = \sqrt{V_{r_2}^2 + V_{u_1}^2} = \sqrt{100^2 + 581.5^2} = 590 \text{ ft. per sec.}$$

$$V'_2 = \sqrt{V_{r_2}^2 + V_{u_1}'^2} = \sqrt{100^2 + 492^2} = 503 \text{ ft. per sec.}$$

$$v_2 = \sqrt{V_{r_2}^2 + (u_2 - V_{u_1})^2} = \sqrt{100^2 + (628 - 581.5)^2} = 110 \text{ ft. per sec.}$$

$$\tan \alpha'_2 = \frac{V_{r_2}}{V'_{u_1}} = \frac{100}{492} = 0.2033, \alpha'_2 = 11^\circ 30'$$

The virtual pressure head developed in the impeller is:

$$H_{\text{vir. } \infty p} = \frac{1}{2g} (u_2^2 - u_1^2 + v_1^2 - v_2^2) = \frac{1}{2g} (628^2 - 306^2 + 358^2 - 110^2) = 6460 \text{ ft.}$$

It may be assumed that, owing to the circulatory flow, friction, and turbulence in the impeller, 15 per cent of this head is lost. Hence the effective head is $0.85 \times 6460 = 5490$ ft.

$$\text{By Eq. 13-7: } \epsilon_p^{0.283} - 1 = \frac{0.283H}{RT_0} = \frac{0.283 \times 5490}{53.34 \times 517.5} = 0.0563 \text{ and } \epsilon_p = 1.2135.$$

Impeller outlet pressure: $p_2 = 1.2135 \times 14.45 = 17.55$ lb. per sq. in. abs.

The friction and turbulence losses will be transformed into heat which raises the temperature of the air. The outlet temperature may be based upon the adiabatic head in the impeller neglecting losses:

$$\epsilon_p^{0.283} - 1 = \frac{0.283 \times 6460}{53.34 \times 517.5} = 0.0663, \text{ and } \epsilon_p^{0.283} = 1.0663.$$

The outlet temperature: $T_2 = T_0(\epsilon_p)^{0.283} = 517.5 \times 1.0663 = 552^\circ$ F. abs.

The outlet specific weight: $\gamma_2 = \frac{P_2}{RT_2} = \frac{144 \times 17.55}{53.34 \times 552} = 0.0858$ lb. per cu. ft.

Leakage Losses. Sufficient information is now available to estimate the leakage through the labyrinth between the impeller and the casing. This was assumed to be $2\frac{1}{2}$ per cent and the figure should be checked.

Assume the following data for a straight-through labyrinth:

Number of strips = 3. Clearance diameter $D = 21\frac{1}{2}$ in.

Pitch of strips $s = \frac{7}{16}$ in. Radial clearance $\delta = 0.040$ in.

Tip thickness of strips, $\Delta = 0.010$ in.

$$\text{The leakage area: } A = \frac{\pi D \delta}{144} = \frac{\pi 21.5 \times 0.040}{144} = 0.01878 \text{ sq. ft.}$$

Pressure before labyrinth: $P_i = 144p_2 = 144 \times 17.55 = 2525$ lb. per sq. ft.

Specific volume before labyrinth: $\bar{V}_i = \frac{1}{\gamma_2} = \frac{1}{0.0858} = 11.65$ cu. ft. per lb.

$$\frac{\delta}{\Delta} = \frac{0.040}{0.010} = 4; \quad \text{from Fig. 13.2(a) } \alpha = 0.67.$$

$$\frac{p_f}{p_i} = \frac{p_0}{p_2} = \frac{14.45}{17.55} = 0.824; \quad \text{from Fig. 13.2(c) for 3 throttlings } \phi = 0.32.$$

$$\frac{\delta}{s} = \frac{0.040}{\frac{7}{16}} = 0.0915; \quad \text{from Fig. 13.2(d) for 3 throttlings } \gamma = 1.51.$$

$$\text{Leakage flow in pounds per second: } w_L = A \alpha \phi \gamma \sqrt{g \frac{P_i}{\bar{V}_i}} =$$

$$0.01878 \times 0.67 \times 0.32 \times 1.51 \sqrt{\frac{32.2 \times 2525}{11.65}} = 0.508 \text{ lb. per sec.}$$

The percentage leakage: $\frac{0.508}{20.35} \times 100 = 2.5$ per cent, which checks the assumed value.

The flow leaving the impeller: $Q_2 = \frac{1.025w}{\gamma_2} = \frac{1.025 \times 20.35}{0.0858} = 243 \text{ c.f.s.}$

The net impeller radial outlet area required: $A_2 = \frac{144Q_2}{V_{r_2}} = \frac{243 \times 144}{100} = 350 \text{ sq. in.}$

Assuming that the vanes have a constant thickness of $\frac{1}{8}$ in., the outlet vane thickness factor: $\epsilon_2 = \frac{\pi D_2 - \frac{zt}{\sin \beta_2}}{\pi D_2} = \frac{40\pi - \frac{20 \times 0.125}{0.9063}}{40\pi} = 0.979.$

Impeller outlet width: $b_2 = \frac{A_2}{\pi D_2 \epsilon_2} = \frac{350}{\pi 40 \times 0.979} = 2.84 \text{ in.}$

The vane thickness factor at the inlet: $\epsilon_1 = \frac{\pi D_1 - \frac{zt}{\sin \beta_1}}{\pi D_1} = \frac{19.5\pi - \frac{20 \times 0.125}{0.530}}{19.5\pi} = 0.925.$ This checks the value assumed previously;

therefore the inlet width b_1 is correct.

Values of the impeller width at other radii could be calculated in a similar manner by the use of Eqs. 13-5 and 13-6. Since the flow conditions are so uncertain, as outlined in Section 13-6, this is not worth the effort involved. If the inlet and outlet widths are connected by smooth curves, the results will be as satisfactory as those that could be obtained with elaborate calculations.

Summary. The calculated dimensions are summarized below and a sketch of the impeller appears in Fig. 13-4.

SUMMARY OF IMPELLER DESIGN

- Shaft diameter: $D_s = 8 \text{ in.}$
- Hub diameter: $D_H = 9 \text{ in.}$
- Eye diameter: $D_0 = 19 \text{ in.}$
- Eye velocity: $V_0 = 175 \text{ ft. per sec.}$
- Flow through eye: $Q_0 = 270 \text{ c.f.s.}$
- Vane inlet diameter: $D_1 = 19\frac{1}{2} \text{ in.}$
- Velocity at vane inlet: $V_1 = 185 \text{ ft. per sec.}$
- Impeller inlet width: $b_1 = 3.80 \text{ in.}$
- Inlet vane thickness factor: $\epsilon_1 = 0.925.$
- Inlet vane angle: $\beta_1 = 32^\circ 0'.$
- Number of vanes: $g = 20.$
- Impeller inlet speed: $u_1 = 306 \text{ ft. per sec.}$

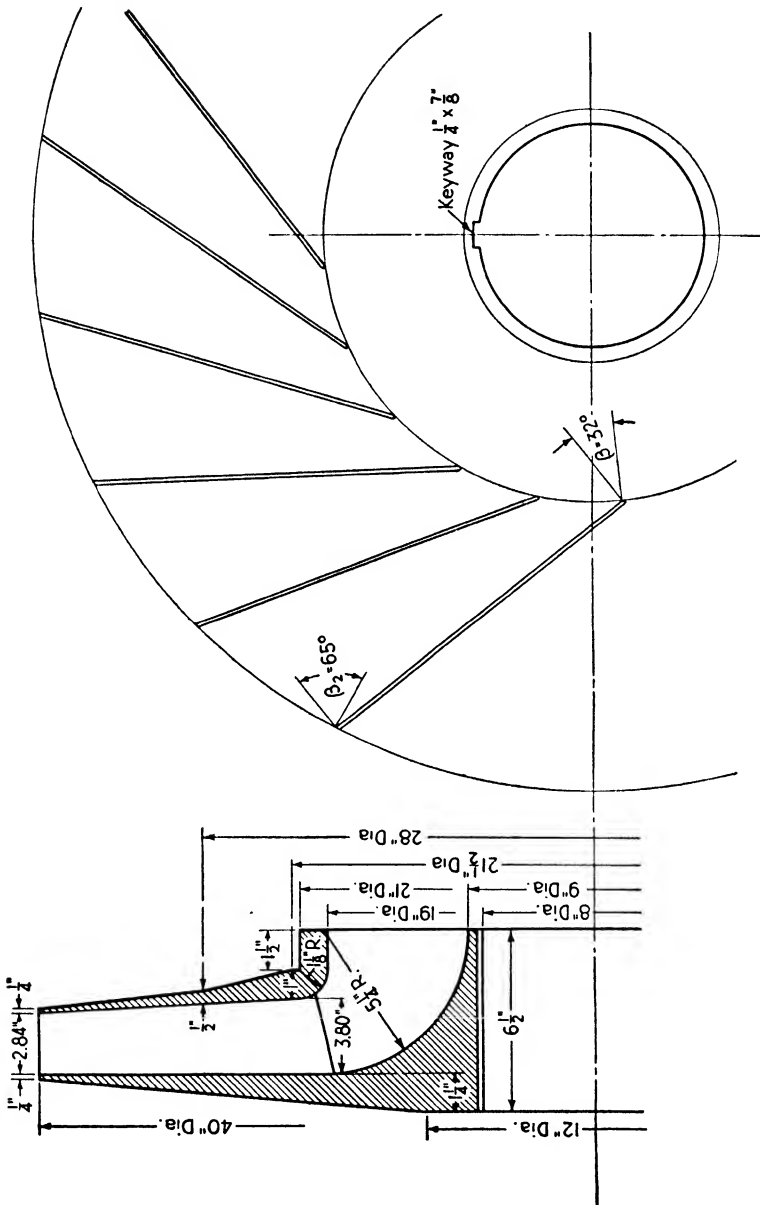


FIG. 13-4. Sketch of impeller designed in Section 13-10.

Outside diameter of impeller: $D_2 = 40$ in.
 Radial component of outlet velocity: $V_{r_2} = 100$ ft. per sec.
 Impeller width at outlet: $b_2 = 2.84$ in.
 Vane outlet thickness correction factor: $\epsilon_2 = 0.979$.
 Impeller tip speed: $u_2 = 628$ ft. per sec.
 Tangential component of outlet velocity: $V'_{u_2} = 492$ ft. per sec.
 Vane outlet angle: $\beta_2 = 65^\circ$.
 Absolute outlet velocity: $V'_2 = 503$ ft. per sec.
 Absolute outlet angle: $\alpha'_2 = 11^\circ 30'$.
 Flow from impeller outlet: $Q_2 = 243$ c.f.s.

13-11 Design of the Volute. Volutes are commonly used for blowers developing low heads, whereas diffusers are usually employed on blowers with high heads.

It was shown in Section 2-12(b) that for a constant specific volume the radial velocity is proportional to the area; that is,

$$bRV_r = C_1 \quad 2-19$$

In Section 2-12(c) it was shown that the tangential component V_u is independent of the area or specific weight and

$$RV_u = C_3 \quad 2-21$$

If the volume flow remains constant and the sidewalls are parallel the path of the flow will be a logarithmic spiral.

As the gas flows through a volute its velocity is decreased with a consequent increase in pressure and temperature, the net result being a decrease in the volume flow. Under these conditions Eq. 2-21 will still hold, but the radial component V_r will decrease more rapidly with increasing radius than indicated by Eq. 2-19. The path of a particle will then lie "inside" that of a logarithmic spiral, as shown by the dotted line of Fig. 2-10. The actual difference is not so great as the theory would indicate since the tangential component is also reduced on account of the friction. Frequently, therefore, the volute is based upon logarithmic flow; in this event the discussion and procedure outlined in Section 6-10 will apply. Since the volume will decrease with the reduced velocities, it will not be necessary to increase the areas as much as for pumps to allow for the frictional effect.

13-12 Example of Volute Design. The impeller designed in Section 13-10 has a rather high outlet velocity. This necessitates the use of a volute having a large outside diameter to reduce the velocity to a reasonable value. However, a volute will be designed for this condition to illustrate the procedure.

The preliminary shape of the volute section will be taken as a trapezoid with the sidewalls at a 30° angle with the radial lines ($\theta = 60^\circ$) and a base width of 3.75 in. at the impeller outlet D_2 . This base width

is found by adding to the outlet width b_2 twice the shroud width and twice the axial clearance. The width of the volute at any point may be scaled from a layout or calculated from the equation $b = b_3 + 2x \tan \frac{\theta}{2} = 3.75 + 2x \tan 30^\circ$, where x is the distance between any radius R and the impeller rim radius R_2 .

The volute is designed by determining the angle ϕ° measured from an assumed radial line by tabular integration of Eq. 6-10: $\phi^\circ = \frac{360R_2 V'_{u_2}}{Q_2} \int_{R_2}^{R\phi} b \frac{dR}{R}$. If R and b are expressed in inches, this equation becomes $\phi^\circ = \frac{360 \times 20 \times 492}{237 \times 144} \sum_{R_2}^{R\phi} b \frac{\Delta R}{R} = 103.8 \sum_{R_2}^{R\phi} b \frac{\Delta R}{R}$. It should be noted that the value of Q_2 used is not increased by the leakage flow because this does not enter the volute. The integration will be performed in tabular form. The explanations given in Section 6-11 apply also to the following table.

R in.	ΔR in.	$R_{ave.}$ in.	b in.	$\frac{b \Delta R}{R_{ave.}}$	$\Delta\phi^\circ$	ϕ°	ΔA sq.in.	$A\phi$ sq. in.	$Q\phi$ c.f.s.	$V_{ave.}$ ft. per sec.
20			3.750			0		0	0	
	2	21	4.904	0.467	48.5		9.81			
22						48.5		9.81	32.0	469
	2	23	7.212	0.627	65.1		14.42			
24						113.6		24.23	74.7	444
	2	25	9.520	0.762	79.0		19.04			
26						192.6		43.27	126.8	422
	2	27	11.828	0.877	91.0		23.66			
28						283.6		66.93	186.7	401
	2	29	14.136	0.975	101.2		28.27			
30						384.8		95.20	253.8	384

It will be noted that the average velocity of the air leaving the volute is about 387 ft. per sec., which is too high. This could be reduced somewhat by increasing the width more rapidly (i.e., by increasing θ), but in any event the volute would not be very satisfactory. The corners of the trapezoidal shape can be rounded off as outlined in Section 6-10, but the area should not be increased as much as was done there, since the decrease in volume flow is equivalent to increasing the area.

The tongue radius is made about 10 per cent greater than the tip

radius R_2 . The tongue angle ϕ_t may be found from Eq. 6-12:

$$\phi_t^\circ = \frac{132 \log_{10} \frac{R_t}{R_2}}{\tan \alpha_2'} \quad 6-12$$

Make the tongue radius $1.1 \times 20 = 22$ in.; $\log_{10} 1.1 = 0.0414$; $\alpha_2' = 11^\circ 30'$; $\tan \alpha_2' = 0.2035$.

$$\phi_t^\circ = \frac{132 \times 0.0414}{0.2035} = 27^\circ$$

The virtual pressure head developed in the volute is

$$\frac{V_2^2 - V_4^2}{2g} = \frac{503^2 - 387^2}{2 \times 32.2} = 1603 \text{ ft.}$$

Assuming an efficiency of 55 per cent in the volute, the actual pressure head is $0.55 \times 1603 = 882$ ft.

$$\epsilon_p^{0.283} - 1 = \frac{k - 1}{k} \frac{H}{RT_2} = \frac{0.283 \times 882}{53.34 \times 552} = 0.00849 \quad \epsilon_p = 1.0303$$

$$p_4 = \epsilon_p \times p_2 = 1.0303 \times 17.55 = 18.1 \text{ lb. per sq. in. abs.}$$

The temperature rise is based upon the full head, or

$$\epsilon_p^{0.283} - 1 = \frac{0.283 \times 1603}{53.34 \times 552} = 0.01542 \quad \epsilon_p^{0.283} = 1.01542$$

$$T_4 = \epsilon_p^{0.283} T_2 = 1.01542 \times 552 = 561^\circ \text{ F. abs.,}$$

and

$$\gamma_4 = \frac{P_4}{RT_4} = \frac{144 \times 18.1}{53.34 \times 561} = 0.0871 \text{ lb. per cu. ft.}$$

$$\text{The volume flow: } Q_4 = \frac{w}{\gamma_4} = \frac{20.35}{0.0871} = 234 \text{ cu. ft. per sec.}$$

The area of the passage to the second stage is $\frac{Q_4}{V_4} = \frac{234}{387} = 0.605$ sq. ft. or 87 sq. in.

If this area is made gradually larger (to avoid turbulence losses) further conversion of velocity to pressure is possible. The ideal volute is sketched in Fig. 13-5. It is necessary to make a more extended tabular integration, using smaller ΔR in laying out this figure. The above table illustrates the method, but the radial differences are too large to be practical.

13-13 Design of the Diffuser.* A diffuser is used for blowers developing high heads and frequently on multistage machines. The design procedure is similar to that for a pump diffuser (Section 6-12).

The diametral clearance between the diffuser vane tips and the impeller is made equal to 10 to 20 per cent of the impeller diameter.

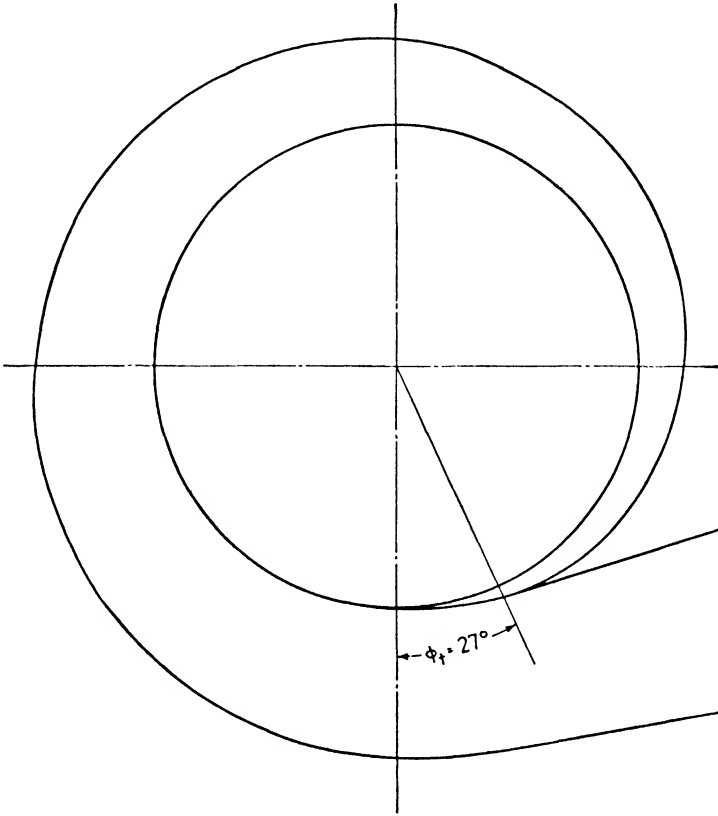


FIG. 13-5. Elevation of volute of Section 13-12.

The efficiency is better with this large clearance and the high-pitched whistle of the unit is eliminated.

It may be assumed that the flow between the impeller tip and the diffuser follows a logarithmic spiral; thus the gas enters the diffuser vanes at the same absolute angle at which it leaves the impeller, α'_2 . The inlet velocity at the diffuser is much lower than the absolute velocity leaving the impeller. In calculating the inlet area of the diffuser

* G. N. Patterson, "Modern Diffuser Design," *Aircraft Engineering*, September, 1938, pp. 267-273.

passages A_3 the velocity V_3 should be taken as 50 to 70 per cent of the outlet velocity V'_2 . This correction includes the change in specific volume, diameter, and passage width between the two points, i.e.,

$$A_3 = \frac{144Q_2}{(0.5 \text{ to } 0.7) V'_2}$$

The velocity of the gas leaving the diffuser is made slightly greater than of that in the discharge flange, i.e., 100 to 200 ft. per sec. By using this value the specific volume of the gas leaving the diffuser can be found according to the method outlined in Section 13-3. From the weight flow, specific weight, and outlet velocity the outlet area A_4 may be found.

The vanes may be made of sheet metal bent to shape or of varying thickness. The principles of vane shape are the same as those developed for pumps (see Section 6-12 and 6-13).

A large number of diffuser vanes will increase the area ratio between the outlet and inlet, and hence the pressure rise, but will also increase the friction and turbulence losses. The number of vanes should have no common multiple with the number of impeller vanes to avoid vibration and resonance. Fifteen to thirty vanes are commonly used.

13-14 Example of Diffuser Design. The principal dimensions of a diffuser to operate with the impeller designed in Section 13-10 will be calculated to illustrate the principles just outlined.

The diametral clearance between the impeller and vane tips is 10 to 20 per cent of the impeller diameter, i.e., 4 to 8 in.; hence a vane tip diameter of 46 in. may be used. The net inlet area A_3 may be found by assuming a correction factor of 60 per cent for the absolute outlet velocity V'_2 :

$$A_3 = \frac{144Q_2}{0.6 V'_2} = \frac{144 \times 237}{0.6 \times 503} = 113 \text{ sq. in.}$$

The inlet width of the diffuser will be made 3.75 in.; this is the same as was used for the volute. If 21 diffuser vanes are used the height of each passage will be

$$h_3 = \frac{A_3}{b_3 z'} = \frac{113}{3.75 \times 21} = 1.435 \text{ in.}$$

The inlet angle of the vanes equals α'_2 or $11^\circ 30'$.

If a velocity leaving the diffuser of 200 ft. per sec. is assumed, the adiabatic head developed between the impeller tip and the diffuser

outlet equals $\frac{V_2'^2 - V_4^2}{2g} = \frac{503^2 - 200^2}{64.4} = 3310$ ft. If an efficiency of 50 per cent is assumed for this portion of the stage, the pressure head = $0.5 \times 3310 = 1655$ ft.

$$\epsilon_p^{0.283} - 1 = \frac{0.283H}{RT_2} = \frac{0.283 \times 1655}{53.34 \times 552} = 0.0159 \quad \epsilon_p = 1.0573$$

$$p_4 = \epsilon_p p_2 = 1.0573 \times 17.55 = 18.55 \text{ lb. per sq. in. abs.}$$

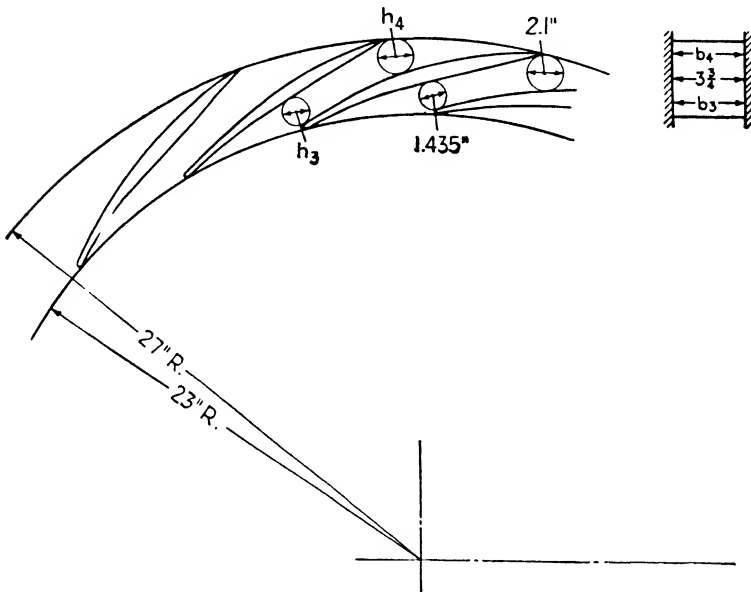


FIG. 13-6. Sketch of diffuser of Section 13-14.

The temperature rise based upon the total head:

$$\epsilon_p^{0.283} - 1 = \frac{0.283 \times 3310}{53.34 \times 552} = 0.0318 \quad \epsilon_p^{0.283} = 1.0318$$

$$T_4 = T_2(\epsilon_p)^{0.283} = 552 \times 1.0318 = 570^\circ \text{ F. abs.}$$

The outlet specific weight: $\gamma_4 = \frac{P_4}{RT_4} = \frac{18.55 \times 144}{53.34 \times 570} = 0.088$ lb. per cu. ft.

$$\text{The volume flow at the outlet: } Q_4 = \frac{w}{\gamma_4} = \frac{20.35}{0.088} = 231 \text{ c.f.s.}$$

$$\text{The outlet area: } A_4 = \frac{Q_4 \times 144}{V_4} = \frac{231 \times 144}{200} = 166 \text{ sq. in.}$$

$$\begin{aligned} \text{The height of each vane passage at the outlet: } h_4 &= \frac{A_4}{b_4 z'} = \frac{166}{3.75 \times 21} \\ &= 2.1 \text{ in.} \end{aligned}$$

The outside diameter of the diffuser is found from a layout which follows the principles outlined in Section 6-13. See Fig. 13-6.

13-15 Disk Friction. The horsepower consumed in disk friction was discussed in Section 3-8. It was shown there that it is proportional to $D^2 u^3 \gamma$ or $D^5 n^3 \gamma$.

Stodola* gives the results of experiments in which boiler plate disks were used; he presents the following equation for the disk friction horsepower:

$$\text{hp}_{DF} = \frac{\beta}{10^6} D_2^2 u_2^3 \gamma \quad 13-13$$

where β is an experimental coefficient equal to 0.0608

D_2 is the outside diameter of the disk in feet

u_2 is the rim speed of the disk in feet per second

γ is the specific weight of the air in pounds per cubic foot.

Kearton,† using the experimental data of Odell‡ who rotated cardboard disks in the open atmosphere, gives the formula in the second form:

$$\text{hp}_{DF} = \frac{\left(\frac{D_2}{10}\right)^5 \left(\frac{n}{1000}\right)^3}{215 \bar{V}} \quad 13-14$$

where D_2 is the outside diameter of the disk in inches

n is the angular speed in revolutions per minute

\bar{V} is the specific volume of the air cubic feet per pound.

Kearton's equation reduces to Eq. 13-13 with a coefficient, β , of 0.0803; hence it gives a horsepower loss about 32 per cent greater than Stodola's equation.

To illustrate the application of these equations, consider the impeller designed in Section 13-10 where $D_2 = 40$ in.; $n = 3600$ r.p.m.; $u_2 = 628$ ft. per sec; $\gamma_2 = 0.0858$ lb. per cu. ft.; and $\bar{V}_2 = 11.65$ cu. ft. per lb.

* Stodola-Loewenstein, *Steam and Gas Turbines*, pp. 194-202.

† W. J. Kearton, *Turbo-Blowers and Compressors*, pp. 91-96.

‡ See *Engineering*, January 1, 1904.

$$\begin{aligned} \text{Eq. 13-13: } hp_{DF} &= \frac{0.0608}{10^6} D_2^2 u_2^3 \gamma_2 = \frac{0.0608}{10^6} \left(\frac{40}{12}\right)^2 628^3 \times 0.0858 \\ &= 14.35 \end{aligned}$$

$$\text{Eq. 13-14: } hp_{DF} = \frac{\left(\frac{D_2}{10}\right)^5 \left(\frac{n}{1000}\right)^3}{215 \bar{V}} = \frac{\left(\frac{40}{10}\right)^5 \left(\frac{3600}{1000}\right)^3}{215 \times 11.65} = 19.1$$

13-16 Multistaging. Multistaging is used when the total head to be developed is too large for a single stage to handle. Several impellers are then mounted on one shaft and operate in series. The head per stage is limited by the impeller tip speed which, if excessive, would induce dangerous centrifugal stresses in the impeller.

For moderate pressure ratios, it is customary to have all the impeller outside diameters of the same size; therefore each will develop approximately the same head. The pressure ratios and pressure rise per stage will not be uniform though, as the temperature is higher in each successive stage.

To illustrate this, consider the complete blower of Section 13-10. The pressure and temperature rise through the two stages will be calculated, first by neglecting losses, and second by assuming a temperature rise ratio of 0.7. The overall adiabatic head was found to be 13,500 ft. and the head per stage 6750 ft. For this example the following subscripts will be used to designate points in the blower: *a* before the blower, *b* between the stages, and *c* at the blower discharge.

Neglecting Losses. First stage:

$$\epsilon_p^{0.283} - 1 = \frac{0.283 \times H}{RT_a} = \frac{0.283 \times 6750}{53.34 \times 520} = 0.0689 \quad \epsilon_p = 1.2655$$

$$p_b = p_a \epsilon_p = 14.70 \times 1.2655 = 18.60 \text{ lb. per sq. in. abs.}$$

$$p_b - p_a = 18.60 - 14.70 = 3.90 \text{ lb. per sq. in.}$$

$$T_b = T_a \epsilon_p^{0.283} = 520 \times 1.0689 = 555.8^\circ \text{ F. abs.}$$

$$T_b - T_a = 555.8 - 520 = 35.8^\circ \text{ F.}$$

Second stage:

$$\epsilon_p^{0.283} - 1 = \frac{0.283H}{RT_b} = \frac{0.283 \times 6750}{53.34 \times 555.8} = 0.0644 \quad \epsilon_p = 1.247$$

$$p_c = p_b \epsilon_p = 18.60 \times 1.247 = 23.20 \text{ lb. per sq. in. abs.}$$

$$p_c - p_b = 23.20 - 18.60 = 4.60 \text{ lb. per sq. in.}$$

$$T_c = T_b \epsilon_p^{0.283} = 555.8 \times 1.0644 = 591.6^\circ \text{ F. abs.}$$

$$T_c - T_b = 591.6 - 555.8 = 35.8^\circ \text{ F.}$$

It may be observed in this example that the temperature rise is the same for both stages. The pressure ratio is less for the second stage on account of the increased temperature at its inlet, but the pressure rise of the second stage is 0.7 lb. per sq. in. greater than that of the first stage, owing to the higher initial pressure.

Including Temperature Rise Ratio. A closer approach to actual conditions will be made by assuming a temperature rise ratio Y of, say, 0.7 for each stage. This will be done for the above example for comparison.

First stage:

$$\epsilon_p^{0.283} - 1 = \frac{0.283 \times 6750}{53.34 \times 520} = 0.0689 \quad \epsilon_p = 1.2655$$

$$p_b = p_a \epsilon_p = 14.70 \times 1.2655 = 18.60 \text{ lb. per sq. in. abs.}$$

$$p_b - p_a = 18.60 - 14.70 = 3.90 \text{ lb. per sq. in.}$$

$$T_b = T_a \epsilon_p^{0.283} = 520 \times 1.0689 = 555.8^\circ \text{ F. abs.}$$

$$(T_b - T_a)_{\text{ad.}} = 555.8 - 520 = 35.8^\circ \text{ F.}$$

$$(T_b - T_a)_{\text{act.}} = \frac{(T_b - T_a)_{\text{ad.}}}{Y} = \frac{35.8}{0.7} = 51.1^\circ \text{ F.}$$

$$T_{b\text{act.}} = 520 + 51.1 = 571.1^\circ \text{ F. abs.}$$

Second stage:

$$\epsilon_p^{0.283} - 1 = \frac{0.283 \times 6750}{53.34 \times 571.1} = 0.0627 \quad \epsilon_p = 1.2397$$

$$p_c = p_b \epsilon_p = 18.60 \times 1.2397 = 23.04 \text{ lb. per sq. in. abs.}$$

$$p_c - p_b = 23.04 - 18.60 = 4.44 \text{ lb. per sq. in.}$$

$$T_c = T_b \epsilon_p^{0.283} = 571.1 \times 1.0627 = 606.9^\circ \text{ F. abs.}$$

$$(T_c - T_b)_{\text{ad.}} = 606.9 - 571.1 = 35.8^\circ \text{ F.}$$

$$(T_c - T_b)_{\text{act.}} = \frac{35.8}{0.7} = 51.1^\circ \text{ F.}$$

$$T_{c\text{act.}} = 571.1 + 51.1 = 622.2^\circ \text{ F. abs.}$$

A comparison of these two examples will show that the losses occurring in the first stage will slightly reduce the pressure rise in the second (in this case from 4.60 to 4.44 lb. per sq. in.).

The value of temperature rise ratio for the impeller and diffuser of

Sections 13-10 and 13-14 may be found from Eq. 11-35:

$$Y = \frac{T_a(\epsilon_p^{0.283} - 1)}{\Delta T_{act.}} = \frac{520 \left[\left(\frac{18.55}{14.7} \right)^{0.283} - 1 \right]}{570 - 520} = \frac{520 \times 0.06807}{50} = 0.708$$

Since the specific volume varies throughout the machine, the eye diameters and impeller widths will not be the same for all the stages, even though the outside diameter is the same.

As in pumps, return guide vanes must be installed between the diffuser of one stage and the impeller eye of the succeeding stage. These eliminate the tangential component of the flow leaving the diffuser and insure radial entry into the next stage. They introduce additional friction and turbulence, and thus decrease the efficiency and overall head factor K' somewhat, but the magnitude of the reduction is difficult to estimate.

PROBLEMS

13-1 Determine the amount of air leakage through a four-strip straight-through labyrinth, given the following data: Clearance diameter 8 in., radial clearance 0.030 in., thickness of strips at tip 0.020 in., pitch of strips $\frac{3}{8}$ in., pressure before labyrinth 3 lb. per sq. in. ga., pressure after labyrinth atmospheric, and temperature before labyrinth 150° F.

Ans. 0.132 lb. per sec.

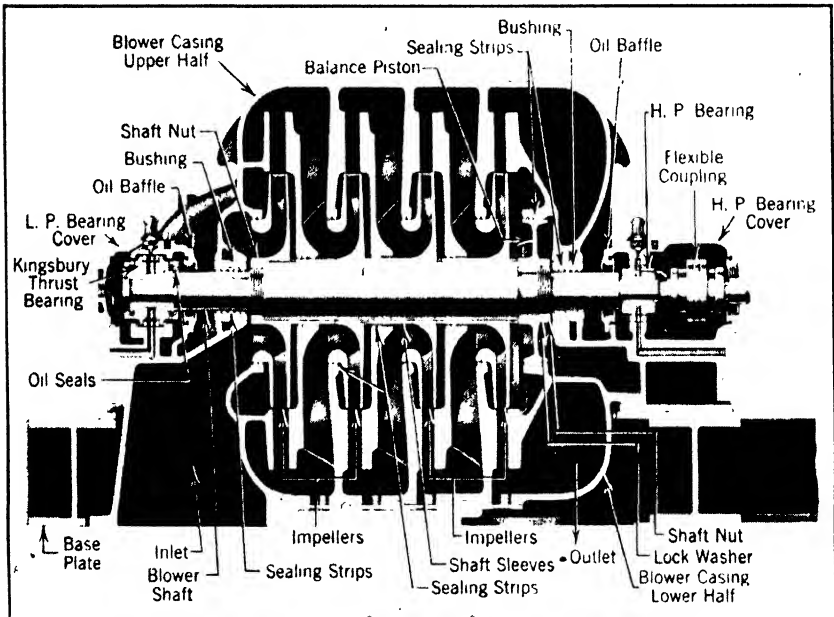
13-2 To obtain a required head an impeller tip speed of 628 f.p.s. is necessary. This may be obtained by the use of a 20-in. impeller rotating at 7200 r.p.m. or a 40-in. impeller rotating at 3600 r.p.m. Assuming that the medium is air with a specific weight of 0.08 lb. per cu. ft. determine the horsepower lost in disk friction for the two possibilities; use Kearton's equation.

Ans. 4.44; 17.76.

CHAPTER 14

CONSTRUCTION DETAILS OF BLOWERS

14.1 Introduction. The usual practice of construction details and materials used for various parts are considered in this chapter. Figures 14-1, 14-2, and 14-3 show sections through the common types of blowers which are referred to throughout the chapter.



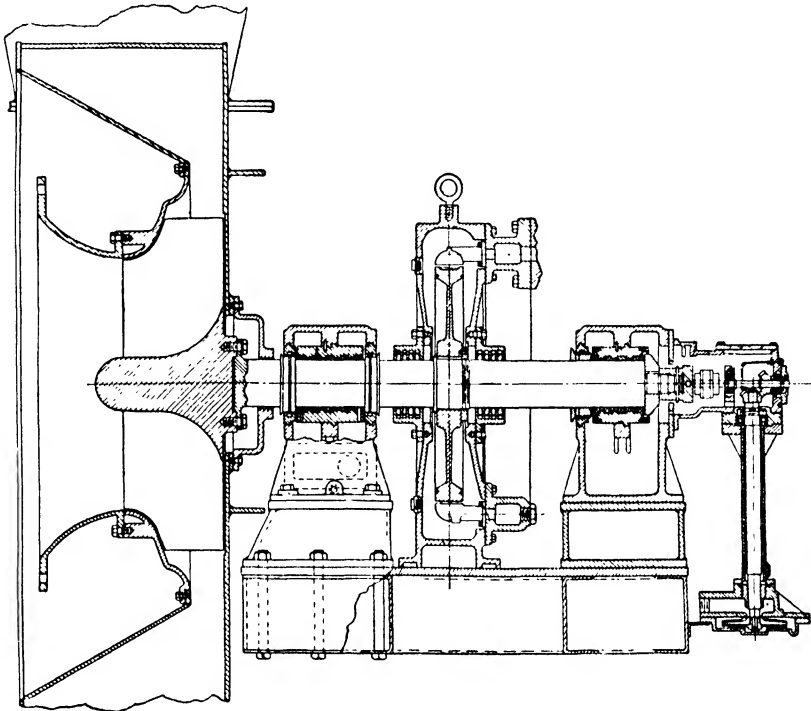
Courtesy Allis-Chalmers Manufacturing Co.

FIG. 14-1. Section through typical multistage blower.

14.2 Shaft and Sleeves. The shaft is usually made of forged carbon steel, machined all over after heat-treating. Sleeves are frequently placed around the shaft to protect it from rubbing and corrosion. They are held in place with nuts threaded counter to the direction of rotation and locked with pins.

The shaft diameter is fixed mainly by the critical speed, as outlined in Section 13.5. As the operating speed is higher for blowers than for pumps and the critical speed is usually kept well above running

speed value, the shaft diameter is made quite large (Figs. 1-1 and 14-1). For ease of assembly, the shaft is usually made stepped with the largest diameter at the center.



Courtesy B. F. Sturtevant Co.

FIG. 14-2. Section through single-stage, end-suction, turbine-driven blower with welded steel casing.

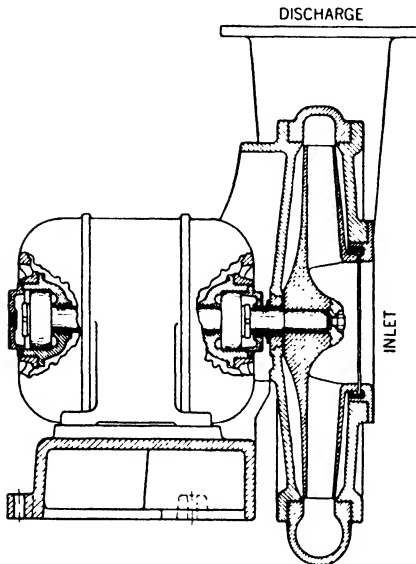
14-3 Leakage. It is desirable to reduce the leakage of the air or gases through the packing boxes where the shaft enters the casing. This may be done by means of a labyrinth, carbon rings, low pressure steam seal, or a water seal.

The labyrinths are usually made of thin strips of stainless steel, lead, or bronze and may be of either the staggered or the straight-through type. The design calculation method is outlined in Section 13-8. If a light rubbing occurs, the shaft will not be injured but the strips will become worn or bent over and their usefulness will be reduced. The labyrinths are illustrated in Figs. 14-1, 14-2, and 14-3.

For higher pressures, carbon rings made of segments held in place by garter springs are frequently used as illustrated in Fig. 1-1. This compressor is also equipped with a steam seal which operates between

Sections A and B of the inner carbon ring. Steam is introduced at Section A and, after leaking past the inner ring, is drained off at B,

as shown in the supplementary view, thus preventing air or gas leakage.



Courtesy Roots-Connersville Blower Corp.

FIG. 14-3. Section through single-stage, end-suction, motor-driven blower.

Packing boxes on exhausters handling gases frequently contain a water seal, as illustrated in Fig. 14-4. A collar is fixed to the rotating shaft and rotates in a groove in the casing. Water introduced into this space is thrown outward by the centrifugal force to form the seal. The seal will be broken when the shaft does not rotate; some device is then required to prevent leakage. This is accomplished by pushing a steel plate against a sleeve on the shaft and the casing to form a tight joint by moving the "stationary seal operating handle" to the closed position.

The plate is constructed so that the rotation of the shaft, when the two are in contact, causes them to separate.

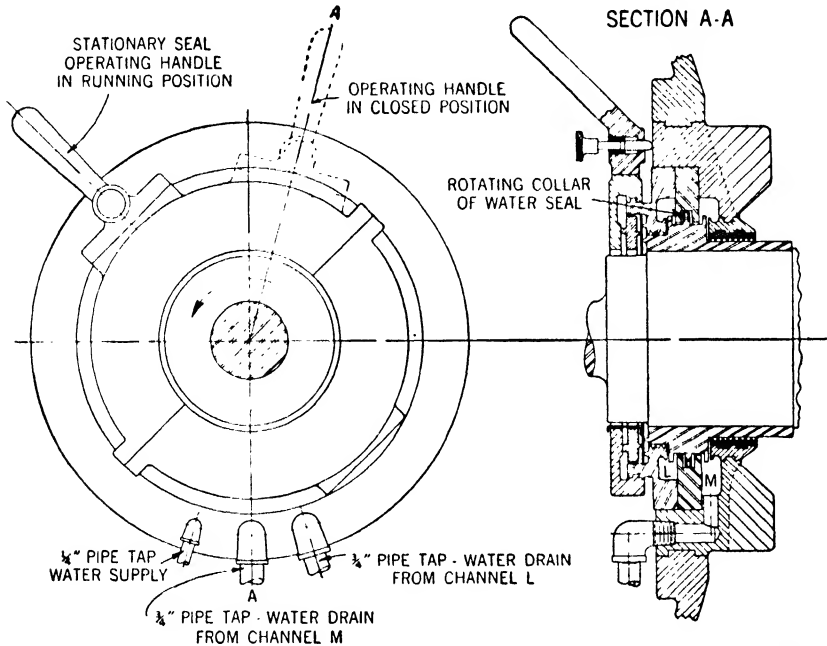
Labyrinths are used to prevent leakage between the stages, at the wearing rings, and on the balance pistons, as shown in Figs. 1-1 and 14-1.

14-4 Bearings. The discussion of bearings in Section 8-3 applies equally well to blower bearings. The journal-type bearings are more commonly used for blowers on account of their higher rubbing speeds. They are usually babbit-lined and may be ring-oiled or may have force feed lubrication with an integral or external pump and an oil cooler.

If the axial thrust is low it may be taken on a collar type thrust bearing as illustrated in Fig. 14-2. If it is larger it may be absorbed by a Kingsbury bearing as shown in Figs. 1-1 and 14-1. Most of the thrust on multistage machines is usually taken by a balance piston or drum which will be described in Section 14-8. In any event, a thrust collar should be used to locate the shaft axially and absorb any sudden changes in the thrust load.

14-5 Casing. The casing may be made of cast iron, horizontally split, or it may be built up of welded steel plates, with reinforcing ribs

as shown in Fig. 14-2. The horizontally split type may have the suction and discharge connections on the bottom half to facilitate inspection and repair. The end-suction type is vertically split. Since there is usually no suction line to disconnect, it is a simple matter to reach the impeller for inspection purposes.



Courtesy Roots-Connersville Blower Corp.

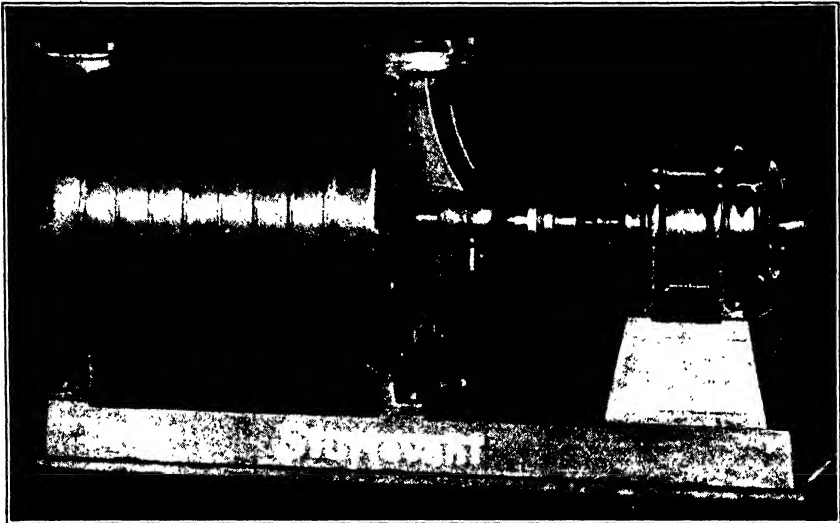
FIG. 14-4. Combined running and stationary seal.

The multistage machines are frequently horizontally split, as shown in Figs. 1-1 and 14-1, with a cast iron casing. Several companies manufacture compressors with barrel-type casings as illustrated in Fig. 14-5. The various parts of the compressor are assembled and slid axially into the casing which is then bolted together.

The casing should be supported as close as possible to the shaft centerline to prevent misalignments due to temperature expansions when the unit is starting up. The discharge nozzle may be placed at any of the angular positions shown in Fig. 8-7.

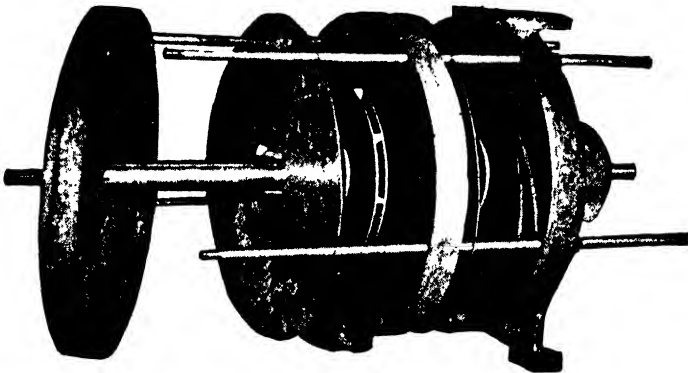
14-6 Impeller and Vanes. The impellers may be single- or double-suction of the open, semi-open, or enclosed type, i.e., they may have no, one, or two shrouds. Impellers having two shrouds are not dependent upon close axial clearances to prevent leakage as they are

equipped with replaceable radial wearing rings. Hence, they will usually maintain high efficiencies for longer periods of time. Since



Courtesy B. F. Sturtevant Co.

FIG. 14-5(a). Eight-stage motor-driven centrifugal blower as used for sewage treatment, etc.

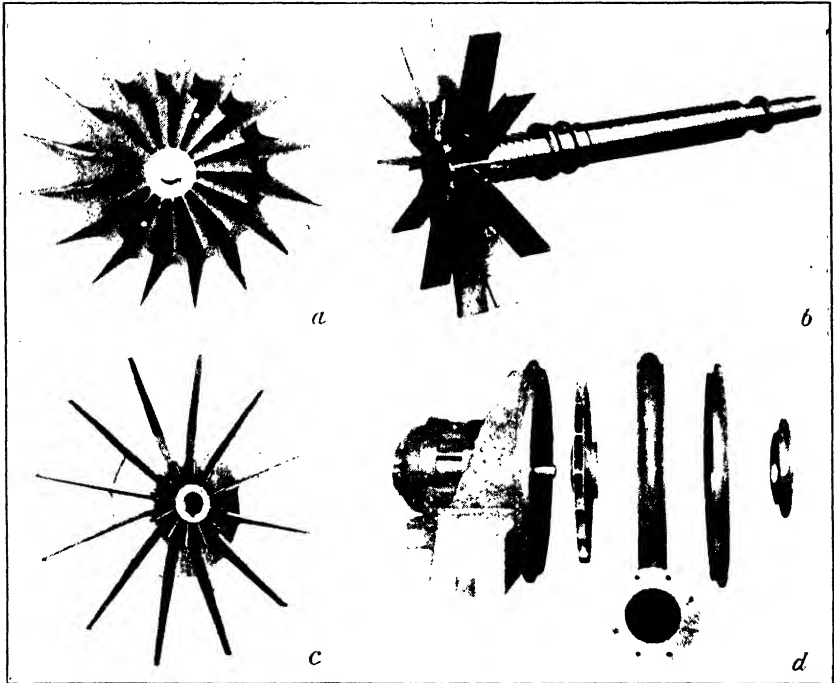


Courtesy B. F. Sturtevant Co.

FIG. 14-5(b). Assembly of blower showing impellers and stationary casings with return guide passages.

the vanes are better supported in an enclosed impeller, vibration failures are not so frequent in this type. For these reasons, the fully enclosed impeller is more commonly used.

The impellers may be made of alloy steel, bronze, or aluminum and, if of the open or semi-open type, may have the vanes either cast integral with the impeller or milled from a solid forging (Fig. 14-6). If they are of the enclosed type, the side plates or shrouds are made of forged alloy steel and have the vanes riveted in place. If the speeds



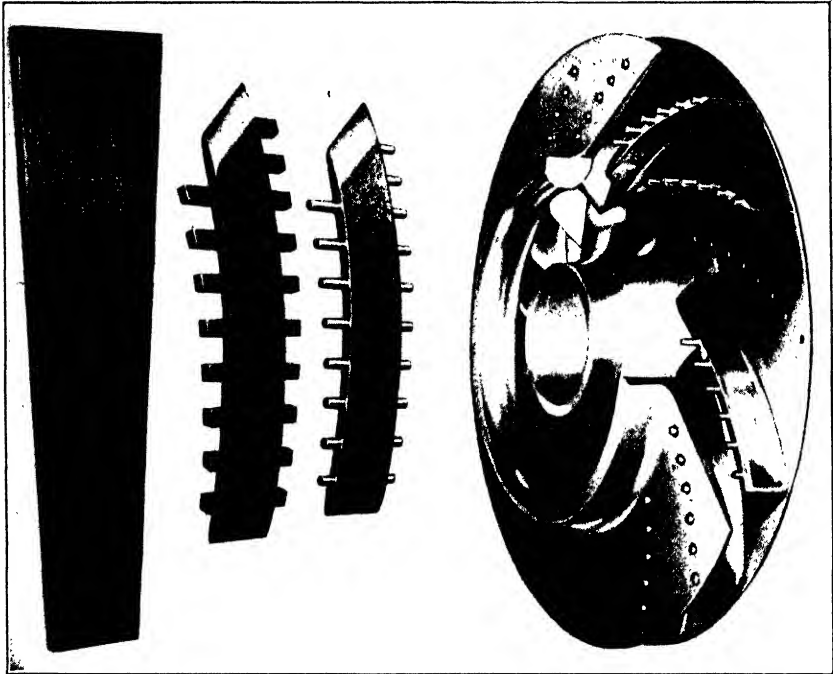
Courtesy Roots-Connersville Blower Corp.

FIG. 14-6. Methods of manufacturing impellers: (a) Cast steel open-type impeller with axial vanes at inlet; (b) impeller and shaft made from one-piece solid forging; (c) stainless steel impeller milled from solid forging; (d) single-stage blower with one-piece cast aluminum impeller.

are low, the complete impeller may be cast in one piece. The vanes, if made separate, may have a variable thickness and may be assembled as shown in Fig. 14-7, or they may be made of sheet metal hot forged to a \sqsubset or \sqsupset section and riveted to the side plates, as shown in Fig. 14-8.

The stresses in the shrouds and hub should be calculated according to the method outlined in Chapter 18. Since the vanes do not contribute to the strength, the centrifugal force due to their mass must be considered as an additional load on the disk. For design purposes it may be assumed that the riveted vane is divided into sections and

that the rivets in any section carry the load of that section. They are calculated on the basis of ultimate shear strength with a safety factor about 5. Owing to the stresses induced when the impeller rotates, the hub will expand. Therefore the fit should be tight enough to prevent the disk from being loose on the shaft at the running speed.



Courtesy Allis-Chalmers Manufacturing Co.

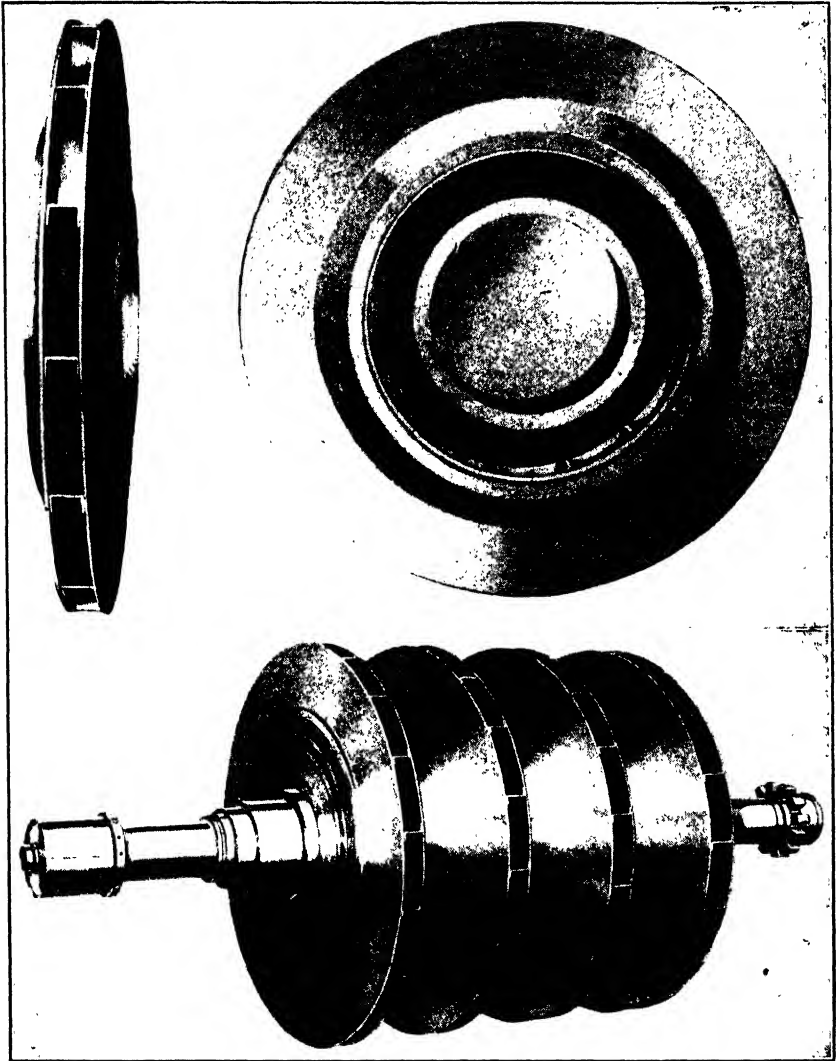
FIG. 14-7. Steps in manufacture and assembly of thick impeller vanes.

The impellers are usually statically balanced, then run at about 25 per cent overspeed as a precautionary measure and to "prestress" them. They are then shrunk on and keyed to the shaft and the complete assembly is dynamically balanced.

14-7 Diffuser and Diaphragm. Most blowers have vaneless-type diffusers, of either the annular or volute type or a combination of the two. For high heads where space is important, as in airplane superchargers, vane diffusers are used.

The diffuser vanes may have a cross section of variable thickness or may be made of sheet steel strips bent to shape. They are either cast with or attached to the interstage diaphragm as illustrated in Fig. 14-5(b).

To guide the gas leaving the volute or diffuser into the succeeding stage in a radial or axial direction, return guide vanes are usually



Courtesy De Laval Steam Turbine Co.

FIG. 14-8. Blower impellers with bent sheet iron vanes.

cast integral with the diaphragm between the stages as illustrated in Fig. 14-9.

14-8 Axial Thrust. An axial thrust is exerted on the impellers of blowers as well as on those of pumps (Section 8-10) but, since the

pressure rise is generally smaller, the magnitude is not so great. This thrust may be reduced by drilling holes axially through the impeller as shown in Fig. 14-6(a).

On multistage machines, a balancing piston or drum is employed to absorb the axial thrust, as shown in Figs. 1-1 and 14-1. As noted



Courtesy Elliott Co.

FIG. 14-9. Blower diaphragm used in multistage blowers showing guide vanes to direct the flow radially into the succeeding stage.

in Section 8-10, the resultant pressure thrust has a magnitude approximately $\frac{\pi}{4} (D_0^2 - D_H^2)(p_d - p_s)$, where p_d and p_s are the discharge and suction pressures of the blower. By placing a labyrinth at a diameter D_0 on the high pressure end of the blower so that one side is subjected to a pressure p_d and the other side to a pressure p_s , the force may be equalized. The suction pressure p_s is obtained by connecting the space on one side of the labyrinth to the suction (equalizing connection of Fig. 1-1).

14-9 Couplings. The couplings are of the flexible type to care for slight misalignments due to temperature changes. Metallic couplings of the Falk or Fast type are commonly used and, if the casing is vertically split, a spacer coupling is required to facilitate inspection and repair.

14·10 Cooling.* The gas passing through a compressor may be cooled by water-jacketing the stages or by being passed through external coolers between the stages. This will increase the pressure rise and efficiency because the average temperature during the compression will be lower. In order to maintain the efficiency of the system, the water-jackets or intercoolers must be frequently cleaned; this procedure is not only expensive but it also removes the unit from service. The cost of installing and operating the cooling system must be balanced against the power saving for each installation in determining if savings warrant cooling. In general, the savings involved are not justified on units having discharge pressures below about 30 lb. per sq. in. ga., hence relatively few machines are cooled.

*W. J. Kearton, *Turbo-Blowers and Compressors*, Pitman, 1926, Chapter V; "Recent Developments in Turbo-Blowers," *Trans. Inst. Mech. Engrs.*, January, 1936.

CHAPTER 15

BLOWER APPLICATIONS

15·1 Introduction. The information presented in Sections 9·1 and 9·3 concerning arrangements of pumps in parallel and in series with their corresponding curves and the economic considerations involved may also be applied to blowers. For blowers to operate successfully in parallel, they should develop approximately the same pressure and have fairly steep characteristic curves of about the same shape.

For many applications a variable speed drive is desirable, hence steam turbines are widely used. If electric motors are employed they are usually either of the squirrel cage or synchronous type and are frequently connected to the blower with speed-up gears. To obtain a variable speed, a hydraulic or magnetic coupling may be used.

Any installation is made only after a considerable amount of study and consultation with the manufacturer. The usual operating conditions, sizes, and special features of blowers and compressors for various applications will now be considered.

15·2 High Pressure Air. Many factories need high pressure air (60 to 120 lb. per sq. in. ga.) to operate tools, clean castings, etc. For smaller capacities (less than about 1000 c.f.m.) reciprocating compressors are commonly used, because the leakage losses, etc., in a centrifugal compressor would result in low efficiencies. For capacities of 10,000 c.f.m. and above, nine- to twelve-stage centrifugal compressors operating at speeds between 4000 and 5000 r.p.m. may be used with two or three intercoolers. They are either directly driven by a steam turbine or motor driven through speed-up gears.

15·3 Sewage Aeration Blowers.* In the activated-sludge process of purifying sewage, air is blown through porous plates in the bottom of tanks containing 10 to 15 ft. of sewage. The air may be supplied by a two- or three-stage blower at a pressure of 6 to 10 lb. per sq. in. ga. A general rule for estimating the required capacity is that 1 cu. ft. of air is required for each gallon of sewage, but this may vary widely with local conditions. The capacity of the blowers ranges from 2000 to 100,000 c.f.m. Frequently, to obtain flexibility, the units operate

* R. G. Regester, "Selection of Centrifugal Blowers for Sewage Works," *Powerfax*, June, 1940.

in parallel, discharging into a common header from which the air is drawn for the process. To prevent backflow into the blower, a check valve is placed in the discharge line in addition to a gate valve.

The units are either motor or turbine driven, the larger ones (over 10,000 c.f.m.) being direct connected and running at speeds ranging from 3000 to 4000 r.p.m., and the smaller ones operating at higher speeds through speed-up gears. The capacity may be controlled by a constant discharge pressure governor which throttles the flow if motor driven, or by varying the speed if turbine driven. Frequently the control is manual.

As shown in Chapter 12, the pressure rise is inversely proportional to the absolute inlet temperature, so the winter discharge pressure is higher than the summer discharge pressure. With a constant speed driver, this means that the air must be throttled for winter operation; this represents a loss of power. If a steam-turbine drive is used, the speed may be varied to meet the operating conditions, but the initial cost of the complete installation, involving boilers and condensing equipment, will be greater. An economic study of the annual charges for the two alternatives should be made for each installation.

15-4 Scavenging Two-Cycle Diesels. Centrifugal blowers are used to scavenge the dead gases out of and introduce fresh air into the cylinders of large Diesel engines. For small sizes, rotary or reciprocating units are used.

The blowers are single-stage, operating at about 3550 r.p.m., and they are motor driven or they may be geared to the crankshaft. The air is delivered at pressures from 2 to 5 lb. per sq. in. ga. and the usual capacities are in the range of 10,000 to 30,000 c.f.m.

15-5 Cupola Blowers.* Blowers are used to supply air to foundry cupolas at a pressure of 1 to 2 lb. per sq. in. ga. They are either single- or double-suction, depending upon the capacity. They generally run at 3550 r.p.m. and have capacities of 600 to 15,000 c.f.m.

A gate valve is placed in the discharge line to regulate the flow. If the units are to operate in parallel a check valve is needed in the discharge line to prevent backflow which would drive the impeller of an idle blower in the wrong direction as a turbine. Methods of regulation of these blowers are considered in the next chapter.

Blowers of this type are used for ventilating tunnels, mines, etc.

15-6 Blast Furnace Blowers. An application similar to that described in the preceding section is supplying air to blast furnaces. The units are quite large and handle from 20,000 to 120,000 c.f.m.

* H. V. Crawford, "The Constant-Air-Weight Method of Cupola Blowing," *General Electric Review*, November and December, 1930, pp. 626, 682.

For average operation a pressure of 15 to 20 lb. per sq. in. ga. is required, but occasionally the charge may become clogged. Then a pressure as high as 35 lb. per sq. in. may be needed to break it up. The blower speed is usually between 2600 and 3000 r.p.m., and is generally direct coupled to a steam turbine because of the large power requirement and the simpler speed regulation. The blower usually has four or five stages and is generally uncooled. If cooling is used the power requirement is lowered, but so is the discharge temperature of the air. The temperature of the air leaving the blower must be increased to 700 to 1000° F. in a heat exchanger. Moreover, the added cost of installation, operation, and cleaning of the cooling system generally outweighs the lower power cost. Hence it is very doubtful if water cooling is justified for this application.

Generally each furnace is served by a single blower, the pressure and volume flow being specified by the furnace superintendent. To secure flexibility in plant operation, several blowers may be connected to a single header which is connected to the various furnaces. Each unit has a check valve and a gate valve in the discharge line to prevent backflow during shut-down periods.

The blowers usually have an automatic governing device to deliver a constant weight flow of air which can be set by the operator, and which is described in the next chapter.

Some installations have the intake air pass through a cold water spray which condenses the moisture in the air and washes out the dust particles which would otherwise pass through the blower and cause erosion. The water chills the air and thus increases the blower efficiency and, by removing the excess humidity, increases the efficiency of both the furnace and the blower.

15-7 Bessemer Converter Blowers. The blower supplying air to a Bessemer converter is similar to a blast furnace blower but, because it is smaller, a motor drive is more often used. The pressure required varies from 5 to 35 lb. per sq. in. ga. and the capacities range from 10,000 to 40,000 c.f.m. The service is intermittent as the time required per heat is from 15 to 20 minutes. The blower is under the direct control of the converter operator, who can vary the pressure and duration of the run to suit the metal being produced. The control may be accomplished by throttling the flow, but more generally by varying the driver speed.

15-8 Blast Furnace Gas Blowers. The gases leaving the blast furnace are generally burned under a boiler to increase the plant efficiency. In some instances this gas is mixed with the coke oven gas before it is burned. A blast furnace gas blower is used to convey

the gas to the boiler. The pressure developed is about 2 lb. per sq. in. ga. and, since the specific gravity of the gas is about unity, a single stage is sufficient. The gases are first cooled in a heat exchanger and mixed with air, so the blower inlet temperature is about 100° F.

The blower is either motor or turbine driven and operates at about 3550 r.p.m. The impeller is either single- or double-suction, depending upon its capacity.

15-9 Water Gas Blowers. In the manufacture of water gas, air is blown through a bed of coke intermittently for periods of 1 to 3 minutes. For the remainder of the period while steam and oil are being blown through the coke no air is required. If a steam-turbine drive is used the blower may idle during these periods, whereas if a motor is employed the unit must operate at shut-off or the flow must be by-passed. The pressure required is from 1 to 3 lb. per sq. in. ga., so a single-stage unit is satisfactory and it is generally run at 3550 r.p.m. The capacity of the units is between 15,000 and 50,000 c.f.m.

15-10 Municipal Gas Plant Blowers. Municipal gas plants use centrifugal blowers to convey the illuminating gas from the storage holders through the trunk distributing lines. The pressure in these main lines is usually 6 to 7 lb. per sq. in. ga. although it may go higher (up to 10 lb. per sq. in. ga.). The gas then passes through a reducing valve into the distributing lines where the pressure is only a few inches of water. The blower must be multistaged because of the low specific gravity of the gas. It may be direct turbine driven, or a motor drive with or without a speed-up gear may be used. The capacities range from about 3,000 to 60,000 c.f.m. The packing box seal is quite important in this application to keep the gas in the blower and the air out. Water or steam seals are commonly used.

15-11 Coke Plant Exhausters and Boosters. *Exhausters.* The gases generated in the coke oven are removed by centrifugal exhausters which, by governor control, maintain a vacuum of 5 to 15 in. of water in the oven. These exhausters discharge the gas at a pressure of 2 to 5 lb. per sq. in. ga. in order to force the gas through a by-product recovery plant and into the main or gas holder. Since the specific gravity of the gas is between 0.33 and 0.4, two to four stages are required. If steam is available a turbine drive is used; if not, a motor drive with a speed-up gear or a variable speed coupling is employed. The capacity of the exhausters ranges from 10,000 to 35,000 c.f.m. or over, at speeds of 4000 to 7000 r.p.m. The packing boxes are equipped with water seals to reduce the leakage.

An important advantage of the centrifugal type of exhauster is its ability to remove a good portion of the tar contained in the gas.

The tar is thrown outward by centrifugal force onto the casing and is then drawn off at the bottom. The heat of compression keeps the tar in liquid form. Just before the unit is stopped a light oil is sprayed on the first-stage impeller and this oil travels through all the stages, dissolving the tar and cleaning the impeller and drains. If this were not done the tar would solidify on the impellers and clog the drains, causing vibration due to unbalance when the unit is next started up.

Boosters. The boosters are used to transfer the coke oven gases from the holder or reservoir to the mains or point of use. They have about the same capacity and speed as the exhausters and generally the same type of drive. They take the gas usually at atmospheric pressure or slightly higher and discharge it at 5 to 10 lb. per sq. in. ga. into the mains, as described in the previous section. They are equipped with water seal packing boxes. A "scrubber" or "washer" is placed between the coke ovens and the exhauster to remove the dust and tar; hence the gas is saturated with water vapor when it passes through both the exhauster and the booster.

15-12 Airplane Superchargers.* As the altitude at which an airplane flies increases, the specific weight of the air decreases (see Fig. 11-4); this means that the engine receives a proportionately smaller weight of oxygen and hence loses power. If the air is compressed to sea level pressure this deficiency will be restored and the engine will have the same power as it had at sea level. This is the purpose of the supercharger.

Superchargers are either single- or double-stage blowers operating at high tip speeds (800 to 1400 ft. per sec.) and high revolutions per minute (15,000 to 30,000). They are either geared to the propeller shaft with a gear ratio between 5 and 10 to 1, or they are driven by exhaust gas turbines. The geared type must run at a constant speed because its speed bears a direct ratio to the engine speed. As a result the ceiling or altitude of the plane at which the engine can produce sea level power is limited. To develop the correct head at lower altitudes the supercharger must be throttled. This may be partially obviated by employing a gear shift giving two ratios. If the supercharger is driven by a gas turbine its speed can be varied by by-passing some of the exhaust gases from the engine. In addition, more power is developed as the altitude increases since the pressure drop across the turbine wheel is increased. The chief difficulty with the turbine drive is securing materials which will withstand the high stresses and temperatures at which the turbine has to operate.

* R. G. Standerwick and W. J. King, "Superchargers for Aircraft Engines," *A. S. M. E. Trans.*, Jan., 1944, p. 61. and bibliography.

The impeller has radial-type vanes because of the necessity of obtaining the greatest possible pressure rise per stage, and it is made single-suction. It is of either the semi-open or the enclosed type. The end thrust is reduced by drilling axial holes between the vanes and the remainder is taken by a thrust bearing, frequently of the Kingsbury type.

The capacity of the supercharger may be estimated from the power developed by the engine, the fuel consumption (which is between 0.4 to 0.5 lb. of fuel per b.hp.-hr.), and the fact that each pound of fuel requires from 13 to 14 lb. of air. The pressure ratio and head may be found by taking the ratio of 30 in. Hg to the atmospheric pressure in inches at the altitude considered and the corresponding head based on the temperature existing at that altitude.

The great importance of weight and space in aircraft design accounts for the high speed and small diameter of the impeller. The air usually enters an air scoop on the outside of the plane; this gives it an initial velocity head or ramming effect, passes through the carburetor, the supercharger (which may be used to aid in thoroughly mixing the air and gasoline vapor), and finally into the intake manifold of the engine.

The principles of design follow those outlined in Chapter 13 although difficulties due to the supersonic velocities* of the air may be encountered.

15-13 Other Applications. There are many other applications besides those already described but many are very specialized and not of general interest.

Among these might be mentioned circulators used in the chemical industries. They are used to circulate gases, usually at high pressures and temperatures, through chemical processes. The volumes are generally relatively small and the pressure ratios are small, but the inlet pressures are quite high — up to 5000 lb. per sq. in. Since they frequently handle corrosive gases, special materials must be used for the rotor and casing and provision must be made to prevent leakage at the packing boxes.

Another specialized field is large refrigeration units handling ammonia, water vapor, and Freon 11. The latter has a specific gravity of about 4.5 and a low specific heat ratio, so the pressure ratio per stage is relatively large.

* K. W. Sorg, "Supersonic Flow in Turbines and Compressors," *Forschung*, November and December, 1939; English translation by L. J. Goodlet, *Journal of Royal Aeronautical Society*, March, 1942.

CHAPTER 16

REGULATION OF BLOWERS

16.1 Introduction. It is evident from the preceding chapter that for most applications of blowers some form of regulation is required. The types of control may be classified as:

- (a) Constant pressure at inlet or exhaust
- (b) Constant inlet volume or weight flow
- (c) Prevention of pulsation

The control may be operated either manually or automatically.

If the unit is turbine driven, the governing is generally effected by varying the speed; this being more economical than throttling the flow. Small- and medium-size units are commonly driven by alternating-current induction or synchronous motors which operate at constant speed. In such cases the regulation is obtained by throttling the flow in the suction line. It is possible to throttle the discharge flow, as is done with pumps. However, there is a slight decrease in the brake horsepower if the suction is throttled, owing to the slightly reduced specific weight of the gas passing through the impeller, so this method is preferred.

It is possible to obtain a blower speed control with a constant speed driver by means of hydraulic or magnetic variable speed couplings and these are occasionally used for smaller sizes. Neither type of coupling can transmit large powers at high speeds, hence speed-up gears must be placed between the coupling and the blower, and this increases the size and cost of the unit.

The flow may be regulated by using movable diffuser vanes which vary the diffuser inlet area and angle, or by placing movable guide vanes in front of the impeller to induce prerotation of the gas. These methods are described in Section 16.5.

The actual governing mechanisms are rather complex because they are generally operated with compensated oil relays to insure stable action. They are not standard and are being continually improved. Rather than a description of any particular mechanism, the general operating principle and a simplified schematic diagram will be given for each type.

16.2 Constant Pressure Regulation. For satisfactory operation, exhausters must maintain a constant vacuum in the suction line.

The control mechanism consists of a sensitive diaphragm-operated oil governor which controls the steam flow in turbine drives or actuates a butterfly valve in the suction line of the blower if the speed is fixed. The latter type is illustrated diagrammatically in Fig. 16-1.

The suction line is connected to a cylinder containing a piston or diaphragm. Atmospheric pressure is exerted on the right side of the piston and is opposed by the spring. Movement of the piston operates

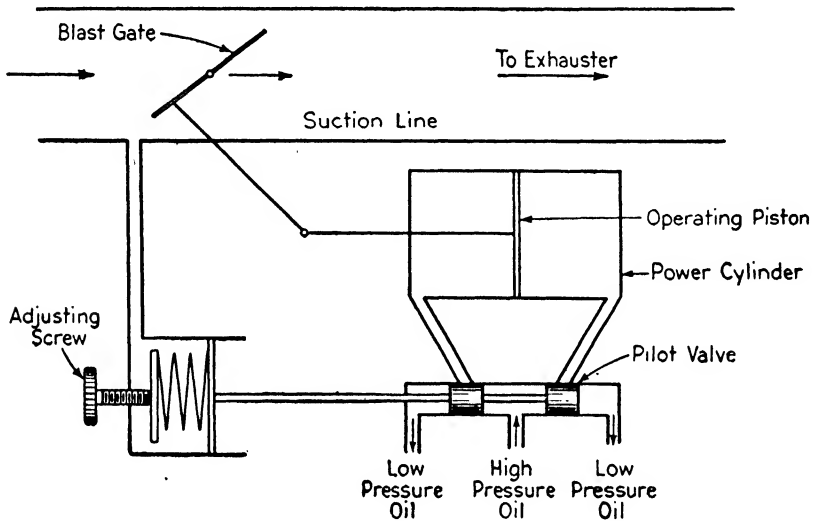


FIG. 16-1. Schematic sketch of governing mechanism to secure constant pressure regulation by throttling.

the pilot valve which admits high pressure oil to one side of an operating piston and allows the oil on the other side to be exhausted. If the pressure in the suction line increases the diaphragm will move to the right, moving the pilot valve in the same direction. This exposes the right port to high pressure oil and the left one to the drain, so the operating piston moves to the left, opening the valve and increasing the flow. The desired suction line pressure may be obtained by turning the adjusting screw; this varies the spring load on the diaphragm. As noted in the previous section the actual mechanisms are much more complex, since over-travel and unstable operation must be prevented, but the diagram serves to illustrate the principle.

A similar arrangement may be used to control the discharge pressure of blowers used as boosters or circulators. A decrease in the discharge pressure would cause the valve to open, increasing the inlet pressure and hence the discharge pressure.

A mechanism to vary the steam supply to a turbine driver and maintain a constant discharge blower pressure is illustrated in Fig. 16-2. A pipe connects the blower discharge line with a cylinder containing a piston or diaphragm. The pressure exerted on the piston by the gas in the discharge line is balanced by a compression spring. A movement of the piston is transmitted to a pilot valve through a lever *AB* pivoted on the moving sleeve of the turbine speed governor. The pilot

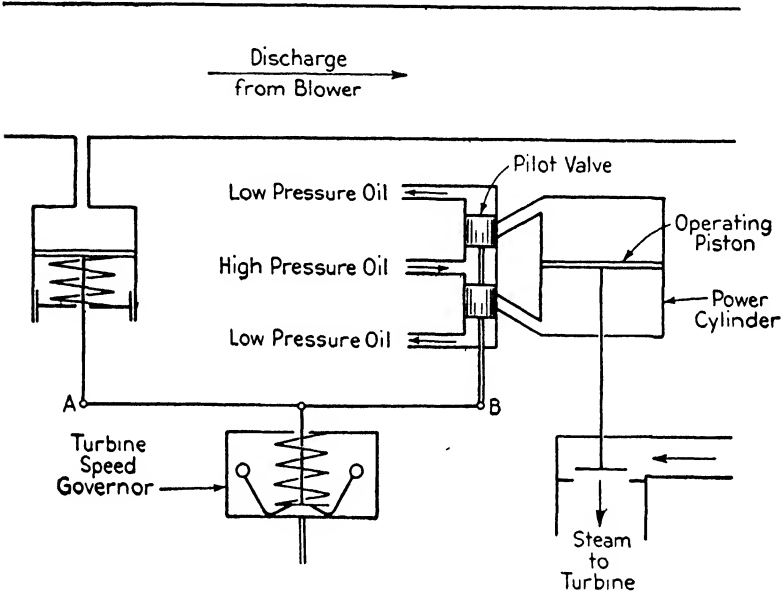
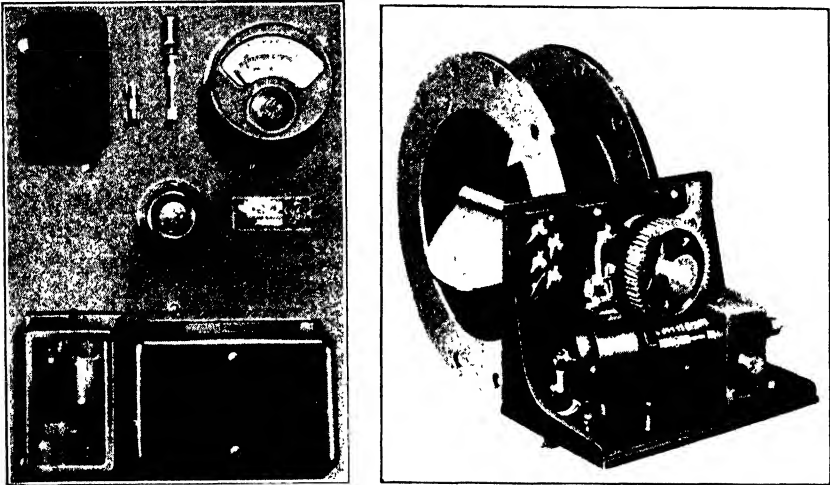


FIG. 16-2. Schematic sketch of governing mechanism to secure constant pressure regulation by speed control.

valve movement uncovers ports which transmit high pressure oil to and low pressure oil from a power cylinder. The force exerted by the oil on the operating piston in the power cylinder opens and closes the governor valve, admitting steam to the turbine. The initial compression in the spring may be adjusted by turning the internal nut to secure any desired discharge pressure from the blower.

To illustrate the action, consider that the discharge pressure from the blower drops off. The diaphragm will then move upward and the lever *AB*, pivoted on the speed governor sleeve, will move the pilot valve downward. This movement admits high pressure oil on the under side of the operating piston and allows the oil above the piston to be released, thus causing the operating piston and governor steam valve to rise. More steam is admitted to the turbine and this

will increase the speed of the unit and restore the discharge pressure of the blower. If the turbine speed is increased to an unsafe value the governor sleeve moves upward and the lever *AB* moves the pilot valve upward. The direction of the operating piston travel is thus reversed and the speed of the unit is decreased.



Courtesy Ingersoll-Rand Co.

FIG. 16-3. Control board and motor-operated blast gate.

16-3 Constant Inlet Volume or Weight Flow. Cupola blowers and blast furnace blowers should deliver a constant inlet volume or weight flow to maintain uniform combustion conditions in the cupola or blast furnace. The amount of air required will depend upon the size of the charge, the quality of and moisture in the coke, the air leakage, etc.*

One method of controlling the weight flow used with motor-driven cupola blowers is based upon the principle that the brake horsepower is proportional to the product of weight flow and head. For a constant speed, the head remains constant so the weight flow is approximately proportional to the kilowatt input to the motor. By graduating a kilowatt meter in cubic feet of standard air per minute, the weight of air handled can be read directly and can be adjusted to any desired value. The control may be manual or may be made automatic by electric relays operating a blast gate by means of a small reversible

* H. V. Crawford, "The Constant-Air-Weight Method of Cupola Blowing," *General Electric Review*, November and December, 1930, pp. 626, 682.

motor. Figure 16-3 shows a typical control board and the motor-operated blast gate.

Another method makes use of the principle that the volume flow through a venturi meter is approximately proportional to the square root of the pressure difference between the mouth and throat. This pressure difference may act across a diaphragm to move a pilot valve and hence regulate the turbine speed or operate a butterfly valve in the suction line. The mechanism is similar to that shown in Figs. 16-1 and 16-2 except that the pressure actuating the diaphragm is taken from a venturi meter in the suction line. The diaphragm spring may be adjusted to care for any inlet pressure or temperature and to secure any desired weight flow.

16-4 Pulsation. In Section 3-20 it was shown that, if the quantity of air removed from the system is less than the quantity corresponding to the highest point on the characteristic curve of a blower supplying the system, unstable conditions prevail. The blower will alternately deliver large quantities of gas or air and operate at shut-off — an undesirable condition. As the pulsation point of blowers normally occurs at 40 to 50 per cent of the design flow, it is desirable to have some means of preventing this phenomenon.

The total head of many blower applications consists mainly of friction head which is approximately proportional to the velocity of the gas squared or the flow squared. If the speed of the unit can be reduced, the pulsation point will be reduced in the same proportion, hence surging may be largely avoided for these applications.

For constant speed machines a simple but uneconomical solution is to provide a relief or blow-off valve in the discharge line of the blower. When the system demand falls below the critical flow at which pulsation occurs the valve is opened and sufficient air is discharged to the atmosphere to bring the total flow through the blower above the critical value. When gases are handled, the excess gas is by-passed to the suction line but care must be taken to prevent sudden or extreme rises in the blower temperature when this is done.

The blow-off valve may be manually operated or may be operated by a volume-type governor. The pulsation point is the highest point on the characteristic curve, so a governor similar to Fig. 16-2 may be set to open the by-pass valve when this maximum pressure is reached or approached.

The pulsation may be eliminated to some extent by throttling the suction line either manually or by means of an oil relay operated by a diaphragm connected to the discharge line. The throttling causes the

characteristic curve to drop more rapidly and moves the pulsation point closer to shut-off.

16-5 Movable Diffuser Vanes and Prerotation. A special device for governing by using movable diffuser vanes was developed by the Brown-Boveri Company in Switzerland and is manufactured in this country by the Allis-Chalmers Co. The diffuser vanes may be moved to vary the inlet angle and area. Each vane is pivoted and all vanes

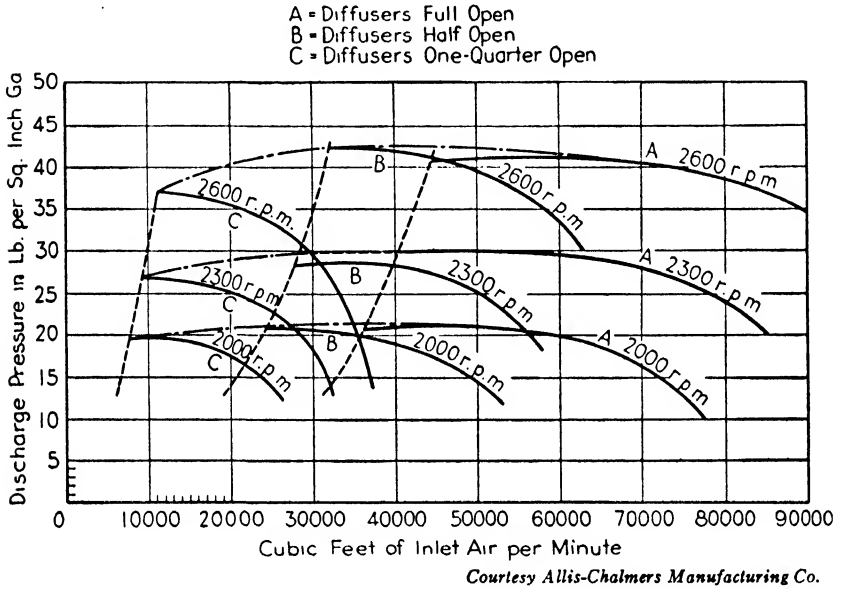
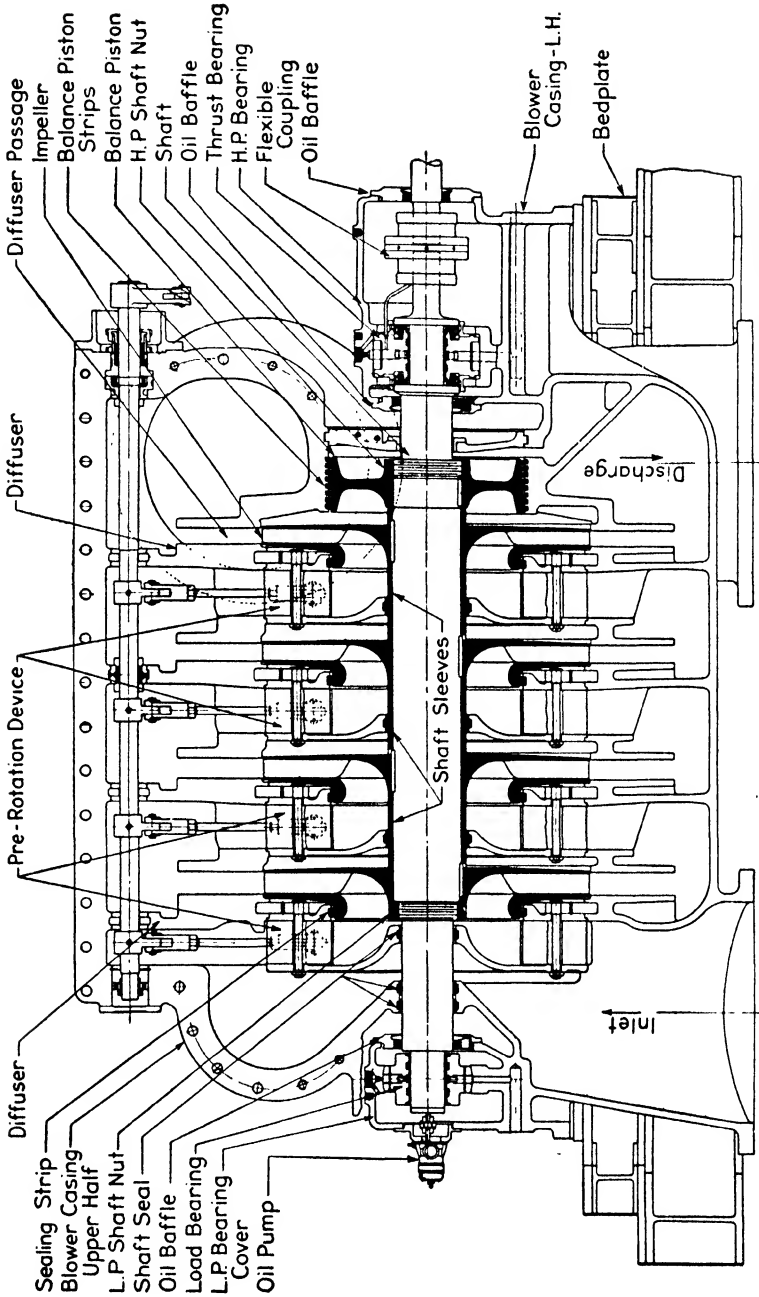


FIG. 16-4. Operating characteristics of a blower operating with movable diffuser vanes.

move together. This device may only be used with gases which are not gummy, corrosive, or erosive.

Figure 16-4 shows the operating characteristics obtained for various diffuser positions. From this figure it may be observed that the pulsation point is moved toward shut-off flow as the diffuser vanes are closed, hence it may be used to control pulsation. Also, the vanes may be adjusted to secure desired suction or discharge pressures. A particularly advantageous use is on blast furnace blowers where wide variations in the weight flows occur. The vane position is usually adjusted manually and the unit is then placed under one of the governor controls mentioned in the preceding sections.

Another method of governing, produced by the same companies, is used with vaneless diffusers, and is accomplished by giving the gas



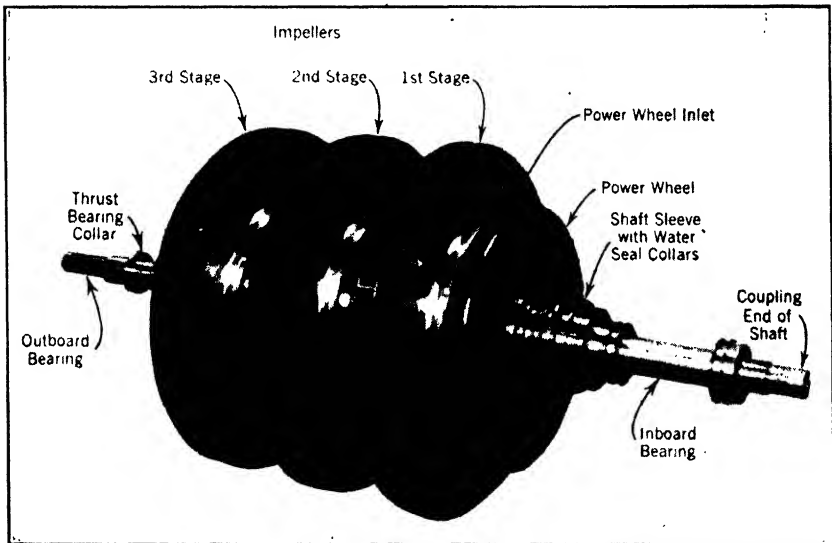
Courtesy Allis-Chalmers Manufacturing Co.

FIG. 16-5. Section through a four-stage blower with pre-rotation on all four stages.

approaching the impeller a whirl in the direction of rotation by means of movable guide vanes. It was shown in Section 3-11 that prerotation decreases the absolute inlet angle α , and increases V_{u_1} .

By Eq. 3-5, $H_{vir.\infty} = \frac{1}{g} (u_2 V_{u_2} - u_1 V_{u_1})$. Hence, increasing V_{u_1} results in a reduction in head delivered by the impeller. Also, since $hp_{vir.\infty} = \frac{w}{550g} (u_2 V_{u_2} - u_1 V_{u_1})$, from Eq. 3-6, an increase of V_{u_1} will reduce the horsepower required.

A blower may then be made to operate at a reduced head by adjusting guide vanes placed before the impeller to give the gas a whirl in the direction of the wheel rotation, and the horsepower requirement will also be decreased. The arrangement is illustrated by the sectional drawing in Fig. 16-5.



Courtesy Ingersoll-Rand Co.

FIG. 16-6. Power wheel method of regulating pressure.

16-6 The Power Wheel. As noted previously, regulation by throttling involves a waste of power because the kinetic energy of the air or gas is destroyed without a corresponding gain. To reduce this loss, the Ingersoll-Rand Co. has developed a turbine or power wheel which is placed in the suction before the first-stage impeller (Fig. 16-6). The air or gas is expanded through a system of movable guide vanes which direct the jets upon the turbine blades. These blades are of

the reaction type and will produce a further pressure drop. Therefore, both an impulse and a reaction effect are produced. The torque which is developed is transmitted to the shaft and relieves the driver of an equivalent amount of power.

The movable guide vanes may be connected to a governing mechanism (similar to Figs. 16·1 or 16·2) to obtain full automatic control, or they may be operated manually. They are generally used with constant speed drivers to regulate the output, but they may also be used to control pulsation, since the effect is similar to that obtained with suction throttling.

CHAPTER 17

BLOWER INSTALLATION, OPERATION, AND TEST

17.1 Installation. When a blower installation is being planned or the units are being erected certain precautions must be observed to insure satisfactory operation. These are similar to those outlined in Section 10.1 for pumps.

The pipe connections to the blower should be independently supported to avoid straining the casing which might cause distortion and rubbing. To reduce the friction and turbulence losses, all lines should be as short and straight as possible. Any elbow should have a large radius, and supplementary guide vanes may be used for the larger sizes.

If the blower takes air from the atmosphere the suction intake should be located outside the compressor house so that the air will be cooler. The inlet should be protected against foreign objects, dust, and rain which might be drawn into the blower and cause damage. The velocity in the suction line should be kept low to reduce the friction and turbulence losses, the maximum value being about 80 ft. per sec. There may be considerable noise manifested at the inlet air opening. For installations where this condition is objectionable, silencers are used. The pressure drop across them should be small (less than 2 in. of water) to prevent excessive throttling of the flow.

As outlined in the previous chapter, the flow may be regulated by throttling either the suction or discharge lines by means of blast gates or butterfly valves. If units are to operate in parallel and in certain installations of single blowers as, for example, blast furnace blowing, a check valve should be placed in the discharge line to prevent back flow. For such applications it is necessary to place a blow-off valve in the discharge line between the blower and the check valve. This permits the unit to pass sufficient flow to build up a delivery pressure higher than the system pressure and permits delivery into the system. When gases are being compressed the valve operates to by-pass the gas back to the suction. These valves may be operated either manually or by governor control, as outlined in the previous chapter.

17.2 Operation. The operation of blowers is quite similar to that described in Section 10.2 for pumps. When starting or stopping, the

flow should be throttled to reduce the load on the driver. About the only attention required while running is an occasional check on the bearing temperature and oil supply.

The unit should be dismantled periodically and examined for excessive wear or corrosion, particularly at the labyrinths, which are easily damaged.

17-3 Blower Test. The usual test is one conducted to determine if the blower meets the conditions of head, capacity, and efficiency as guaranteed by the manufacturer. For small blowers the test is generally conducted in the manufacturer's plant, whereas for large units

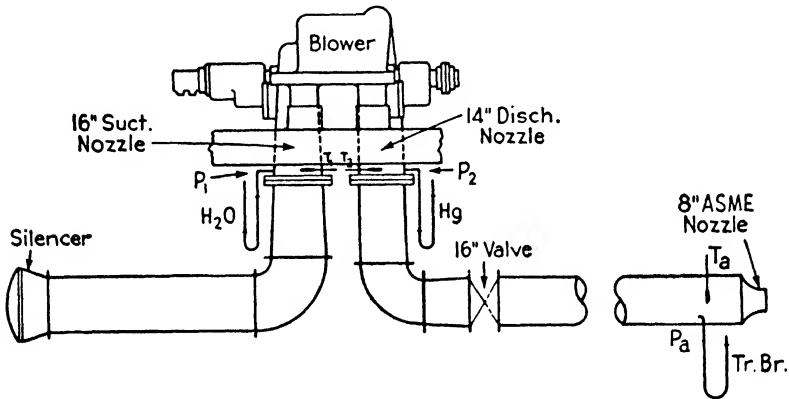


FIG. 17-1. Typical blower test arrangement.

the test may be run after final installation. Tests in this country are conducted in accordance with the A.S.M.E. Test Code for "Centrifugal Compressors, Exhausters and Fans" (1935).

Usually only the design point is guaranteed by the manufacturer, hence this point is accurately determined, and other points are found merely to fix the curve shape and the pulsation point.

The unit is run at full speed before readings are taken to insure steady conditions in both the blower and driver. The unit is then run at the design point and several readings are taken at equal time intervals. These are averaged to determine the performance at this point. Readings are then taken at about five-minute intervals for various flows to determine the curve shape.

All instruments should be calibrated before and after the test to insure their accuracy. Before the test is started the blower should be checked mechanically, i.e., the bearings and the condition of the labyrinths should be inspected and the rotating parts should turn freely.

Figure 17-1 shows a typical test set-up with the various instruments

in place. The dimensions given on the figure apply to the sample test of Section 17.5.

17.4 Test Instruments and Apparatus. The theory of test instruments is given in the A.S.M.E. Test Code and books on experimental engineering.* It will not be repeated here, but a brief description of the instruments used will be given.

Measurement of Pressure. For low pressures (less than 10 lb. per sq. in. ga.) manometers are usually used. If the pressure is quite low the manometers are filled with water and may be of the inclined type, like boiler draft gages. For higher pressures, mercury with a specific gravity of 13.6 or acetylene tetrabromide with a specific gravity of 2.96 may be used. For high pressures (above 10 lb. per sq. in. ga.) Bourdon gages are employed.

Measurement of Speed and Power. The measurement of speed and power input of blowers is the same as described in Section 10.4 for pumps.

Measurement of Temperature. The temperatures are measured with bare-bulb-type thermometers. The bulb should project well into the air stream to avoid any cooling effect from the casing. If the pressures are high, provision must be made to prevent the thermometers from being blown out of the casing.

Measurement of Capacity. Greater accuracy may be obtained if the volume flow is measured both before and after the gases pass through the blower. If this is not practical the flow is usually measured in the discharge line.

The flow could be measured by either drawing the gas from or discharging it into a holder and measuring the variations in volume, pressure, and temperature. With large volumes the temperature in the holder will not be uniform, hence this method may not be too accurate. For most applications no holder is available, therefore, the method is seldom used.

The usual arrangement is to place a constriction in the line and to calculate the flow from the pressure drop across it. This constriction may be a venturi meter, a thin plate orifice, or a rounded inlet nozzle. Guide vanes are usually placed before the constriction to even out the flow and prevent any whirling of the gas which would cause inaccuracies in the measurement. The pressure drop across the constriction and the temperature before it are measured as shown in Fig. 17.1. The size should be selected to obtain low pressure ratios. If the pressure ratio is too large there is danger that the critical flow may be reached.

* Diederichs and Andrae, *Experimental Mechanical Engineering*, Vol. I, Wiley, 1930.

The pressure measured before the constriction may be the static pressure alone but it usually includes the impact pressure due to the velocity head as measured by a pitot tube facing the flow. The pressure after the constriction is always taken to be the static pressure.

The A.S.M.E. has adopted a series of standard homologous nozzles with a rounded inlet which are widely used in test work. The following equations for calculating the weight and volume flow of air based on the total pressure before the nozzle, and a pressure drop across the nozzle of less than 10 per cent of the total pressure before the nozzle, are taken from the Code.*

$$w = 0.8596cD^2 \sqrt{\frac{(p_a - p_b)p_b}{T_a}} \text{ lb. per sec.} \quad 17.1$$

$$Q_s = \frac{19.16cD^2 T_s}{p_s} \sqrt{\frac{(p_a - p_b)p_b}{T_a}} \text{ c.f.m.} \quad 17.2$$

For pressure drops between 10 and 50 per cent of the total pressure before the nozzle:

$$w = 0.8627cD^2 \sqrt{\frac{(p_a - p_b)}{T_a} [p_b - 0.0755(p_a - p_b)]} \text{ lb. per sec.} \quad 17.3$$

$$Q_s = \frac{19.23cD^2 T_s}{p_s} \sqrt{\frac{(p_a - p_b)}{T_a} [p_b - 0.0755(p_a - p_b)]} \text{ c.f.m.} \quad 17.4$$

where c = coefficient of discharge, which depends upon the nozzle throat diameter D and is between 0.97 and 0.995

D = nozzle throat diameter, inches

p_a = total pressure at nozzle inlet, pounds per square inch absolute

w = weight flow, pounds per second of air

p_b = static pressure at nozzle outlet, pounds per square inch absolute

T_a = temperature of the air at nozzle inlet, degrees Fahrenheit absolute

p_s = pressure to which the volume flow is referred, pounds per square inch absolute

T_s = temperature to which the volume flow is referred, degrees Fahrenheit absolute

Q_s = Flow through nozzle referred to T_s and p_s , cubic feet of air per minute.

* A.S.M.E. *Power Test Code for Centrifugal Compressors, Exhausters, and Fans*, A.S.M.E., 1935.

For other gases and further information concerning the nozzle proportions or test arrangements, the Code should be consulted.

The same equations may be used for thin plate orifices or venturi meters by using the correct flow coefficients. These depend upon the pressure drop, size, and ratio of mouth to throat diameters. It should be observed that Eqs. 17-2 and 17-4 correct the flow to any specified conditions of temperature T_s and pressure p_s , hence it is only necessary to correct the results for inconsistencies in speed before plotting the results, if T_s and p_s are taken as the actual temperature and pressure at the blower inlet.

17-5 Sample Blower Test. Figure 17-2 is a typical blower data and result test sheet for the blower illustrated in Fig. 17-1. The sizes given on Fig. 17-1 apply to this particular test.

The sample test is for a three-stage, single-suction motor-driven blower with a 16-in. suction flange and a 14-in. discharge flange. The blower is designed to handle 10,000 c.f.m. of air at 60° F. and 30 in. Hg and deliver it at 8 lb. per sq. in. with an efficiency of 68 per cent when operating at 3550 r.p.m. The flow is measured at the discharge with an 8-in. diameter standard rounded inlet A.S.M.E. nozzle. Figure 17-1 shows the location of the various manometers and thermometers. The power input to the blower was measured with a torsion meter.

The blower was run for 20 minutes at the design point and readings were taken every 5 minutes. Seven other points ranging from almost maximum flow to the pulsation point were taken at five-minute intervals to determine the curve shape. The last four columns of Fig. 17-2 give the test results corrected to the specified design conditions. The method of calculation is illustrated below for the design point (run 1).

Sample Calculation. Before the calculation is begun the various pressure readings must be converted to pounds per square inch absolute and the temperature readings to degrees absolute (1 in. water = 0.0361 lb. per sq. in.).

$$\begin{aligned} \text{Barometric pressure } p_b &= 30.07 \text{ in. Hg} \times 0.491 \\ &= 14.764 \text{ lb. per sq. in. abs.} \end{aligned}$$

$$\begin{aligned} \text{Blower inlet pressure } p_1 &= 14.764 - 8 \times 0.0361 \\ &= 14.475 \text{ lb. per sq. in. abs.} \end{aligned}$$

$$\begin{aligned} \text{Blower outlet pressure } p_2 &= 14.764 + 14.4 \times 0.491 \\ &= 21.835 \text{ lb. per sq. in. abs.} \end{aligned}$$

$$\begin{aligned} \text{Pressure before nozzle } p_a &= 14.764 + 18.95 \times 0.0361 \times 2.96 \\ &= 16.790 \text{ lb. per sq. in. abs.} \end{aligned}$$

Corresponding temperatures $T_1 = 550^\circ \text{ F.}$; $T_2 = 644^\circ \text{ F.}$;
 $T_a = 636.2^\circ \text{ F.}$

Customer XYZ Manufacturing Corp. Location Boston, Mass. Serial No. 4 A 2371
 Date 6-1-43 Type 3 Stage Single Suction R.P.M. 3550
 Design Conditions: 10,000 c.f.m. @ 60 °F & 14.7 p.s.i.a. Discharge Pressure 80 p.s.i.g. Eff. 68%
 Barometer Reading 30.07 Hg

Run No.	Time	RPM	Tor Meter Deg	INLET		OUTLET		8" NOZZLE		TEST CONDITIONS				CONTRACT CONDITIONS				
				t ₁ °F	P ₁ H ₂ O	t ₂ °F	P ₂ Hg	T _a °F	P _a lbf/br	Q cfm	P ₂ p.s.i.g.	η %	b h p	Q cfm	P ₂ p.s.i.g.	η %	b h p	
	9 30	3560	1460	89.5	8.00	183.5	14.40	176.0	18.90									
	9 35	"	1465	90.0	8.10	184.0	14.35	176.5	18.95									
	9 40	"	1458	90.0	7.80	184.0	14.40	176.0	18.97									
	9 45	"	1455	90.5	8.00	184.5	14.40	176.0	19.00									
	9 50	"	1457	90.0	8.10	184.0	14.45	176.5	18.93									
	1 Ave	3560	1459	90.0	8.00	184.0	14.40	176.2	18.95	10,070	7.21	67.1	410.5	10030	7.90	67.1	437	
	2 10 00	3550	1607	89.0	11.50	171.5	7.75	166.0	27.62	12340	4.05	46.0	451.0	12340	4.68	46.0	488	
	3 10 05	3550	1560	89.5	9.95	179.0	11.62	171.5	23.70	11,320	5.89	60.0	437.8	11320	6.65	60.0	472	
	4 10 10	3580	1340	90.0	5.85	189.0	16.75	180.5	14.20	8,650	8.34	70.2	378.8	8580	8.93	70.2	395	
	5 10 15	3580	1197	90.0	3.90	196.0	18.50	186.0	9.50	7,000	9.15	68.8	338.2	6950	9.70	68.8	350	
	6 10 20	3580	966	89.0	2.00	204.0	19.15	192.0	4.50	4,785	9.43	59.8	273.0	4640	9.91	59.8	282	
	7 10 25	3550	1370	90.5	6.40	192.0	15.80	186.0	15.65	9,060	7.86	69.0	384.0	9060	8.65	69.0	411	
	8 10 30	3540	1483	90.5	8.75	188.0	13.25	184.0	20.95	10,500	6.66	64.1	415.0	10530	7.45	64.1	451	

FIG. 17-2. Blower test data and result sheet.

The results will be calculated for the test conditions of pressure and temperature, i.e., the values of T_s and p_s will be those at the blower inlet, T_1 and p_1 . The values thus found will later be corrected to the contract conditions of 60° F. and $14.7 \text{ lb. per sq. in.}$ when the speed correction is introduced.

The coefficient of discharge for an 8-in. throat diameter is 0.995 according to the Code. As the pressure drop across the nozzle is $p_a - p_b = 16.790 - 14.764 = 2.026 \text{ lb. per sq. in.}$, which is between 10 and 50 per cent of the pressure before the nozzle, Eqs. 17-3 and 17-4 will apply.

$$\begin{aligned}
 w &= 0.8627cD^2 \sqrt{\frac{(p_a - p_b)}{T_a} [p_b - 0.0755(p_a - p_b)]} & 17.3 \\
 &= 0.8627 \times 0.995 \times 8^2 \sqrt{\frac{2.026}{636.2} [14.764 - 0.0755 \times 2.026]} \\
 &= 11.88 \text{ lb. per sec.}
 \end{aligned}$$

$$\begin{aligned}
 Q_s &= \frac{19.23cD^2T_s}{p_s} \sqrt{\frac{(p_a - p_b)}{T_a} [p_b - 0.0755(p_a - p_b)]} & 17.4 \\
 &= \frac{19.23 \times 0.995 \times 8^2 \times 550}{14.475} \sqrt{\frac{2.026}{636.2} [14.764 - 0.0755 \times 2.026]} \\
 &= 10,070 \text{ c.f.m.}
 \end{aligned}$$

The pressure readings at the inlet and outlet do not include the velocity head. The inlet area is $\frac{16^2\pi}{4 \times 144} = 1.40$ sq. ft., and the discharge area $\frac{\pi}{4} \frac{14^2}{144} = 1.07$ sq. ft. The specific weight of the air at the

blower inlet is $\gamma_1 = \frac{P_1}{RT_1} = \frac{144 \times 14.475}{53.34 \times 550} = 0.071$ lb. per cu. ft., and

at the blower discharge it is $\gamma_2 = \frac{P_2}{RT_2} = \frac{144 \times 21.835}{53.34 \times 644} = 0.0916$ lb.

per cu. ft. The velocities in feet per second are: $V_1 = \frac{Q_1}{60A_1} = \frac{10,070}{60 \times 1.40} = 120$ at the inlet and $V_2 = \frac{Q_2}{60A_2} = \frac{w}{\gamma_2 A_2} = \frac{11.88}{0.0916 \times 1.07} = 121$ at the outlet.

Since both velocities are practically the same, the velocity head at the inlet and discharge is given by $H_v = \frac{V^2}{2g} = \frac{120^2}{64.4} = 224$ ft. In

terms of pressure, the velocity head at the inlet is $\frac{H_v \gamma_1}{144} = \frac{224 \times 0.071}{144}$

$= 0.110$ lb. per sq. in., whereas at the outlet it is $\frac{H_v \gamma_2}{144} = \frac{224 \times 0.0916}{144}$

$= 0.143$ lb. per sq. in.

The total pressure at the inlet is $14.475 + 0.110 = 14.585$ lb. per sq. in. abs.; at the discharge it is $21.835 + 0.143 = 21.978$ lb. per sq. in. abs.

The pressure ratio $\epsilon_p = \frac{21.978}{14.585} = 1.507$, and $\epsilon_p^{0.283} - 1 = 0.12307$.

The adiabatic head = $\frac{RT_1}{0.283} (\epsilon_p^{0.283} - 1) = \frac{53.34 \times 550}{0.283} \times 0.12307 = 12,760$ ft.

The air horsepower = $\frac{wH}{550} = \frac{11.88 \times 12760}{550} = 275.5$.

A calibration of the torsion meter shows the torque coefficient to be 498; the power equation thus becomes: $b.hp. = \frac{Tn}{63,000} = \frac{498\alpha n}{63,000} = 0.0079\alpha n$. The brake horsepower for the design point = $0.0079 \times 14.59 \times 3560 = 410.5$ b.hp.

The blower efficiency = $\frac{a.hp.}{b.hp.} = \frac{275.5}{410.5} = 67.1$ per cent.

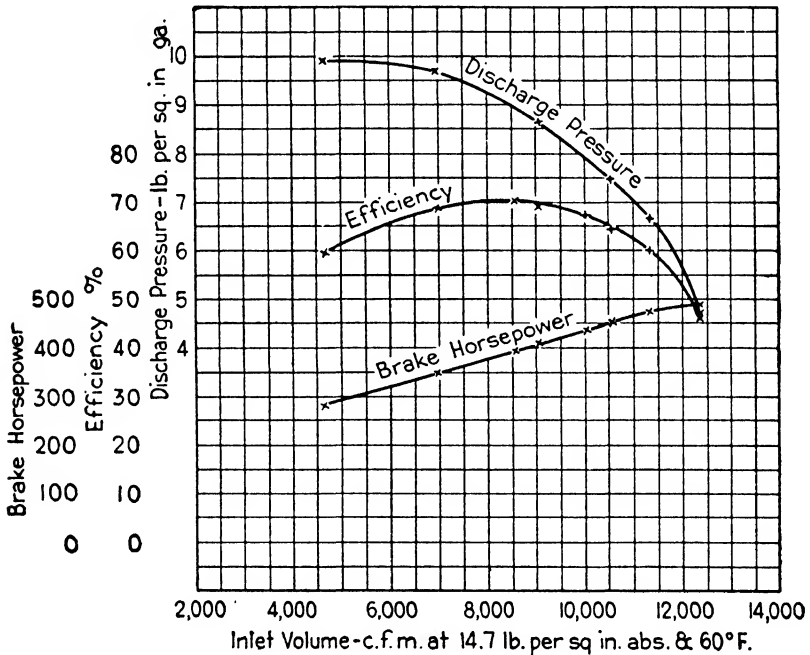


FIG. 17-3. Performance curves of blower test.

These results should now be corrected to the specified contract conditions of 14.7 lb. per sq. in. abs., 60° F., and 3550 r.p.m. in accordance with Chapter 12.

$$Q_b = Q_a \frac{n_b}{n_a} = 10,070 \times \frac{3550}{3560} = 10,030 \text{ c.f.m.} \quad 12.3$$

$$\begin{aligned} \epsilon_{p_b}^{0.283} - 1 &= (\epsilon_{p_a}^{0.283} - 1) \left(\frac{n_b}{n_a} \right)^2 \frac{T_{0_a}}{T_{0_b}} \\ &= 0.12307 \left(\frac{3550}{3560} \right)^2 \times \frac{550}{520} = 0.1294 \end{aligned} \quad 12.6$$

$\epsilon_{p_b} = 1.5373$ and $p_b = 1.5373 \times 14.70 = 22.60$ lb. per sq. in. abs.

The pressure rise = $22.60 - 14.70 = 7.90$ lb. per sq. in.

$$\begin{aligned} \text{b.hp.}_b &= \text{b.hp.}_a \left(\frac{n_b}{n_a} \right)^3 \left(\frac{p_{0_b}}{p_{0_a}} \right) \left(\frac{T_{0_a}}{T_{0_b}} \right) \\ &= 410.5 \left(\frac{3550}{3560} \right)^3 \left(\frac{14.700}{14.475} \right) \left(\frac{550}{520} \right) = 437 \end{aligned} \quad 12.8$$

or

$$\begin{aligned} \text{b.hp.}_b &= \text{b.hp.}_a \left(\frac{p_{0_b}}{p_{0_a}} \right) \left(\frac{Q_b}{Q_a} \right) \left(\frac{\epsilon_{p_b}^{0.283} - 1}{\epsilon_{p_a}^{0.283} - 1} \right) \\ &= 410.5 \left(\frac{14.70}{14.475} \right) \left(\frac{10,030}{10,070} \right) \left(\frac{0.12940}{0.12307} \right) = 437 \end{aligned} \quad 12.9$$

The performance curves as corrected for the contract conditions are plotted in Fig. 17·3.

CHAPTER 18

DISK STRESSES

18.1 Introduction. One of the important factors to be considered in designing impellers rotating at high speeds is the stress induced by the centrifugal force of the disk itself and of the attached vanes. The stresses created by the action of the fluid on the impeller are minor compared with those due to the rotation.

Any element of the disk will have three stresses acting on it, namely, radial, tangential, and axial. The latter is quite small and is neglected. Fundamental equations to determine the radial stress R and the tangential stress T existing in the disk were derived by Dr. A. Stodola of Zurich,* but the derivation is too lengthy to be repeated here. The equations are based upon the following assumptions:

(a) The disk is symmetrical about a plane perpendicular to the axis of rotation.

(b) The disk thickness varies only slightly, so the slope of the radial stresses toward the plane of symmetry is negligible.

(c) The stresses are uniformly distributed over the cross section.

In applying the basic equations, it is necessary to express the shape of the profile by some mathematical equation or have the profile closely approximate it. For special applications, a single equation may be used,** e.g., the De Laval constant strength disk. However, for general work the disk is usually divided into a number of sections having some particular shape such as conical rings,† constant thickness rings,‡ hyperbolas,§ etc., and then the stresses in these sections are found.

* Stodola-Loewenstein, *Steam and Gas Turbines*, McGraw-Hill, 1927, pp. 372-404, 1075-1090.

** Stodola-Loewenstein, *Steam and Gas Turbines*, p. 376; I. Malkin, "Design and Calculation of Steam-Turbine Disc Wheels," *A.S.M.E. Trans.*, APM-56-8, August, 1934.

† Dr. F. Selzman, "Families of Curves for Determining Stresses in Rotating Discs by Means of Conical Rings According to the Method of Keller," *Escher Wyss News*, July-September, 1938, p. 63.

‡ H. Haerle, "Strength of Rotating Discs," *Engineering*, August 9, 1918; Stodola-Loewenstein, *Steam and Gas Turbines*, McGraw-Hill, 1927, p. 380.

§ S. H. Weaver, "Disc Wheel Stress Determination," *A.S.M.E. Trans.* 39, p. 173.

The method using parallel-sided or constant-thickness rings gives accurate results and will be described here. Because of its simplicity and general adaptability to any type of disk or load condition it is widely used.

18.2 Sum and Difference Curves. This method uses the sum S and the difference D of the tangential T and radial R stresses as applied to parallel-sided disks, i.e.:

$$S = T + R \quad 18.1$$

$$D = T - R \quad 18.2$$

For the special case of a constant thickness disk, Stodola's basic equations reduce to

$$S = (1 + \nu) \frac{\gamma}{2g} [K_1 - u^2] \quad 18.3$$

$$D = (1 - \nu) \frac{\gamma}{4g} \left[u^2 + \frac{K_2}{u^2} \right] \quad 18.4$$

where $K_1 = \frac{4gb_1E}{\gamma(1 - \nu^2)}$ and $K_2 = \frac{8g\omega^2b_2E}{\gamma(1 - \nu^2)}$

ν = Poisson's ratio, or the ratio of the strain perpendicular to a force to the strain in the direction of the force
(0.3 for steel)

γ = specific weight of the material in pounds per cubic inch
(0.283 for steel)

u = tangential velocity in inches per second

g = acceleration of gravity = 386 in. per sec.²

ω = angular velocity in radians per second

E = modulus of elasticity = 29,000,000 for steel

b_1 and b_2 = constants depending upon the stress conditions at the bore and rim.

For a disk rotating at a given speed, the only variables for any given radius are K_1 and K_2 . Hence, arbitrary values of K_1 and K_2 may be assumed, and the values of S and D may be plotted against the tangential velocity u . In this way the chart shown in Fig. 18-1 is obtained.*

By means of the chart, the tangential and radial stresses at any radius in a parallel-sided disk can be found. As K_1 and K_2 are constants, any pair of curves which will satisfy the given stress conditions

* Figure 18-1 is in a pocket in the back cover of the book.

at the bore and rim will also give the values of S and D at points between. The correct pair is chosen by trial.

To illustrate, assume a parallel-sided disk rotating at 5000 r.p.m. has inside and outside diameters of $5\frac{1}{2}$ in. and $22\frac{1}{4}$ in. There is no external load at either bore or rim, i.e., the radial stress is zero at these two radii. The corresponding peripheral velocities are 120 and 486 ft. per sec. respectively, and the S and D curves should intersect on both these lines. By trial it may be seen that the only pair of curves which do this on Fig. 18-1 intersect at a stress of 20,700 lb. per sq. in. at the bore and at 5500 lb. per sq. in. at the rim. The values of K_1 and K_2 used in plotting these two curves were the correct ones for this particular case. The values of the radial and tangential stress at any point along the disk can be found from Eqs. 18-1 and 18-2:

$$R = \frac{S - D}{2} \quad 18-5$$

$$T = \frac{S + D}{2} \quad 18-6$$

18-3 Disk of any Profile. The sum and difference curves may be applied to an impeller of any profile by approximating its shape with a number of constant-thickness sections as shown by the dotted lines in Fig. 18-2 and assuming that the stress varies over each section as for a parallel-sided disk. These imaginary parallel-sided sections will have different widths. In the transition from one width to the adjoining width it is assumed that the radial stress varies inversely with the thickness and that the change in the tangential stress equals the change in the radial stress times Poisson's ratio.

The procedure for calculating the stresses follows the outline given below.

1. Make a scale drawing of the impeller on the chart with the widths plotted in inches, but in place of radial dimensions use tangential velocities in feet per second as shown in Fig. 18-2.

2. Divide the impeller into a series of constant-thickness rings; this gives the impeller the stepped profile shown by the dotted lines.

3. Calculate the radial stress at the rim and bore (if any). It is the external load divided by the circumferential area of the impeller at the point considered.

4. Assume a tangential stress at the rim.

5. Determine the values of S and D at the rim on the basis of the radial stress R at this surface (from step 3) and the assumed tangential stress T (from step 4), by means of Eqs. 18-1 and 18-2.

6. Plot the values of S and D from step 5 on the chart at the rim tangential velocity and follow the respective curves to the tangential velocity line corresponding to the first transition point or change in thickness.

7. The radial stress at the base of the ring is given by Eq. 18-5, $R = \frac{S - D}{2}$. If t is the thickness of the upper ring and t' is the thickness of the lower ring, the change in radial stress ΔR is

$$\Delta R = R \left(1 - \frac{t}{t'} \right) \quad 18-7$$

8. From the assumption that the change in the tangential stress equals the change in the radial stress times Poisson's ratio (which is taken as 0.3 for steel), these changes in the sum and difference values at the transition point follow:

$$\Delta S = \Delta R + \Delta T = \Delta R + \nu \Delta R = \Delta R(1 + \nu) = 1.3\Delta R \quad 18-8$$

$$\Delta D = \Delta T - \Delta R = \nu \Delta R - \Delta R = \Delta R(\nu - 1) = -0.7\Delta R \quad 18-9$$

9. From step 8 points on the new S and D curves may be found for starting the second ring. These new curves may be followed to the base of the second ring, where the above process is repeated, and so on to the bore of the disk.

10. The S and D curves at the bore must give the calculated value of radial stress from step 3. If it does not, the proper tangential stress at the rim was not assumed in step 4. Hence, another trial must be made with a new assumed tangential stress. At the most, only three trials need to be made, as it has been found* that a straight-line relationship exists between the assumed tangential stress at the rim and the calculated radial stress at the hub. If the first two trials are plotted, the tangential stress to be assumed for the third trial can be found by either interpolation or extrapolation.

11. Upon finding the correct set of S and D curves, the values of the tangential and radial stress at any radius may be found from Eqs. 18-5 and 18-6. It is more exact to find these stresses at the mid-points of the rings and, after plotting them, to draw smooth curves through these points to get a complete curve of the radial and tangential stresses along the disk.

The S and D curves will intersect at any point where the radial stress is zero. In most cases, there will be no external load at the

* M. G. Driessen, "A Simplified Method of Determining Stresses in Rotating Disks," *A.S.M.E. Trans.*, APM-50-10, 1928.

rim of the impeller, hence the curves should intersect at this radius. If there is no radial pressure between hub and shaft at the running speed the radial stress will again be zero. However, if a pressure does exist here as a result of a shrink fit its value is equal to the radial stress.

18.4 Dead Weight of Vanes. The impeller vanes, because of the centrifugal force acting upon them, increase the stresses induced in the impeller; but since these stresses are not continuous they do not contribute to the strength. The additional stress due to this dead load may be cared for by the following procedure through the use of the sum and difference curves.

(a) The vanes are divided into a number of imaginary lengths, generally extending between the points of transition of the imaginary parallel-sided rings making up the impeller.

(b) The centrifugal force of each length is found from the equation

$$F = \frac{W u^2}{g r} \quad 18.10$$

where W = the weight of the length in pounds

u = the peripheral velocity of the approximate center of gravity of the length in feet per second

r = the radius of the approximate center of gravity of the length in feet

g = acceleration due to gravity = 32.2 ft. per sec.²

(c) The additional radial stress R' due to this load may be considered to act at the outer side of the inner ring of the step. It equals the total force for all the vanes, zF , divided by the circumferential area of the outer side of the inner ring, i.e.,

$$R' = \frac{zF}{\pi t' d}$$

(d) After the change in radial stress ΔR at the step is found (Eq. 18.7), the additional external radial stress R' is subtracted from it before the change in the sum and difference curves of step 8 of Section 18.3 is found.

(e) The rest of the procedure is the same as that outlined in the previous section.

If the impeller has two shrouds, it may be assumed that each carries an equal share of the dead load.

18.5 Notes on the Use of the Chart. The impellers are generally run at 25 per cent above the normal speed before leaving the factory to guard against manufacturing defects, and the stresses are usually calculated for this condition.

Occasionally the peripheral speeds or induced stresses may exceed the chart limits. Since the stresses are proportional to the speed squared, the calculation may be made at a lower speed and the stresses may be stepped up in the ratio of the square of the speed.

Figure 18-1 may be used indefinitely by drawing the lines on a piece of tracing paper placed upon it. This tracing may be filed with the other design calculations.

In the procedure outlined previously, the method was to start at the rim and work toward the bore. It may often be desirable to reverse this and start at the bore. This will, of course, not effect the results or the amount of work involved.

The general rule is to keep the maximum stresses in the disk at 15 to 20 per cent overspeed below one-third of the yield point of the material to care for stress concentrations, fatigue, etc. However, the tangential stress at the bore is sometimes allowed to go considerably higher (up to 60 per cent). This may result in local yielding when the disk is first rotated, but the impeller then acquires a permanent set which offsets the high stress. It may cause the disk to become loose on the shaft, so should be used with discretion.

On the chart a line is shown starting at zero stress and velocity and curving upward to the left. This shows the tangential stress existing in a thin ring at the various velocities; it may be used to determine whether the ring will carry itself or impose an additional load on the impeller.

Rim and Bore Conditions. The sum and difference curves will intersect at any point where the radial stress is zero. This will occur at the rim unless the vanes overhang as for an open-type impeller. It may also occur at the bore provided there is no radial pressure between the hub and shaft.

Generally the radial pressure between the hub and shaft should have a slight positive value at overspeed to prevent any looseness of the impeller. This condition determines the fit between the hub and shaft.

Where the disk at some radius merges into a solid rotor or drum, the assumption may be made that the drum is a disk of constant strength, or that the radial and tangential stresses are equal and constant, i.e., the D curve should cross the zero stress line at or near this point.

The diameter of the bore should include keyways, as they break up the tangential stress lines. Small holes well spaced, especially if quite far from the center, may be neglected, but again this is a matter for judgment. The holes are usually well rounded and polished to avoid any stress concentrations which might start fatigue failures.

Impellers not Made of Steel. The usual sum and difference charts are plotted for steel. For any other material, a new chart could be plotted, but it would be quite laborious. An inspection of Eqs. 18-3 and 18-4 shows that the only factors involving the material are the specific weight γ and Poisson's ratio ν , since the chart is plotted with assumed values of K_1 and K_2 . Approximate values of these properties, as taken from handbooks for common impeller materials, are

Steel	$\gamma = 0.283$	$\nu = 0.30$
Brass	$\gamma = 0.315$	$\nu = 0.33$
Cast aluminum	$\gamma = 0.100$	$\nu = 0.33$
Cast iron	$\gamma = 0.256$	$\nu = 0.27$
Bronze	$\gamma = 0.308$	$\nu = 0.35$

A value of Poisson's ratio of 0.30 may be used for all these materials without a great error. If this is done the values of S and D or stress will be directly proportional to the specific weights, i.e., the stress scale is compressed or extended in that ratio. Thus, an impeller of any common material may be calculated as if it were made of steel; but the resulting radial and tangential stresses must be reduced in the ratio of $\gamma_m/0.283$, where γ_m is the specific weight of the impeller material.

18-6 Example. To illustrate the calculation procedure the stresses in the back shroud of the steel impeller, designed in Section 13-10 (Fig. 13-4) will be found at 25 per cent overspeed, i.e., 4500 r.p.m. The dead weight due to the 20 vanes riveted to the shrouds will be included.

The impeller is drawn to scale with the radial dimensions expressed in feet per second and the axial dimensions in inches (see Fig. 18-2). It should be observed that the hub diameter is taken as $8\frac{1}{2}$ in. (167 ft. per sec.) rather than 8 in. (157 ft. per sec.) to allow for the $\frac{1}{4}$ in. x $\frac{7}{8}$ in. keyway. The profile is then approximated by eight parallel-sided rings as shown by the dotted lines. The width of each ring is scaled on the drawing and noted there.

There is no radial stress at the rim, and a tangential stress there of 8500 lb. per sq. in. is assumed; so the S and D curves meet at a speed of 786 ft. per sec. and a stress of 8500 lb. per sq. in. This is entered in the first line of Table 18-2.

Before proceeding, the induced stresses due to the centrifugal loading of the steel vanes must be found. For this purpose the vane is divided into three lengths and the centrifugal force acting on each is calculated as shown in Table 18-1.

The normal vane thickness is $\frac{1}{8}$ in. and the circumferential thickness t_θ equals $0.125/\sin \beta$. The thickness at the inlet and outlet are calculated and the other values are found by proportion, as shown above. The vane is made of sheet metal with a $\frac{1}{2}$ -in. strip bent over for rivet-

TABLE 18-1

u ft. per sec.	D in.	β	$t_v = \frac{0.125}{\sin \beta}$ in.	b in.	L in.	$V = bLt_v$ cu. in.	r ft.	CF per Vane lb.	CF_{TOT} lb.
786	40.00	65°	0.138	3.84					
718			0.156	4.00	3.42	2.135	1.524	6360	127,200
650	33.16		0.171	4.16					
584			0.187	4.32	3.42	2.760	1.239	6670	133,400
517	26.32		0.203	4.48					
450			0.220	4.64	3.41	3.480	0.954	6550	131,000
383	19.50	32°	0.236	4.80					

ing on each side. Hence, the gross vane width is the actual width plus 1 in. The length L is the radial length; therefore the volume V equals bLt_v and the centrifugal force equals $\frac{\gamma V u^2}{g r}$ per vane. The total centrifugal force is the product of the force per vane and the number of vanes, 20.

Assuming that these loads act at the outer side of the inner ring of the step and that each shroud carries one-half the total centrifugal load, the radial stresses induced are:

d in.	t' in.	$A = \pi dt'$ in. ²	CF per Shroud lb.	R' lb. per sq. in.
33.16	0.615	64.1	63,600	993
26.32	0.860	71.2	66,700	937
19.50	1.300	79.7	65,500	822

Following the S and D curves from 8500 at $u = 786$ to $u = 650$, the values at the inner side of the outer step are $S = 22,000$ and $D = 3500$

By Eq. 18-5, $R = \frac{22,000 - 3500}{2} = 9250$. The width correction is

$1 - \frac{0.375}{0.615} = 0.39$, and hence the change in radial stress ΔR is $0.39 \times$

9250 or 3610 lb. per sq. in. The external radial stress R' of 993 lb. per sq. in. is subtracted from this, or $3610 - 993 = 2617$. By Eqs. 18-8 and 18-9,

$$\Delta S = 1.3(\Delta R) = 1.3 \times 2617 = 3400 \text{ lb. per sq. in.}$$

$$\Delta D = -0.7(\Delta R) = -0.7 \times 2617 = -1830 \text{ lb. per sq. in.}$$

and the values of S' and D' for the next step are

$$S' = S - (\Delta S) = 22,000 - 3400 = 18,600$$

$$D' = D - (\Delta D) = 3500 - (-1830) = 5330$$

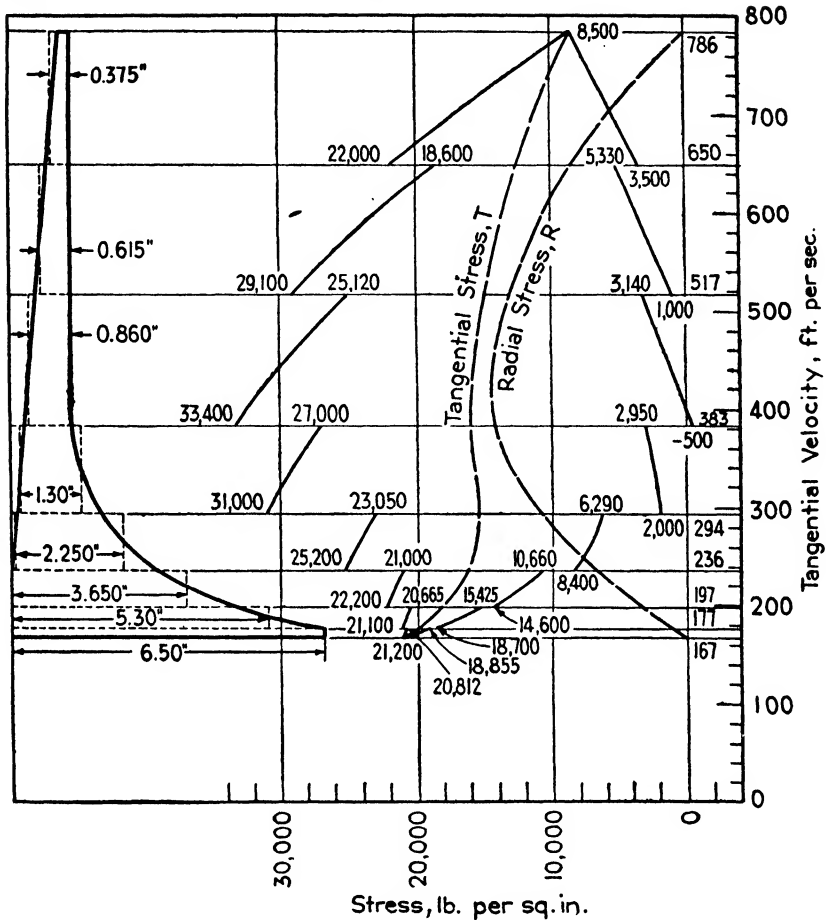


FIG. 18-2. Determination of stresses in impeller of Fig. 13-4 when rotating at 4500 r.p.m.

This procedure is repeated for the succeeding rings with the values noted in Table 18-2 and the curves as shown in Fig. 18-2.

The radial and tangential stresses are found by Eqs. 18-5 and 18-6 from the curves, at points where the assumed rings coincide with the actual impeller, and they are plotted. These points are then joined by smooth curves labeled *R* and *T* to give the values of these stresses at any point in the impeller.

PROBLEMS

18-1 A constant-thickness disk has a rim speed of 500 ft. per sec. and a bore speed of 165 ft. per sec. If the radial stress at the bore and rim is zero, what are the tangential stresses at these points?

Ans. Rim 7,000; bore 22,000.

18.2 The disk shown in Fig. 18.3 rotates at 5000 r.p.m. The radial stress at the bore and rim is zero. Thirteen 1-lb. vanes are attached to the disk at *AA*.

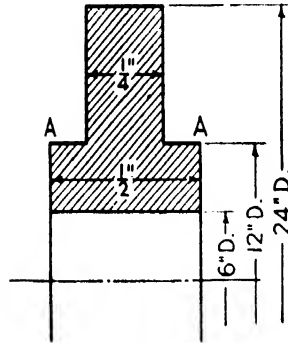


FIG. 18.3.

Assuming the center of gravity of the vanes is at a radius of 6 in., determine the radial and tangential stresses throughout the disk.

Ans. Tangential stresses: rim, 6000; bore, 21,600.

CHAPTER 19

CRITICAL SPEEDS

19·1 Introduction. As the speed of rotation of a machine is gradually increased it will be observed that at certain speeds the shaft may vibrate violently whereas at speeds below and above these it will run relatively quietly. The speeds at which the severe vibrations occur are known as the *critical speeds* of the shaft. If a unit operates at or near a critical speed, large amplitudes will be built up. Such a condition results in dangerously high stresses, possible rubbing of the rotating parts, and an undesirable vibration being transmitted to the foundations. It is, therefore, quite important that the shaft be designed so that the critical speeds are 20 to 30 per cent above or below the running speed. Further information on critical speeds may be found in books on vibration.*

19·2 Action at the Critical Speed. Extremely few shafts are in perfect balance. Owing to slight machining inaccuracies the center of mass and the geometric center of rotation do not coincide, although the difference may amount to only a few ten-thousandths of an inch. Rotation produces a centrifugal force of the mass center which is balanced by the springing action of the shaft.

Kimball and Hull† explain the physical action which takes place while the shaft passes through the critical speed. They show that below the critical speed the center of mass rotates in a circle about the geometric center, whereas above it the shaft rotates about the center of mass. Thus the axis of rotation is changed at the critical speed from the geometric center to the mass center. When the shaft rotates at the critical speed the restoring force of the shaft is neutralized and the action is dynamically unstable, hence large amplitudes of vibration may occur.

The critical speed coincides with the natural frequency of vibration of the shaft, which may be found by the principles developed by Lord

* Den Hartog, *Mechanical Vibrations*, McGraw-Hill, 1940; Freberg and Kemler, *Elements of Mechanical Vibrations*, John Wiley, 1943; Timoshenko, *Vibration Problems in Engineering*, Van Nostrand, 1937.

† Kimball and Hull, "Vibration Phenomena of a Loaded Unbalanced Shaft," *A.S.M.E. Trans.*, 1925, p. 673.

Rayleigh.* He found that a body vibrating at its natural frequency does so with simple harmonic motion and that all points on the body come to rest at the same time and attain their maximum velocity simultaneously, even though they are completely out of phase.

A vibrating body contains energy. When the points on the body are at rest their displacement is a maximum and all the energy is potential, equaling $\frac{1}{2}Wy$ where W is the weight of the point in pounds and y is the corresponding displacement in inches. When the displacement is zero the energy is entirely kinetic and, since the motion at the natural frequency is simple harmonic, equals $\frac{1}{2} \frac{W}{g} y^2 \omega^2$, where ω is the angular velocity in radians per second and g equals 386 in. per sec.².

Since the total energy in the system remains constant (neglecting losses) the maximum potential and kinetic energies may be equated to determine the frequency. If a shaft has a number of weights W_1, W_2 , etc., placed along it and the corresponding maximum deflections of the weights are y_1, y_2 , etc.,

$$\text{Maximum potential energy} = \frac{1}{2} W_1 y_1 + \frac{1}{2} W_2 y_2 + \text{etc.}$$

$$\text{Maximum kinetic energy} = \frac{1}{2} \frac{W_1}{g} \omega^2 y_1^2 + \frac{1}{2} \frac{W_2}{g} \omega^2 y_2^2 + \text{etc.}$$

Equating:

$$\omega = \frac{\sqrt{\frac{1}{2} W_1 y_1 + \frac{1}{2} W_2 y_2 + \text{etc.}}}{\sqrt{\frac{1}{2} \frac{W_1}{g} y_1^2 + \frac{1}{2} \frac{W_2}{g} y_2^2 + \text{etc.}}} = \sqrt{g} \sqrt{\frac{\sum Wy}{\sum Wy^2}} \text{ radians per second}$$

or

$$F = \frac{60\omega}{2\pi} = \frac{60\sqrt{g}}{2\pi} \sqrt{\frac{\sum Wy}{\sum Wy^2}} = 187.5 \sqrt{\frac{\sum Wy}{\sum Wy^2}} \text{ cycles per minute } 19\cdot1$$

Lord Rayleigh developed an important principle which is of great use in vibration work. This principle states that in any vibrating system the displacements of the system are such that, when the maximum potential and kinetic energies are equated to each other, the lowest frequency is obtained. If the displacements are taken any other way, the frequency will be higher, i.e., the system deflects naturally so that its frequency is a minimum. This principle is applicable to any of the possible modes of vibration.

* Lord Rayleigh, *Theory of Sound*, 1894.

If many deflection curves are assumed for the assembled shaft and the values of W_1 , W_2 , etc., and y_1 , y_2 , etc., are substituted in Eq. 19-1, the critical speed will approximate the lowest frequency F obtained.

A good initial assumption for the deflection curve would be to use the static deflection curve based upon the shaft and impeller weights combined with the shaft dimensions. The resulting frequency will be slightly high as the actual deflection curve is due to the centrifugal force $\frac{W}{g}y\omega^2$ rather than the static weight W . If a more

accurate value is desired the shaft loading may be taken as $\frac{W}{g}y\omega^2$, where ω is an assumed angular velocity and y is taken from an assumed deflection curve. The new deflection curve will more closely approximate the actual curve. Equation 19-1 may then be used to secure a new frequency by using the product of centrifugal force in place of W and the revised deflections due to this centrifugal force for y .

For practical cases the frequency based upon the static deflection curve alone is sufficiently accurate. The critical speed has not one particular value but extends over a fairly broad range. It has been found from experience that a considerable change in the loading is required to change the deflection curve appreciably. The calculated value may be altered by other factors such as bearing flexibility, gyroscopic action of the impellers, and the fit between the impeller and the shaft. It is difficult to predict the magnitude of these effects. They are discussed further in Section 19-5.

From the above discussion it is apparent that the critical speed is approximately inversely proportional to the square root of the static deflection. For beams or shafts the static deflection is proportional to WL^3/EI , so the critical speed is proportional to $1/\sqrt{W}$, $1/L^{3/2}$, \sqrt{E} , \sqrt{I} or D^2 . These ratios are quite useful in estimating the changes which may be made in a shaft to bring the critical speed to a safe value.

The critical speed may be placed either above or below the operating speed. If the unit is to operate at high speeds which do not vary widely the critical speed may be below the operating speed and the shaft is said to be flexible. If the operating speed is low or must vary through wide ranges the critical speed is placed above it and the shaft is called rigid or stiff.

19-3 Critical Speed of a Two-Bearing Stepped Shaft. The determination of the lowest critical speed of a two-bearing stepped shaft is essentially a problem in graphic statics to determine the static deflection curve due to the impeller loads and the shaft weight. The

basic principles are covered in books on strength of materials* so need not be repeated here. The procedure will be outlined with the aid of an example shown in Fig. 19-1. The various portions of this figure will be designated by capital letters in parentheses throughout the remainder of this section. The scales to which the figure is drawn apply to the original. These were necessarily reduced in printing.

Part (A) shows an overhung stepped shaft, fully dimensioned, drawn to a space scale of 1 in. = 8 in. It has two impellers, one weighing 50 lb. and the other 10 lb., located on it. The left bearing is located at the left end of the shaft and the right bearing is 10 in. in from the right end. The impeller weights are listed under the loads in line (B). The shaft weight is found by dividing the shaft into a number of lengths, calculating the weight of each, and assuming that these loads act at the midpoint of each length. These loads are listed in line (C). The shaft weights are added to the impeller weights to give the total loads in line (D). The loads between the bearings act downward, whereas those to the right of the right bearing act upward. Owing to the shaft deflection while whirling at the critical speed, the centrifugal forces will act outward and the static loading must be taken accordingly.

These total forces of line (D) are represented vectorially in line (E) and labeled according to Bow's notation. The forces are laid off successively to a scale of 1 in. = 30 lb. on the vertical line of part (F) (the distance ab represents force ab , etc.), and they are laid off in the direction in which they act. A pole p is located $1\frac{1}{4}$ in. from the vertical line and the radial lines from p to a , b , etc., are drawn. The pole distance is made $1\frac{1}{4}$ in. to make the moment scale an even value, so the moments may be read off directly with the aid of an engineer's decimal scale. The vertical location of the pole p does not matter, but a neater diagram generally results if it is placed opposite the midpoint of the vertical line.

The moment diagram (G) is now drawn starting at the left bearing with line a parallel to line pa of part (F), line b parallel to pb , etc. The lines in part (G) are located directly below the correspondingly labeled spaces of part (E); thus the d line is located in the d space between the loads cd and de , and the h line in the h space between the loads gh and hk , etc. The polygon is closed by drawing in the k line between the bearings. A line drawn parallel to this k line on part (F) gives the bearing reactions graphically by the lengths hk and ka . The moment at any point on the shaft is given by the vertical distance between lines k or h and the other lines to a scale of 1 in. = space

* A. Morely, *Strength of Materials*, Longmans, 1935, pp. 197-208.

scale \times force scale \times pole distance, or $1 \text{ in.} = 8 \times 30 \times 1\frac{1}{4} = 300 \text{ in.-lb.}$ The values of the moment M as scaled from part (G) are listed on line (H).

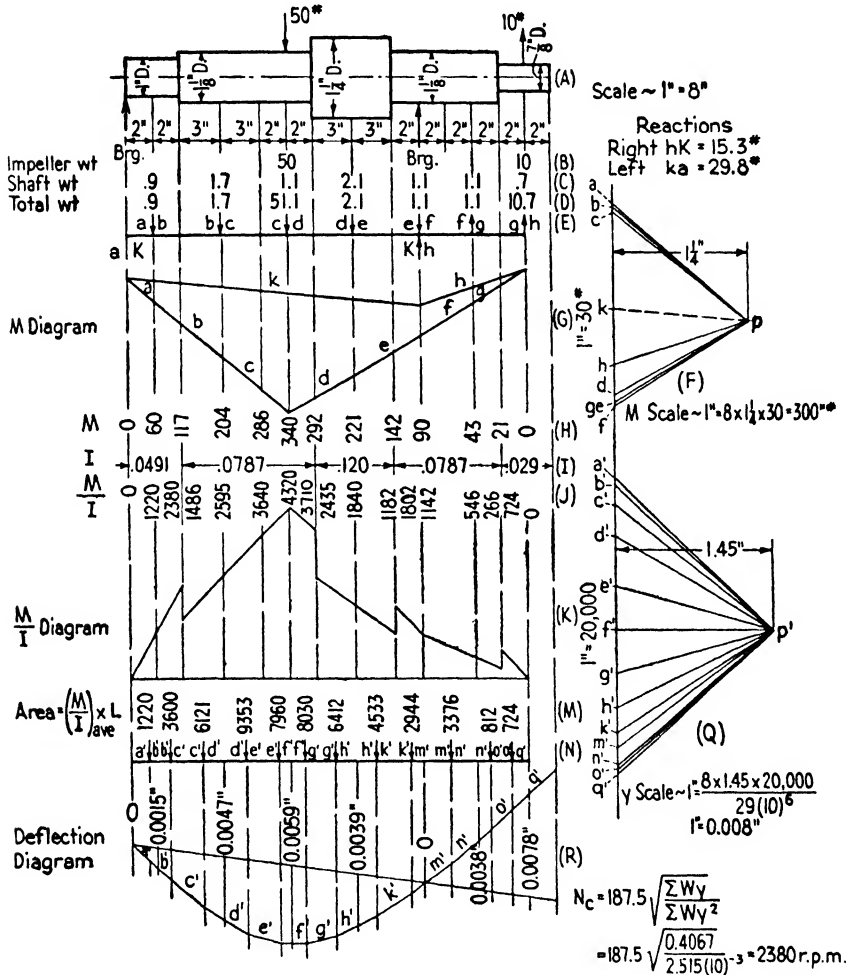


FIG. 19-1. Graphical determination of critical speed of two-bearing, stepped shaft.

The moment of inertia I of the various sections are calculated and shown on line (I). The values of M/I are calculated, listed on line (J), and plotted to form an M/I diagram (K). The value of M/I changes instantaneously with a change in shaft diameter.

A conjugate beam is assumed to be loaded with the area under the M/I diagram. These areas are calculated and listed on line (M) and

represented by the vectors on line (*N*). For example, for vector $b'c'$, area = $\left(\frac{M}{I}\right)_{\text{ave.}} L = \left(\frac{1220 + 2380}{2}\right)2 = 3600$. These imaginary loads will act at the center of gravity of the areas, which may be approximated with sufficient accuracy. They are laid off successively on the vertical line of part (*Q*) to a scale of 1 in. = 20,000. A pole p' is assumed 1.45 in. to the right of the vertical line, and the radial lines $p'a'$, $p'b'$, etc., are drawn. The pole distance is again selected to make the deflection scale an even value to facilitate reading off deflections with an engineer's decimal scale. The vertical location of the pole p' is again immaterial.

The deflection curve (*R*) is drawn similarly to the moment diagram, i.e., line a' is parallel to $p'a'$ in the a' space, b' is parallel to $p'b'$ in the b' space, etc. As it is assumed that the bearings do not deflect, the closing line crosses the deflection curve at the bearings. The deflection scale is given by multiplying the space scale by the pole distance of part (*Q*) by the area scale and dividing by the modulus of elasticity E ; y scale 1 in. = $\frac{8 \times 1.45 \times 20,000}{29,000,000} = 0.008$ in. The vertical distance between the closing line and the curve at any point represents the deflection. The deflections under the loads are listed on the deflection diagram.

The critical speed is then found from Eq. 19·1:

<i>W</i>	<i>y</i>	<i>y</i> ²	<i>Wy</i>	<i>Wy</i> ²
0.9	0.0015	2.25 (10) ⁻⁶	0.0013	2.03 (10) ⁻⁶
1.7	0.0047	22.09 (10) ⁻⁶	0.0080	37.55 (10) ⁻⁶
51.1	0.0059	34.81 (10) ⁻⁶	0.3015	1778.80 (10) ⁻⁶
2.1	0.0039	15.21 (10) ⁻⁶	0.0082	31.94 (10) ⁻⁶
1.1	0	0	0	0
1.1	0.0038	14.44 (10) ⁻⁶	0.0042	15.88 (10) ⁻⁶
10.7	0.0078	60.84 (10) ⁻⁶	0.0835	651.00 (10) ⁻⁶
			0.4067	2517.20 (10) ⁻⁶

$$n_c = 187.5 \sqrt{\frac{\sum Wy}{\sum Wy^2}} = 187.5 \sqrt{\frac{0.4067}{2517.2(10)^{-6}}} = 2380 \text{ r.p.m.}$$

The running speed of the shaft should be at least 20 per cent away from the critical, i.e., it should not operate between speeds of 1900 and 2860 r.p.m.

It is not necessary to construct the M/I diagram (*K*). It was done in Fig. 19·1 to clarify the procedure, but the M/I values are all that are required to get the deflection curve.

19.4 Higher Critical Speeds of Two-Bearing Shafts. A vibrating system may have as many modes of vibration as it has degrees of freedom. Each mode has a particular frequency which is unique to it. A shaft having a distributed load has an infinite number of lateral modes of vibration and consequently an infinite number of natural frequencies or critical speeds. Only the first one or two of these are of practical importance, the others being much higher than any ordinary running speed. The first four modes are shown in Fig. 19-2 for a shaft with a uniformly distributed load (vibrating string). The more complex the curve shape, the higher the critical speed and the smaller the maximum deflection.

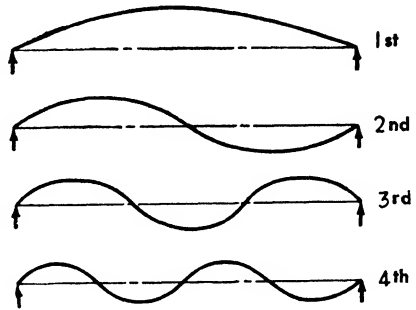


FIG. 19-2. Modes of vibration of uniformly loaded two-bearing shaft.

When a stepped shaft with many loads spaced unequally along it is considered, the higher critical speeds are quite difficult to determine. The usual procedure is to assume a curve shape and from this is found the centrifugal loading $\frac{W}{g} y \omega_{ass}^2$. With this loading the deflection curve is found graphically; it should coincide with the assumed curve.

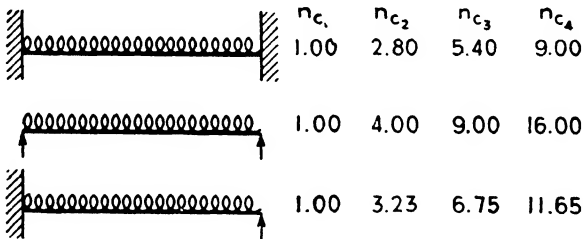


FIG. 19-3. Ratios of higher critical speeds for various end conditions of two-bearing uniformly loaded shafts.

If it does not, a second assumption must be made until agreement is reached. The process is not convergent as it is for the first critical speed. Usually many trial assumptions must be made and several days may be consumed in finding a satisfactory value.

For a uniform diameter shaft with symmetrical loads, the curve shape may be predicted sooner. Figure 19-3 gives the ratio of the higher speeds to the lowest for several special cases with continuous

loads. They may be used as a guide in estimating the higher speeds in more complicated cases.

19-5 Factors Influencing the Critical Speed. There are many factors which may change the critical speed from the calculated value. Frequently the magnitude of their effect cannot be determined accurately. When special cases arise in which they become important or in which it is necessary to account for discrepancies between test results and calculated values, the references given below in footnotes may be consulted for further details.

Bearing Length. It is usually assumed that the shaft is simply supported and this assumption is justified if the bearings are free to oscillate and adjust themselves to the shaft deflections. Often the bearings are fixed and, if long compared to their diameter, they may tend to create the effect of a fixed support. This decreases the shaft deflection and raises the critical speed.

As the shaft deflects, the center of pressure of the oil film is no longer at the bearing centerline but tends to move in toward the main mass. A general rule is to move the assumed bearing center "in" toward the main mass about one-sixth of the bearing length when fixed bearings are used.*

Gyroscopic Effect of the Impellers. If the impellers are heavy and have a large diameter, they create a gyroscopic action and resist any change in the direction of their axis. When the shaft begins to whirl, the impeller resists the motion and tends to keep it straight, thus reducing the deflection and raising the critical speed. This effect is greater for impellers nearer to the bearings where the slope of the shaft is greater.†

Bearing Elasticity. The usual assumption made in calculating the deflection curve is that the bearings are rigid and do not deflect. Actually every bearing will deflect somewhat because of the load on it. This will tend to lower the critical speed, since the deflection is greater than calculated, and may be as much as 25 to 50 per cent. The bearings may deflect more in one direction than another (as for the pedestal type which is not so rigid horizontally as it is vertically), resulting in two distinct critical speeds for the same shaft. It is very difficult to predict the bearing deflection in advance, but it may be measured in a unit already manufactured to account for discrepancies.‡

Shrink Fits of Impeller Hubs. If the hubs are quite heavy and

* See Stodola-Loewenstein, *Steam and Gas Turbines*, p. 430.

† See Stodola-Loewenstein, *Steam and Gas Turbines*, McGraw-Hill, pp. 430-437; Timoshenko, *Vibration Problems in Engineering*, Van Nostrand, 1937, p. 290.

‡ See A. L. Kimball, *Vibration Prevention in Engineering*, Wiley, 1932, p. 72.

shrunk tightly on the shaft they tend to stiffen it and raise the critical speed. It is difficult to predict the amount of the stiffening because of manufacturing uncertainties in the tolerances but the effect may be appreciable.

19-6 Critical Speeds of Three-Bearing Shafts. The critical speeds of three-bearing shafts are rather difficult to determine, especially if the loading and shaft sizes are not symmetrical. The procedure of assuming a deflection curve and frequency and deriving a new deflection curve on the basis of the centrifugal loading, as outlined in Section 19-4, may be followed. This may require many trials and may be very tedious. For a three-bearing shaft, a graphical method developed by W. von Borowicz* may be used.

Borowicz's method determines influence factors for each portion of the shaft, i.e., for the two portions of the shaft between the pairs of bearings. After a number of these portions have been calculated the critical speeds may be found for various combinations of the portions. The need for adopting the cut-and-try procedure mentioned above is obviated.

The procedure for locating the first critical speed will be outlined here with the aid of Fig. 19-4. The loading on the left portion of the shaft (between the left and center bearings) will be designated as I, and that on the right portion (between the center and right bearings) as II. These loadings will be considered separately. The loads on the shaft may be taken as the centrifugal forces based upon an assumed deflection and frequency (this is the more accurate method) or the static deflections due to the weight may be used. For the first critical speed the loads on the two portions of the shaft will act in opposite directions. The procedure follows.

1. Draw the shaft to scale and determine the loading, using either centrifugal forces or weights (*A*). In this example the static deflections due to the impeller weights are considered and the shaft weight is neglected for simplification.

2. Consider that the right-hand bearing is removed and that loads act on the left portion of the shaft only. Construct the moment diagram (not shown) and the deflection curve for the complete shaft. Between the center and right bearing this will be a straight line (only partially shown) tangent to the curve at the center bearing since no loads act upon it.

* *Beitrag zur Berechnung der kritischen Geschwindigkeiten von zwei- und mehrfach gelagerten Wellen, dissertation*, München, 1915. For a complete discussion of the theory see the original dissertation, or Section 92, p. 457, of *Steam and Gas Turbines* by Stodola-Loewenstein.

3. The total value of M/I areas for step 2 is designated as I and equals 1700 for this case. It will act at the intersection of the end tangents to the deflection curve as shown in (B) .

4. Steps 2 and 3 are repeated in (C) , considering that the left bearing is removed and that loads act on the right portion of the shaft only. The total value of the M/I areas is called II and equals 2646.

5. For each of the load conditions considered above a load must be applied at the free end of the shaft to bring it back to the bearing. If this is the only load acting on the shaft the bending moment diagram will appear as shown at (D) for both cases. The maximum moment will occur at the center bearing. Any value may be used for this moment (100 in.-lb. is used in the example).

6. If the moment diagram of step 5 is created by a free load acting at the left bearing (which has been removed) the shaft deflection curve for the right portion of the shaft alone is shown at (E) . The sum of the M/I areas for this portion is called II_0 and equals 264. The line of action of II_0 is again at the intersection of the end tangents to the deflection curve.

7. This is a repetition of step 6 except that the right bearing is removed and the load is applied at that point. The deflection curve of the left portion of the shaft is shown at (F) . The sum of the M/I areas for this portion is designated as I_0 and equals 734. The line of action of I_0 is at the intersection of the end tangents of the deflection curve as shown.

8. The four deflection curves shown at (B) , (C) , (E) , and (F) must be combined to give a resultant deflection curve. This may be done graphically as illustrated at (G) .

9. On a horizontal base line ab project the line of action of I , I_0 , II , and II_0 as found above.

10. On the line of II_0 lay off to a convenient scale a distance equal to I_0 , i.e., 734, below the base line.

11. On the line of I_0 lay off to the same scale a distance equal to II_0 , i.e., 264, above the base line.

12. Join steps 10 and 11. This line crosses the base line to locate the point of action of $I_0 + II_0$.

13. Draw any line from a , and then the following lines as shown on the diagram: dcf , efg , and gmb .

14. Lay off bh to the same scale as used in steps 10 and 11, a distance equal to II , i.e., 2646.

15. Draw hm parallel to ef , mj parallel to ad , and mk parallel to cd .

16. The distance hk is designated as I'_0 and scales as 510; the distance hj as II'_0 and scales as 1430.

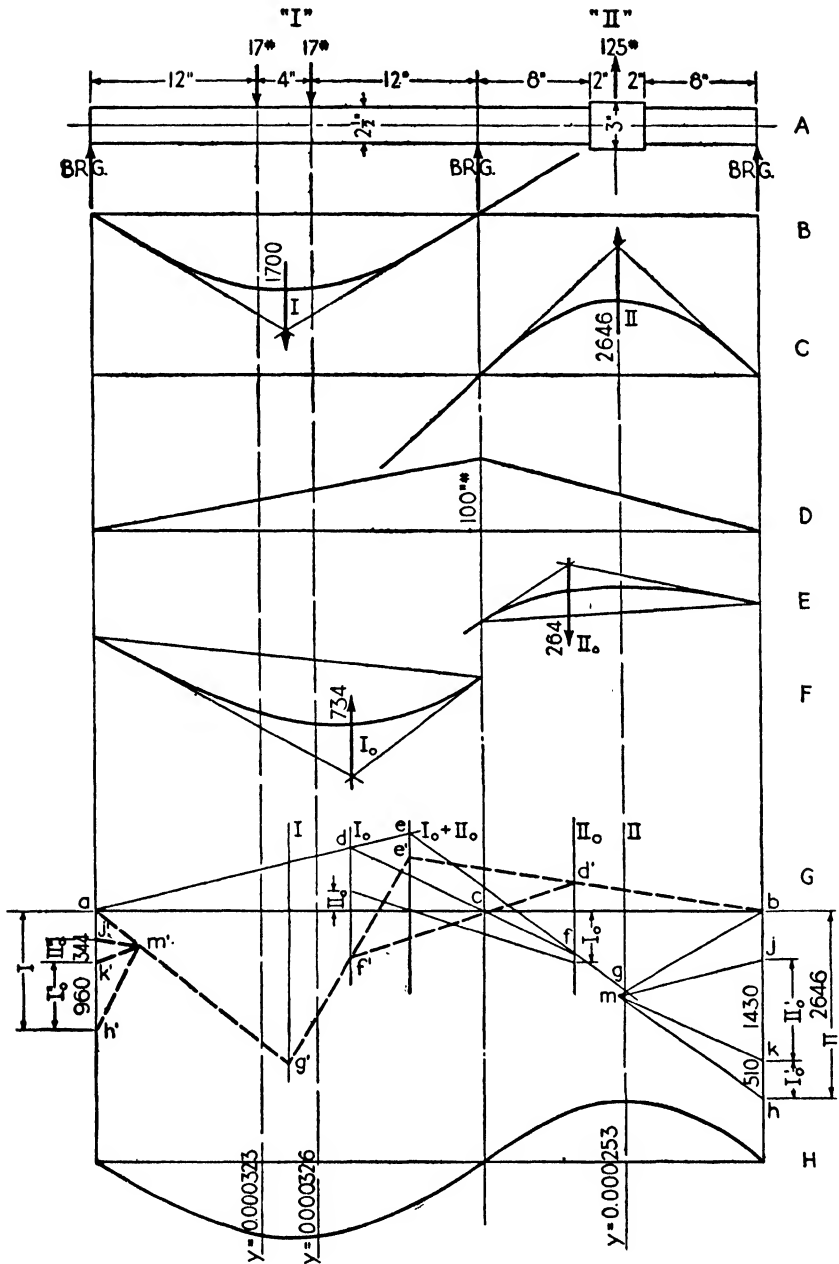


FIG. 19-4. Determination of critical speed of three-bearing stepped shaft considering impeller weights alone.

17. A coefficient α_2 is now found and equals

$$\alpha_2 = \frac{I'_0}{II_0} = \frac{hk}{II_0} = \frac{510}{264} = 1.93$$

or

$$\alpha_2 = \frac{II'_0}{I_0} = \frac{kj}{I_0} = \frac{1430}{734} = 1.95$$

An average value of 1.94 may be used for α_2 .

18. Steps 10 to 15 are repeated for the left portion of the shaft as shown by the dotted lines and primed letters in part (G).

19. The distance $h'k'$ is designated as I''_0 and scales as 960, and the distance $k'j'$ as II''_0 and scales as 344.

20. A coefficient α_1 is now found; it equals

$$\alpha_1 = \frac{I''_0}{I_0} = \frac{h'k'}{I_0} = \frac{960}{734} = 1.307$$

or

$$\alpha_1 = \frac{II''_0}{II_0} = \frac{k'j'}{II_0} = \frac{344}{264} = 1.302$$

An average value of 1.304 may be used for α_1 .

21. The resultant deflection on the left portion of the shaft is given by

$$y'_{10} = y_1 - y_{10}(\alpha_1 - \alpha_2) \quad 19.2$$

where y'_{10} is the resultant deflection at any point on the left portion

y_1 is the deflection due to the left loading alone (B)

y_{10} is the deflection due to the load at the free end (E).

Since $\alpha_1 - \alpha_2 = 1.304 - 1.940 = -0.636$, Eq. 19.2 becomes

$$y'_{10} = y_1 - y_{10}(-0.636) = y_1 + 0.636y_{10}$$

22. The resultant deflection on the right portion of the shaft is given by

$$-y'_{20} = -y_2 - y_{20}(\alpha_1 - \alpha_2) \quad 19.3$$

$$-y'_{20} = -y_2 - y_{20}(-0.636) = -y_2 + 0.636y_{20}$$

The negative sign signifies that the deflection is upward rather than downward.

23. By using Eqs. 19.2 and 19.3 the actual resultant deflection curve may be drawn as shown at (H) and the deflections under the loads noted.

24. The critical speed may then be found by Eq. 19-1 as in two-bearing shafts.

W	y	y^2	Wy	Wy^2
125	0.253 (10) ⁻³	0.0639 (10) ⁻⁶	31.60 (10) ⁻³	7.990 (10) ⁻⁶
17	0.326 (10) ⁻³	0.1063 (10) ⁻⁶	5.55 (10) ⁻³	1.808 (10) ⁻⁶
17	0.323 (10) ⁻³	0.1043 (10) ⁻⁶	5.50 (10) ⁻³	1.772 (10) ⁻⁶
			42.65 (10) ⁻³	11.570 (10) ⁻⁶

$$n_c = 187.5 \sqrt{\frac{\sum Wy}{\sum Wy^2}} = 187.5 \sqrt{\frac{42.65(10)^{-3}}{11.57(10)^{-6}}} = 11,380 \text{ r.p.m.}$$

19-7 Torsional Critical Speeds. In addition to the lateral critical speeds just considered, rotating masses connected by shafts have torsional critical speeds which must be avoided. As an impeller of a pump or blower unit rotates, small torque impulses may develop and be transmitted to the shaft. These may be caused by slight misalignments, the passing of the impeller vanes by the volute tongue or diffuser vanes, etc. If the frequency of these impulses coincides with or is an even multiple of the natural frequency or torsional critical speed of the unit, oscillations of large amplitude will build up with resulting high stresses and a possible shear fatigue failure.

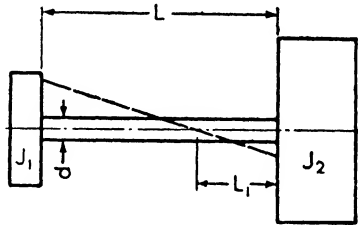


FIG. 19-5. Two-mass-system torsional vibration.

If two masses are connected by a shaft and one is given a torsional impulse relative to the other, oscillations will occur even though the shaft and masses are rotating. Three or more masses connected by shafts will have several critical speeds, one for each manner or mode in which they may oscillate relative to each other. Most pump and blower installations have only two masses. This discussion will, therefore, confine itself to the determination of the natural frequency and location of the node for two mass systems.*

If two masses are connected by a constant diameter shaft as shown in Fig. 19-5 the natural frequency of the system is given by:

$$F = \frac{60}{2\pi} \sqrt{\frac{I_p E_s (J_1 + J_2)}{J_1 J_2 L}} \tag{19-4}$$

* Derivations of the formulas and information for systems having more than two masses may be found in *Practical Solution of Torsional Vibration Problems*, by W. K. Wilson, Wiley, 1935, and *Torsional Vibration*, by W. A. Tuplin, Wiley, 1934.

where F = natural frequency in cycles per minute

$$I_p = \text{the polar moment of inertia of the shaft} = \frac{\pi d^4}{32} \text{ in.}^4$$

d = the shaft diameter in inches

E_s = shearing modulus of elasticity in pounds per square inch

L = shaft length in inches

$$J = \text{mass moment of inertia of the mass} = \frac{W}{g} \bar{R}^2 \text{ in pound- inches-second}^2$$

W = weight of the mass in pounds

\bar{R} = radius of gyration of the mass in inches

g = acceleration due to gravity = 386 in. per sec.²

and the node or point of zero amplitude will be located a distance L_1 inches from mass J_1 as given by

$$L_1 = \frac{J_2 L}{J_1 + J_2} \quad 19.5$$

where the symbols are the same as those given above.

It may be observed from Eqs. 19·4 and 19·5 that F and L_1 are independent of the actual amplitudes, and that the frequency is reduced with larger masses J , greater shaft length L , and smaller shaft diameter d .

If the shaft diameter is not uniform but is stepped, an equivalent length must be found on the basis of some arbitrary diameter. The equivalent length of each constant diameter section is found from the equation

$$L_e = \left(\frac{d_e}{d}\right)^4 L \quad 19.6$$

where L_e is the equivalent length

L is the actual length

d_e is the shaft diameter to which the lengths are referred

d is the actual shaft diameter.

The total shaft length used in Eqs. 19·4 and 19·5 is the sum of the equivalent lengths of the various sections.

To illustrate this, the natural torsional frequency and node position of a motor-driven vertical sewage pump having three vanes will be determined. This unit is illustrated diagrammatically in Fig. 19·6 with the sizes noted.

The equivalent length of a 1-in.-diameter shaft is found from Eq. 19-6 by means of a table:

L	d	d^4	$L_e = L/d^4$
10.0	3.75	198	0.0505
15.5	3.81	211	0.0735
4.5	3.31	120	0.0375
5.5	3.00	81	0.0679
248.6	4.00	256	<u>0.9711</u>
			1.2005

Total equivalent length = 1.2005 in. of 1-in.-diameter shaft

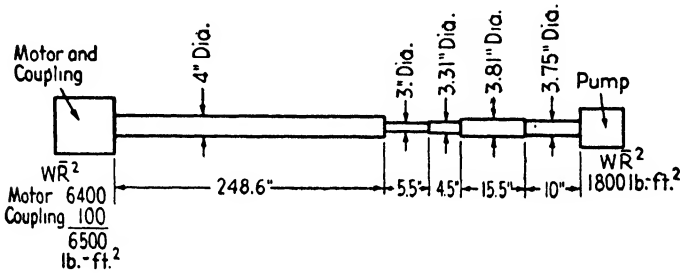


FIG. 19-6. Pump shaft with two masses.

A given torque will produce the same deflection in 1.2005 in. of 1-in.-diameter shafting as it does in the actual shaft shown in the figure.

The mass moments of inertia in inch-pounds-second² are

$$J_1 = \text{motor mass} = 6500 \times \frac{144}{386} = 2420 \text{ in.-lb.-sec.}^2$$

$$J_2 = \text{impeller mass} = 1800 \times \frac{144}{386} = 674 \text{ in.-lb.-sec.}^2$$

Shearing modulus for steel = $E_s = 12,000,000$ lb. per sq. in.

Polar moment of inertia of a 1-in.-diameter shaft = $\frac{\pi}{32} 1^4 = 0.0983$ in.

The natural frequency, by Eq. 19-4, is

$$F = \frac{60}{2\pi} \sqrt{\frac{I_p E_s (J_1 + J_2)}{J_1 J_2 L}} = \frac{60}{2\pi} \sqrt{\frac{0.0983 \times 12,000,000 (2420 + 674)}{2420 \times 674 \times 1.2005}}$$

= 412 cycles per minute

The node is located L_1 in. from the motor, as given by Eq. 19-5,

$$L_1 = \frac{J_2 L}{J_1 + J_2} = \frac{674 \times 1.2005}{2420 + 674} = 0.262 \text{ in.}$$

This value of L_1 is based on the equivalent 1-in.-diameter shaft. The actual distance from the motor is found from Eq. 19-6:

$$L_1 = L_e \left(\frac{d}{d_e} \right)^4 = 0.262 \left(\frac{4}{1} \right)^4 = 67.1 \text{ in. from the motor}$$

To avoid any torsional vibration trouble the operating speed of the unit should not be in the neighborhood of 412 r.p.m. or even multiples thereof.

PROBLEMS

19.1 A constant diameter pump shaft has an impeller located approximately midway between two bearings. What would be the approximate effect in per cent on the lateral critical speed of (a) increasing the shaft diameter 20 per cent; (b) increasing the impeller weight 5 per cent; (c) decreasing the bearing span 10 per cent?

Ans. (a) Increase 44 per cent; (b) decrease 2.3 per cent; (c) increase 17 per cent.

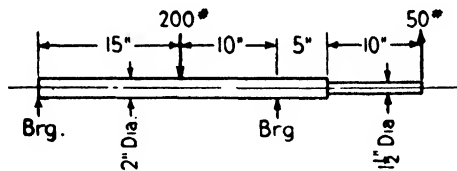


FIG. 19-7.

19.2 Determine the lateral critical speed of the shaft shown in Fig. 19-7, neglecting the weight of the shaft itself. Use the following scales: space 1 in. = 10 in.; force 1 in. = 100 lb.; pole distance $p = 2$ in.; area scale 1 in. = 20,000; pole distance $p' = 1.45$ in. Divide the M/I diagram into 10 in. lengths and work the problem on a sheet of $8\frac{1}{2} \times 11$ in. paper held vertically.

Ans. 2010 r.p.m.

19.3 The left mass of the shaft of Prob. 19-2 has a WR^2 of 1400 in.²-lb. and that on the right has a WR^2 of 150 in.²-lb. What is the torsional critical speed of the shaft?

Ans. 10,270 c.p.m.

INDEX

- Adiabatic process, 192
 Adiabatic temperature rise ratio, 197, 242
 Air, free, 192
 horsepower, 34, 228
 properties of, 8, 205
 standard, 192
 Alignment of shaft, 177
 Altitude-atmospheric relations, 205
 Arrangement of units, parallel, 161, 269
 series, 163
 Atmospheric-altitude relations, 205
 Avogadro's Law, 203
 Axial thrust, 157, 251
 Balancing axial thrust, 157, 251
 Balancing disk, 158, 252
 Bearings, blower, 246
 pump, 145
 Bernoulli's theorem, 10
 Bessemer converter blower, 256
 Bid analysis, 164
 Blast furnace air blower, 255
 Blast furnace gas blower, 256
 regulation of, 263
 Blast gate, 263
 Blower, 208
 Blow-off valve, 264, 269
 Boiler feed pump, 171
 Boyle's Law, 189
 Brake horsepower, 34
 Camerer model law, 65
 Capacity, measurement of blowers, 271
 measurement of pumps, 182
 speed effect of blowers, 210
 speed effect of pumps, 68
 Casing construction, of blowers, 246
 of pumps, 153
 Cavitation, 73-88
 cause of, 73
 effects of, 73
 factors affecting, 81
 Cavitation parameters, 82
 Centrifugal machines, action of, 2
 comparison with reciprocating, 1
 Characteristic curve, *see* Head-capacity curves
 Characteristic equation, 189
 Charles' Law, 189
 Circulating pump, 170
 Circulator, 259
 Circulatory flow, 28, 32, 35
 coefficient for blowers, 224
 coefficient for pumps, 98
 Classification, of blowers, 208
 of pumps, 54, 57, 64
 Clogless pump, 172
 Cupola blower, 255
 regulation of, 263
 Coefficients, circulatory flow, 32
 K factor, 33
 overall head, 33
 relationships between, 35
 Coke plant boosters and exhausters, 257
 Compressibility, effect on design, 217
 Compression of gas, adiabatic, 192
 isothermal, 195
 Compressor, 208
 high-pressure air, 254
 Condensate pump, 172
 Continuity equation, 9
 Contraction factor, 99, 106, 117, 232
 Cooling of blowers, 253
 Corrosion allowance, 154
 Corrosion of pumps, 156
 Costs, *see* Economic considerations
 Couplings, of blowers, 252, 260
 of pumps, 159
 Critical speed, action at, 289
 factors influencing, 296
 higher of two-bearing shaft, 295
 importance of, 289
 lateral, 289-301
 shaft changes, effect on, 291
 three-bearing shaft, 297
 torsional, 301-304
 two-bearing shaft, 291
 Cupola blowers, 255
 regulation of, 263
 Dalton's Law, 203
 Darcy equation, 11
 Deep well pump, 168
 Density, 6
 Diaphragm, blower, 250
 Diffusers, 39
 construction of blower, 250
 construction of pump, 156
 design of blower, 237
 design of pump, 124
 example of blower, 238
 example of pump, 125
 movable vane regulation, 265
 Discharge, position of flange, 154

- Disk friction, 30
 - air and gas, 239
 - water, 127
- Disk stress, 278-288
 - allowable, 283
 - any profile, 280
 - basic assumptions, 278
 - dead weight of vanes, 282
 - examples, 280, 285
 - impellers not made of steel, 284
 - parallel-sided disk, 279
 - procedure, 280
 - rim and bore conditions, 283
- Drainage pump, 170
- Drivers, of blowers, 254
 - of pumps, 164
- Dredge pump, 166
- Eccentric reducer, 176
- Economic considerations, 164-166
 - cost of units, 164
 - efficiency evaluation, 166
- Efficiency, adiabatic-isothermal ratio, 197
 - financial equivalent of, 166
 - hydraulic, 33
 - mechanical, 35
 - overall, 34
 - variation with performance for pumps, 56-64
 - volumetric, 34
- Enthalpy, 191
- Entropy, 191
- Fan, 208
- Fire pump, 166
- Flexible shaft, 291
- Flow, in blower impeller, 222
 - in pump impeller, 95
 - types of, 6
- Fluid horsepower, 34
- Foot valve, 160
- Foundation, 177
- Francis-type impeller, 54
 - design, 130-143
 - dimensions, 130
 - pattern maker's sections, 138
 - streamline determination, 132
 - vane shape, 137
- Free air, 192
- Friction loss, in machine, 29
 - in passage, 11
- Gas, average composition of, 205
 - constant, 190
 - properties of, 204
- Gas mixtures, average composition of, 205
 - properties of, 202
- Gland, 149
- Governing, *see* Regulation of blower
- Head, 9
 - Head, adiabatic, 194
 - of blowers, 209
 - isothermal, 196
 - measurement, 182
 - overall coefficient, 33, 97-104
 - pressure, 9, 219
 - required of machine, 14
 - suction, *see* Suction head
 - velocity, 9, 182
 - virtual, 24, 36
 - Head-capacity curves, actual, 44
 - curve shapes, 71
 - parallel operation, 161
 - series operation, 163
 - speed, effect of, 38, 68, 210
 - suction pressure changes, 212
 - suction temperature changes, 213
 - vane alteration effect, 70
 - virtual, 27, 36
 - Horsepower, adiabatic, 194
 - curve shapes, 72
 - fluid, 34
 - isothermal, 196
 - measurement, 184, 271
 - virtual, 27
 - Horsepower-capacity curves, actual, 45
 - curve shapes, 71
 - parallel operation, 161
 - series operation, 163
 - speed, effect of, 38, 68, 210
 - suction pressure changes, 212
 - suction temperature changes, 213
 - Hot water pump suction head, 87
 - Hydraulic Institute suction head curves, 84-88
 - Hydraulic radius, 11
 - Hydraulic efficiency, 33
 - Impeller, construction of blower, 247
 - construction of pump, 152
 - dimensions of blower, 221, 223, 228
 - dimensions of pump, 92, 96, 109, 131
 - Inspection of pump, 178
 - Installation, of blower, 269
 - of pump, 176
 - Internal energy of gas, 191
 - Irrigation pump, 170
 - Isothermal process, 195
 - Isentropic process, 192
 - Joule's experiment, 191
 - K factor, 33, 35, 98, 223
 - Labyrinth construction, 245
 - Labyrinth leakage, 224, 231
 - Laminar flow, 6
 - Lantern ring, 149
 - Leakage, 31
 - Leakage loss, in blower, 224, 231, 245
 - in pump, 91, 111, 153
 - Liner, dredge pump, 166
 - Losses, disk friction, 30

- Losses, friction, 11, 29**
 in blower, 220
 of head, 11
 leakage, 31
 mechanical, 31
 turbulence, 13, 30
- Maintenance of pump, 178**
Materials of pump, 156
Mean effective pressure, 195
Mechanical efficiency, 35
Mechanical equivalent of heat, 190
Mechanical losses, 31
Mixed-flow-type impeller, 55, 142
Model laws of pumps, 65
Moody, cavitation parameter, 81
 model law, 65
Multistaging, 55
 of blower, 241
 of pump, 127
Municipal gas plant blower, 257
- Nomenclature of parts, 2**
Nozzles, A.S.M.E., 272
NPSH, see Suction head
- Operation, blower, 269**
 pump, 178
 faulty, 179
- Packing, 147**
Packing box, 147
Parallel operation, 161
Pattern maker's sections, 138
Performance curve, 36, 44, 45
 blower, 210
 impeller effects on, 70
 parallel operation, 161
 series operation, 163
 speed changes, 38, 68, 210
 shapes, 71
 suction condition changes, 211
 viscosity changes, 72
Piping, installation, 176, 269
 standard sizes, 90
Poise, 7
Power measurement, 184
Power wheel, 267
Prerotation, 31
 governing of blower, 265
Pressure, effect of changes on performance, 212
 head, 10, 26, 219
 measurement, 182, 271
Priming, 159, 177
Propeller-type impeller, 55, 144
Pulsation, 46
 in blower, 260, 264
 in pump, 161
- Radial thrust, 41, 159**
Radial-type impeller, 54
 design of, 90-117
- Rayleigh's principle, 290**
Reciprocating machines, 2
Regulation of blower, 260-268
 constant inlet volume, 263
 constant pressure, 260
 constant weight flow, 263
 movable diffuser vanes, 265
 prerotation, 265
 power wheel, 267
Return guide passage, 128, 243, 251
Reynold's number, 8
- Saybolt second, 8**
Scavenging Diesel blower, 255
Seal, blower, 245
 mechanical, 151
Selection of pump, chart, 57
Series operation, 163
Sewage blower, 254
Sewage pump, 172
Shaft, alignment, 177
 blower, 221, 244
 pump, 92, 131, 145
Shaft sleeves, blower, 244
 pump, 145
Slurry pump, 167
Specific gravity, 6
Specific heat, 190
Specific speed, 49
 blower, 208
 cavitation, 84-88
 chart, 51
 classification, 54
 and efficiency, 61-64
 equation, 49
 and wheel proportions, 52
Specific volume, 189
Specific weight, 6
Speed, of blowers, 217
 effect on performance, 38, 68, 210
 measurement, 184, 271
 of motors, 90, 164
 of pumps, 90
 regulation of blowers, 262
Spiral flow, 19
Standard air, 192
Stiff shaft, 291
Streamlines, 16
 Francis-type impeller, 132
Streamtubes, 16
 Francis-type impeller, 132
Stresses, casing, 154
 disk, 278-287
 impeller, 278-287
 shaft, 92
 vane, 106, 250
Stuffing box, pump, 147
Suction head, 74
 available, 75
 design effect on, 78
 equation of, 74
 examples of, 75
 how measured, 74, 80

- Suction head, required, 75, 78, 80
 - safe values of, 84-88
- Suction line, installation, 176
 - velocities, 90, 221
- Suction volute, 153
- Sum and difference curves, 278-287
- Supercharger, 258
- Surging, 46
 - prevention in blower, 260, 264
- Temperature, changes in, effect on performance, 213
 - measurement, 271
 - rise ratio, adiabatic, 197, 242
- Testing instruments, blower, 271
 - pump, 182
- Testing procedure, blower, 270
 - pump, 180
- Testing sample, blower, 273
 - pump, 185
- Thoma cavitation parameter, 81
- Thrust, axial, 157, 251
 - radial, 41, 159
- Tongue angle of volute, 119, 236
- Torsional critical speed, 301-304
 - equivalent shaft lengths, 302
 - example, 303
- Torsion meter, 184
- Turbulence, 30
- Turbulent flow, 6
- Valves, blower, 269
- Valves, pump, 176
- Vanes, angles of blower, 221, 223, 228
 - angles of pump, 95, 96, 109, 131
 - construction of blower, 247
 - construction of pump, 106, 152
 - design of blower, 225
 - design of pump, 99
 - Francis-type pump, 132-142
 - number of blower, 225
 - number of pump, 106
- Velocity, in blower lines, 221, 269
 - changes in machine, 41, 217
 - diagrams, 22
 - in pump lines, 90
- Venturi meter, 183
- Viscosity, of fluids, 7
 - kinematic, 7
 - and performance curves, 72
- Volumetric efficiency, 34
- Volute, 39
 - design of blower, 234
 - design of pump, 118
 - example of blower, 234
 - example of pump, 120
- Water, properties of, 8, 76
 - horsepower, 34, 107, 131
- Water gas blower, 257
- Waterworks pump, 170
- Wearing ring clearance, 92
 - construction, 92, 153

DATE OF ISSUE

This book must be returned within 3/7/14 days of its issue. A fine of ONE ANNA per day will be charged if the book is overdue.

--	--	--	--	--	--

